MODIFICATIONS IN AP2 AND CLATHRIN-MEDIATED ENDOCYTOSIS AS A MECHANISM OF SYNAPTIC PLASTICITY

Dissertation

for the award of the degree

"Doctor rerum naturalium"

of the Georg-August-Universität Göttingen

within the doctoral program

"Molecular Biology of Cells"

of the Georg-August University School of Science (GAUSS)

submitted by

Göksemin Fatma Sengül

born in Ankara, Turkey

Göttingen, April 2022

Dedicated to my supervisor Prof. Dr. Peter Schu

and to my beloved family and friends.

To express my gratitude and respect for their constant guidance, support and motivating attitudes throughout my PhD studies. This work also belongs to you as much as it is mine.

Members of the Thesis Committee and Examination Board:

Prof. Dr. Peter Schu   Department of Cellular Biochemistry
(Supervisor and first referee)   University Medical Center Göttingen
                                       Göttingen, Germany

Prof. Dr. Silvio O. Rizzoli   Department of Neurophysiology
(Second   University Medical Center Göttingen
referee)   Göttingen, Germany

Prof. Dr. med. Martin Oppermann   Institute of Cellular and Molecular
                                       Immunology
                                       University Medical Center Göttingen
                                       Göttingen, Germany

Extended members of Examination Board:

Prof. Dr. Michael Thumm   Department of Cellular Biochemistry
                                       University Medical Center Göttingen
                                       Göttingen, Germany

Prof. Dr. Susanne Lutz   Institute of Pharmacology and Toxicology
                                       University Medical Center Göttingen
                                       Göttingen, Germany

Prof. Dr. Alexander Stein   Max-Plank Institute for Multidisciplinary
                                       Sciences
                                       Göttingen, Germany

Date of oral examination: 22nd of June 2022

Affidavit

I hereby declare that my PhD thesis dissertation, entitled as "Modifications in AP2 and clathrin-mediated endocytosis as a mechanism of synaptic plasticity" has been written independently and with no other aids or sources than quoted.

Göksemin Fatma Sengül
Göttingen, 29th April 2022

TABLE OF CONTENTS

LIST OF FIGURES

LIST OF TABLES

ABBREVIATIONS

Activated Cdc42-associated kinase 1	ACK1
Adaptor-associated kinase 1	AAK1
Adaptor protein complex	AP
Adenosine diphosphate	ADP
Adenosine triphosphate	ATP
ADP ribosylation factor	ARF
Action potential	AP
α-amino-3-hydroxy-5-methyl-4- isoxazolepropionic acid	AMPA
AP180 N-terminal homology	ANTH
Bin/Amphiphysin/Rvs	BAR
Bone morphogenic proteins-induciple kinase	BIKE/BMP2K
Calcium-binding protein 39	Cab39
Calcium/Calmodulin-dependent kinase II δ	CaMK-IIδ
Casein Kinase 2	CK2
Chondritin sulfate proteoglycan	CSPG
Clathrin assembly lymphoid myeloid leukemia	CALM
Clathrin-coated pit	CCP
Clathrin-coated vesicles	CCV
Clathrin coated vesicle associated kinase 104	CVAK104
Clathrin heavy chain	CHC
Clathrin light chain	CLC
Clathrin-mediated endocytosis	CME
Close homolog of L1	CHL1
Coat protein complex I	COPI
Coat protein complex II	COPII
Cyclin G-dependent kinase/auxilin2	GAK/auxilin2
Dual specificity tyrosine phosphorylation-regulated Ser/Thr kinase	DYRK1A
Doublecortin-like kinase 1	DCLK1
Early endosome	EE
Endocytic accessory proteins	EAPs
Endoplasmic reticulum	ER

Endoplasmic reticulum-Golgi intermediate complex	ERGIC
Epidermal growth factor receptor	EGFR
Epidermal growth factor receptor substrate 15	Eps15
Epidermal growth factor receptor substrate 15L1	Eps15L1
Epsin-homology domains	EHDs
Fer/Cip4 homology domain-only proteins 1/2	FCHo1/2
Fes/CIP4 homology-Bin/Amphiphysin/Rvs	F-BAR
G-protein coupled receptor	GPCR
G-protein receptor kinase 2	GRK2
Guanosine diphosphate	GDP
Guanosine triphosphate	GTP
Guanine nucleotide exchange factor	GEF
GTPase activating protein	GAP
Heat shock protein 70/90/110	Hsp70/90/110
Heat shock cognate 70 protein	Hsc70
Hungtington-interacting protein 1	Hip1
Hungtington-interacting protein 1-related protein	Hip1R
Intersectin 1	ITSN1
Knockdown	KD
Knockout	KO
Leucine-rich-repeat-kinase 2	LRRK2
Mouse protein 25 α	MO25α
Messenger ribonucleic acid	mRNA
Nuclear Dbf2-related kinase 1/2	NDR1/2
Neuronal cell adhesion molecule	NCAM
Neuronal cell adhesion molecule like 1	NCAM-L1
Neuroglia cell adhesion molecule	NgCAM
NgCAM-related cell adhesion molecule	NrCAM
Neurotransmitter	NT
Numb-associated kinase	NAK
Adaptin-ear-binding-coat associated protein	NECAP
Nucleotide exchange factor	NEF

Neural Wiskott-Aldrich syndrome protein	N-WASP
Oculocerebrorenal Lowe syndrome protein	OCRL
Ras-related/ADP ribosylation factor	Sar/ARF
Rough endoplasmic reticulum	RER
Phosphatidylinositol phosphate	PIP
Phosphatidylinositol 3-kinase	PI3KC2α
Phosphatidylinositol-4,5-bisphosphate	PI-4,5-P$_2$
Plasma membrane	PM
Post translational modification	PTM
Protein phosphatase 2A	PP2A
PP2A regulatory subunit B	PP2R2B
PP2A regulatory subunit C	PP2R2C
Ribonucleic acid	RNA
Saccharomyces cerevisiae pseudokinase 1	SCY1
Saccharomyces cerevisiae-like pseudokinase 1	SCYL1
Secretion associated Ras-related/ADP ribosylation factor	Sar/ARF
Ser/Thr protein kinase 38/39	STK38/39
STK38-like	STK38L
Sterile20 (Ste20)/SPS1-related proline-alanine-rich protein kinase	SPAK
Soluble N-ethylmaleimide sensitive factor attachment protein receptors	SNARE
Sorting nexin 9	SNX9
Src homology 3	SH3
Synaptic vesicle	SV
Synaptic cell adhesion molecule 1	SynCAM1
Trans Golgi network	TGN
Tyrosine-kinase non-receptor protein 2	TNK2

ABSTRACT

AP2 CME fulfills essential functions in embryonic development and cell survival. The AP2 complex and clathrin form AP2 CCV together with sixty other coat proteins. Due to this complex protein network, the regulation of CCV life cycle still remains elusive. The tissue-specific AP1/σ1B complex mediates intracellular protein sorting and coordinates endolysosomal protein transport together with the ubiquitous AP1/σ1A complex. The AP1/σ1B complex knockout mice are viable and fertile, but they have severe learning-memory and motor coordination deficiencies. Hippocampal AP1/σ1B ko synapses showed impaired synaptic vesicle recycling and enhanced endolysosomal protein transport. These alterations in AP1/σ1B ko synapses stimulates protein endocytosis by canonical (canCCV) and by stable, longer-lived AP2 CCV as an indirect, secondary phenotype. In addition, the longer-lasting stable AP2 CCV of these ko synapses are even more stabilized than the corresponding wt stable AP2 CCV and thus, they are named as stCCV. The comparisons of the coat protein composition between wt and ko synaptic AP2 CCV classes revealed three molecular mechanisms, which enhance AP2 stCCV stability, thereby extending their lifetime. These regulatory mechanisms influence all three layers of a CCV: the outer clathrin-basket, the middle AP2 layer and the inner layer, the vesicle membrane phospholipid composition. Firstly, the ko stCCV contain only half the amount of the clathrin basket disassembly protein Hsc70 compared to wt stable CCV. Secondly, the AP2 membrane and cargo binding are hyperactivated via the phosphorylation of its µ2 adaptin by the AAK1 kinase, whose amount and activity are increased in stCCV compared to wt stable CCV. Thirdly, stCCV contain much less of the PI-4,5-P$_2$ phosphatase Synaptojanin1 than wt stable CCV, whose activity is required for AP2 membrane dissociation. Firstly, we analyzed which protein(s) of the Synaptojanin1 CCV interactome determines its level in AP2 CCV. Our results show that the reduction of ITSN1 closely resembles the reduction of Synaptojanin1 levels in ko stCCV. Therefore, ITSN1 regulates the recruitment of Synaptojanin1 into stCCV. Additionally, the excess of Sgip1/AP2 complex over ITSN1 can efficiently compete with Synaptojanin1 for ITSN1 binding lowering Synaptojanin1 level even further. The ITSN1 AP2 CCV levels are controlled by Eps15 only, whereas its close homolog Eps15L1 is not involved. This was not

expected because Eps15L1 is indispensable for neurodevelopment and can substitute the absence of Eps15, but not vice versa. Apparently, Eps15 has specific functions in selected protein transport routes. Pacsin1 is, like ITSN1, a member of the Synaptojanin1 CCV interactome. Its level in a stCCV is also reduced, but its reduction is counter-balanced by its higher phosphorylation and thus its higher activation level. This compensatory activation highlights the complexity of the mechanisms regulating the AP2 CME pathways.

The mechanism controlling the CCV-associated Hsc70 levels and activity was analyzed next. The levels of the Hsc70 CCV co-chaperons, auxilin1 and GAK/auxilin2, its NEF Hsp110 and its co-worker Hsp90 are not changed in stCCV, in ways which would enable a CCV class specific regulation of Hsc70 levels and its uncoating activity. Hsc70 clathrin cage disassembly activity is regulated by differences in its phosphorylation patterns. All AP2 CCV from wt and ko synapses have two main Hsc70 pools, a hyper- and a hypo-phosphorylated pool, each of them contains Hsc70 proteins with different phosphorylation patterns. Only the Hsc70 homodimerization and activation of hypo-Pi Hsc70 proteins associated with the stCCV is inhibited by their binding of CaM/Ca^{2+} and most likely also by their binding of CaM. The regulation of Hsc70 and Pacsin1 activities via phosphorylation and the stimulation of AAK1 kinase activity led us to analyze the CCV class specific kinome. The amounts of DYRK1A, CaMK-IIδ, STK38L and SPAK(STK39)/CAB39 kinases are specifically reduced in ko stCCV, suggesting their involvement in the destabilization of AP2 CCV. Of all 12 investigated kinases, only AAK1 levels and its activity are specifically increased in ko stCCV, while being reduced in ko canCCV. Thus, AAK1 appears to be one of the master kinases regulating the AP2 CCV life cycle. Lastly, among the investigated neuronal cell adhesion proteins, only CHL1 and Neurocan are identified as novel, specific stCCV cargo proteins emphesizing particular functions of the AP2 stCCV pathway in synaptic plasticity. Overall, our findings will contribute to better understandings of diverse functions and mechanisms of AP2 CME pathways. Eventually, these data will provide more insights for developing treatments against neurological disorders caused by altered protein transport in endocytic routes.

Key words: AAK1, AP1/σ1B ko mice, AP2, Calmodulin, clathrin-mediated endocytosis, CCV life cycle, Hsc70, ITSN1, kinases, NCAMs, stabilized CCV, synaptic platicity, Synaptojanin1, X-linked mental retardation disorder.

CHAPTER 1

1. INTRODUCTION

1.1. The vesicular transport of proteins between organelles

Protein synthesis takes place either at soluble ribosomes in the cytoplasm or at the rough endoplasmic reticulum (RER) [1], [2]. Proteins that are newly synthesized have to be to be further processed and transported to the organelles in which they fulfill their cellular functions [1], [3]. After mRNAs are translated into proteins at the RER and then, they have received their core-glycosylation in the RER, they are exported into the Golgi apparatus, in which the carbohydrate side chains are further glycosylated. From the Golgi apparatus, proteins are transported into the trans-Golgi network, in which they receive their final chemical modifications, including phosphorylation, acetylation, methylation and sulfation etc. [1], [4], [5]. In addition, biologically inactive, pro-forms of proteins, like inactive receptors and hormones, are proteolytically matured by endoproteinases of the convertase family and subsequently by amino- and carboxy-exopeptidases [6], [7]. A subset of post-translational modifications (PTMs) function as protein targeting signals along their transport route into their final organelles [1], [4]. Proteins will be transported retrogradely, if they are RER-resident proteins or if they are incorrectly folded or processed [1], [4]. The correctly processed proteins continue their way through the organelles of the late secretory pathway, which intersects with endocytic pathways, and finally reach either to the plasma membrane (PM) of target cellular compartments, or to the lysosome or to the lysosome-related organelles [4], [8]. All transport steps of these membrane bound proteins along the compartments of secretory and endocytic pathways are mediated via vesicular intermediates, that bud off from the donor compartment and fuse with the membrane of the acceptor compartment, releasing their content [1], [8]. There are four main types of transport vesicles, which are named based on their proteinaceous vesicle coat composition (Figure 1.1) [8], [9]. The two types of transport vesicles that function in the early secretory pathway are the coatomer or COP (coat

protein complex) coated vesicles, COP-I and COP-II. The COP-II vesicles mediate anterograde protein trafficking from the RER to the Golgi apparatus and through the Golgi apparatus, while COP-I coated vesicles retrieve proteins and mediate retrograde protein transport through the Golgi apparatus and back into the RER [8], [9]. The third and fourth types of transport vesicles are named as clathrin-coated-vesicles (CCV). The clathrin protein is bound to these vesicles by two different adaptor-protein complexes (AP). The AP1 CCV mediate the transport of proteins between the trans-Golgi network (TGN) and endosomes and the AP2 CCV mediate protein endocytosis at the PM and protein transport into early endosomes [9], [10]. The vesicular protein transport is essential for maintaining the cellular protein homeostasis and cell signalling pathways [11].
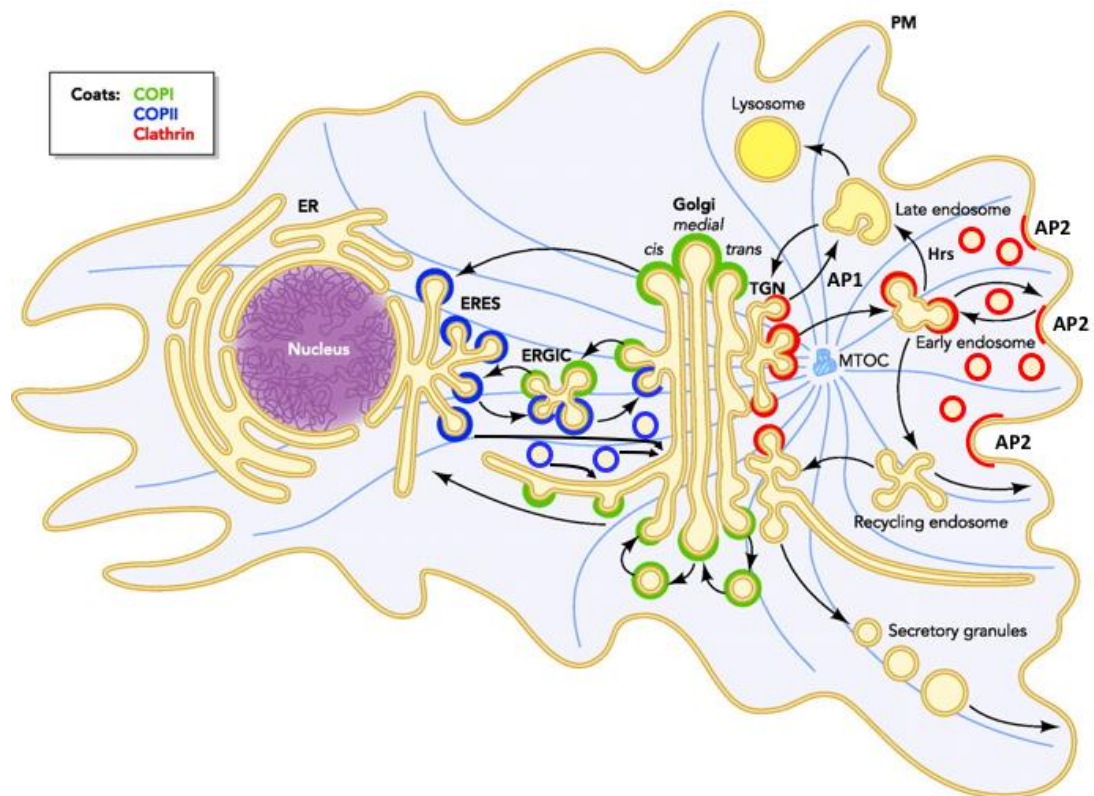
Figure 1.1. The intracellular membrane transport pathways via coated vesicles. The endocytic routes of COPI (green), COPII (blue) and clathrin-coated vesicles (red) in the intracellular protein transport pathways are demonstrated as schematic diagram. The scheme is modified from the original presented in Szul and Stzul *et al.* 2011 [4]. Abbreviations, endoplasmic reticulum (ER), ER exit sites (ERES), ER-Golgi intermediate compartments (ERGIC), trans Golgi network (TGN), Hepatocyte growth factor (Hrs), Adaptor protein (AP) and plasma membrane (PM). The original figure is reprinted with the permission from The American Physiology Society, provided licence number is 5295990674770.

1.2. Coated vesicles in the membrane trafficking

The biogenesis of COP-I and COP-II protein complexes and vesicles are evolutionarily conserved among yeast, worm, insect, plants and vertebrates [4]. The functions of both COP-I and COP-II coated complexes are regulated by Ras-related/ADP ribosylation factor (Sar/ARF) GTPases and their activating guanine-nucleotide-exchange factors (GEFs) and their deactivating GTPase-activating proteins (GAP) and vesicle-organelle membrane tethering factors like the soluble, N-ethylmaleimide sensitive factor attachment protein receptors (SNAREs) [4]. The formation of COP-I and COP-II coated vesicles is mechanistically similar [12]. Firstly, cytoplasmic coatomer is recruited to the membrane by the small GTPase protein, ARF1:GTP, as activated by GEFs which replaces ARF1:GDP bound state with ARF1:GTP bound state [12]. The activated ARF1:GTP is anchored to the the outer leaflets of the organelle membrane via its N-terminal amphipathic helix and stabilizes membrane binding to the COP complexes, which recruit the vesicle cargo proteins through the recognition of specific peptide motifs [12]. The dissociation of ARF1 and of the COP coat proteins requires GTP hydrolysis [12]. Since ARF1 lacks intrinsic GTPase activity, GAPs are required and regulated for the release of ARF1 from the membrane [12]. Also the formation of the third type of transport vesicle, the AP1 CCV, which mediate protein transport between the TGN and early endosomes (EEs) [4], [12], [13], is regulated by ARF1, but by different ARF1 GEF and GAP proteins [12], [14]–[16]. In contrast, formation of the AP2 CCV at the PM is not regulated by ARF1 or a related small GTPase. The formation of AP2 CCV is completed via the activity of large dynamin GTPase which wraps around the neck of vesicles as short helical rings for the membrane scission process [16].

1.2.1. COP-II vesicles in the anterograde vesicular transport

COP-II vesicles orchestrate anterograde protein transport from the RER towards and through the Golgi apparatus [4]. Selected cargo-engulfing COP-II coated vesicles are composed of the three core proteins Sar1p, Sec23/24p and Sec13/31p [17]. The first step in the formation of COP-II coated vesicles is the activation of Sar1p:GDP via its GEF Sec12p into Sar1p:GTP [17], [18]. Sar1p:GTP recruits Sec23/24p complex to the membrane of the RER [17]. Afterwards, Sar1p-Sec23/24p binds to the

heterotetrameric Sec13/31p complex [17]. The Sec24 subunit is responsible for the sorting of cargo proteins into the nascent COP-II vesicles [4]. The four different Sec24a, Sec24b, Sec24c and Sec24d isoforms can bind to the cytoplasmic tails of transmembrane cargo proteins via specific sorting motifs, thereby increasing the variety of cargo proteins that can depart the RER [4]. Sec24a and Sec24b captures cargo proteins via DxE and also via LxxL/ME amino acid sorting motifs, whereas Sec24c and Sec24d recognizes cargo proteins only via IxM sorting motifs (x stands for any amino acid) [4]. Additionally, the Sec23 subunit of COP-II, which functions as a GAP for Sar1p, also plays a role in the sorting of cargo proteins [4]. The Sar1p GTPase activity is triggered by the incorporation of the heterotetrameric Sec13/Sec31p complex, so that the polymerization of the COP-II coat protein complex is finalized after engulfment of the selected cargo into the nascent COP-II vesicles [4]. Deformation of the donor membrane into a pit requires Sar1 and Sec23/24 complex, which is globally kept stable through the Sec13/31p complex [4]. *In vitro* studies indicated that Sar1 is required for the pinching off the COP-II vesicles from the donor membrane [19] by the insertion of the amphipathic NH_2-terminal helix of Sar1, which is activated when bound by GTP, lowering the energy required for the vesiculation of the donor membrane [4], [19], [20]. Experimental blockage of GTP hydrolysis does not inhibit the formation of COP-II vesicles [20], however, the formed COP-II vesicles are unable to detach from the RER membrane [20].

Following the disassembly of the COP-II vesicle coat, the initial interactions between the cargo-carrying vesicle and Golgi membrane are carried out by tethers and then by SNARE-complexes to promote the fusion of vesicles with the recipient Golgi membrane [4], [21]. The initial studies regarding tethering mechanism were performed in yeast cells [4]. It has been shown that yeast Uso1p (homologue of mammalian p115) is responsible for the tethering of vesicles with the Golgi membrane [4], [22]. Activated small GTPase Ypt1p (ortholog of mammalian Rab1) recruits Uso1p to COP-II vesicles [4], [22]. It has been demonstrated that mammalian ortholog of yeast Uso1p p115, associates with SNAREs for the fusion of the vesicle with the Golgi [4], [22], [23]. Therefore, one can assume that Uso1p fulfills the same function by binding to SNAREs, like Bos1p, Sec22p, Bet1p and Ykt6p, in yeast [4], [22]. Besides Uso1p, yeast Grh1p (ortholog of mammalian GRASP65) has been proposed to interact with

Sec23/24p subunits of COP-II coat [4], [24]. Even though the exact function of yeast Grh1p is not known, it is supposed that the interaction of Grh1p with Bug1p (ortholog of mammalian GM130) is involved in the tethering of COP-II vesicles with the acceptor membrane [4], [24]. However, the binding partners of the Uso1p, Grh1p and Bug1p on the Golgi membrane are not identified, yet [4]. Furthermore, it could be also possible that Uso1p-Grh1p-Bug1p form a tripartite complex to facilitate the tethering of COP-II vesicles with the Golgi membrane [4]. Further experiments are required to elucidate the novel mechanisms behind the tethering and fusion of COP-II vesicles with the Golgi membrane.

1.2.2. COP-I vesicles in the retrograde vesicular transport

COP-I vesicles mediate the retrieval of proteins from the distal Golgi stack through the Golgi apparatus, to the endoplasmic reticulum-Golgi intermediate compartment (ERGIC) and all the way back to the RER [4]. COP-I coatomer complex is a heptameric complex and consists of α, β, β', γ, δ, ε and ζ protein subunits, which form a trimeric and a tetrameric subcomplex [4], [25]. The trimeric subcomplex contains α, β' and ε protein subunits and the tetrameric subcomplex contains γ, δ, β and ζ proteins [4], [25]. The trimeric α, β' and ε subcomplex is homologous to the Sec13/31p complex of the COP-II complex [4]. Based on this structural analysis, it can be suggested that trimeric complex is responsible for the formation of the outer layer of the COP-I coat [4], [26]. The γ subunit of COP-I complex is structurally similar to the large α and β adaptin subunits of the AP2 complex, which mediates the formation of CCV and forms the inner protein layer of that coat [4], [27]. Also the tetrameric subcomplex of γ, δ, β and ζ forms the inner core of the COP-I coat [4], [27]. Activated small ARF GTPases are involved in the recruitment of the COP-I complex to the membrane [4], [28]. Sec7p is responsible for the activation of ARFs in yeast [4], [29]. The mammalian orthologs of Sec7p were identified as five families of ARF GTPases based on sequence similarity, comprehensive structure and domain organization: GBF1/BIG, cytohesins, EFA6, BRAGs and F-box [4], [30]. Of all ARF GTPases, GBF1 is sufficient and required to activate ARFs for the recruitment of COP-I to the membrane and eventually for the formation of COP-I coated vesicles [4], [31]. Additionally, the formation of COP-I coated vesicles is also regulated by ARF GAPs,

because they have a scaffolding function to support the assembly of the huge protein complexes [4], [32], [33]. The recruitment of ARF GAPs to the budding COP-I coated vesicles is conducted by their direct interaction with activated ARF GTPases, cargo protein (via its cytoplasmic tail) and the COP-I coat (via the γ and β´subunits), which leads to the formation of tetrapartite ARF-ARF GAP-COP-I coat-cargo complex [4], [34], [35]. COP-I coat proteins and the cargo trigger the activity of the ARF GAP, leading to ARF:GDP and the exclusion of ARF from the tetrapartite complex [4], [34], [35]. It has been proposed that cargo-COP-I coat-ARF GAP complex ensures the formation of cargo loaded COP-I vesicles [4]. However, it is not known whether ARF GAPs still retain this interaction in the mature COP-I vesicle [4]. Moreover, the mechanisms behind the disassembly of COP-I coated vesicles are not well-established [4]. Initial studies suggested that ARF-mediated GTP hydrolysis is not solely enough to induce disassembly of the COP-I coat [4]. Therefore, further scientific studies are necessary to uncover the novel regulatory mechanisms in the dissociation of the COP-I coated vesicles [4]. The final two steps in the transport of cargo to the recipient compartment require tethering and fusions of COP-I coated vesicles with the target [4]. The tethering and fusion mechanisms of COP-I vesicles are more complicated than those of COP-II vesicles, because COP-I vesicles can bud off from multiple distinct cellular compartments including different Golgi stacks and as well as ERGIC and they can fuse with several others containing the distinct Golgi stacks, the ERGIC and eventually the RER [4]. In contrast, COP-II vesicles are needed to be pinch off only from the RER and fuse with just two cellular compartments, the ERGIC and the cis-Golgi to deliver their cargo content [4]. For example, trimeric Dsl1 is responsible for the tethering of COP-I vesicles to the RER [4], [36], [37]. Afterwards, RER-SNAREs such as Ufe1, Use1 and Sec20 are bound by Dsl, thereby assembling the SNARE complexes [4], [36], [37]. As it can be predicted, medial-Golgi COP-I vesicles and/or cis-Golgi COP-I vesicles are tethered and fused to their target membranes via multiple different tethers and SNARE proteins [4].

1.2.3. Clathrin-coated-vesicles in late secretory and endosomal pathways

Clathrin coated vesicles (CCV) transport proteins between TGN and EE and also mediate protein traffic from the PM to early endosomes [38]–[40]. Three clathrin-heavy-chains (CHC) assemble to a stable clathrin triskelion, to which a maximum of three clathrin-light-chain (CLC) may bind [38]–[40]. The clathrin triskelia interact with each other to form a network of pentagonal and hexagonal lattices [38]–[40]. This clathrin cage forms the outer proteinaceous layer of the CCVs [38]–[40]. Clathrin is not able to directly interact either with membrane phospholipids or with cargo proteins [39]. Clathrin is recruited by the adaptor-protein complex 1 (AP1) to form CCVs at the membranes of TGN, whereas the adaptor-protein complex 2 (AP2) recruits clathrin to the PM [38], [39]. Protein transport by CCVs regulates lysosome biogenesis, cell-cell communication and nutrient and ion transport [41]. The detailed structure and functions of clathrin and CCVs will be described in the sections 1.6 and 1.7.

1.3. The family of AP complexes

Adaptor-protein complexes (AP) are heterotetrameric protein complexes that control transport of intracellular proteins via vesicles along the secretory and endocytic pathways [42]–[44]. Five homologous APs, AP1-5 have been described in vertebrates [45]–[47]. The numbering of AP1-5 was assigned based on the chronological order of their discovery [45]–[47]. AP1 and AP2 are the only one, which mediate the formation of CCV, whereas AP3-5 function independently of clathrin [45]–[47]. All AP complexes are composed of four adaptin subunits, two ~100-130 kDa large subunits, one ~50 kDa medium-sized µ adaptin (µ1-5) and one small ~15-20 kDa σ adaptin (σ1-5) [42], [45], [48] as indicated in Figure 1.2. The two large adaptin subunits comprise a N-terminal core domain, a long, proline rich, unstructured hinge domain and a C-terminal globular, called 'ear', domain [44]. One of the large adaptins of the AP1-5 complexes are the β-adaptins (β1-5) show the highest sequence homology (up to 85%) among the AP adaptins [48]. The 'ear' domains of the β adaptins interact with additional vesicle coat proteins, which recruit cargo proteins not directly recognized by AP complexes [10], [49]–[54]. The 'ear' domains of β1 and β2 adaptins also bind and recruit clathrin to the site of vesicle formation on the PM [50]–[52]. The other large adaptins of the five AP-complexes, γ1, α, δ, ε, and ζ subunits of AP1-AP5,

respectively, display the lowest sequence homology among the adaptins of the five AP complexes [42], [55]. Despite that the γ1 and α adaptins of AP1 and AP2, respectively, they share only 25 % of amino acid sequence homology and their ternary structures are almost identical [55]. The N-terminal core domains of these five γ1, α, δ, ε, and ζ adaptins target AP1-AP5 to the membranes of the respective donor organelles, e.g. via binding of phosphatidyl-inositol phosphates, PI4P in the case of γ1 and PI-4,5-P_2 in the case of α adaptin. Their C-terminal domains interact with accessory proteins and co-adaptor proteins to facilitate budding of vesicular membranes and the formation of the vesicles, however we still know very little in this respect about the more recently discovered AP-complexes [56]–[58]. The medium-sized adaptins µ1-5 and the smaller adaptins σ1-5 of AP1-5 respectively, show an overall ~40 % sequence homology among each other, while subdomains may have remarkably larger or less sequence homologies [59], [60]. The µ and the σ adaptins recognize evolutionarily conserved short amino acid sequence motifs in proteins to be sorted and transported by them. The µ-adaptins bind tyrosine-based YxxØ motifs (x refers to any amino acids and Ø refers to a bulky and hydrophobic amino acid e.g. isoleucine or phenylalanine) and σ-adaptins bind dileucine-based D/ExxxLL/I motifs in the cargo proteins [61]–[64]. In vertebrates, AP1, AP2 and AP3 complexes can also be formed by tissue-specific adaptin isoforms, which then replace their ubiquitous isoform in a complex, but these tissue-specific complexes are present in addition to their ubiquitous complexes in a given tissue [42]–[45].
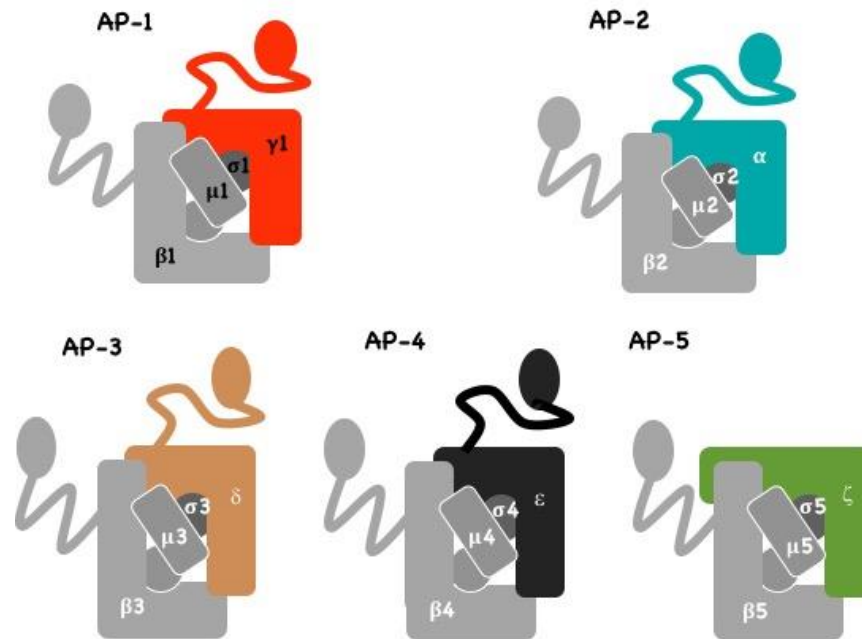
Figure 1.2 The family of five homologous adaptor-protein complexes and their adaptins. Each complex is composed of one large β1-5 adaptin and one large γ, α, δ, ε, and ζ adaptin in AP1-AP5, respectively. They all contain one medium sized μ and one smaller sized σ adaptin. The core domains of APs are required for their interactions with membranes and cargo proteins, while the appendages of the two large adaptins, referred to as 'ears', recruit additional vesicle coat proteins [65]. The Figure, family of five homologous AP complexes and their adaptins courtesy of Prof. Schu.

AP1 complexes form by far the largest AP family. Firstly, there are two ubiquitous γ isoforms γ1 and γ2. The γ1AP1 complexes are found in all eukaryotes, while γ2AP1 complexes are only found in vertebrates and plants. Besides the ubiquitous μ1A adaptin, mammals contain the polarized epithelial tissue-specific μ1B adaptin [42]–[45]. Zebrafish contains a second isoform μ1C, whose sequence is more similar to μ1A than to μ1B [66]. Vertebrates express three σ1 isoforms, the ubiquitous σ1A and the two tissue-specific isoforms σ1B and σ1C, which differ in their tissue-specific expression pattern [42]–[45]. The γ1AP1 and the γ2AP1 have essential and nonoverlapping functions during early developmental processes in vertebrates [66], [67]. However, γ2 does not bind σ1C and thus only two γ2AP1/σ1A and γ2AP1/σ1B complexes are formed. The tissue-specific adaptin isoforms can partially compensate for the loss of their ubiquitous isoforms, so as documented that knockouts of ubiquitous adaptins cease embryonic development at different stages [66].

An AP2 complex can be composed by either one of the two ubiquitous αA (AP2A1/α1) and αC (AP2A2/α2) isoforms, however, they do have tissue-specific

expression levels [42]–[44]. Current knowledge annotated only two splice variants of αA gene [68]. An AP3 complex contains either the ubiquitous β3, μ3 and σ3 adaptins or the brain-specific β3B, μ3B or σ3B isoforms [42]–[44], [65]. Isoforms of AP4 and AP5 adaptins are not known, yet and their expression levels are much lower compared to the other family members [44].

The specificity of AP complex functions is defined by their targeting to the peculiar intracellular compartments (Figure 1.3) [65]. AP1 complex plays a role in the formation of CCV at the trans-Golgi network (TGN) and early endosomes (EE) and mediates protein transport bidirectionally between TGN and EE [69]. This AP1 CCV pathway is involved in the lysosome biogenesis and in the regulation of PM levels of receptors [69]. In addition, AP1 performs essential functions in the regulation of secretory pathways, like the formation of von Willebrand factor containing granules [70]. The AP2 complex takes part in the formation of CCVs particularly at the PM and mediates the endocytosis of numerous PM proteins and their transport into EE [38]–[40]. AP1 and AP2 are indispensable for early embryonic development and survival of embryos in vertebrates, while a deficiency in any of the additional three AP-complexes is compatible with life, but mutations in those three AP-complexes causes severe diseases (will be discussed in detail in Section 1.5) [67], [69].

The AP3 complex mediates protein transport between early and late endosomes [44], [71], [72]. In the absence of AP3, the lysosomal membrane protein 1 (LAMP1) recycles repeatedly between the PM and EE before reaching to its final destination, the lysosome [44], [71]–[73]. The indispensable function of AP3 is the biogenesis of lysosome-related organelles such as melanosomes and dense-core-vesicles in platelets [44], [71], [72]. So, AP3 is essential to direct cargo proteins from the TGN into lysosome-related-organelles [44], [71]–[73], e.g. the transport of the tyrosinase enzyme into melanosomes [74].

The AP4 complex is found at the membranes of TGN and EE and recruits cargo proteins with Yx[FYL][FL]E endocytic motifs to convey them also from apical into basolateral endosomes [75], [76]. For example, AP4 has a role in the basolateral/dendritic transport of AMPA (α-amino-3-hydroxy-5-methyl-4-isoxazolepropionic acid) receptors in neurons [77]. In AP4/ε adaptin deficient cells, ATG9A was constrained to the TGN [78], [79]. ATG9A is the only transmembrane

protein that regulates autophagy [78], [79]. Therefore, the proper transport of ATG9A out of the TGN is important for the biogenesis of autophagosomes [78]. Eventually, defective sorting of axonal ATG9A gives rise to the formation of damaged autophagosomes [78], [79]. The impaired axonal protein sorting in AP4 deficient patients causes the Hereditary-Spastic-Paraplegia (HSP) syndrome, due to defects in motor axon functions [78], [79].

The AP5 complex is the least studied of all complexes. It has been located primarily on late endosomes, mediates protein sorting from late endosomes to lysosomes or protein transport from late endosome back to TGN [80]. The mutations in the AP5/ζ adaptin is associated with the spastic paraplegia disorder, in which axons of motor neurons are degenerated [80]. Studies in AP5/ζ ko mice demonstrated the accumulation of autophagosomes and autolysosomes. Defects in autophagic flux and in the reformation of lysosomes from the autophagosomes were observed in cell lines *in vitro* [80]. AP4 and AP5 complexes have much lower protein expression levels than the other three AP1, AP2 and AP3 complexes and this is a limitation in studying their cellular roles [44]. Therefore, more studies have to be conducted to discover the molecular mechanisms by which these complexes fulfil their functions.
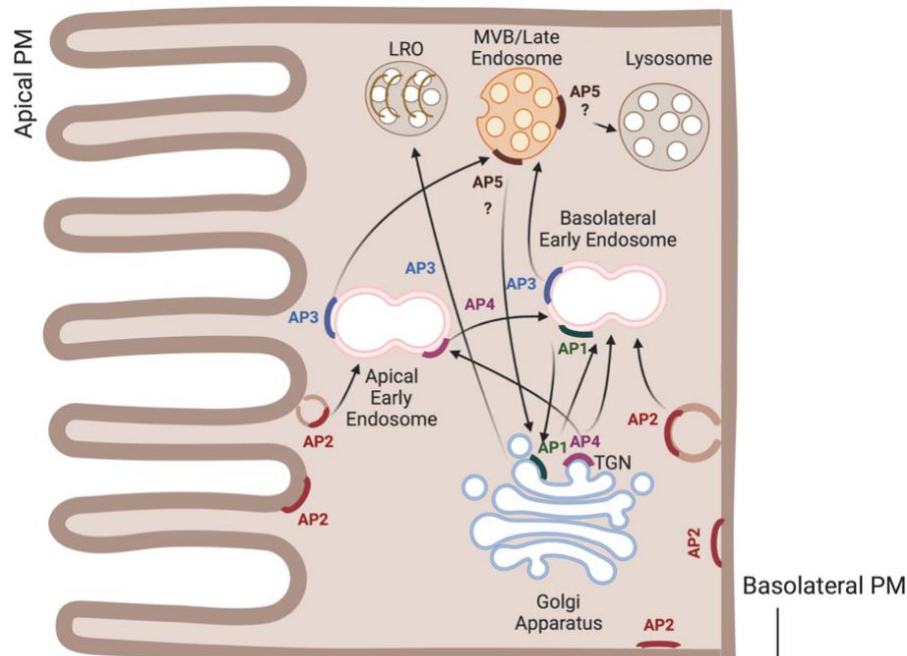
Figure 1.3. The subcellular localizations and intracellular protein transport pathways of AP1-5 protein complexes. The intracellular protein transport pathways of AP1-5 and their subcellular localizations are demonstrated in the schematic figure. Abbreviations: adaptor protein complexes (AP); lysosome-related-organnels (LRO); trans-golgi network (TGN); plasma membrane (PM). The figure is made in BioRender.com based on the current knowledge in the cited literatures [44], [65], [71], [76], [80].

1.4. Clathrin

The clathrin-heavy-chain protein (CHC), usually just referred to as clathrin, is the principal component of the clathrin cage of CCVs. Clathrin forms the outer layer of a CCV and it engulfs the forming vesicles, thus contributing to the energy required for membrane vesiculation and determining the size of a CCV [38]–[40], [81]. The building block of the clathrin cage is a triskelion assembled by three ~190 kDa CHC proteins [40]. A ~25 kDa Clathrin-light-chain (CLC) interacts with CHC via the CHC α-helical heptad repeats at the vertex of its proximal domains (Figure 1.4.A) [40], [82]–[84]. CLC is present at various substochiometrical amounts to CHC in different tissues, except the brain (the ratio of CLC/CHC in brain is equal to 1). It is believed that CLC ensures the static stability of the clathrin lattice and therefore, it might also be involved in the regulation of CCV life cycle [40], [82]–[84]. The vertex proximal legs of clathrin triskelia wrap around each other forming lattices made of hexagons and pentagons (Figure 1.4.B) [39], [40], [84]. The clathrin lattices found at the PM are exclusively formed by hexagons, while the clathrin basket of a CCV is formed by hexagons and pentagons [39], [40], [84]. The clathrin-cage is stable *in-vivo*, but it is not stable *in-vitro* at the physiological pH 7.4. So, the purification of CCV has to be performed in slightly acidic buffers at pH 6.4 [40], [85]–[88].

A   **B**
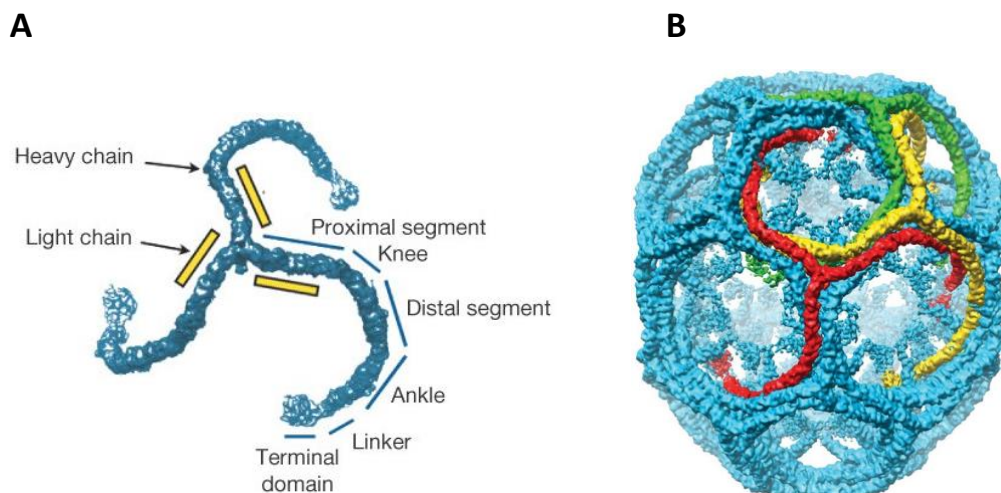
Figure 1.4. Clathrin triskelia assemble into cages with pentagonal and hexagonal lattices. (A) Clathrin triskelion (left) and **(B)** pentagonal and hexagonal lattices forming the clathrin-cage (right) are indicated in the schematic cartoon. Individual clathrin triskelion of the cage are shown in red, yellow and green [40]. The pictures are adapted from Fotin *et al.* 2004. The figure is reprinted with the permission from Springer Nature, granted licence number is 5295570548100.

Clathrin is mainly recruited to the site of transport vesicle formation by AP1 or AP2 complexes, but co-adaptor proteins of a CCV are also able to bind clathrin, like AP180, Eps15, Epsin etc. Recently, a specialized class of endocytic CCV have been identified, which do not contain AP2 and are mainly formed by Eps15 and Epsin [89]. These CCV have a special function in epidermal-growth-factor-receptor (EGFR) endocytosis [89]. Importantly, clathrin-cage assembly does not require a membrane and assembly mediating proteins, like AP1 or AP2, because it is an intrinsic property of the triskelia to form a cage made of hexaogons and pentagons. Such empty clathrin cages are form readily in the cytoplasm and they have to be continuously disassembled, because they would limit the availability of clathrin for the formation of CCV [39]. Two genes encode the CLC proteins CLCa and CLCb in vertabrates sharing 60 % sequence homology [81], [84]. Both CLC isoforms are alternatively spliced in neurons [81]. CLCa and CLCb interactions with CHC are believed to regulate clathrin triskelia stabilization and cage rigidity [81], [84]. CLC splicing variants differentially contribute to the clathrin knee conformations within the clathrin-cage assemblies [81]. It has been shown that neuronal CLC mixtures are much more advantages over single neuronal isoforms of either CLCa or CLCb for the efficient deformation of membranes [81]. The electrophysiological recordings from the neurons of mice, which lack either CLCa or CLCb, revealed defects in SV recycling [81]. Mice exclusively expressing CLCb have a reduction in SV numbers and also have impaired synaptic transmission as compared to their wt littermates, whereas mice with exclusively CLCa show accumulation of SVs and sustain normal neurotransmission [81]. All these results emphasize the differences between the two CLCs and indicate how their mixture in clathrin assemblies could be important to control clathrin function in neurons [81]. The CHC and CLCa of a CCV also bind to peripheral CCV proteins, like the Hungtington-interacting protein 1 (Hip1R), which links CCV with the actin cytoskeleton and controls intracellular membrane trafficking between the TGN and endosomes by promoting the budding of CCV *in vitro* [90], [91]. In addition, CLC isoforms also contribute to the selection of particular receptor proteins as CCV cargos thereby regulating the receptor-mediated endocytosis. To exemplify, CLC plays a role in the endocytosis of G-protein coupled receptors (GPCR), thereby regulating the GPCR signaling pathway [92]. They have been indicated that CLC KDs (CLCa KD and CLCb

KD) cause inhibition of GPCR endocytosis, thus inhibition of GPCR signalling [92]. They have further identified the regulatory mechanism showing that the phosphorylation of CLC by G-protein receptor kinase-2 (GRK2) is necessary for the efficient uptake of GPCRs [92]. Taken together, clathrin triskelia components do not only play an important role in the rigidity of clathrin coat but also regulates intracellular protein trafficking and as well as GPCR signalling [90]–[92].

1.5. The functions of AP1 complexes

The members of the family of AP1 complexes has been introduced in Section 1.3. The γ1 and γ2 adaptin isoforms form the two ubiquitous γ1AP1 and γ2AP1 complexes together with β1, μ1A and σ1A adaptins [44], [66]. γ1AP1 is expressed in all eukaryotes, whereas γ2AP1 is exclusively found in vertebrates and plants [44], [66]. The γ1AP1 complex was discovered first, together with AP2, by the biochemical characterization of CCV purified from bovine, rats and pig brains [13], [38], [93]. The brain is the tissue with the highest expression levels of AP1 and AP2, followed by the liver [94], [95]. Therefore, γ1AP1 complex functions have been studied since many years, while γ2 adaptin has been identified much later, based on its sequence homology to γ1 [96]. Each of the two complexes is essential for vertebrate development [67], [97]. The mouse γ1 adaptin knockout ceases embryonic development already at the blastocyst stage at day 3.5 *in-utero,* prior to the hatching of the blastocyst out of the zona pellucida [67]. γ2AP1 functions in development has been analyzed in zebrafish and it is essential for development as well [66]. Interestingly, also heterozygous γ1 +/- mice showed phenotypes. They grew slower than their wt littermates during nursing and have a defect in T-cell differentiation, demonstrating essential γ1AP1 functions also in post-natal adaptive immune system development [67]. The γ1AP1 and γ2AP1 complexes bind to the TGN and endosomal membranes and have only a partially overlapping distribution. A major difference between the two is the regulation of their membrane binding [96]. As already described in Section 1.3, γ1AP1 membrane binding is stabilized by ARF1:GTP, besides its binding to PI4P and cargo proteins. This ARF1 function is regulated by GEF proteins containing a Sec7 domain and their function can be inhibited by the drug brefeldin A. Therefore, γ1AP1 does not bind to membranes in the presence of brefeldin A [29]. However, γ2AP1 membrane binding

is not inhibited by brefeldin A and therefore γ2AP1 membrane binding either does not require ARF1:GTP or ARF1:GTP is required, but the respective GEF protein does not contain a Sec7 domain and thus its function is not inhibited by brefeldin A [96]. Based on these data, one can assume that the two AP1 complexes have non redundant functions in parallel secretory and endocytic pathways.

γ1AP1 and clathrin were detected on TGN membranes and the TGN is actually defined as the first compartment in the biosynthetic, secretory pathway which carries a clathrin coat [53], [66]. The *in-vitro* binding of the cytoplasmic tail of the mannose-6-phosphate receptor (MPR) to AP1 and AP2 complexes and the presence of the MPR in CCV proposed that AP1 CCV transport MPRs, loaded with lysosomal pro-enzymes, from the TGN to early and/or late endosomes. Afterwards, MPRs are retrieved from late endosomes back to the TGN for another rounds of protein transport [53], [97]. The AP1/μ1A ko mice cease development during mid-organogenesis (at day 13.5 *in-utero*) which enables the establishment of μ1A -/- mouse embryonic fibroblast (MEF) cell lines [69]. The μ1A -/- embryos develop further due to partial compensation of μ1A by the polarized epithelial cells μ1B, as demonstrated by the ability of μ1B to correct the protein sorting defects of μ1A -/- MEF cells [69]. In μ1A -/- MEF cells, the γ1 adaptin forms γ1-β1 dimeric and γ1-β1-σ1A trimeric complexes, which are not able to bind stably to membranes and thus cannot mediate protein sorting and transport [69]. In the μ1A -/- MEF cells, MPRs accumulate in early endosomes (EE) and are not transported back to the TGN [69]. The formation of AP1 CCV on endosomes could not be demonstrated directly, but it has been shown that TGN tethers bind and collect AP1 CCV [69]. These data demonstrated that γ1AP1 is required for bidirectional TGN-EE protein transport. Interestingly, due to the accumulation of the entire intracellular pool of MPRs in EE, their recycling rate between EE and the PM is increased, specifically the endocytic capacity of the MPR300 is increased by sevenfold [69]. Thus, the γ1AP1 complex also regulates receptor functions at the PM by the intracellular sorting of receptor proteins such as MPRs [69].

Polarized epithelial cells contain the ubiquitous γ1AP1 complex and the cell type specific γ1AP1/μ1B complex, in which μ1B replaces μ1A [69], [97]. γ1AP1/μ1B is located at recycling endosomes, where it supports protein recycling back to the basolateral PM of the polarized epithelial cells [98], [99]. The γ1AP1/μ1B ko mouse

is viable, but suffers from impaired gut development and gut regeneration, leading to severe bacterial infections and associated disease symptoms. In addition, mice suffers from impaired renal functions [98], [99].

Three isoforms of σ1 adaptin exist in vertebrates, as already described in Section 1.3. Each one is encoded by individual genes which are *AP1S1* gene encoding the ubiquitous σ1A, *AP1S2* and *AP1S3* genes encoding the tissue-specific σ1B and σ1C, respectively [63], [100]. Glyvuk *et al.* 2010 reported the highest expression of σ1A and σ1B in the brain, while σ1C isoform is highly expressed in the intestine and is hardly expressed in the brain [100]. In general, tissues contain only two σ1 adaptins at high levels, which are the ubiquitous σ1A either with σ1B or σ1C [100]. In AP1/σ1B ko fibroblast cells, the distribution of MPR were analyzed and the sorting of MPR was not altered as opposed to AP1/μ1A deficient cells [69], [98]. This result suggests that AP1/σ1B adaptin is not required for ubiquitous functions of the γ1AP1 complex [69], [98]. Also, the σ1B ko mouse is viable, although the animals were hypoactive. Thus, the viable σ1B ko mice enable to analyze synaptic functions and revealed key AP1/σ1B functions in the regulation of synaptic vesicle (SV) recycling [100]. AP1/σ1B deficient synapses contained fewer SVs due to inefficient and slowed-down SV recycling and enlarged EE and as well as late, multi-vesicular-body (MVB) endosomes were accumulated in parallel [100]. These results demonstrated the importance of AP1 function and EE in SV recycling [100]. The further biochemical characterization of the accumulating EE and the MVB endosomes exclaimed that they are canonical, Rab5 and PI3P enriched EE and exhibited an increased binding of γ1AP1/σ1A, but not γ2AP1/σ1A, complexes to these EE. Although these EE were enriched in PI3P, the Vps34 enzyme (PI3 kinase, PI3KC3)   which synthesizes PI3P out of PI, was present at wt levels [100], [101].

The analysis of the molecular basis for the increased Vps34 catalytic activity revealed a novel, non-canonical function of γ1AP1 complexes [101]. The work of my predecessor Ermes Candiello and colleagues revealed that γ1AP1/σ1A stimulates the maturation of EE into MVB endosomes, while γ1AP1/σ1B inhibits this pathway [101]. The activation is achieved by the formation of tripartite AP1/σ1A-ArfGAP1-Rabex5 complex [101]. Even though ubiquitous ArfGAP1 can be also incorporated into the complex, the brain-specific ArfGAP1 isoform binds σ1A with a much higher affinity.

The formation of this complex increases the amount of EE Rabex5, a GTP/GDP exchange factor of Rab5 protein [100]–[102]. Rab5:GTP activates the Vps34 kinase activity via binding to Vps15, which is present as a Vps34/Vps15 complex on EE. The increase in PI3P leads to enhanced recruitment of ESCRT complex proteins and thus triggers MVB formation [101]–[104]. In wt synapses, γ1AP1/σ1B binds to Rabex5 competing with its binding by ArfGAP1 and therefore, prevents the formation of the stable tripartite AP1/σ1A-ArfGAP1-Rabex5 complex [101]. Therefore, γ1AP1/σ1A stimulates maturation of EE into MVB endosomes and also stimulates protein degradation via this pathway [101].

While diseases have been associated with mutations in the σ1C encoding gene, AP1S3, the molecular functions of its protein product are not known. However, it may very well be specialized for the binding of a subset of cargo proteins with distinctive di-leucine based sorting motifs, as it has been shown by our group for σ1B [63] . In addition, much more still has to be learned about the functions of γ2AP1 complexes. However, the absence of σ1B in the knockout synapses is compensated by increased levels of γ2AP1/σ1A complexes, which is not the case for γ1AP1/σ1A. Therefore, the functions of the two γ2AP1 complexes may be largely redundant unlike the functions of the γ1AP complexes, at least in synapses [66].

1.6. The functions of AP2 complexes

The functions of the AP2 complex are also essential for early embryonic development and survival, like the functions of AP1 complexes [67], [105]. The composition of its adaptin subunits has already been described in Section 1.3. It has been shown by Sosa *et al.* 2012 that distruption of β1/2 gene expression leads to drastic defects in the developmental, growth and cytokinesis processes in *Dictyostelium discoidium* [106]. Moreover, the depletion of β1/2 causes significant decrease in the amounts of AP1/µ1 and AP2/µ2 proteins which indicates the involvement of β subunits in the stabilization of µ subunits [106]. Additionally, heterozygous AP2/β2 mutant mice are viable and show no phenotypic abnormality but they express significantly lower amounts of AP2/β2 mRNA and proteins as compared to their expressions in wt mice [107]. However, homozygous AP2/β2 mutant mice, expressing no AP2/β2 mRNA and protein, can continue their development only till prenatal

periods [107]. Furthermore, mice heterozygous for a targeted disruption of AP2/μ2 adaptin are viable and exhibit normal phenotype whereas AP2/μ2 homozygous mutant embryos cease development before day 3.5 post-coitus [105]. All these studies emphasize the indispensable functions of AP2 complex for the early embryonic development and survival in different non-animal and animal models [105].

Neuronal communication junctions are known as synapses. Signal transmission are conveyed either chemically or electrically from one neuron to another along the synapses. Electrical synapses communicate via ionic currents whereas chemical synapses transmit signals using chemical messengers, namely called as neurotransmitters (NTs) [108]–[110]. NTs are packed in the SVs at the pre-synaptic nerve terminals. In response to action potential (AP), voltage-gated Ca^{2+} channels are activated so that Ca^{2+} influx stimulates fusion of NTs-filled SVs with PM to release their contents into synaptic-cleft (synaptic exocytosis). Ultimately, NTs are bound by their receptors at the post-synaptic neurons. SVs are mainly recycled back from pre-synaptic PM via clathrin-mediated endocytosis (CME) in order to be re-filled with NTs for another rounds of exocytosis [108]–[110]. Major clathrin-adaptor protein AP2 complex takes role in the retrieval of SVs directly from the pre-synaptic PM (see Section 1.7 for detailed information) [111]. Besides recycling of SVs, AP2 CME also mediates the endocytosis of numerous proteins, such as receptors or cell adhesion proteins [38]–[40]. The AP2 complex binds exclusively to the PI-4,5-P_2 enriched PM in order to control the endocytosis of cargo and/or SV proteins at synapses [38]–[40]. High affinity membrane binding of AP2 does not involve ARF1:GTP, unlike the AP-complexes which bind to intracellular membranes. Instead, AP2 membrane binding is controlled via its interaction with cargo and PI-4,5-P_2 PM domain. Besides its PI-4,5-P_2 binding motifs in the α and β2 adaptins, AP2 contains additional PI-4,5-P_2 binding site in μ2 adaptin which is under the control of a kinase-stimulated conformational change. The conformational change in AP2 complex is supported by μ2 phosphorylation on Thr156 by the AAK1 kinase (AP2-associated-kinase) which removes the steric hindrance of the cargo binding domains in μ2 and σ2 adaptins and enables PI-4,5-P_2 binding motifs in μ2 to come into close proximity with the PM [85], [112]–[114]. This transition in AP2 conformation ensures the stable AP2 membrane association. Therefore, AAK1 activity has been considered to regulate the initiation of

AP2 membrane and cargo protein binding and thus AP2 CCV formation and CME [85]. Recent studies indicated the AP2 co-adaptor proteins Eps15 and Epsin are able to form endocytic CCV independent of AP2. This AP2-independent CME is specialized for EGFR mediated endocytic sorting as mentioned in Section 1.4 [89]. The alterations in the SV protein sorting and the AP2 CCV coat protein composition in AP1/σ1B ko synapses enable to study the functions of AP2 CME as secondary phenotypes [85], [100], [102] that are described in detail in section 1.9-11.

1.7. The clathrin-coated-vesicle life cycle

The CCV life cycle starts with the concentration of AP1 or AP2 complexes and their cargo proteins in a small membrane domain, and then, AP1 or AP2 complexes recruit clathrin for the formation of a clathrin-coated-pit (CCP). This CCP invaginates to form a clathrin coated bud, which is connected to the donor membrane by a narrow membrane neck. After membrane scission via a large dynamin GTPase, the CCV formation is completed and the CCV can be transported away from the donor compartment [115]–[117]. The proteinaceous coat of a CCV has to be disassembled to enable the interaction of vesicle and membrane SNARE proteins, which eventually leads to the fusion of the vesicle and acceptor organelle membranes and event the delivery of the CCV cargo proteins [109], [118]. The studies analyzing CCV formation focused exclusively on AP2 mediated CME, because endocytosis can be more easily tackled with experiments than CCV formation on intracellular membranes. Despite the sequence and structural homologies between AP1 and AP2 complexes, differences exist in molecular mechanisms regulating the life cycles of AP1 and AP2 CCV. They share in common molecular mechanisms for the recruitment of clathrin and for the capturing of their cargo proteins, but all other mechanisms regulating their life cycles are specific for AP1 and AP2 pathways [116].

Advanced scientific techniques, like TIRF microscopy, expanded our knowledge about the many proteins involved in the CME pathway. More than 60 different proteins can be involved in CME (Figure 1.5) [119]. However, TIRF microscopy only allows the analysis of the earliest events in AP2 CCV formation and so, many questions remain to be answered [115], [116], [119]. AP2 CCV formation can be subdivided into the four main stages initiation, stabilization, maturation and membrane fission, as

depicted in Figure 1.5-6 [116], [119]. CME does not only demand AP2 and clathrin, but also requires several endocytic accessory proteins (EAPs) that can be function in protein scaffolding, cargo capturing, generation and sensation of membrane curvature (Figure 1.5-1.6) [116], [117]. The crucial EAPs and the order in which they function in CME pathway as analysed by TIRF microscopy are provided in Figure 1.7 [116]. Dynamin GTPase is recruited at comparably low amounts to nascent CCPs during early stages of CME and is recruited in larger amounts only later in the maturation process [116], [117]. Finally, dynamin forms short helical rings around the neck of CCPs, that are deeply invaginated, and eventually catalyzes the pinching off CCVs from the PM at the late stages of CME [116], [117].
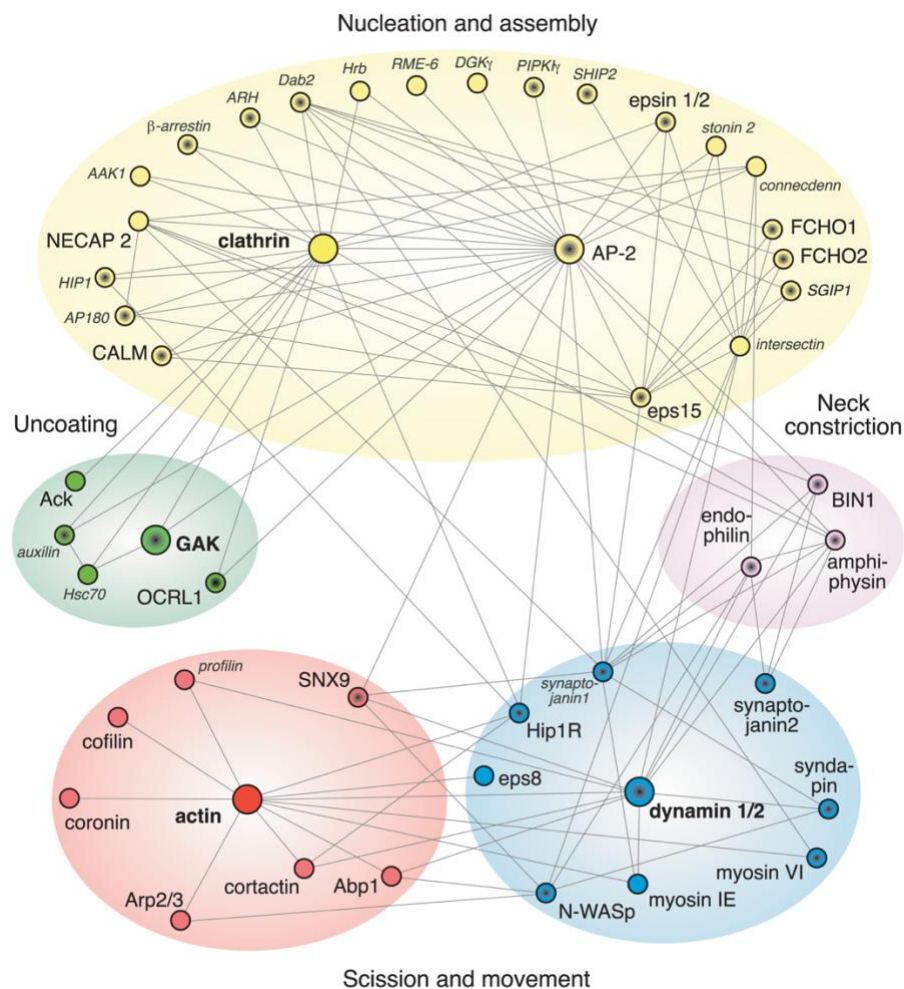
Figure 1.5. The interaction network of endocytic clatrin-coated vesicles in vertabrates. The stages of CME are depicted with different colors and functionally-related proteins are clustered within respective modules. Circle represented proteins with black center directly bind to PM PI-4,5-P_2 domain. The established protein-protein interactions are indicated with grey nodes. This figure visualizes the complex interactome behind the CME process and illustrates different binding partners of AP2 and clathrin throughout the distinct CME stages [119]. This figure is adapted from Traub *et al.* 2011. The figure is reprinted with the permission from PLOS open access Creative Commons CC BY provided a licence for the unrestricted use of any part of the article without special permission.
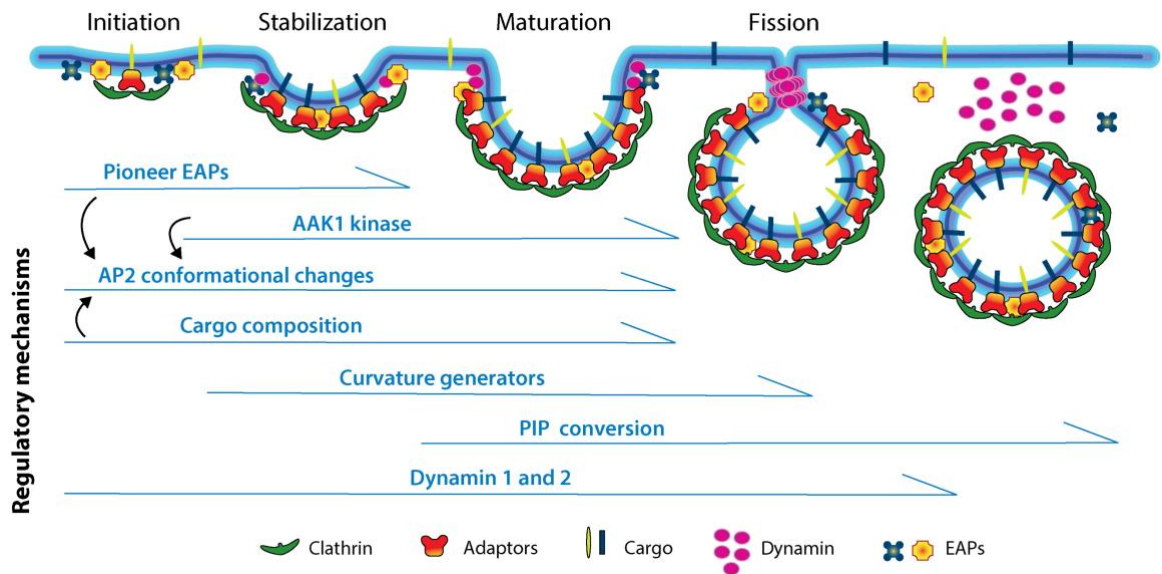
Figure 1.6. The multiple stages and regulatory mechanisms in CME. The stages including initiation, stabilization, maturation and the final step, membrane scission, and as well as the regulatory mechanisms of CME during CCV formation are demonstrated. The cartoon is obtained from Mettlen *et al.* 2018 [116]. The figure is reprinted with the permission from Annual Reviews granted licence number is 1214991-1.

The participation of numerous proteins, their numerous interactions by a limited and lower number of interaction mediating domains makes the formation of AP2 CCV a complicated process (Figure 1.5) [119]. The fact that the same protein interaction mediating domains connect different proteins suggest that AP2 CCV formation requires the sequential interactions of several proteins [116], [119].

CCP formation is the first stage of AP2 CCV formation [116]. AP2 interacts with the PM targeting PI-4,5-P$_2$ domain and as well as with the selected cargo protein via endocytic amino acid sequence motifs for the stable membrane binding [116]. Thereafter, AP2 forms a tripartite complex with EAPs, consisting of proteins of the family of Fer/Cip4 homology domain-only proteins 1/2 (FCHo1/2) and the epidermal-growth-factor-receptor-substrate proteins 15 or 15L1 (Eps15, Eps15L1). These proteins are followed by the scaffolding protein intersectin1 (ITSN1), the adaptin-ear-binding-coat-associated-proteins (NECAP1 and -2) and AP180 or its homologue clathrin-assembly-lymphoid-myeloid-leukemia (CALM) protein [116], [119]. These EAP-AP2 clusters are responsible for the initiation and stabilization of the CCP and they increase the recruitment of clathrin whose lattices contribute to the stabilization and further maturation of CCPs [116]. The F-BAR (Bin/Amphiphysin/Rvs) domain of

FCHo1/2 proteins bind specifically to slightly curved membranes and thus shallow CCP [116], [120]. Therefore, absence of or mutations in EAPs delays the initiation and stabilization of CCPs and thus slows down the formation of CCV [116], [119]–[122].

Stabilization of CCPs also involves supporting of AP2 conformational shift from its closed to open state as already described in Section 1.6 [112], [114], [116]. Only the open conformation of AP2 is able to bind cargo proteins and this change in AP2 conformation is induced and stabilized via μ2 adaptin phosphorylation by the AAK1 kinase [85], [113], [116]. AAK1 belongs to Numb-associated kinase (NAK) family like the Hsc70 co-chaperone and protein kinase cyclin G-dependent kinase/auxilin2 (GAK/Auxilin2), the bone morphogenic proteins-induced kinase (BIKE/BMP2K) and the Ark/Prk kinases, the yeast homologs of mammalian AAK1 BIKE/BMP2K [112]–[114], [116], [123].

The maturation of CCPs involves their growth into round, coated buds [116], [124]. The AP2 complex recruits more clathrin from the cytoplasm and clathrin assembly into the clathrin cage contributes to the energy required to bend the membrane into a vesicle [116], [124]. The accumulation of many large proteins and protein complexes on the membrane and their space requirements also contribute to membrane binding referred to as 'molecular crowding' [116], [125], [126]. Additionally, it has been shown that high concentrations of cargo proteins also support the AP2 open conformation and AP2 concentration, thereby stimulating clathrin-coat polymerization [116], [124].

The final **scission** of the narrow membrane-vesicle shaft releases the formed CCV from the PM [116]. The assembly of the large dynamin GTPase into rings and the constriction of this ring mediates this scission event [116], [127], [128]. The SRC-homology 3 (SH3) domain of BAR-domain containing proteins such as endophilin, amphiphysin and sorting-nexin 9 (SNX9), interact with dynamin via its proline-rich sequence domain [129]–[131]. These interactions recruite dynamin to the neck of the budding CCV [129]–[131]. It has been shown that dynamin ring assembly around the neck of the CCVs stimulates dynamin GTPase activity [132], which induces conformational changes in dynamin [133] and eventually buds off the formed CCV from the donor membrane [134], [135].

Figure 1.7. The list of endocytic accessory proteins and their specific functions in the CME pathway. Abbreviations: activation (A); adaptor protein complex 2 (AP2); clathrin assembly lymphoid myeloid leukemia (CALM); clathrin-coated pit (CCP); clathrin heavy chain (CHC); clathrin light chain (CLC); Dynamin (Dyn); endocytic accessory proteins (EAPs); EGF-receptor phosphorylation substrate (Eps15); Fer/Cip4 homology domain-only proteins 1/ 2 (FCHo1/2); cyclin G associated kinase (GAK); Huntingtin interacting protein-1 related (Hip1R); heat shock protein 70 kD (Hsc70); knockdown (KD); knockout (ko); mutation (M); not determined (ND); adaptin-ear-binding coat-associated protein (NECAP); neural Wiskott-Aldrich syndrome protein (N-WASP); oculocerebrorenal Lowe syndrome protein (OCRL); overexpression (OX); phosphatidylinositol 3-kinase (PI3KC2α); phosphatidylinositol phosphate (PIP); sorting nexin 9 (SNX9) [116]. The image is obtained from Metleen *et al.* 2018. The table is reprinted with the permission from Annual Reviews, provided licence number is 1214991-1.

After pinching off CCVs from their donor membranes, they are transported towards their acceptor membranes to release their cargo content [116], [119]. However, before the fusion of cargo containing vesicles with the target membrane can take place, the CCV coats have to be removed [116], [119]. Currently, there are only two molecular mechanisms known that regulates the uncoating of the CCV. These two mechanisms will be described in detail in the sections 1.8.1 and 1.8.2, respectively.

1.8. The disassembly of the CCV clathrin cage

AP2 binds to the PM PI-4,5-P$_2$ domains and recruits clathrin to the inner leaflets of the PM from the cytosol to initiate CME process. The assembly of clathrin-coat is supported by the recruitment of other coat-proteins from the cytosol. The selected cargo proteins are captured while nascent CCPs are continuing to assemble. During membrane scission stage, the neck of the CCPs is constricted and then, they pinch off from the donor PM through dynamin GTPase and actin cytoskeleton machinery. Finally, clathrin-coat has to be removed in order to fuse cargo molecule-filled vesicles with the recipient compartments and eventually they deliver their content to activate certain signaling pathways [116], [119], [136]. Furthermore, the disassembly of the CCV also liberate the endocytic machinery free for the next round of CME cycle [116], [136]. Two important molecular mechanisms have been identified to regulate the dissociation of clathrin coat from the endocytic vesicles. First mechanism involves the disassembly of clathrin-basket by the heat-shock-cognate (Hsc70) and its co-chaperons auxilin1 and GAK/auxilin2 (Section 1.8.1). Secondly, the PI-4,5-P$_2$ phosphatase Synaptojanin1 is required to support the release of AP2 from the vesicle membrane (Section 1.8.2), thereby triggering the dissociation of the CCV inner proteinaceous coat [116], [119], [136].

1.8.1. Hsc70-mediated clathrin-basket disassembly

Hsc70 is a member of 70 kDa heat-shock-protein (Hsp70) family [137], [138]. Hsp70 family proteins function as molecular chaperons and are involved in protein folding quality control processes, the repair of misfolded proteins and the solubilization of protein aggregates [139], [140]. These activities require conformational changes in Hsp70 family members, which are regulated by their ATP hydrolysis activity, ADP:ATP cycles. The family member Hsc70 has been shown to

mediate the disassembly of the clathrin-cage of CCV [137], [138]. This Hsc70 activity requires the two co-chaperones auxilin1 and GAK/auxilin2 [139], [141], [142]. Auxilin1 and GAK/auxilin2 are bound by CHC proximal legs and with Hsc70 via their J- domains [142]. The dissociation of clathrin-coat by Hsc70 and its co-chaperons are indicated in Figure 1.8. Even though auxilins-dependent Hsc70 recruitment to the uncoating CCV is well-established, the precise mechanism of Hsc70 mediated clathrin-cage disassembly is still controversial [142]. Two models are described below namely, the Brownian/Steric wedge model and the wrecking ball model for Hsc70-driven coat disassembly [140], [142].
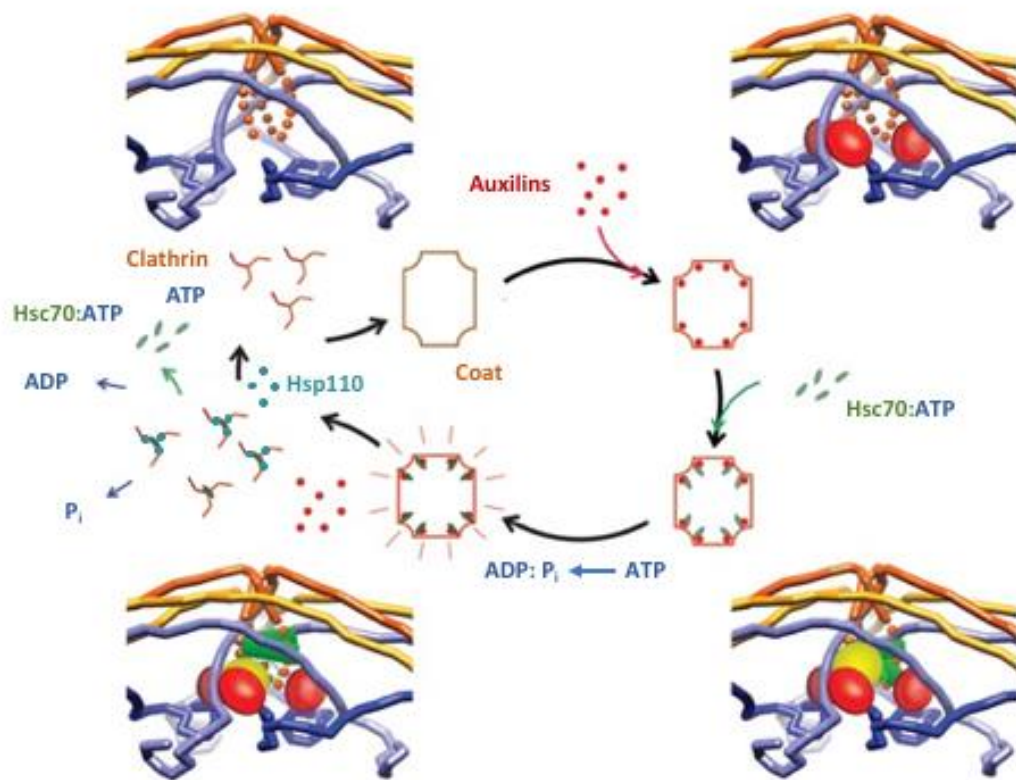
Figure 1.8. The model of CCV uncoating mechanism mediated by Hsc70 and its co-chaperons auxilin1 and GAK/auxilin2. The inner diagram indicates the Hsc70/clathrin cycle, while the four outer corner diagrams zoom in the detailed binding events at each clathrin triskelion vertex. Following the clockwise direction from the top left towards the bottom left side, auxilins (red) bind to the clathrin-coat and recruit Hsc70:ATP to the clathrin triskelia vertex (Hsc70 ATPase domain is shown in yellow and Hsc70 substrate binding domain is shown in green). Upon ATP hydrolysis and Hsc70 conformational changes, the dissociation of clathrin-cage takes place and results in the release of auxilins, clathrin:Hsc70:ADP and Pi. Hsc70 NEF, Hsp110 (turquois) exchanges ADP with ATP, which causes the dissociation of clathrin:Hsc70:ADP complex. This makes clathrin available for the next rounds of CCV formation [140]. The figure is modified from Xing Yi *et al.* 2010 and updated based on the currently reviewed model by Sousa and Lafer *et al.* 2015 [140], [143]. The original figure is reprinted with the permission from European Molecular Biology Organization provided open access Creative Commons Attribution Licence for the unrestricted re-use and reproduction of any part of the manuscript without special permission.

The **Brownian-Steric Wedge model** proposes that bound Hsc70 induces the disassembly of the clathrin-cage [140]. Xing Yi *et al.* 2010 and colleagues have suggested that clathrin-coats undergo constantly random fluctuations which are able to weaken the interactions among the CHC triskelia [140]. However, these fluctuations are never adequate to induce CHC triskelia dissociation [140]. The binding of Hsc70:ATP to CHC, just beneath each triskelion vertex, may sterically impede the reversal of these loosening fluctuations so that the legs of the triskelia are driven apart, eventually [140].

The **wrecking ball model** describes how Hsc70 itself disassembles the clathrin-cage [142], [144], [145]. Sousa *et al.* 2016 present a model in which Hsc70 does not simply shifts trsikelia-binding equilibria, like in the Brownian-Steric Wedge model, but actually Hsc70 proteins actively drive the triskelia legs apart [140], [142]. Instead, positioning of Hsc70 proteins right underneath the individual triskelia vertices by its CCV co-chaperones and by conformational changes on Hsc70 push the triskelia outwards which then pulls the triskela legs apart [142], [144], [145]. This mechanism is accompanied with Hsc70 homodimerisation, and even higher Hsc70 order complexes may be involved, whose collisions with the clathrin basket triskelia produce the force for the dissociation of the clathrin-cage [142], [144], [145]. It is still unresolved which of these two models explains the Hsc70-driven clathrin-coat dissociation best and it is also possible that both contribute to clathrin-cage dissociation [142].

After the clathrin coat disassembly process is completed, Hsc70:ADP stably binds to the clathrin triskelia. This prevents recycling of triskelia to reform the just disassembled clathrin cage [146]. It has been indicated that mutations in Hsc70 cause defects in the assembly and disassembly of CCV and eventually leads to impairments in the endocytosis process [147]. Hsc70 Nucleotide-Exchange-Factors (NEFs) regulate the association of Hsc70 with protein substrates via exchanging ADP with ATP [143], [148]. Hsp110, which also belongs to the Hsp70 protein family, is one of the most abundant NEFs in the brains of vertebrates and it is involved in the regulation of Hsc70 activity in CCV [143], [149]. The activity of Hsp110 is regulated via phosphorylation of its Ser509 residue by Casein Kinase II (CKII), which implies the

regulation of Hsc70-mediated clathrin-coat disassembly mechanism by CKII [143], [150].

1.8.2. PI-4,5-P$_2$ dephosphorylation and the dissociation of the CCV coat

The function of PI-4,5-P$_2$ in AP2 membrane binding and in CCV coat formation has been explained in the previous section 1.7 [85], [151]. Therefore, dephosphorylation of PI-4,5-P$_2$ is required for the release of AP2 from the vesicle membrane and thus the completion of CCV disassembly [151]. The Synaptojanin1 phosphatase catalyzes the dephosphorylation of PI-4,5-P$_2$ into PI-4-P and in PI [152]. Synaptojanin1 exists as a 170 kDa ubiquitious protein and as a 145 kDa brain-specific protein, with a truncated C-terminal domain [151]. Synaptojanin1 has as functional domains the N-terminal, Sac1-like domain with 4´-phosphatase activity, the central 5´-phosphatase domain and a C-terminal, proline-rich domain (PRD) acting as a protein-protein interaction domain [151]. Microscopic imaging have fluorescently tagged proteins revealed that these two isoforms are recruited to AP2 CCV just before they are pinched off from the donor PM [151]. Moreover, the accumulations of CCV and PI-4,5-P$_2$ were also observed in neurons of brain-specific Synaptojanin1 ko mice [153]. Furthermore, Synaptojanin1 depleted fibroblast cells did not contain a clathrin pool available for the formation of CCP [154]. It has been also demonstrated that impaired PI-4,5-P$_2$ metabolism is responsible for the defects in the SV endo- and exocytotic cycle in the synapses of Synaptojanin1 ko mice implying an importance of PI-4,5-P$_2$ metabolism in the regulation of SV recycling [155].

In addition to Synaptojanin1, the PI-4,5-P$_2$ phosphatase OCRL1 was also detected in the CME pathway [156] and has a role in the regulation of protein transport between EE and the TGN [157]. Immunoprecipitation experiments show the direct interaction of OCRL1 with clathrin as well as with AP2, indicating that OCRL1 may also dephosphorylate PI-4,5-P$_2$ for the uncoating of CCV [157], [158].

1.9. Alterations in protein sorting in AP1σ1B ko synapses

The AP1/σ1B encoding gene *AP1S2* is located on the X-chromosome in humans and in mice [100]. In the AG Schu lab, AP1/σ1B ko mice were produced by targeted mutation of the σ1B encoding locus [100]. AP1/σ1B ko mice replicate the disease

phenotypes of human patients with mutations in the *AP1S2* gene and thus these mice are a model organism for a severe, X-linked human mental retardation disorder [100]. The *AP1S2* gene in human patients contains a premature STOP codon. AP1/σ1B ko mice are viable and fertile, but the animals show a severe memory and learning deficiency and impaired motor coordination, like the human patients, who have delayed motor development and intellectual disabilities, requiring life-long comprehensive care [100].

Electron microscopy analysis of AP1/σ1B ko hippocampal synapses have displayed that they contain fewer SVs. Therefore, SV recycling rate was measured in AP1/σ1B ko hippocampal synapses (Figure 1.9). After the SV pool depleting stimulus, only 45 % of exocytosed SVs were recovered in AP1/σ1B ko hippocampal synapses within the first 10 secs, compared to 90 % SV recovery in wt controls. Furthermore, only 70 % of SVs were reformed in AP1/σ1B ko hippocampal synapses compared to the wt. These experiments suggested that reduced numbers of SV are caused due to slower and inefficient SV recycling [100].
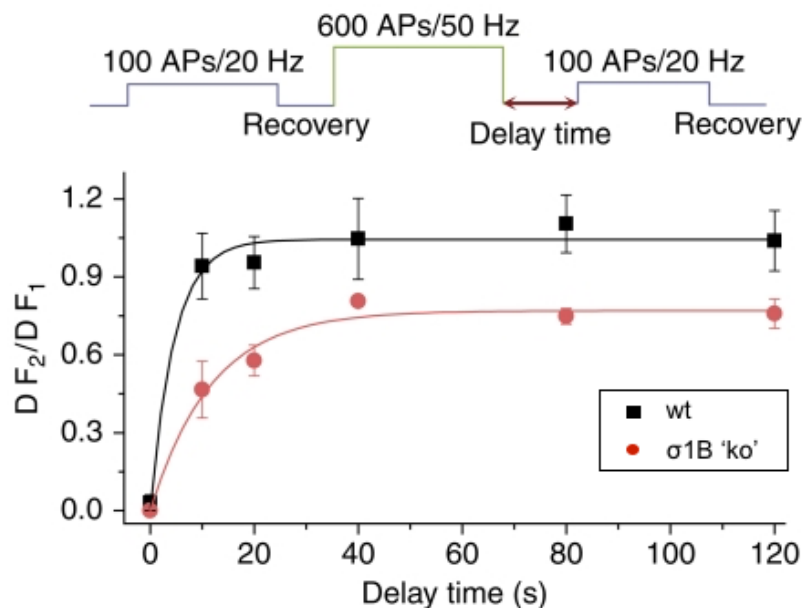
Figure 1.9. Impaired SV recycling rate in AP1/ σ 1B ko hippocampal synapses. The protocol of AP stimulation is shown above the diagram consisting of test stimulus 100 APs/20 Hz is followed by depleting stimulus 600 APs/50 Hz with respect to variable delay time for the next rounds of test and depleting stimulus. The ratio of recovered fluorescence amplitude to test stimulus fluorescence amplitude (DF_2/DF_1) is plotted over delay time. After depleting AP stimulation within the first 10 secs, approximately 45 % of exocytosed SVs were recovered in AP1/σ1B ko hippocampal synapses as compared to approximately 90 % in wt controls. The figure is adaptod from Glyvuk *et al.* 2010. [100]. The figure is reprinted with the permission from European Molecular Biology Organization provided open access Creative Commons Attribution Licence for the unrestricted use of any part of the manuscript without special permission.

The microscopic analysis also demonstrated the accumulation of enlarged endosomes and the presence of MVB endosomes as already discussed in Section 1.5. Even more surprising was the increase in CCV numbers despite decreased SV numbers and inefficient SV recycling. Therefore, they were expected to be AP1 CCV, somehow dysfunctional due to the absence of the AP1/σ1B complex. However, they turned out to be AP2 CCV [102]. The increase in synaptic AP2 CCV numbers can be explained in two ways. Firstly, it could be caused by a stimulation of AP2 CME pathway. Secondly, the life cycle of AP2 CCV can be extended and AP2 CCV may have longer life-span [85], [102]. The analysis of the synaptic AP2 CCV pools revealed the existence of two AP2 CCV classes [85]. Besides canonical AP2 CCV, which undergo fast CCV uncoating, AP2 CCV with a stabilized CCV coat and thus an extended life time were identified in wt and in AP1/σ1B ko synapses [85]. The size of both AP2 CCV classes are doubled in AP1/σ1B ko synapses and the AP2 CCV of the pool of stable AP2 CCV are even more stabilized and therefore, they were named as stCCV [85]. The changes in AP1/σ1B ko synapses are summarized in Figure 1.10.
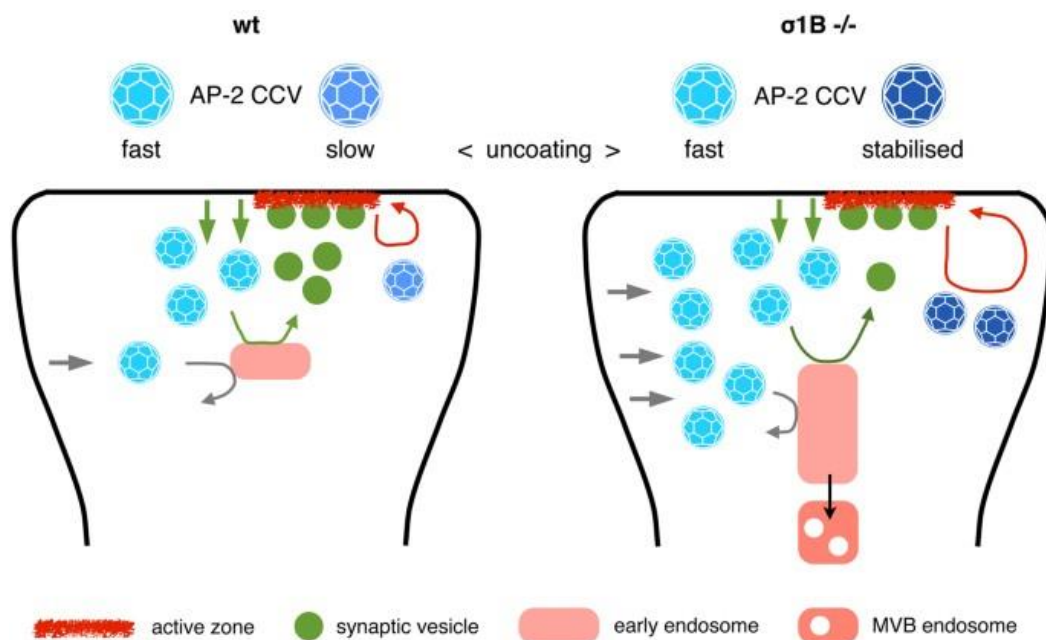
Figure 1.10. The differences between wt and AP1/σ1B ko synapses. The fast-uncoating canonical CCV (canCCV) and slow-uncoating stable CCV were shown with lighter and dark blue colors, respectively. Both AP2 CCV classes are increased in AP1/σ1B ko synapses as compared to their wt levels. The stable CCVs are even more stabilized in AP1/σ1B ko synapses thus, named as stCCV. Cartoon also summarizes the different forms of synaptic plasticity in AP1/σ1B ko synapses. Besides increase in AP2 CCVs, accumulation of enlarged EEs, activation of MVB pathway for the degradation of SV porteins and lastly the regulation of AZ plasticity via specialized AP2 CME pathway were shown in AP1/σ1B ko synapses. The figure is adapted from Candiello *et al.* 2017 [85]. The figure is reprinted with Creative Commons Attribution 4.0 International Licence allows the unrestricted use of any part of the paper without special permission.

Comparison of the coat protein composition of wt and AP1/σ1B synapses CCV revealed three molecular mechanisms underlying the enhanced stabilization of the AP2 stCCV [85]. An increase in CCV numbers was only observed in AP1/σ1B ko synapses and not in their cortex or their adipocytes, whose numbers are reduced due to impaired adipogenesis [63], [85]. Therefore, the observed alterations in AP2 CCV pathways in AP1/σ1B ko synapses represent a mechanism of synaptic plasticity [85].

1.10.   Mechanisms for AP2 stCCV formation

Three molecular mechanisms have been identified for the enhanced stabilization of AP2 CCV and stCCV formation [85]. These mechanisms influence all three layers of a CCV, firstly the outer clathrin basket layer, secondly the middle AP2 layer and finally the inner layer, the membrane phospholipid composition [85]. It has been shown that clathrin-coat disassembly protein Hsc70 levels were reduced in AP1/σ1B ko stCCV as compared to its wt stable CCV levels [85]. However, the CCV co-chapaerons of Hsc70, namely auxilin1 and GAK/auxilin2, were not decreased in AP1/σ1B ko stCCV. Apparently, they should be able to activate Hsc70 for the disassembly of clathrin-cage [85]. There must be additional yet unknown regulatory mechanisms that regulate recruitment of Hsc70 into CCV, thus delaying the clathrin-cage dissociation, which results in the extension of their life-span [85]. The second mechanism is a hyperactivation of AP2 complexes, stabilizing high-affinity AP2 membrane binding [85]. The AAK1 kinase levels and also the levels of phosphorylated AP2/μ2 adaptin are increased in stCCV [85], [113], [114], [123]. This modification induces the conformational change of the AP2 complex into its open state, which enable the binding of AP2/μ2 to additional PI-4,5-P_2 domain and as well as to cargo proteins [85], [112], [159]. Therefore, high affinity AP2-mebrane associations can be responsible for the stabilization of AP2 CCV, thereby leading to extension in their life time [85]. Thirdly, a stCCV contains with 10 % of wt stable CCV levels, only trace amounts of, the PI-4,5-P_2 phosphatase Synaptojanin1. As it was described in Section 1.8.2, Synaptojanin1 phosphatase activity is required for release of AP2 from the vesicle membrane and for the completion of clathrin-coat dissociation [151]. Therefore, the recruitment of less Synaptojanin1 into AP1/σ1B ko stCCV also enhances their stabilization [85]. The given schematic diagram summarizes three

molecular mechanisms for the enhanced stabilization and extended half-life of AP2 CCV in Figure 1.11. The regulation of Synaptojanin1 recruitment into AP2 CCV and also the regulation of Hsc70 CCV uncoating activity were studied in my thesis to reveal the novel molecular mechanisms controlling AP2 CCV life cycle.
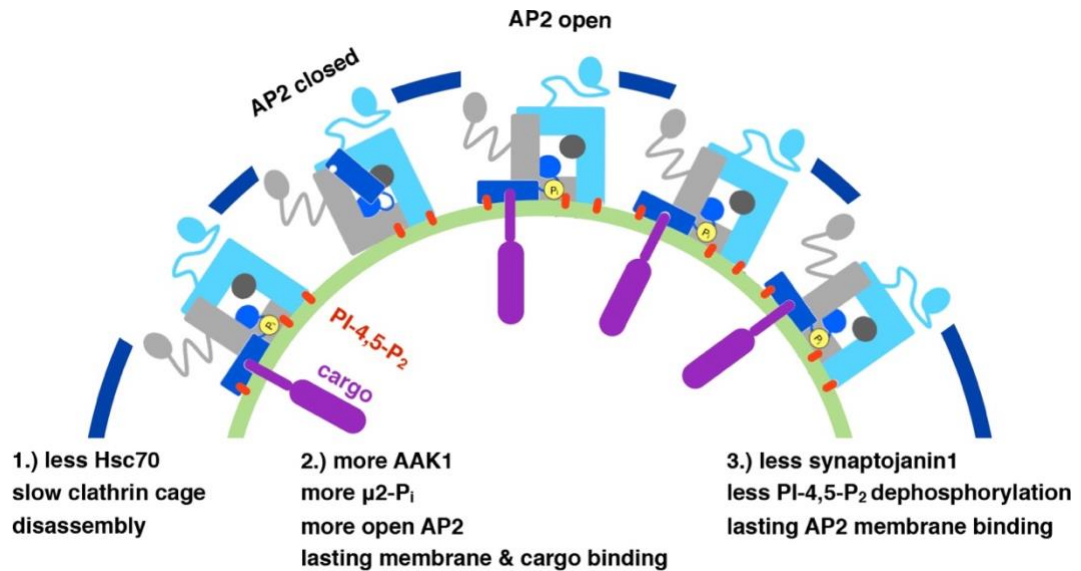
Figure 1.11. The three molecular mechanisms regulating the stabilization and extended life-span of AP2 CCV in AP1/ σ 1B. These mechanisms affect all three layers of a CCV: firstly the outer clathrin basket layer, secondly the middle AP2 layer and thirdly the inner layer vesicle membrane phospholipid composition. The figure is sketched based on the published data in Candiello *et al.* 2017 [85], courtesy of Prof. Peter Schu.

1.11. Functions of AP2 stCCV in synaptic protein sorting

A major question about the function(s) of stCCV, and eventually of wt stable CCV, in synaptic protein sorting remains to be answered. In a recent publication of the AG Schu, Candiello *et al.* 2017, it has been shown that wt stable AP2 CCV and the stCCV make up 15% of the total synaptic AP2 CCV pool [85]. The cargo proteins specifically enriched in stCCV point out their specific functions in the regulation of synaptic plasticity [85]. Candiello *et al.* 2017 and his colleagues have shown that structural active zone (AZ) proteins Git1 and Stonin2 were enriched in AP1/σ1B ko stCCV as compared to their wt stable CCV levels [85]. Morever, Munc13 isoforms, an AZ protein, which takes part in the regulation of SV fusion at presynaptic AZs [160], [161], were differentially recruited into AP2 CCV [85]. All these recent findings offer a novel molecular mechanism for the regulation of AZ plasticity via this specialized AP2 CME pathway [85]. Therefore, it can be concluded that this AP2 CME pathway does not simply mediate the uptake of numerous cargo proteins to be transported into

cellular compartments, but also regulates synaptic PM protein composition as a form of synaptic plasticity in AP1/σ1B ko synapses [85].

1.12. Aims of the study

In this study, three goals are aimed at to be reached. The first question to be answered is about the molecular mechanisms regulating the CCV levels of Synaptojanin1. The second question to be answered is about the molecular mechanisms regulating the clathrin-cage disassembly activity of Hsc70. Thirdly, it is also intended to determine the stCCV specific cargo proteins and thus to identify functions of these specialized AP2 stCCV in synaptic plasticity. Depending on the progress of these three project parts, also the mechanism regulating AAK1 recruitment and activity is also studied.

The analysis of the molecular mechanism that determine the amount and activity of Synaptojanin1 had been started by my predecessor. After I learned the biochemical experimental techniques and data quantification approach, I joined to this project and completed the experiments. It had been a widely accepted view in the field that Synaptojanin1 is recruited to CCV by Endophilin A1, which is recruited just prior to the membrane scission event [162], [163]. The Endophilin A1 BAR-domain binds preferably to highly curved membranes, like the shaft of the budding CCV [162]. Therefore, the levels of Endophilin A1 were compared between wt and AP1/σ1B ko cellular fractions by previous PhD students in the AG Schu lab. They showed that the levels of Endophilin A1 are reduced down to 50 % of wt stable CCV levels in AP1/σ1B ko stCCV [85]. This reduction does not match with the reduction in the Synaptojanin1 levels, which was 10 % of wt stable CCV levels in AP1/σ1B ko stCCV [85]. Therefore, the obtained results suggest that Endophilin A1 does not determine the amount of Synaptojanin1 in stCCV and thus in AP2 CCV in general [85]. However, modifications of Endophilin A1 can change the mode of its association with the budding CCV, from membrane to protein binding, and this might impair its ability to recruit Synaptojanin1 [164]. Such a modification on Endophilin A1 is its BAR-domain phosphorylation by the Leucine-rich-repeat kinase 2 (LRRK2) [165]. So, I started this project with the analysis of the CCV levels of LRRK2 and of putative CCV class specific differences in LRRK2 catalytic activity [164]. After I could rule out a

participation of LRRK2 and thus of Endophilin A1, I started to analyse the distribution of additional CCV proteins known to also interact with Synaptojanin1 [164]. After the completion of this project, the paper Mishra *et al.* 2021 was published in Scientific Report-Nature journal with me as a co-author.

Secondly, I started to analyze the molecular mechanisms regulating Hsc70 activity in clathrin-cage disassembly. My predecessors in this project had already shown that the levels in the Hsc70 co-chaperones auxilin1, GAK/auxilin2 and also in the pre-synapse specific CCV chaperone CSPα are not altered in a way, that they could be accepted as the regulators of the Hsc70-mediated increased stability of stCCV [85], [102]. Therefore, I started to analyze the synapse and CCV levels of other proteins known to regulate and to interact with Hsc70 including its NEF Hsp110 and its co-worker, Hsp90 in many cellular peocesses. Moreover, the post-translational modifications, specifically phosphorylation, on Hsc70 are investigated whether playing a role in the formation of stCCV. Proceeding analysis leads to the identification of hypo- and hyper-phosphorylated Hsc70 proteins in wt and AP1/σ1B ko synaptic CCVs. Additionally, the inhibition of Hsc70 dimerization, thereby its activity, due to the association(s) of different Hsc70 phosphorylation patterns with CaM/Ca^{2+} and/or CaM was also tested to elucidate the reason why stCCV contains less Hsc70. Furthermore, I also compare the CCV specific kinases including CVAK104, CK2, DYRK1A, ACK1, CaMK-IIδ, DCLK1, SPAK/CAB39, STK38S and STK38L and phosphatase including PP2A regulatory domains PP2R2B and PP2R2C profiles between wt-ko synapses to identify the putative mechanism regulating AP2 CCV life cycle and its stabilization. Furthermore, I also compared the association of several kinases and phosphatases with CCV, because it has been published that coat protein phosphorylation patterns are altered during the CCV life cycle.

Previous analysis of AP2 CCV coat composition discovered AZ scaffolding protein Git1 and its CCV co-adaptor protein Stonin2 as specific cargo proteins of the AP2 stCCV pathway, suggesting their sorting via stCCV affects AZ and synapse plasticity [85]. More cargo proteins should be identified in order to develop a model for the functions of the AP2 stCCV pathway in synaptic plasticity. The analysis of Hsc70 interacting proteins led me to compare the levels of several neuronal cell adhesion molecules (NCAMs), between wt and ko synaptic CCV as well as between

their synapses and cortices. Overall, our experimental aims are not only intended to give rise to better understandings of the molecular mechanisms regulating the AP2 CCV life cycle and their enhanced stabilization, but also to elucidate the novel functions of AP2 CME pathway in synaptic plasticity.

CHAPTER 2

2. MATERIALS AND METHODS

2.1. Materials

2.1.1. Lab equipments and machines

Table 2.1. Lab equipments and machines

Equipment and machines	Manufacturing companies
Agarose gel electrophoresis system	Bio-Rad, Germany
Bachofer Speed Vac Concentrator, SVC-100H	Savant, Germany
Beckman Coulter Optima MAX-XP Ultracentrifuge (TLA55)	Beckman Coulter, US
Beckman Coulter Optima L-90K Ultracentrifuge (SW60-Ti)	Beckman Coulter, US
Cell homogenizor	Isobiotech, Germany
Electrophoresis power supply	GE Healthcare, Sweden
Eppendorf 5424-R centrifuge	Eppendorf, Germany
Eppendorf 5417-R centrifuge	Eppendorf, Germany
Eppendorf thermomixer comfort	Eppendorf, Germany
Epson Perfection V850 Pro	SilerFast, Germany
Glass tissue homogenizer potter (2 ml)	Wheaton®, US
LAS-300 luminescent image analyzer	FujiFilm, Japan
NanoDrop One	Thermo Scientific, Germany
Gradient station IP	BioComp Instruments, Canada
SDS PAGE mini-gel systems	Bio-Rad, Germany
Sonicator W-220F cell disrubter	Heat Systems Ultrasonics Inc, Canada
Western blot wet transfer system	Bio-Rad, Germany
PCR Labcycler gradient	SensoQuest, Germany
Vortex-Genie 2 mixer	Scientific Industries, Inc., US
UV transilluminator for agarose gel documentation	Biometra, Germany
Mass Spectrometer ultrafleXtreme™ MALDI-TOF/TOF Systems	Brucker, US

2.1.2. Buffers and solutions

SDS Running Buffer (10x stock solution)

Components	Amount	Supplier/distributors
0.25 M Tris	151 g	CARL ROTH GmbH, Germany
1.924 M Glycine	720.5 g	CARL ROTH GmbH, Germany
0.1% Sodium dodecyl sulfate (SDS)	50 g	CARL ROTH GmbH, Germany

The volume of the solution is completed to 5 liter with with ddH_2O.

Running Gel Buffer

Components	Amount	Supplier/distributors
1.5 M Tris	60.57 g	CARL ROTH GmbH, Germany
0.4 % Sodium dodecyl sulfate (SDS)	4 g	CARL ROTH GmbH, Germany

1.5 M Tris and 0.4% SDS were dissolved in ~800 ml ddH_2O. After pH was adjusted to 8.8 with HCl, the total volume was completed to 1 liter with ddH_2O.

Stacking Gel Buffer

Components	Amount	Supplier/distributors
0.5 M Tris	181.7 g	CARL ROTH GmbH, Germany
0.4 % Sodium dodecyl sulfate (SDS)	4 g	CARL ROTH GmbH, Germany

0.5 M Tris and 0.4% SDS were dissolved in ~800 ml ddH_2O. After pH was adjusted to 6.8 with HCl, the total volume was completed to 1 liter with ddH_2O.

Anode buffer recipe (2x stock solution)

Components	Amount	Supplier/distributors
150 mM Tris	18.2 g	CARL ROTH GmbH, Germany
40 % Methanol	400 ml	CARL ROTH GmbH, Germany
HCl fuming 37 %	adjust pH 7.4	CARL ROTH GmbH, Germany

After the pH is adjusted to pH 7.4 with HCl, the volume is completed to 1 liter with ddH_2O.

Cathode buffer recipe (2x stock solution)

Components	Amount	Supplier/distributors
40 mM Tris	4.8 g	CARL ROTH GmbH, Germany
80 mM 6- Aminocaproic Acid	10.5 g	CARL ROTH GmbH, Germany
40 % Methanol	400 ml	CARL ROTH GmbH, Germany
HCl fuming 37 %	adjust pH 9	CARL ROTH GmbH, Germany

After the pH is adjusted to pH 9 with HCl, the volume is completed to 1 liter with ddH_2O.

Wet transfer buffer (10x stock solution)

Components	Amount	Supplier/distributors
0.25 M Tris	30.3 g	CARL ROTH GmbH, Germany
1.924 M Glycine	144 g	CARL ROTH GmbH, Germany

After Tris and Glycine are first dissolved in ~800 ml ddH_2O, total volume is completed to 1 liter with ddH_2O. The 10x stock solution is stored at room temperature.

Wet transfer buffer (1x transfer buffer)

Components	Amount	Supplier/distributors
10x Wet transfer buffer	100 ml	
20 % Methanol/Ethanol	200 ml	CARL ROTH GmbH, Germany

After mixing 10x transfer buffer and methanol, the total volume is completed to 1 liter with ddH_2O. The 1x transfer buffer is stored at 4 °C till transfer process.

Coomassie brilliant blue (CBB) staining solution

Components	Amount	Supplier/distributors
10 % (v/v) orthophosphoric acid	100 ml	Merck, Germany
45 % (v/v) Ethanol	450 ml	CARL ROTH GmbH, Germany
0.125 % (w/v) CBB G-250	1.25 g	CARL ROTH GmbH, Germany

To the glass measure, 450 ml ddH_2O is put. Then, orthophosphoric acid, Ethanol and CCB are added and stirred with magnetic fish till obtaining homogenous staining solution.

Destaining solution

Components	Amount	Supplier/distributors
5 % (v/v) orthophosphoric acid	50 ml	Merck, Germany
40 % (v/v) Ethanol	400 ml	CARL ROTH GmbH, Germany

To the glass measure, 550 ml ddH_2O is put. Then, orthophosphoric acid and Ethanol is added and destaining solution is mixed properly with magnetic stirrer.

Fixation solution I

Components	Amount	Supplier/distributors
10 % (v/v) orthophosphoric acid	100 ml	Merck, Germany
40 % (v/v) Methanol	400 ml	CARL ROTH GmbH, Germany
10 % (v/v) Ethanol	100 ml	CARL ROTH GmbH, Germany

To the glass measure, 400 ml ddH_2O is put and orthophosphoric acid, Methanol and Ethanol are added. The solution is mixed properly with magnetic stirrer.

Fixation solution II

Components	Amount	Supplier/distributors
1 % (v/v) orthophosphoric acid	10 ml	CARL ROTH GmbH, Germany
10 % (w/v) ammonium sulfate	100 g	CARL ROTH GmbH, Germany

To the glass measure 990 ml ddH$_2$O is put. Then, orthophosphoric acid and ammonium sulfate are added and the solution is mixed properly with magnetic stirrer.

6X Laemli buffer for loading proteins for SDS-PAGE gels

Components	Amount	Supplier/distributors
750 mM Tris	9.09 g	CARL ROTH, Germany
9 % SDS	9 g	CARL ROTH, Germany
60 % Glycerol	60 ml	Sigma Aldrich, Germany
0.15 % Bromophenol blue	0.15 g	Merck, Germany
HCl fuming 37 %	adjust pH 6.8	CARL ROTH, Germany
6 % 2-mercaptoetnanol	60 µl in 1ml 6x loading dye aliquot	CARL ROTH, Germany

The volume of the 6x loading dye solution is completed to 100 ml with ddH$_2$O and 60 µl 2-mercaptoethanol was added in 1 ml 6x loading dye aliquot prior to use.

Tris Buffered Saline (TBS) (20x stock solution)

Components	Amount	Supplier/distributors
0.4 M Tris	242 g	CARL ROTH GmbH, Germany
1.24 M NaCl	362.5 g	AppliChem, Germany
HCl fuming 37 %	adjust pH 7.5	CARL ROTH GmbH, Germany

After the pH is adjusted to pH 7.5 with HCl, the volume is completed to 5 liter with ddH$_2$O.

Tris Buffered Saline with Tween (TBST)

Components	Amount	Supplier/distributors
20 mM Tris	12.1 g	CARL ROTH GmbH, Germany
62 mM NaCl	18.1 g	AppliChem, Germany
0.05 % Tween 20	5 ml	AppliChem, Germany

250 ml 20x TBS is diluted by completing the total volume to 5 liter with ddH$_2$O and 5 ml 0.05 % Tween 20 is added into the solution and is stirred to dissolve it in the solution properly.

Mild Stripping Buffer

Components	Amount	Supplier/distributors
1.5 % Glycine	15 g	CARL ROTH GmbH, Germany
0.1 %SDS	1 g	Serva GmbH, Germany
1 % Tween 20	10 ml	AppliChem, Germany

After the pH is adjusted to pH 2.2 with HCl, the volume is completed to 1 liter with ddH$_2$O.

Non-Fat Dry Milk (NFDM) Blocking Buffer

Components	Amount	Supplier/distributors
5 % NFDM	5 g	Frema Reform GmbH, Germany

5 g NFDM is dissolved in 100 ml 1x TBST to block the membranes for Western blotting.

Bovine Serum Albumin (BSA) Blocking Buffer

Components	Amount	Supplier/distributors
5 % BSA (Albumin Fraction V)	5 g	CARL ROTH GmbH, Germany

5 g BSA is dissolved in 100 ml 1x TBST to block the membranes for Western blotting.

Enhanced Chemiluminescence (ECL) Detection kits

Kits	Supplier/distributors
SuperSignal^{TM} West Pico Plus Chemiluminescence Substrate	Thermo Fisher Scientific, USA
SuperSignal^{TM} West Femto Plus Chemiluminescence Substrate	Thermo Fisher Scientific, USA
SuperSignal^{TM} West Dura Plus Chemiluminescence Substrate	Thermo Fisher Scientific, USA

Phosphate-Buffered Saline (PBS) (10x Stock Solution)

Components	Amount	Supplier/distributors
1.4 M NaCl	81.8 g	AppliChem, Germany
25 mM KCl	1.86 g	CARL ROTH GmbH, Germany
65 mM Na_2HPO_4	9.2 g	CARL ROTH GmbH, Germany
15 mM KH_2PO_4	2.04 g	CARL ROTH GmbH, Germany

After the pH is adjusted to pH 7.4-7.5 with HCl, the volume is completed to 1 liter with ddH_2O.

Phosphate-Buffered Saline (PBS)

Components	Amount	Supplier/distributors
140 mM NaCl	8.18 g	AppliChem, Germany
2.5 mM KCl	0.186 g	CARL ROTH GmbH, Germany
6.5 mM Na_2HPO_4	0.92 g	CARL ROTH GmbH, Germany
1.5 mM KH_2PO_4	0.2 g	CARL ROTH GmbH, Germany

100 ml 10x PBS is diluted in 900 ml ddH_2O to prepare 1x PBS solution.

Trypsin-EDTA (0.05 %)

Components	Amount	Supplier/distributors
Trypsin	0.5 g/L	Gibco Invitrogen, Germany
EDTA	0.2 g/L	Gibco Invitrogen, Germany

Clathrin coated vesicle (CCV) isolation buffer (10x stock solution)

Components	Amount	Supplier/distributors
10 mM MES	0.976 g	AppliChem, Germany
0.5 mM EGTA	0.0951 g	Sigma Aldrich, Germany
0.5 mM $MgCl_2$	0.024 g	Merck, Germany
1 mM $NaNO_3$	1 µl	Sigma Aldrich, Germany
10 mM NaF	10 ml	Sigma Aldrich
10 nM Calyculin A	500 µl	Abcam, UK

After 10 mM MES, 0.5 mM EGTA and 0.5 mM $MgCl_2$ are dissolved in ddH_2O, pH is adjusted to 6.4 for the stabilization of isolated CCVs. Then, 1 mM $NaNO_3$, 10 mM NaF, 10 nM Calyculin A are added and total volume is completed to 50 ml with ddH_2O.

Clathrin coated vesicle (CCV) isolation buffer (1x CCV buffer)

Components	Amount	Supplier/distributors
10x CCV buffer	50 ml	
320 mM Sucrose	54.7 g	CARL ROTH GmbH, Germany
Complete EDTA free Protease inhibitor cocktail (PIC)		Roche, Germany

10x CCV buffer is diluted in ~400 ml ddH_2O and 320 mM sucrose (54.7 g in 500 ml) is dissolved. The volume is completed to 500 ml with ddH_2O. CCV buffer is aliquoted into falcons and prior to use for isolation 5 PIC tablets are dissolved in each 50 ml 1x CCV buffer.

Cell culture medium

Components	Amount	Supplier/distributors
Dulbecco´s Modified Eagle Medium (DMEM)	4.5 g/L	Gibco Invitrogen, Germany
10 % Fetal Calf Serum (FCS)	0.1 g/L	PAN, Germany
1 % Penicilin/Streptomycin (100x solution)	100 µl	Gibco Invitrogen, Germany
1 % Glutamine (100x solution)	100 µl	Gibco Invitrogen, Germany

Freezing medium

Components	Amount	Supplier/distributors
Dulbecco´s Modified Eagle Medium (DMEM)	4.5 g/L	Gibco Invitrogen, Germany
10 % Fetal Calf Serum (FCS)	0.1 g/L	PAN, Germany
1 % Penicilin/Streptomycin (100x stock solution)	100 µl	Gibco Invitrogen, Germany
1 % Glutamine (100x stock solution)	100 µl	Gibco Invitrogen, Germany
5 % Dimethyl sulfoxide (DMSO)	50 ml	Merck, Germany

2.1.3. Chemicals

Table 2.2. List of chemicals

Chemicals	Catalog number	Supplier/distributors
Acetonitrile gradient grade for liquid chromatography LiChrosolv® Reagent	1000302500	Merck, Germany
Amersham Protran 0.45 µm pore size nitrocellulose Western blotting membranes	GE 10600003	GE Healthcare, Sweden
Ammonium bicarbonate, ReagentPlus® ≥ 99.0%	A6141	Sigma-Aldrich, Germany
Ammonium sulfate (99.5 %) powder	3746.1	CARL ROTH GmbH, Germany
6-Aminocaproic acid	A2504-100 g	CARL ROTH GmbH, Germany
Agarose NEEO ultra quality	2267.3	CARL ROTH GmbH, Germany
Bovine Serum Albumin (BSA)	A6003-100 g	Sigma-Aldrich, Germany
Calmodulin agarose beads (CABs)	A6112-5 ml	Sigma-Aldrich, Germany
Complete proteinase inhibitor cocktail tablets	45148300	Roche, Germany
Coomassie brilliant blue (CBB) G-250	9598.2	CARL ROTH GmbH, Germany
Dimethyl sulfoxide (DMSO)	1.02952.1000	Merck, Germany
1,4-dithiothreitol	6908.2	CARL ROTH GmbH, Germany
DMEM High Glucose w/sodium pyruvate	DMEM-HPSTA	Copricorn Scientific
EDTA disodium salt solution	1E23.1	CARL ROTH GmbH, Germany
EGTA	3054.2	CARL ROTH GmbH, Germany
Ethanol	9065.4	CARL ROTH GmbH, Germany
Fetal Bovine Serum	SG30070.03	Hyclone laboratories
Glycine	3187.4	CARL ROTH GmbH, Germany
HEPES	HN78.3	CARL ROTH GmbH, Germany
Hygromycin B	10687010	Invitrogen, Germany
Instant skimmed milk powder	0202V01	Frema, Germany
Iodoacetemide (IAM)	A3221-56 mg	Sigma-Aldrich, Germany
Methanol	4627.5	CARL ROTH GmbH, Germany
MES sodium salt, 3-N-morpholino propanesulfonic acid (MOPS)	6979.4	CARL ROTH GmbH, Germany

Nonidet^{TM} P 40 (NP40) detergent	74385-1L	Sigma-Aldrich, Germany
Orthophosphoric acid (85 %)	1.00563.1000	Merck, Germany
Potassium chloride (KCl)	6781.1	CARL ROTH GmbH, Germany
Potassium hydroxide (KOH)	6751.1	CARL ROTH GmbH, Germany
2-Propanol	6752.4	CARL ROTH GmbH, Germany
Precision plus protein All blue Prestained Protein Standards	1610372	Bio-Rad, Germany
Proteinase K	7528.2	CARL ROTH GmbH, Germany
Protein G Sepharose 4 fast flow beads	GE17-0618-05	GE Healthcare, Sweden
Puromycin	ant-pr-1 100 mg	Invivogen, Germany
Rotiphorese ® Gel 30 (37, 5:1) Acrylamide/Bisacrylamide	2029.1	CARL ROTH GmbH, Germany
Roti ® Quant 5x Bradford	K015.1	CARL ROTH GmbH, Germany
SDS pellets	CN30.3	CARL ROTH GmbH, Germany
Sequencing Grade Modified Trypsin	V5111	Promega, Germany
D (+) saccharose	9286.2	CARL ROTH GmbH, Germany
Tag Man ® Universal PCR Master Mix	4304437	Applied Biosystems
N,N,N′,N′- Tetramethylethylene-1,2-diamine (TEMED)	2367.1	CARL ROTH GmbH, Germany
Trifluoroacedic acid, peptide synthesis grade	15820273	Applied Biosystems^{TM}, US
Tris	5429.2	CARL ROTH GmbH, Germany
Triton ® X-100	1.08643.1000	Merck, Germany
TRIzol ® Reagent	15596018	Ambion
Tween ® 20	9127.2	CARL ROTH GmbH, Germany
0.05 % Trypsin-EDTA	25300-054	Gibco, Germany
Urea	3941.1	CARL ROTH GmbH, Germany
Wattman blotting filter paper sheets	FT-2-519-580600N (580XX699 mm)	Sartorious Stedim, Biotech, Germany
Zinc chloride	208086	Sigma-Aldrich, Germany

2.1.4. Primary antibodies

Table 2.3. List of primary antibodies for Western blot experiments

Antibody	Species	Source	Dilution ratio
Anti-ACK1 (TNK2)	Rabbit	Proteintech, 14304-1-AP	1:1000
Anti-α-adaptin (AP2)	Mouse	BD Biosciences, BD 610502	1:1000
Anti-γ1-adaptin (AP1)	Mouse	BD Biosciences, BD 610386	1:1000
Anti-ArhGEF7	Rabbit	GeneTex, GTX55517	1:1000
Anti-Auxilin (DNAJC6)	Rabbit	Proteintech, 21941-1-AP	1:1000
Anti-Auxilin2/GAK	Rabbit	Santa Cruz Biotechnology, sc-7864	1:500
Anti-CAB39 (MO25α)	Rabbit	Bioss Antibodies, bs-3636R	1:1000
Anti-Calmodulin	Mouse	Merck Millipore NP_008819	1:1000
Anti-CHL1	Goat	R&D Systems, AF2127	1:1000
Anti-CK2β	Rabbit	Origene, AP06515PU-N	1:500
Anti-CVAK104 (SCYL2)	Rabbit	Antibodies, ABIN6567812	1:500
Anti-DCLK1	Rabbit	Proteintech, 21699-1-AP	1:1000
Anti-Dynamin123	Mouse	Synaptic Systems, SySy 115 002	1:1000
Anti-DYRK1A	Rabbit	Cell Signaling Technology, 2771	1:1000
Anti-Endophilin A1	Rabbit	Synaptic Systems, SySy 159002	1:1000
Anti-Epsin1	Rabbit	Abcam, ab75879	1:500
Anti-Eps15	Mouse	BD Biosciences, BD 610806	1:1000
Anti-Eps15L1	Rabbit	Biorbyt, orb156764	1:500
Anti-Hsc70	Mouse	Synaptic Systems, SySy 149011	1:1000
Anti-Hsp90α	Rabbit	Bioss Antibodies, BS10100R	1:1000
Anti-Hsp110	Mouse	BD Biosciences, BD 610510	1:1000
Anti-Intersectin1 (ITSN1)	Mouse	BD Biosciences, BD 611574	1:1000
Anti-LRRK2	Rabbit	Novus Biologicals, NB300-268	1:1000
Anti-LRRK2 Ser935-Pi	Rabbit	Abcam, ab133450	1:1000
Anti-NCAM1	Mouse	Origene, TA323611	1:1000
Anti-Neurocan	Rabbit	Origene, TA322754	1:1000
Anti-NrCAM	Mouse	Origene, AM60049PU-N	1:1000
Anti-Pacsin1	Rabbit	Synaptic Systems, SySy 196002	1:1000
Anti-Pacsin1 Ser346-Pi	Rabbit	Merck Millipore, ABS39	1:1000
Anti- PTPTZ1	Rabbit	Origene, TA314410	1:500
Anti-PPP2R2B	Rabbit	Proteintech, 13123-1-AP	1:1000
Anti-PPP2R2C	Rabbit	Proteintech, 12747-1-AP	1:1000
Anti-Sgip1	Rabbit	Acris, AP53888PU-N	1:1000
Anti-STK38S (NDR1)	Mouse	Origene, AM31888PU-N	1:1000
Anti-STK38L (NDR2)	Mouse	Origene, TA505176	1:1000
Anti-Synaptojanin1	Rabbit	Synaptic Systems, SySy 159002	1:300
Anti-SynCAM1	Goat	Origene, AP21519PU-N	1:500

2.1.5. Secondary antibodies

Table 2.4. List of secondary antibodies for Western-blot experiments

Antibody	Species	Source	Dilution ratio
Anti-mouse HRP	Goat	Dianova, GtxMU-003-DHPRX	1:10000
Anti-Rabbit	Goat	Dianova, 11-035-045	1:10000
Anti-Goat	Rabbit	Jackson ImmunoResearch Laboratories, INC. 305-035-003	1:5000

2.1.6. Mouse embryonic fibroblasts cell lines

Table 2.5. The mouse embryonic fibroblasts cell lines used for cell culture experiments

Cell lines	Genetics background	Source
MEF S1B111 D5	AP1/σ1B +/+	AG Schu (Glyvuk *et al.* 2010)
MEF S1B111 E8	AP1/σ1B -/-	AG Schu (Glyvuk *et al.* 2010)
MEF 24A	AP1/µ1A-/-::µ1A cDNA	AG Schu (Meyer *et al.* 2000)
MEF 24	AP1/µ1A-/-	AG Schu (Meyer *et al.* 2000)

2.2. Methods

2.2.1. Subjects

The AP1/σ1B knock-out (ko) mice were generated via homologous recombination by targeting the X-chromosomal σ1B locus to exchange the endogenous wild-type (wt) gene sequence with the mutated gene insertion as described in Glyvuk *et al.* 2010 [100]. Isogenic +/+ wt mice and AP1/σ1B ko -/- mice are generated from heterogeneous +/- matings in order to establish mice colonies and also conduct tissue isolations for animal experiments. Both established wt and AP1/σ1B ko mice lines are kept in the central animal facility of the faculty of medicine in Georg-August University Göttingen by following the ethical guidelines. Mice are euthanized with CO_2 and subsequent cervical dislocation. The etchical guidelines and protocols for animal housing and sacrification were approved by the Niedersächsisches Landesamt für Verbraucherschutz und Lebensmittelsicherheit´ (LAVES). Brains were dissected from 4-6 mounts-old wt and AP1/σ1B ko animals in the late afternoon, were snap frozen in liquid nitrogen and were stored at -80 °C till further cortex, synaptosome and synaptic CCVs protein extraction processes.

2.2.2. Brain subfractionation

2.2.2.1. Extraction of proteins from mice cortices

Proteins were isolated from wt and AP1/σ1B ko mice brains in parallel at the same day in order to take into account unavoidable variations in the sample preparation. The frozen brains were thawed on ice. After the cerebellum has been removed, cerebral cortex was chopped into small pieces via scalpel in 1 ml CCV buffer in a petri-dish. The entire dish content was transferred in to a glass potter with additional 1 ml CCV buffer. The minced cortex was homogenized first using a 'loose' piston (~20 strokes) until there were no tissue particles visible. Then a 'tight' piston is used until the heavy resistance was defeated (~40 strokes). Homogenized cortices were transferred into 2 ml eppendorf tubes, and were centrifuged at 3300 rpm (1000x g) for 10 minutes at 4^0 C. The supernatant (S1) was transferred into a new 2 ml Eppendorf tube and stored on ice. The pellet (P1) was dissolved in ~1 ml CCV buffer and again centrifuged at 3300 rpm (1000x g) for 10 minutes at 4^0 C. The supernatant S2 was added to the S1, and P2 was discarded. The protein concentrations were determined with Bradford Assay (ROTI® Quant, K015.1, Roth, Germany). The protein concentrations of cortex proteins were normalized and were incubated with reducing SDS-PAGE loading buffer including dye for 5 min at 95^0 C. Protein solutions were stored at -20 ^{0} C until they are used in further semi-quantitative Western-blot experiments.

2.2.2.2. Isolation of synaptosomes from crude cortex extracts

Synaptosomes are isolated, sealed pre- and post-synaptic terminals, which lack axons and dendrites [166]. Synaptosomes were isolated from the crude cortex homogenates (as described in Section 2.2.2.1) through differential centrifugation. Pooled S1 and S2 cortex homogenates were centrifuged at 9200x g (9800 rpm) for 15 min at 4^0 C. After centrifugation, the supernatant was discarded and the pellet was dissolved in 1.5 ml CCV buffer. Next, this resuspended pellet was centrifuged at 10200x g (10400 rpm) for 15 minutes at 4^0 C. After centrifugation, the supernatant was discarded and the pellet was resuspended in 600-800 µl CCV buffer. The concentrations of the synaptosomes were normalized, they were incubated with

reducing loading dye for 5 min at 95 °C and stored at -20^0 C freezer till they were analyzed in further semi-quantitative Western-blot experiments.

2.2.2.3. Isolation of synaptic Clathrin-coated vesicles from synaptosomes

Clathrin-coated vesicles (CCV) are isolated from synaptosomes. The clathrin-coat of a CCV is not stable at the physiologic pH of 7.4 *in-vitro* and undergoes more rapid disassembly at slightly higher pH values. The clathrin cage is stabilized at the slightly acidic pH of 6.4 [40], [85]–[88], [167]. The isolated synaptosomes (as described in section Section 2.2.2.2) were lysed using a steel ball cell homogenizer (Isobiotech, Heidelberg, Germany). The gap width used was 12 µm and synaptosomes were lysed by 40 passages. The lysed synaptosomes were transferred into 1.5 ml Beckman Eppendorf microcentrifuge tubes and centrifuged at 25.000 x g for 20 min at 4°C (Beckman Coulter Optima MAX-XP Ultracentrifuge, rotor TLA55, US). The supernatant was disposed and the pellet was resuspended in 550 µl CCV buffer. The protein concentration of the synaptosomal membranes was determined using the Bradford Assay (ROTI® Quant, K015.1, Roth, Germany). The protein concentration of each sample was adjusted to 2-3 µg/µl in a total volume of 600 µl and loaded onto a 20-50 % sucrose density gradient. The 20 % and 50 % sucrose solutions were prepared in CCV buffer. Firstly, 1.75 ml ice-cold 50 % sucrose solution was added into SW60 Ti centrifuge tubes and then 1.75 ml ice-cold 20 % sucrose solution was added on top of 50 % sucrose, slowly in order not to disrupt the interphase between them. Afterwards, 20-50 % continuous sucrose gradient was prepared by mixing the solutions using a density gradient machine (Gradient Station IP, Biocomp, Canada). The 500 µl normalized synaptosomal membrane samples were loaded onto the continuous 20-50 % sucrose density gradient and centrifuged (Beckman Coulter Optima L-90K Ultracentrifuge, SW60-Ti rotor, US) at 33.000 x g for 1.5 hours at 4°C. The 4 ml of the total tube volume was fractionated into 10 fractions, 400 µl each. CCV were enriched in fractions 6-9 [85] and were combined into Eppendorf tubes.

2.2.2.4. Immunoisolation of stabilized CCV

The synaptic CCV purified by density gradient centrifugation (as described in Section 2.2.2.3) were used for the immunoisolation of the subpopulation of stabilized CCV. Hsc70 is responsible for the disassembly of the clathrin-cage and it is recruited

to the clathrin-basket by its co-chaperons auxilin1 and GAK/auxilin2. Hsc70 has to undergo ATP hydrolysis, which triggers collision pressure, thereby leading to the dissociation of clathrin lattice. Hsc70:ADP binds to additional sites on the clathrin-coat in a more stable and promiscuous manner [142]. Immunoprecipitation is performed with the anti-Hsc70 antibody (mouse monoclonal anti-Hsc70 antibody from Synaptic Systems, Goettingen, Germany). The anti-Hsc70:CCV complexes are isolated with protein G sepharose beads (Protein G sepharose 4 Fast Flow, GE Healtcare, Uppsala, Sweden). The stable CCV isolated from wt synaptosomes are called as wt stable CCV, whereas the stabilized and thus longer lived CCV of AP1/σ1B ko synaptosomes are called as stCCV. Both pools represent 15% of the total pool of synaptic CCVs. The unstable, shorter lived canonical CCV are abbreviated as canCCV. The protein G sepherose beads, preserved in 20 % ethanol, were washed with CCV buffer for 5 times. The protein G sepharose beads were diluted in CCV buffer and 40-60 µl protein G sepharose beads (50% slurry in CCV buffer) were added into each tube. The CCV samples were incubated with protein G sepharose beads for one hour at 4 ^{0}C on wheel, were centrifuged at 2000 rpm for 30 seconds at room temperature (Centrifuge 5254, Eppendorf, Germany). This pre-cleared CCV solution was transferred into a new tube for stCCV immunoisolation. The pelleted protein G sepharose beads were discarded. The pre-clearing of synaptic CCV proteins were optional. If non-specific protein-protein interaction is not a concern for the target proteins, the isolated canCCV fractions are directly used for the immunoisolation experiments without pre-clearing step. The CCV solutions were incubated with anti-Hsc70 antibody at a concentration of 5 mg/ml overnight at 4 ^{0}C end-over-end on a wheel. Protein G sepharose beads were washed in CCV buffer for 5 times and 60 µl protein G sepharose beads (50 % slurry in CCV buffer) were added into each tube and incubated on wheel at room temperature for 3 hours or at 4 ^{0}C, overnight. The beads were harvested at 2000 rpm for 30 secs at room temperature (Centrifuge 5254, Eppendorf, Germany) and the supernatant was discarded. The beads were washed 5 times with CCV buffer, were resuspended in 50 µl 3x SDS-PAGE loading dye and incubated at 90 ^{0}C for 5 min and beads were spun down at 400 rpm in the table top centrifuge. This supernatant was the first wash or elution fraction and this elution step was repeated [85]. The elution fractions Elution 1 (Elu1) and Elution 2 (Elu2) and the

washed beads were loaded onto SDS-PAGE and analyzed by semi-quantitative Western-blot analyses.

2.2.3. CCV coat protein interactions

Protein:protein interactions of CCV coat proteins were analyzed by co-immunoprecipitation experiments after the disassembly of the coat of purified CCV (sections 2.2.2.3 and 2.2.2.4). CCV coat disassembly was induced by a pH shift from the CCV buffer pH 6.4 to a basic pH by adding 500 µl CCV buffer adjusted to pH 8 and by incubating the solution for 15 min at RT. Vesicles were removed from solubilized CCV coat proteins by centrifugation at 100.000 x g (Beckman Coulter Optima MAX-XP Ultracentrifuge, rotor TLA55, US) for 20 min at 4°C. The supernatants were transferred into fresh tubes and the pH was shifted back to slightly acidic conditions by adding 500 µl CCV buffer adjusted to pH 6.4, in order to re-establish the condition of stable CCV protein:protein interactions *in-vitro*. The solubilized proteins of wt and ko canCCV and of wt stable CCV and ko stCCV were incubated with 5 µg of anti-ITSN1 antibody (BD611574, BD Biosciences, US) overnight at 4°C on an end-over-end rotor. The antibody bound protein complexes were isolated with protein G Sepharose ® beads (Protein G Sepharose® 4 Fast Flow GE Healthcare, Uppsala, Sweden) by overnight incubation at 4°C or for 3-4 hours at room temperature on an end-over-end rotor. The protein G beads containing interacting proteins were spun down and washed with CCV buffer at pH 6.4 for 3-5 times. The ITSN1-interacting CCV proteins were eluted in 80 µl SDS-PAGE, non-reducing, 3x loading dye buffer and incubated at 90 °C for 5 min. Eluates from 3 wt canCCV and 3 ko canCCV and of 3 wt stable CCV and 3 ko stCCV were pooled respectively, to increase the amounts of CCV proteins [164]. Elution fractions from wt and ko CCV proteins were loaded next to each other onto SDS-PAGE gels for subsequent semi-quantitative Western-blot analysis. Beads were also loaded onto the gels to control the efficiency of the protein elution.

2.2.4. Calmodulin-Hsc70 pull-down experiments of CCV associated Hsc70

To test for a calcium dependence of Hsc70 clathrin disassembly activity, isolated CCV (described in sections 2.2.2.3, 2.2.2.4 and 2.3) were incubated with Calmodulin-agarose beads (CABs) (CABs, A6112, Sigma Aldrich). Calmodulin

(CaM) beads were loaded with calcium (Ca^{2+}) by washing them with EGTA free CCV buffer supplemented with 1 mM Ca^{2+} and a second fraction was washed with CCV buffer containing 1 mM EGTA for 3 times to remove any potentially CaM bound Ca^{2+}. Afterwards, beads were washed with EGTA free CCV buffer in the Ca^{2+} treatment groups and with regular CCV buffer containing 0.5 mM EGTA in the treatment groups w/o Ca^{2+} for 3 times. Isolated synaptic wt and ko canCCV and wt stable CCV and ko stCCV were added to CaM/Ca^{2+} and Ca^{2+} free CaM beads and incubated overnight at 4 °C on an end-over-end wheel. Beads were isolated by centrifugation at 500 x g for 30 sec. Supernatants were transferred into new cups and incubated with reducing 6x loading dye at 90 °C for 5 min. Beads were washed with EGTA free and regular CCV buffers for 3 times, respectively, to get rid of proteins bound by weak and non-specific protein interactions. The washed beads were incubated with reducing 3x SDS-PAGE loading dye at 90 °C for 5 min. Proteins were separated on the phospho-tag™ SDS-PAGE gels (see section 2.2.11), on which protein migration was slowed down by the interactions of phosphorrylated proteins with phospho-tag. Proteins were subsequently transferred onto nitrocellulose membranes, which were developed with anti-Hsc70 antibody (see section 2.2.8). The Hsc70 proteins bound to isolated canCCV or wt stable CCV were used as a positive control and as a size marker for hypo- and hyperphosphorylated Hsc70 proteins.

2.2.5. Determination of the protein concentration with the Bradford Assay

The concentration of the isolated total cortex and synaptosome proteins were determined using the Bradford Assay (ROTI® Quant, K015.1, Roth, Germany). The reactions were prepared by mixing 800 µl of distilled water, 4 µl of protein sample and 200 µl of 5x Bradford reagent (ROTI® Quant, K015.1, Roth, Germany) in an eppendorf tube. The solution was mixed very-well, transferred into a UV spectroscopy cuvette and incubated for 5 minutes at room temperature. The blank solution was prepared in parallel by mixing distilled water and the Bradford reagent. Firstly, the blank was read to set the machine to zero absorbance at 595 nm and then the absorbance of each individual sample was detected. The concentrations of the protein samples were calculated based on Bovine Serum Albumin (BSA) standards. The 2-16

μg of BSA dilutions were prepared from 1 mg/ml BSA main stock and the absorbance of the BSA samples were measured at 595 nm.

2.2.6. Protein separation by electrophoresis

Sodium dodecyl sulfate poly-acrylamide gel electrophoresis (SDS-PAGE) analysis was used in order to separate proteins based on their molecular mass. Sodium Dodecyl Sulfate (SDS pellets, CN30.3, Roth, Germany) is a detergent, which unfolds proteins by binding to their amino acid hydrocarbon chains and this results in a uniform negative charge of each protein. Reducing agents such as dithiothreitol (DDT, Roth, 6908.2) or 2-mercaptoethanol cleave disulfide bonds to enable full protein unfolding. The gel matrix is composed of polyacrylamide (acrylamide/bisacrylamide (Rotiphorese® Gel30, 37 5:1, Acrylamide/Bisacrylamide, 2029.1, Roth, Germany). The cross-links between two acrylamide molecules is formed by bisacrylamide and the polymerization of the gel is initiated by Ammonium persulfate (APS, 3746.1, Roth, Germany) a free radical, and the radical buffer compound N,N,N′,N′-Tetramethylethylene-1,2-diamine (TEMED, 2367.1, Roth, Germany) [168]. The SDS-PAGE gel is a discontinuous polyacrylamide gel. The top part is a stacking gel, which has lower acrylamide concentration and lower pH (pH 6.8) than the bottom resolving part of the gel, with a higher acrylamide concentration and with a higher pH (pH 8.8). The concentration of the acrylamide and thus the the pore size is adjusted to optimally separate proteins within the molecular mass range of interest. A 7.5 % acrylamide resolving gel is used to separate proteins ranging from 100 kDa to 250 kDa, a 10-12.5 % acrylamide resolving gel is used to separate proteins ranging from 50 kDa to 100 kD and a 15 % acrylamide resolving gel is used to separate proteins of masses lower than 50 kDa. The acrylamide gel was run in SDS-PAGE buffer containing 50 mM Tris, 400 mM Glycine and 0.1 % (w/v) SDS in 10x stock solution which was diluted into 1x prior to use and pH of the SDS-PAGE running buffer should be 8.3. The protein samples were pre-mixed with 6x Laemmli buffer with 2-mercaptoethanol as a reducing agent and incubated at 95 ° C for 5 minutes. They were cooled down to room temperature and then were loaded onto gels or stored at -20 ° C till performing Western-blot analysis. The samples were loaded onto the gel together with protein ladder (Precision plus protein All blue Prestained Protein Standards, 1610372, Biorad,

Germany) to mark the reference molecular weights thereby estimating the molecular weight of the protein of interest. The samples were run at 20 mA constant current (for 2 gels) till reaching to the resolving part for 30-45 minutes. After the proteins reached to resolving part, the current was increased to 30-40 mA (for 2 gels) and run for additional 2-3 hours till the samples appeared at the bottom part of the gels and about to leak out of the gels [102], [168].

2.2.7. Semi-dry and wet Western blot transfer

After proteins were run on SDS-PAGE, they are transferred onto nitrocellulose membranes (Amersham Protran 0.45 µm pore size nitrocellulose Western blotting membranes, GE 10600003, GE Healthcare Life Sciences, Sweden). The transfer sandwiches were assembled as indicated below in Figure 2.1. Three Wattman filter papers (Sartorius Stedim Biotech, Göttingen, Germany) and nitrocellulose membranes were pre-wetted in Anode buffer. The polyacrylamide gel was equilibrated in Anode buffer in order to remove running buffer´s salts and detergents and then it was placed onto the nitrocellulose membrane avoiding air bubbles. Afterwards, three Wattman filter papers were pre-wetted in cathode buffer and layered on top of the polyacrylamide gel. In order to remove the excessive moisture and air bubbles trapped in between filter papers and nitrocellulose membrane, the stack was gently pressed using a plastic roller. The protein transfer in a semi-dry blotting chamber was run as 1 mA/cm^2 per gel, which required 90 mA current (for 2 gels). The transfer duration varies between 30 to 120 minutes depending on the molecular mass of the proteins, which ranged from 25 kDa to 250 kDa.
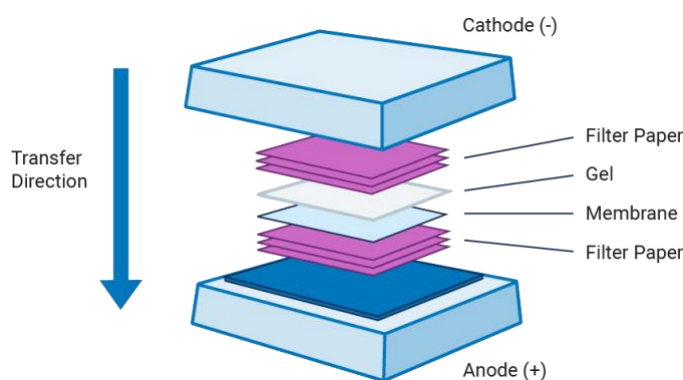
Figure 2.1. The semi-dry transfer sandwich assembly order. The cartoon representation of semi-dry transfer sandwich is shown. The transfer chamber is carefully closed and the transfer of proteins onto nitrocellulose membranes takes place under constant current. The image is obtained from *LI-COR* webpage (Transfer options, Wet tank vs. Semi-dry) [169]. The figure is reprinted with the permission from LI-COR Inc. provided a copyright permission for the unrestricted use of any substantial part of the paper upon special request.

The Wet protein transfer system is recommended for proteins of high molecular mass and for proteins resolved in phos-tag™ SDS-PAGE (see section 2.2.11). The stack of nitrocellulose membrane, the gel and Watmann papers were pressed together in a cassette (see Figure 2.2) and proteins are blotted onto membranes in transfer buffer at a constant 150 mA (300 V; 75 mA per gel of 9 by 6 cm) for 10 hours at 4 ^{0}C.
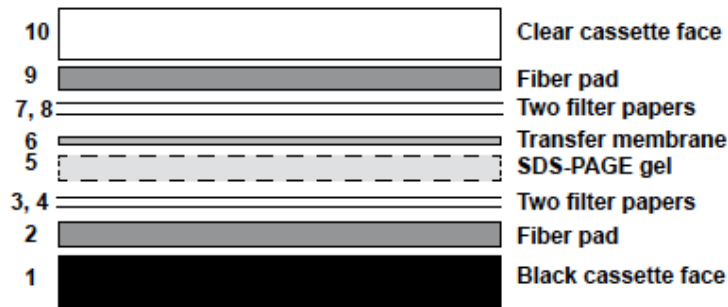
Figure 2.2. Wet transfer cassette assembly order. Wet transfer cassettes are assembled as indicated, from bottom (cathode side) to top direction (anode side). Wet fiber pad is placed onto the black cassette face. Secondly, two pre-wetted Wattman filter papers are put onto the fiber pad. Polyacrylamide gel is put onto the Wattman papers. Nitrocellulose membrane, pre-wetted in transfer buffer, is placed onto the gel. Two more pre-wetted Wattman filter papers are put onto the gel subsequently and possibly trapped air bubbles are pressed out using a plastic roller. The assembled cassettes are closed and they are placed into the transfer chamber. The electrotransfer of proteins onto the nitrocellulose membranes is performed under the constant current. The image is obtained from [170]. The figure is reprinted with Attribution-NonCommercial-ShareAlike 4.0 International (CC BY-NC-SA 4.0) licence for the unrestricted use of the any part of the paper without special permission.

2.2.8. Immunoblot detection of the transferred proteins

After proteins were transferred onto the nitrocellulose membranes as described in Sections 2.2.7, the membranes were blocked in 5 % non-fat dry milk (NFDM, instant skimmed milk powder, 0202V01, Frema, Germany) or 5 % Bovine Serum Albumin (BSA, A6003-100 g, Sigma, Germany), both diluted in TBS-T, for 1 hour at RT on the shaker. The blocking solution was discarded and the membranes were incubated with a primary antibody (diluted in 5% blocking solution as 1:250-1:5000 ratio) for 3-4 hours at room temperature or overnight (for 16 hours) at 4 °C on shaker. Membranes were washed three times with TBS-T or with 5 % NFDM 3 times over 10 minutes each. Next, membranes were incubated with HRP (Horseredish peroxidase)-conjugated secondary antibodies (diluted in 5 % NFDM as 1:5.000-1:10.000 ratio) for 1 hours at RT on the shaker. The list of used primary and secondary antibodies were given in Table 2.3-2.4. After the secondary antibody incubation, the membranes were

washed three times with TBS-T for 10 minutes each. The membranes were developed with Femto (SuperSignal[TM] West Femto Maximum Sensitivity Substrate, 34095, Thermo Fisher Scientific, US) or Pico PLUS (SuperSignal[TM] West Pico PLUS Chemiluminescent Substrate, 34580, Thermo Fisher Scientific, US) enhanced chemiluminescent (ECL) kits and then the protein bands were imaged in LAS-300 luminescent image analyzer (FujiFilm, Japan).

2.2.9. Stripping of Western-blot membranes for re-immunoblotting

Stripping refers to the removal of primary and secondary antibodies from the Western-blot membranes to enable the repeated use of the membranes. Therefore, re-probing of the same membrane can be advantageous to save precious samples, materials and time. In order to avoid potential loss of transferred proteins, a mild stripping protocol from Abcam [171] was carried out. The membranes were incubated twice with mild-stripping buffer (containing 1.5 % Glycine, 0.1 % SDS and 1 % Tween 20) adjusted to pH 2.2 for 10 min on shaker at room temperature. Afterwards, membranes were washed twice with PBS for 10 min on the shaker at RT. The stripped membranes were ready for the incubation with different antibodies according to the protocol described in Section 2.2.8, after blocking.

2.2.10. Analysis of protein phosphorylation by phos-tag SDS-PAGE

Phos-tag ™ SDS-PAGE is used to discriminate protein phosphorylation levels. The phosphate chelating phos-tag ™ (Phos–tag[TM], AAL-107, Wako Pure Chemicals Corp., Japan) group is attached to acrylamide, which can be added at variable concentrations to regular SDS-PAGE acrylamide solutions. Due to the binding of the phosphate groups of proteins with the phos-tag ™ group, phosphorylated proteins migrate slower than their non- or lower phosphorylated variants on the gel [10]. The basics SDS-PAGE protocol for 7.5% or 10% acrylamide gels (Section 2.6) was followed in the presence of 20 μM phos-tag ™ acrylamide (from 5 mM stock solution) and 50 μM $MnCl_2$ (from 10 mM stock solution) [172]. A range of 20-80 μg of proteins were loaded and separated at constant 20 mA (for 2 gels) for 1 hour until proteins were reached to resolving gel. The current was increased to constant 30-40 mA for 3-4 hours. Before transferring the proteins onto nitrocellulose membranes, phos-tag gels were washed in transfer buffer with 10 mM EDTA for 10 min twice at RT to remove

Mn^{2+} salts. This step significantly increases protein transfer efficiency [172]. Afterwards, gels were washed in transfer buffer to remove EDTA. The wet Western-blot protein transfer system is recommended for phos-tag gels (Section 2.2.7) [172]. The membranes were immunoblotted with primary and secondary antibodies as described in Section 2.2.8.

2.2.11. Coomassie brilliant blue SDS-PAGE staining

The isolated cortex, synapse and/or synaptic CCV proteins were separated on the SDS-PAGE. After the run, gels were incubated with fixation solution I, to immobilize the proteins in the gel, for 1 h on a shaker at room temperature. The Fixation solution I was discarded and the gels were incubated with Fixation solution II for 2 hours on a shaker at room temperature. The Fixation solution II was discarded after 2 hours and the gels were incubated with Coomassie protein staining solution overnight on a shaker at room temperature. After discarding the staining solution, the gels were washed with destaining solution for 3-4 hours on a shaker at RT. The destaining solution was changed 2-3 times during the incubation period. Afterwards, the gels were destained in ddH_2O for 16-24 hours on a shaker at RT [173], [174]. The gels were scanned (Epson Perfection V850 Pro, SilverFast, Germany) and the stained proteins were labelled based on the expected molecular weight. Proteins of interest were excised from the gels and gel slices were stored in Eppendorf tubes at -20°C for the subsequent proteomic analysis.

2.2.12. Protein Mass Spectrometry Analysis

Mass Spectrometry (MS) is a technique to determine the mass of molecules based on their mass-to-charge ratios. MS provides a qualitative and also a quantitative profiling of chemical substances [175]. MS methodology allows to identify proteins, peptides, DNA or RNA sequences within the investigated target chemicals (qualitative MS analysis). A protein quantification is achieved by different methods, e.g. comparing the relative signal intensities of mixed samples (quantitative MS analysis) [176], [177]. The proteins isolated from phos-tag™ SDS PAGE gels were prepared for the MS analysis by Olaf Bernhard (Department of Cellular Biochemistry, Medical Faculty, University Göttingen) and the MS analysis was performed by Dr. Oliver Valerius (Department of Molecular Microbiology & Genetics, University Göttingen).

The purified synaptic canCCV isolated from wt and AP1/σ1B ko mice were loaded onto the phos-tag^{TM} SDS-PAGE. The hyper- and hypo-phosphorylated Hsc70 bands were excised and the gel pieces were further proceeded for the MS Analysis including steps: reduction and alkylation of cysteine amino acids to irreversibly break the disulfide bonds between cysteines [178]; digestion of the proteins with trypsin [179] to generate peptides [178], [179]; extraction and resuspension of the peptides for MS measurements. The excised gel pieces were incubated with 100 µl 25 mM Ammonium bicarbonate/water (Ammonium bicarbonate, ReagentPlus® ≥ 99.0%, A6141, Sigma, Germany) for 15 min at 37 °C at 1000 rpm in a thermo shaker (Eppendorf® Thermomixer Comfort, T1317, Eppendorf, Germany). Gel pieces were spun down by a quick centrifugation and the supernatant was discarded. Gel pieces were washed twice with 100 µl 50 % Acetonitrile (AcN) (Acetonitrile gradient grade for liquid chromatography LiChrosolv® Reagent, 1000302500, Merck, Germany) in 25 mM Ammonium bicarbonate/water for 30 min each at 37 °C with gentle shaking. The gel pieces were spun down quickly with a table-top centrifuge and the supernatant was removed. The gel pieces were incubated with 100 µl 100 % AcN for 10 min at 37 °C with gentle shaking. Gel pieces were harvested by centrifugation and the supernatant was discarded. Gel pieces were left to dry for 5 min at RT by opening the lid of the eppendorf tubes. Gel pieces were incubated for 1 hour at 56 °C with gentle shaking in 10 µl 10 mM DTT (DTT BioChemica BC, A1101, Applichem, Germany), in 25 mM Ammonium bicarbonate/water, to cleave disulfide bonds between peptides. At the end of this incubation, the tubes were cooled down on ice, gel pieces were centrifuged and the supernatant was discarded. Gel pieces were incubated with 25 mM 10 µl Iodoacetamide (IAM) (Iodoacetemide single use vial of 56 mg, A3221, Sigma, Germany), dissolved in 25 mM Ammonium bicarbonate/water, for 30 min at room temperature with gentle shaking for the alkylation of cysteine residues. IAM covalently binds to the thiol groups on the cysteine amino acids and prevents the reformation of disulfide bonds [180], [181]. At the end of the incubation time, the gel pieces were spun down and the supernatant was discarded. The gel pieces were again incubated with 10 µl reducing reagent (10 mM DTT in 25 mM Amonium bicarbonate/water) for 10 min at 37 °C with gentle shaking. After discarding the supernatant, the gel pieces were washed firstly with 100 µl 50% AcN (in 25 mM

Ammonium bicarbonate/water) and then with 100 % AcN for 10 min each at 37 °C with gentle shaking. After quick centrifugation, the supernatant was discarded and the gel pieces were allowed to dry at RT for 5 min by opening the lid of the Eppendorf cups. For the digestion of proteins, 6 µl 20 ng/µl trypsin (Sequencing Grade Modified Trypsin, V5111, Promega, Germany), in 25 mM Ammonium bicarbonate/water, was added onto dried gel pieces and incubated for 15 min on ice. Afterwards, they were further incubated at 37 °C for at least 4 hours or over-night. After quick centrifugation, the supernatant was transferred into fresh 500 µl eppendorf cups and the gel pieces were incubated with 20 µl 1% Trifluoroacetic acid (TFA) (Trifluoroacedic acid, Peptide Synthesis grade, 15820273, Applied Biosystems™ 400137, US), dissolved in water, for 30 min 37 °C with gentle shaking. The gel pieces were quickly spun down and the supernatant was transferred to the new 500 µl Eppendorf cups. Extracted peptides were pooled and dried completely in a Speed Vac vacuum concentrator (Bachofer Speed Vac Concentrator, SVC-100H Vakuumzentrifuge, Germany). The dried peptides were dissolved in 10 µl 0.1% TFA/water by vortexing (Vortex-Genie 2, Scientific Industries, Inc., US) and sonication. The peptide solutions were either directly used for MS Analysis (Mass Spectrometer ultrafleXtreme™ MALDI-TOF/TOF Systems, 259900, Bruker, US) or stored at -20 °C for later MS measurements.

2.2.13. Mouse embryonic fibroblast cell culture

2.2.13.1. Mouse embryonic fibroblast cell lines

Mouse embryonic fibroblasts (MEFs) cells had been established from isogenic wt AP1/σ1B+/+ and ko AP1/σ1B -/- mice. AP1/µ1A-/- MEF cells were rescued via ectopic expression of µ1A cDNA [69], [100]. The cell lines used are provided in the Table 2.5.

2.2.13.2. Thawing the frozen MEF cell lines

The frozen MEF cell lines are stored in liquid nitrogen for long-term cryopreservation. In the liquid nitrogen tanks, the cells can be kept for years without losing their viability [182]. The protocol for the preservation of cell lines in the liquid nitrogen will be provided in Section 2.2.13.5. The frozen resuspended MEF cells

containing vials were removed from the liquid nitrogen tanks and cell vials were thawed in 70 % EtOH at 37 ° C in a water bath in order to protect the cells from any source of contamination. The thawed cells were cultured and maintained as described in detail in the following sections.

2.2.13.3. Cultivation of MEF cells

After the frozen MEF cells were thawed as mentioned earlier in Section 2.2.13.2, they were transferred into a falcon tube. Since the freezing medium contains 5 % dimethyl sulfoxide (DMSO), 10 ml pre-warmed Dulbecco´s Modified Eagle Media (DMEM) was added into the falcon tube to prevent the toxic effect of DMSO by diluting DMSO down to 0.1-0.5 % (v/v) DMSO, which is nontoxic for the cell viability and proliferation [183]. The cells were spun down at 300 x g for 5 min at room temperature (Centrifuge 5804 R, Eppendorf, Germany). The supernatants were discarded and the cell pellets were resuspended in 5 ml fresh DMEM and then the cells were seeded into a sterile 25 cm^2 flask. Additional 10 ml fresh DMEM were added and cells were incubated at 37 °C, 5 % (v/v) CO_2 and at >90 % humidity. Cell adherence and growth were controlled approximately two hours after the initial seeding process. Cells were grown in the incubator for 2-3 days after which they reached up to 90-95 % confluency.

2.2.13.4. Subculturing of MEF cells

After the MEF cells reached up to 90-95 % confluency, they were diluted into new flasks or to a bigger flask. First, the cell culture medium was discarded and then the cells were washed with 1x PBS for three times. For the detachment of adherent MEF cells from the 25 cm^2 cell culture flask, 500 µl Trypsin-EDTA (0.05 % Trypsin-EDTA, 25300-054, Gibco, Germany) were added. Cells were incubated with Trypsin-EDTA for 5 min at 37 °C, 5 % (v/v) CO_2 and at >90 % humidity. At the end of the incubation period, 4.5 ml pre-warmed DMEM was added to solubilize the cells and the cells were distributed among three new 25 cm^2 flasks or transferred into larger culture dishes or flasks.

2.2.13.5. Long-term cryopreservation of MEF cells

MEF cells are stored in liquid nitrogen at -196 °C for long-term cryopreservation. After cells reach 90-95 % confluency, they were detached from the flask using Trypsin-EDTA as described in Section 2.2.13.4. The cell suspension was transferred into a falcon tube and centrifuged at 300xg for 5 minutes at room temperature (Centrifuge 5804 R, Eppendorf, Germany). The supernatant was discarded and the pelleted cells were dissolved in 1 ml freezing medium. The freezing medium was supplemented with 5 % DMSO to prevent formation of large ice crystals during the process of cell freezing as well as during their long-term storage in the liquid nitrogen [184]. The resuspended cells were aliquoted in 250 µl volumes per 1 ml cryotube and the tubes were chilled on water ice, then they were transferred to -20 °C for 1-2 hours, then to the -80 °C freezer for additional 2 hours and finally they were transferred into liquid nitrogen for long-term storage.

2.2.13.6. Extraction of CCV and proteins from MEF cells

After MEF cells reached 90-95 % confluency, the growing medium was discarded and the cells were rinsed in 1x PBS for three times. Then, 1 ml PBS was added to the 25 cm^2 flask and cells were scraped off with a cell scraper. The cells were transferred into 2 ml Eppendorf tubes and centrifuged at 200x g for 10 minutes at room temperature (Centrifuge 5805 R, Eppendorf, Germany). The supernatants were discarded and the pelleted cells were resuspended in PBS with proteinase inhibitor cocktail (PIC). The cells were centrifuged at 200x g for 5 minutes at 4 °C (Centrifuge 5417 R, Eppendorf, Germany) and the washing step was repeated one more time. Finally, cells were resuspended in 1.5 ml cell lysing or CCV buffer. The resuspended cells were homogenized by passing them several times through a 22G needle. After homogenization, additional 500 µl cell lysis or CCV buffer was added into each eppendorf tube and after mixing they were centrifuged at 500x g for 10 minutes at 4 °C (Centrifuge 5417 R, Eppendorf, Germany). The supernatant was transferred into fresh tubes and pellets were discarded. The concentrations of proteins were determined via Bradford assay and normalized as described previously in Section 2.2.5. Protein lysates were stored at -20 °C freezer after they were incubated in loading dye at 95 °C for 5 minutes until further use for semi-quantitative Western blot analysis. The cell

culture experiments were mainly performed for the initial optimization of the experimental conditions for the semi-quantitative Western blot analysis.

2.14. Statistical analysis

The experiments comparing the protein levels between wt and AP1/σ1B ko mouse tissue samples were repeated at least three times with independent biological samples. The processing of wt and AP1/σ1B ko cortex, synapse and synaptic CCV preparations were handled in parallel and only the protein contents of these samples were compared with each other on the same Western-blot membrane. The Western-blot signal values from wt protein samples were defined as 100 % and the values of ko samples were calculated relative to wt. Only the data sets in which all ko values were either below or above their respective wt values were accepted as significant. Statistical analysis of the quantified data were shown as box-plot diagrams, which were calculated by the DataGraph software tool (Visual Data Tools, USA) [85], [164].

CHAPTER 3

3. RESULTS

3.1. Endophilin A1 and LRRK2 do not regulate Synaptojanin1 CCV levels

It has been shown that Endophilin A1 and Synaptojanin1 are recruited at the same time to budding CCV, at the very end of CCV budding stage [162], [185], [186]. This has convinced people that Endophilin A1 regulates the levels of Synaptojanin1 in CCV and thereby the CCV life time [162], [185], [186]. So, in our first characterization of the alterations in the composition of the stCCV coat, we found the levels of Endophilin A1 to be reduced in ko synaptic canCCV and stCCV down to ~40 % and ~50 % of the respective wt CCV levels [85]. However, the reduction of Endophilin A1 level in stCCV compared to the wt stable CCV level does not match the reduction in Synaptojanin1 stCCV level, which is 10 % of wt stable CCV Synaptojanin1 levels (Figure 3.1) [85], [164]. This suggests that Endophilin A1 may not regulate the amount of Synatojanin1 in a CCV. However, regulatory mechanisms may inhibit the binding of Synaptojnin1 by Endophilin A1 in stCCV. Leucine-rich-repeat-kinase 2 (LRRK2) phosphorylates Endophilin A1 in its Bin/Amphiphysin/Rvs (BAR) domain at residue Ser75 and this is predicted to inhibit BAR domain membrane binding [165]. In this scenario, Endophilin A1 would be recruited to CCV via binding of its SH3-domain to either ITSN1, Dynamin, Pacsin, VGLUT1, N-type Ca^{2+}-channels or Parkin. This sets up a competition among Synaptojanin1 and these other proteins for the binding of the Endophilin A1 SH3 domain, thereby impairing the recruitment of Synaptojanin1 [165]. So, LRRK2 level and its catalytic activity should be increased in stCCV, if Endophilin A1 determines Synaptojanin1 CCV levels. The levels of LRRK2 are reduced down to 60 % and 65 % of wt CCV levels in AP1/σ1B ko canCCV and stCCV, respectively (Figure 3.2.A) [164]. However, these changes do not match with the alterations in Endophilin A1/Synaptojanin1 CCV ratios [85], [164]. The binding of ArhGEF7 to LRRK2 leads to the formation of LRRK2:GTP and this stimulates LRRK2 kinase activity [187]. The level of ArhGEF7 is slightly increased in the

AP1/σ1B ko synapses compared to wt synapses, 110 % of wt ArhGEF7 synapse levels. ArhGEF7 levels are reduced down to ~60 % and ~42 % of wt levels per CCV in ko canCCV and stCCV, respectively (Figure 3.2.B) [164]. The phosphorylation of LRRK2 on Ser935 leads to inhibition of the kinase activity [188]. The LRRK2 Ser935 phosphorylation, e.g. by PKA, results in 14-3-3 protein binding and eventually leads to LRRK2 inactivation [188]. The LRRK2 Ser935-Pi level is 85 % of wt in ko canCCV (Figure 3.2.C.) [164]. So, the LRRK2 activity is slightly inhibited in ko canCCV as compared to wt canCCV. However, stCCV are expected to have increased LRRK2 activity, if Endophilin A1 recruitment is mainly regulated by its SH3 domain and protein-protein interactions [165]. There is only 55 % of wt Pi-LRRK2 levels in ko stCCV (Figure 3.2.C.) [164]. Even though LRRK2 seems less inhibited in ko stCCV, its level is reduced and it is not more activated by ArhGEF7 [164] . However, it could be inferred from the cumulative effect of LRRK2 activation/inhibition cycles, that LRRK2 kinase activity is reduced in ko stCCV, which suggests that it may contribute to the shortening of the CCV half life [164]. Collectively, these data demonstrate that Endophilin A1 does not determine the amount of Synaptojanin1 in CCV[164]. Furthermore, the level of LRRK2 is reduced down to 65 % of wt levels and the Pi-LRRK2 amount is increased to 140 % of wt levels in AP1/σ1B ko synapses (Figure 3.2.A, C). This decreased synaptic LRRK2 kinase activity is in consistency with the stimulation of endosomal protein transport in AP1/σ1B ko synapses, as LRRK2 suppresses many Rab proteins, that are essential players in endolysosomal protein trafficking [189].
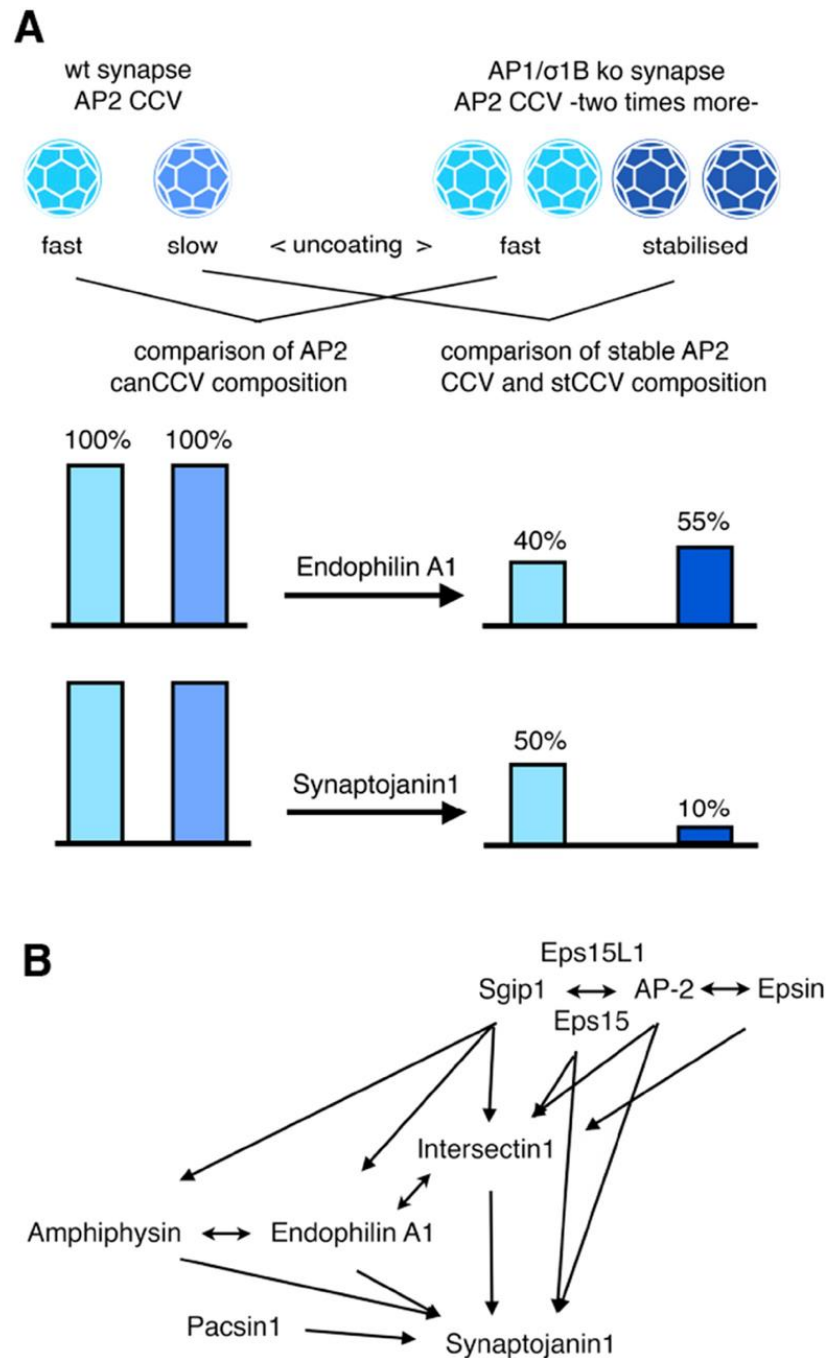
Figure 3.1. The changes in the coat composition and lifespan of AP2 CCV classes in ko synapses and the interaction network of Synaptojanin1 CCV coat proteins. (A) The alterations in the AP2 CCV classes in AP1/σ1B ko synapses are shown. Both ko canCCV and stCCV numbers are increased two-folds. Additionally, wt stable CCV become more stabilized in ko synapses, the stCCV. Due to both synaptic CCVs are doubled in size, the reduction in Endophilin A1 and Synaptojanin 1 levels are given per CCV. The published data in Candiello *et al.* 2017 is summarized in Mishra *et al.* 2021 as bar diagrams [85], [164]. **(B)** The CCV proteins interactome of Synaptojanin1 and their interactions with each other are shown. The order of proteins from top to bottom indicates their appearance during CCV formation, from CCP formation till pinching off CCVs from the PM. The figure is obtained from Mishra, R., **Sengül, G.F.** *et al.* 2021. The figure is reprinted with the permission from Springer Nature, Scientific Reports open access Creative Commons CC BY provided a licence for the unrestricted use of any part of the manuscript without special permission.
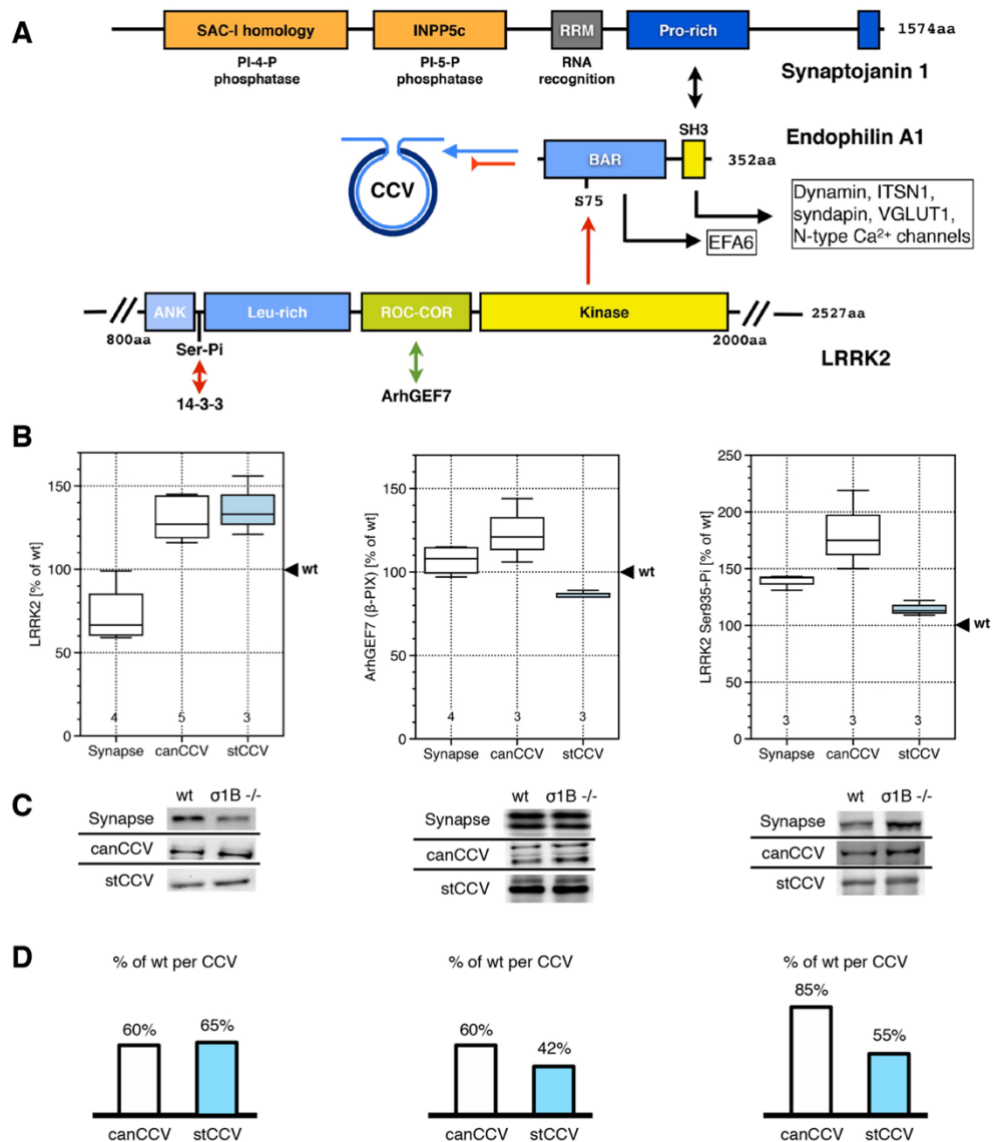
Figure 3.2. The protein domain organization of Synaptojanin1, Endophilin A1 and LRRK2 and the comparison of LRRK2 protein and its kinase activity levels between wt-ko synapses and between wt-ko synaptic AP2 CCV. (A) The cartoon demonstrates the protein domain organizations of Synaptojanin1, Endophilin A1 and LRRK2. Endophilin A1 interacts with Synaptojanin via its SH3 domain and with LRRK2 via its BAR domain. The binding of the Endophilin A1 BAR domain to the neck of budding CCV can be inhibited by LRRK2. In this case, Endophilin A1 could still be recruited to budding CCV via binding of its SH3-domain to either ITSN1, Dynamin, Pacsin, VGLUT1, N-type Ca^{2+}-channels or Parkin. These interactions would compete with Synaptojanin1 for its binding to the Endophilin A1 SH3 domain. **(B)** The levels of LRRK2 protein (240 kDa) and its activity (stimulated by ArhGEF7; 74 kDa, shown with green arrow and inhibited by LRRK2 Ser935-Pi ;240 kDa shown with red arrow) are compared between wt and AP1/σ1B ko synaptosomes, canCCV and the wt stable and AP1/σ1B ko stCCV. The quantified band intensities from wt samples are defined as 100 % and signal intensities of ko samples are expressed relative to wt. The numbers below each box-plot in the diagrams denote the numbers of independent biological replicates for a given data set. **(C)** Representative Western-blot images used for the quantifications are shown. **(D)** The alterations in the levels of each protein per CCV in AP1/σ1B ko canCCV and stCCV compared to their relative wt levels are depicted as bar diagram [164]. The figure is adapted from Mishra, R., **Sengül, G.F.** *et al.* 2021. The figure is reprinted with the permission from Nature Springer, Scientific Reports open access Creative Commons CC BY provided a licence for the unrestricted use of any part of the paper without special permission. Author contribution: R. Mishra contributed to the synapse (LRRK2) and stabilized CCV (LRRK2), E. Candiello contributed to the canCCV (LRRK2) and G.F. Sengül contributed to the synapse (LRRK2, ArhGEF7, LRRK2 Ser935-Pi), canCCV (LRRK2, ArhGEF7, LRRK2 Ser935-Pi) and stabilized CCV (ArhGEF7 and LRRK2 Ser935-Pi).

3.2. Compensation of reduced Pacsin1 CCV levels by its enhanced activation

The CCV protein Pacsin1, also known as syndapin1, is composed of a F-BAR (Fes/CIP4 homology-Bin/Amphiphysin/Rvs) and a SH3 (Src-homology) domains [190], [191] (Figure 3.3.A) [164]. The F-BAR domain of Pacsin1 regulates the membrane curvature by interacting with PM phospholipids and its SH3 domain initiates membrane scission via its interaction with Dynamin, which mediates vesicle-PM scission, and with N-WASP, which induces actin polymerization [190], [191]. The intramolecular interactions between the F-BAR and SH3 domains of Pacsin1 lead to its autoinhibition. The intermediate sequence between F-BAR and SH3 domains of Pacsin1 is separated by 100 amino acid residues. This intermediate sequence is not structured [191]. The NPF (Asparagine-Proline-Phenylalanine)-motifs in this sequence are responsible for the interaction with CCV co-adaptor proteins via their EHDs (Epsin-homology domains) [191].

There are wt levels of Pacsin1 in AP1/σ1B ko synapses and in their canCCV (Figure 3.3.B) [164]. However, stCCV have only 30 % of wt Pacsin1 levels (Figure 3.3.B) [164]. This 70 % reduction in the levels of Pacsin1 could be also responsible for the reduced incorporation of Synaptojanin1 into stCCV [85], [164]. The autoinhibition of Pacsin1 is released through its phosphorylation on Serine residues [192]. The Ser343 residue on Pacsin1 is phosphorylated by Pak5, which can also phosphorylate Synaptojanin1 on its proline-rich domain (where Synaptojanin1 binds to Endophilin A1 SH3 domain) [192]. Either of these two protein phosphorylations can stabilizes the interaction between Pacsin1 and Synaptojanin1 [192]–[196]. So, the levels of phospho/activated-Pacsin1 are also analyzed by performing Western-blot experiments with anti-Pacsin1 Ser346-Pi antibody [164]. While the levels of Pacsin1 is reduced down to 30 % of wt levels in stCCV, there are 65 % of wt levels of Pi-Pacsin1 in stCCV (Figure 3.3.B) [164]. Thus, the fraction of Pi/activated-Pacsin1 in stCCV is two-fold higher than in a wt stable CCV [164]. This result can not completely exclude a contribution of the reduced Pacsin1 stCCV level in the reduced Synaptojanin1 recruitment into stCCV. However, the compensation of the reduced Pacsin1 levels by its enhanced activation does not suggest a regulatory function of Pacsin1 in Synaptojanin1 recruitment [164]. These Pacsin1 data demonstrate the complexity behind the regulation of the CCV life cycle.

3.3. CCV class specific ITSN1 levels

ITSN1 can interact directly with both Synaptojanin1 and Endophilin A1 as indicated in Figure 3.3.A [164]. Pechstein *et al.* 2015 suggests that ITSN1 acts as a platform to coordinate the recruitment of Synaptojanin1 by Endophilin A1 [186]. ITSN1 can also bind to N-WASP, regulating actin organization [197], [198] and other CCV coat proteins [186], [198] such as AP2 [199], Dynamin [198], [200], SGIP1 [199], [201], Epsin [198] and Stonin2 [198]. There are two predominantly expressed transcripts of ITSN1 in mammals, the ubiquitously expressed short ITSN1 isoform (ITSNS1) and the long ITSN1 isoform (ITSNL1), specifically expressed in the brain [198], [202], [203]. ITSNS1 is composed of two N-terminal Eps15 homology (EH) domains, one central coiled-coil (CC) domain and five SH3 (A-E) domains, whereas ITSNL1 contains additional extensions at its C-terminus, including Dbl homology (DH)/RhoGEF domain, Pleckstrin homology (PH) domain and C2 domain [198], [202], [203] (Figure 3.3.A) [164]. The evolutionarily inclusion of five amino acid residues into the ITSNL1 SH3A domain prevents an autoinhibitory conformation and makes brain ITSNL1 constitutively active [204]. ITSN1 proteins binds to the PM at early stages of the CCV budding process and its level elevates throughout this process [198], [199]. As it has been already mentioned above, ITSN1 interacts with Synaptojanin1 via its SH3A domain [198], [199] and with Endophilin A1 via its SH3B domain [186] and it binds to AP2 via the SH3A-SH3B linker domain [199]. There are 80 % of wt ITSN1 levels in AP1/σ1B ko synapses as compared to its wt levels (Figure 3.3.B-D) [164]. Commercially available anti-ITSN1 antibody recognizes two bands of ITSN1 proteins exclusively in the synapses. The 20 % reduction in ko synapses as compared to wt synapses is detected in the both, the slow and fast migrating ITSN1-protein bands [164]. Even though a canCCV in AP1/σ1B ko synapses contains wt levels of ITSN1, its level is reduced down to 30 % of wt stable CCV levels in ko stCCV (Figure 3.3.B-D) [164]. As already explained, the level of Synaptojanin1 was reduced down to 10 % of wt stable CCV levels in ko stCCV [164]. These reductions are quite close to each other. Therefore, it can be strongly suggested that ITSN1 determines the amount of Synaptojanin1 in stCCV and thus the CCV life time (Figure 3.3) [164].
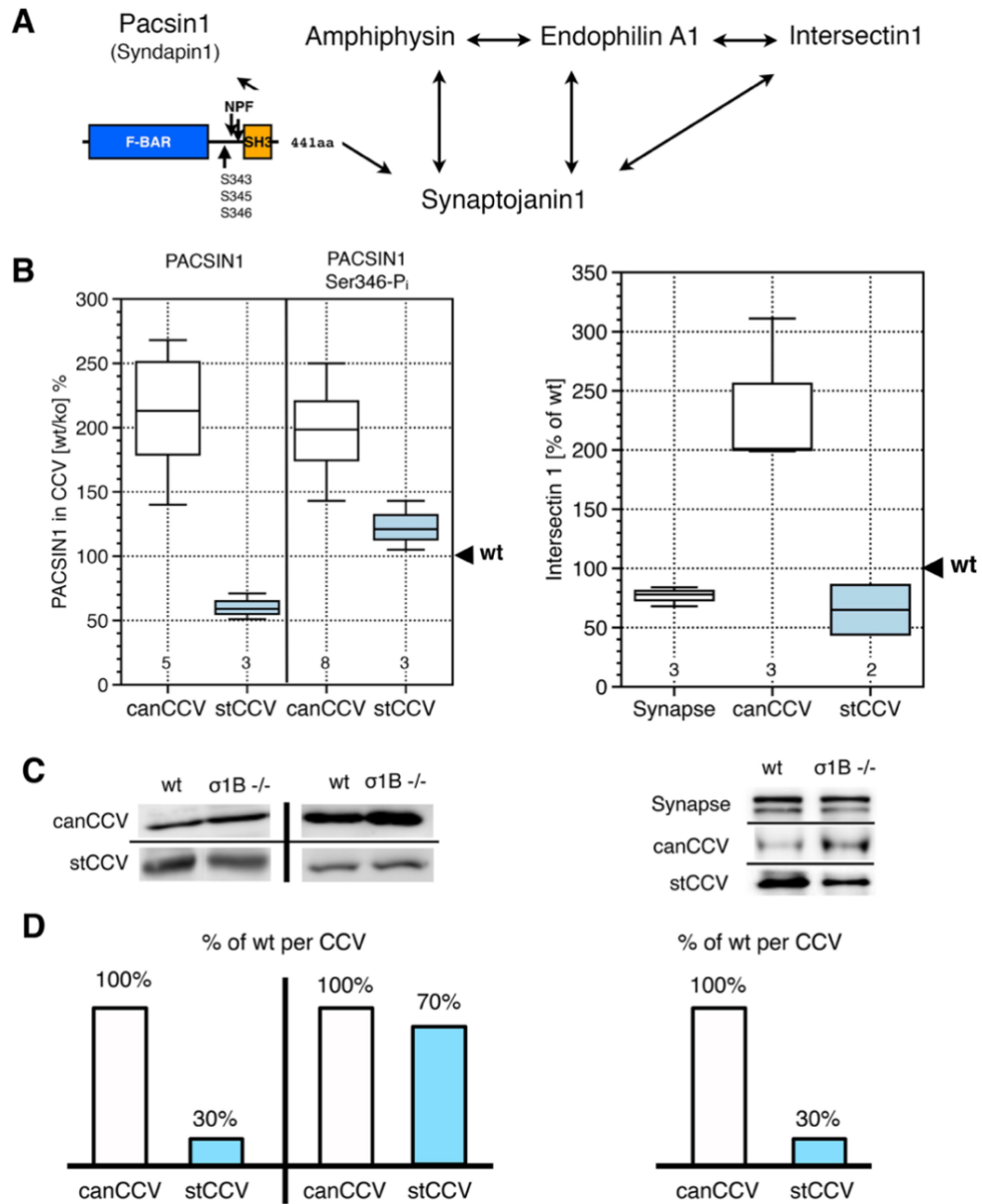
Figure 3.3. The CCV protein interactome of Synaptojanin1, and the levels of Pacsin1, activated Ser346-Pi Pacsin1 and ITSN1 in wt-ko subcellular fractions. (A) Protein-protein interaction scheme of CCV proteins binding to Synaptojanin1 is presented. **(B)** Pacsin1, activated Ser346-Pi Pacsin1 and ITSN1 wt synapse, canCCV and stable CCV levels are compared with AP1/σ1B ko synapse, canCCV and stCCV levels. The Western-blot signal intensities from wt samples are defined as 100% and values from ko samples are expressed relative to wt. Numbers in box-blot diagrams indicate the numbers of experiments with independent biological samples. **(C)** Representative Western-blot images used for quantifications are shown. **(D)** Bar diagrams indicate the changes in protein levels of Pacsin1, activated Ser346-Pi Pacsin1 and ITSN1 per CCV in both ko AP2 CCV classes relative to wt CCV [164]. The estimated molecular weight of Pacsin1 is 52 kDa; activated Ser346-Pi Pacsin1 is 52 kDa; ITSN1 is 200 kDa. The figure is adapted from Mishra, R., **Sengül, G.F.** *et al.* 2021. The figure is reprinted with the permission from Nature Springer, Scientific Reports open access Creative Commons CC BY provided a licence for unrestricted use of any part of the manuscript without special permission. Author contribution: E. Candiello contributed to the canCCV (Pacsin1, activated Ser346-Pi Pacsin1), stabilized CCV (Pacsin1, activated Ser346-Pi Pacsin1). R. Mishra contributed to synapse (ITSN1), canCCV (ITSN1), stabilized CCV (ITSN1). G.F. Sengül contributed to the canCCV (Pacsin1, activated Ser346-Pi Pacsin1).

3.4. The regulation of Synaptojanin1 CCV levels by ITSN1

CCV have to be purified at slightly acidic conditions at pH 6.4, because the CCV coat is unstable at physiological pH 7.4 *in-vitro* [85]–[88], [164]. In order to verify preferential ITSN1-Synaptojanin1 binding, the CCV coat proteins were solubilized via a pH shift from 6.4 to 8 [164]. The vesicles were removed via centrifugation and the pH of the protein solution was re-adjusted to pH 6.4 to stabilize the coat protein interactions again. The same amounts of ITSN1 are immunoisolated by anti-ITSN1 antibody from wt and ko canCCV proteins and also from wt stable CCV and ko stCCV proteins. Importantly, Dynamin is not co-immunoprecipitated with ITSN1, which implies that ITSN1 and co-isolated proteins are not a part of a huge protein network (Figure 3.4.B-C) [164]. The amounts of co-immunoprecipitated Endophilin A1 with ITSN1 are increased by the same level in ko canCCV and ko stCCV compared to the respective wt CCV (Figure 3.4.B-C). The amounts of Endophilin A1 in ko canCCV was 40 % of wt levels and it was 55 % of wt stable CCV levels in ko stCCV [85], but relatively more Endophilin A1 has been co-immunoprecipitated with ITSN1 from both ko CCV classes compared to their corresponding wt CCVs. This increased interaction may be linked to the increase in AP2 CCV formation and CME [85], [164]. However, the levels of Endophilin A1 are not differentially regulated between wt and ko canCCV and wt stable CCV and ko stCCV [85]. The ko stCCV contain only 10 % of wt stable CCV Synaptojanin1 levels, as shown in Candiello *et al.* 2017 [85]. So, ITSN1 should co-isolate much less of Synaptojanin1 out of ko stCCV. However, ITSN1 co-isolated almost as much Synaptojanin1 from ko stCCV than from wt stable CCV. This enhanced ITSN1:Synaptojanin1 interaction strongly indicates the regulation of Synaptojanin1 CCV levels by ITSN1 [164]. So, these data speak against the established view that Endophilin A1 regulates Synaptojanin1 recruitment and thus the uncoating of CCV [85], [164].
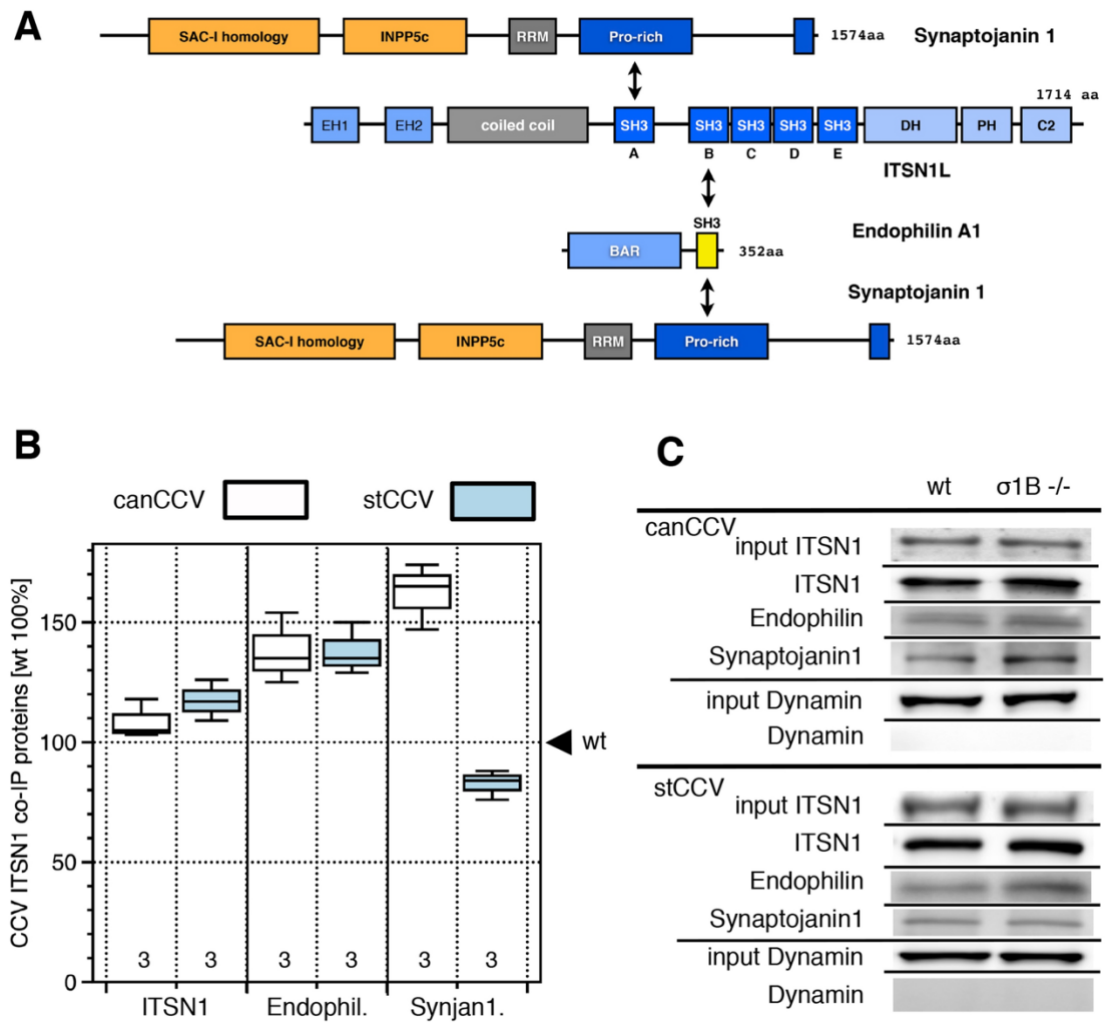
Figure 3.4. The protein domain organization of Synaptojanin1, ITSN1 and Endophilin A1 and co-immunoprecipitation of Synaptojanin1 and Endophilin A1 with ITSN1 from wt-ko solubilized synaptic AP2 CCV. (A) The cartoon represents the protein domain organizations of Synaptojanin1, ITSN1 and Endophilin A1. The interactions of Synaptojanin1 with ITSN1 and Endophilin A1 via its proline-rich domain and the binding of Endophilin A1 with ITSN1 via their SH3 domains are illustrated. **(B)** ITSN1:EndophilinA1 and ITSN1:Synaptojanin1 binding ratios are compared between wt and AP1/σ1B ko canCCV and wt stable CCV and ko stCCV by ITSN1 co-immunoprecipitations after CCV coat protein solubilisation. Samples are immunoblotted with Dynamin as a negative control. Numbers below each box-plot show the numbers of independent experiments performed in triplicate. **(C)** Representative Western-blot images for the quantifications are shown. The estimated molecular weight of ITSN1 is 200 kDa; Endophilin A1 is 37 kDa; Synaptojanin1 is 145 kDA; Dynamin is 100 kDa. The figure is adapted from Mishra, R., **Sengül, G.F.** *et al*. 2021. The figure is reprinted with the permission from Nature Springer, Scientific Reports open access Creative Commons CC BY provided a licence for the unrestricted use of any part of the paper without special permission. Author contribution: G.F. Sengül performed the co-immunoprecipitation experiments and obtained the complete figure.

3.5. Competition of Synaptojanin1 binding to ITSN1 with other ITSN1 binders

As described beforehand, the level of Synaptojanin1 is reduced down to 10 % of wt stable CCV in ko stCCV [85] and the ITSN1 level is reduced down to 30 % of wt stable CCV (Figure 3.3.B-D) [164]. This 20% difference needs to be explained, if ITSN1 is the major, if not sole, protein determining Synaptojanin1 CCV levels [164]. Therefore, the next aim is to find out molecular mechanim that could be responsible for this additional 20 % reduction in Synaptojanin1 levels as compared to ITSN1 levels in ko stCCV [164]. Besides Synaptojanin1, ITSN1 can be also bound by other proteins that are involved in CCV formation [197]–[201] such as AP2 [199] [22], Eps15, Eps15L1, Epsin [198] and Sgip1 [199], [201], as summarized in Figures 3.1.B [164].

3.5.1. Sgip1 levels are not changed in stCCV

It has been proposed that tripartite Sgip1-AP2-Eps15 and/or Sgip1-AP2-Eps15L1 complexes assist and even initiate the AP2 CCV budding process by the ability of Sgip1, the brain-specific homolog of ubiquitous FcHO1/2 BAR-domain proteins, to bind especially low curvature membranes with highest affinity [205]–[208]. Sgip1 binds to the ITSN1 SH3A domain as does Synaptojanin1 [198], [199], [201], whereas AP2 binds to the ITSN1 SH3A-SH3B linker domain [199]. Therefore, Sgip1/AP2 compete with Synaptojanin1 for ITSN1 binding and this might explain the further reduction in the Synaptojanin1 stCCV levels (Figure 3.5) [164]. The ratio of ITSN1 to a Sgip1/AP2 complex should determine how efficiently ITSN1 can bind Synaptojanin1. Therefore, next the levels of Sgip1 in wt-ko canCCV and wt stable CCV and ko stCCV are compared. In Figure 3.5.B-C, it is shown that AP1/σ1B ko synapses contain wt levels of Sgip1 [164]. There are also wt levels of Sgip1 in both ko canCCV and ko stCCV as compared to wt canCCV and wt stable CCV, respectively [164]. However, stCCV contain slightly more Sgip1 than wt stable CCV (Figure 3.5.B-C) [164]. It has been already shown in Candiello *et. al* 2017 that both ko canCCV and ko stCCV also contain wt levels of AP2 as compared to respective wt CCV pools [85]. The Sgip1 and AP2 levels match, thereby implying identical budding kinetics of canCCV and stCCV in ko synapses [85], [164]. The excess of Sgip1/AP2 over ITSN1 in ko stCCV can further reduce the binding of Synaptojanin1 to ITSN1 [85], [164]. Even though these data clearly indicate that a competition among Sgip1/AP2 and

Synaptojanin1 for ITSN1 binding is responsible for the further reduction (20 %) in Synaptojanin1 levels in ko stCCV, it does not explain the lower amounts of ITSN1 in stCCV compared to wt stable CCV. Thus, the potential contribution of other ITSN1 binders to the regulation of ITSN1 CCV levels is needed to be investigated [164].

3.5.2. The ITSN1 EH-domain binding proteins Stonin2 and Epsin

Stonin2 and Epsin interact with ITSN1 through its two N-terminal EH-domains [198]. It is possible that their levels determine the amount of ITSN1 in a CCV. Therefore, the Stonin2 and Epsin levels are also compared between both CCV classes from wt and ko synapses [85], [102]. It has been shown in Kratzke *et al.* 2015 and in Candiello *et al.* 2017 that Stonin2 levels were reduced down to 40 % of wt canCCV levels in ko canCCV [85], [102]. However, the ko stCCV contained the same amount of Stonin2 as the wt stable CCV [85], [102]. So, the Stonin2 level does not limit the ITSN1 amount in stCCV [85], [102]. Epsin is the second protein that interacts with ITSN1 through those two EH-domains [198] as indicated in Figure 3.5.A [164]. Besides interacting with ITSN1, Epsin also interacts with PI-4,5-P_2 of the PM, with AP2 and with clathrin [49], [52], [209]–[211]. Its ubiquitin-interacting motif (UIM) binds to ubiquitinated cargo proteins [212], [213]. Furthermore, its ENTH domain binds to the PM and inserts itself into the cytoplasmic leaflet, which pushes the head groups of the phospholipids apart. This decreases the force required to bend the membrane into a clathrin-coated pit and to form a vesicle [214]. The key function of Epsin is defined as being an endocytic clathrin co-adaptor for the selection of specific cargo proteins in the CME pathway [215], [216]. However, its critical roles in CCV coat dynamics are still not fully elucidated. In 2014, Messa *et al.* showed impaired CME in Epsin ko embryonic fibroblasts and they have also observed an accumulation of early stage clathrin-coated pits (CCPs) [215]. Moreover, they showed that Epsin facilitates the interaction of actin cytoskeleton with CCPs suggesting its involvement in the generation of force for the invagination and fission of the CCPs into a vesicle [215]. In our previously published data in Kratzke *et al.* 2015 and Candiello *et al.* 2017, AP180 endocytic accessory protein, whose ANTH domain acts like the Epsin ENTH domain, is decreased down to almost 50% of wt levels in both ko canCCV and in ko stCCV [85], [102]. Thus, it is reasonable to expect an increase in the levels of

Epsin in both CCV classes of the ko in order to compensate the functionally equivalent ANTH domain containing AP180 levels in CCVs. The levels of Epsin in AP1/σ1B ko synapses was slightly increased to 115 % of wt levels [102]. In contrast to the expected results, the levels of Epsin are reduced down to 30 % of wt in ko canCCV [102]. and to 65 % of wt stable CCV levels in ko stCCV (Figure 3.5.A) [164].
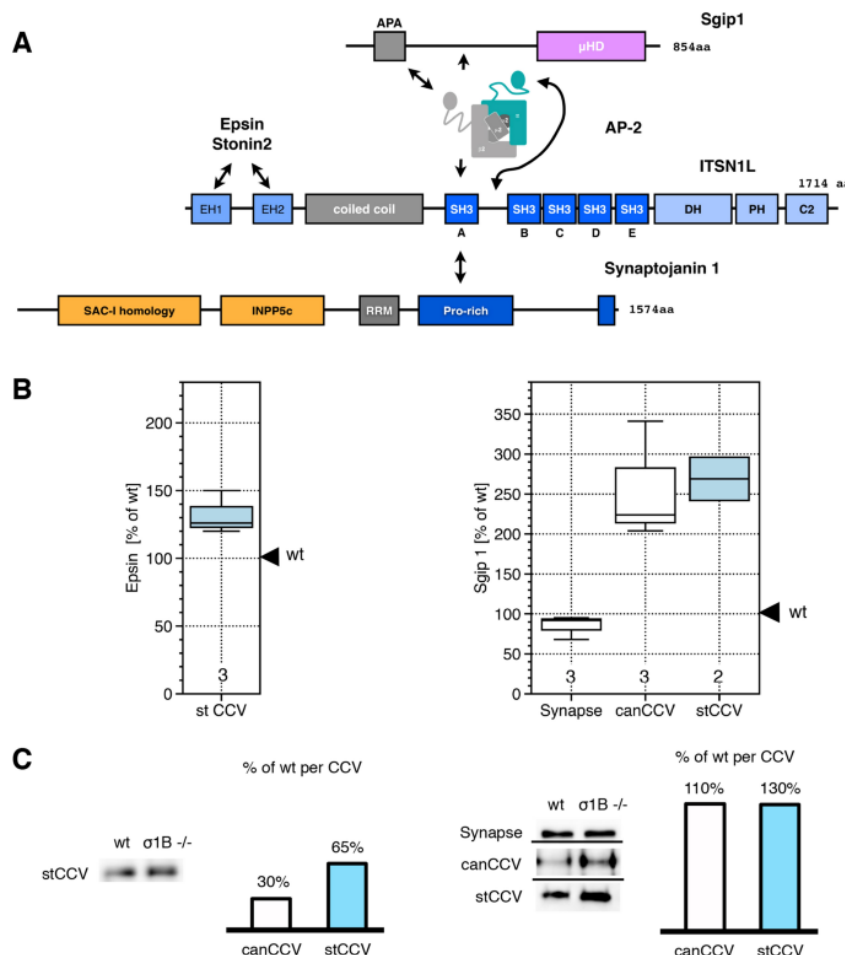
Figure 3.5. The protein domain organization of Sgip1, ITSN1 and Synaptojanin1, and the comparision of Epsin and Sgip1 levels between wt-ko fractions. (A) Epsin, Sgip1/AP2 and Synaptojanin1 binding of ITSN1 are demonstrated. Epsin and Stonin2 bind ITSN1 via its EH-domains, Sgip1 binds ITSN1-SH3A, as does Synaptojanin1, and AP2 α-adaptin ,ear' domain binds ITSN1 between SH3A-SH3B linker domains and the β2-adaptin ,ear' domain binds the APA domain of Sgip1. Sgip1/AP2 complex competition with Synaptojanin1 for the binding of ITSN1 SH3A domain is also indicated. **(B)** For Epsin (85 kDa) only stCCV levels are shown, because synapse and canCCV data have been published previously in Kratzke *et al.* 2015 (see text in Section 3.5.2) [102]. Alterations in the levels of Sgip1 (95 kDa) between wt- AP1/σ1B ko subfractions are shown. The Western-blot signal intensities from wt brain subfractions are defined as 100% and the values from ko samples are expressed relative to wt samples. Numbers below the box-plots denote the repeats of experiments with independent biological wt-ko pairs. **(C)** Representative Western-blot images used for quantifications are demonstrated. Bar diagrams indicate changes in protein levels per CCV [164]. The figure is adopted from Mishra, R., **Sengül, G.F.** *et al.* 2021. The figure is reprinted with the permission from Nature Springer, Scientific Reports open access Creative Commons CC BY provided a licence for the unrestricted use of any part of manuscript without special permission. Author contribution: R. Mishra contributed to the synapse (Sgip1), canCCV (Sgip1) and stabilized CCV (Epsin, Sgip1).

Alterations in the levels of Epsin in both canCCV and stCCV also do not match with the levels of ITSN1 in the respective CCVs [102], [164]. Therefore, it can be concluded that Epsin does not take a role in the recruitment of ITSN1 into a CCV. Additionally, these data also indicate that specialized pathway of stable and thus longer lived AP2 CCV is not stimulated to endocytose more Epsin cargos [102], [164].

3.5.3. The ITSN1 binding proteins Eps15 and Eps15L1

Eps15 and its homologue Eps15L1 bind to the ITSN1 coiled-coil domain, which is also known as its homodimerization domain [198] as indicated in Figure 3.6.A [164]. In addition, Eps15 and Eps15L1 form a tripartite complex with Sgip1 and AP2 during early CCP formation [205]–[208]. Therefore, the levels of Eps15 and Eps15L1 are compared between both wt-ko synaptic CCV classes [164]. Eps15 ko mice are viable and fertile [217]. These mice do not show a significant neuronal phenotype even though its ortholog in *Drosophila melanogaster* plays a key role in SV recycling [217]–[219]. In contrast, Eps15L1 is essential for neonatal viability. Eps15L1 ko mice die within the first two days after birth. Eps15L1 has nonredundant functions for the neonatal survival and it appears that Eps15L1 can compensate the absence of Eps15 [217]. Based on these data, it could be expected that Eps15L1 determines the CCV specific ITSN1 distributions rather than Eps15. The levels of Eps15 are not changed in AP1/σ1B ko synapses and also not in canCCV compared to the respective wt samples. However, Eps15 levels are reduced down to 50% of wt stable CCV levels in ko stCCV (Figure 3.6.B-C) [164]. The ko synapses contain slightly more Eps15L1 than wt synapses and Eps15L1 levels are reduced down to 65 % of wt levels in both ko canCCV and in ko stCCV (Figure 3.6.B-C) [164]. Even though Eps15L1 shows clear reduction in ko canCCV and stCCV, the recruitment of Eps15L1 is not differentially regulated between two CCV classes. Interestingly, Eps15 CCV levels are differentially regulated, but not the CCV levels of its indispensable homolog Eps15L1. Therefore, Eps15 specific functions exist and it regulates the stably incorporation of ITSN1 into AP2 CCV [164]. It has been shown that the highly homologous Eps15 and Eps15L1 proteins are regulated via numerous post-translational modifications such as phosphorylation, ubiquitination and acetylation [220], [221]. So, post-translational modifications may be responsible for the specific

function(s) of Eps15 in CCV pathway regulation, while the primary function of Eps15 appears to be the recruitment of specific cargo proteins [217], [220], [221]. Overall, our data propose a model indicating Eps15 determines the levels of ITSN1 stably incorporated into AP2 CCV and ITSN1 controls the levels of Synaptojanin1 stably incorporated into AP2 CCV. The CCV coat protein interactions regulating ITSN1 and Synaptojanin1 CCV levels and thus CCV stability and half-life are summarized in Discussion section (in Figure 4.1).
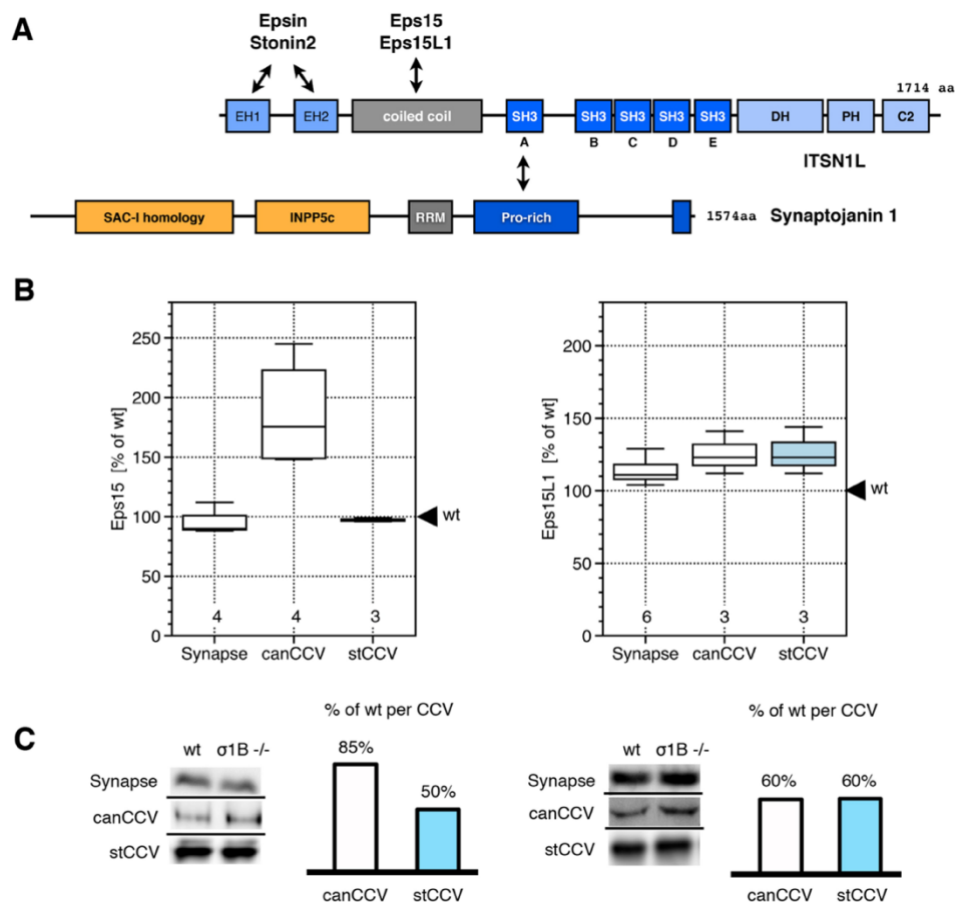
Figure 3.6. The protein domain organization of Synaptojanin1 and ITSN1, and the comparison of Eps15 and its homolog Eps15L1 between wt-ko synapse and synaptic AP2 CCV pools. (A) The protein domain organization of ITSN1 and Synaptojanin1 and the interactions of ITSN1 with Eps15 and its homolog Eps15L1 via its coiled coil domain are demonstrated in the cartoon. **(B)** Changes in the levels of Eps15 and Eps15L1 are shown between wt and AP-1/σ1B ko synapse, canCCV and wt stable and ko stCCV. The wt protein levels in each cellular fraction are defined as 100 % and AP-1/σ1B ko protein levels are calculated relative to wt. The numbers at the bottom of box-plots in each subfraction indicate the numbers of wt-ko biological replicates. **(C)** The representative gel images from Western blot experiments used for quantifications are shown for Eps15 (140 kDa) and Eps15L1 (75 kDa). The bar diagrams are drawn to indicate alterations in the levels of Eps15 and Eps15L1 per CCV [164]. The figure is adapted from Mishra, R., **Sengül, G.F.** *et al.* 2021. The figure is reprinted with the permission from the Nature Springer, Scientific Reports open access Creative Commons CC BY provided a licence for the unrestricted use of any part of the manuscript without special permission. Author contribution: R. Mishra contributed to canCCV (Eps15), stabilized CCV (Eps15, Eps15L1) and G.F. Sengül contributed to synapse (Eps15, Eps15L1), canCCV (Eps15, Eps15L1).

3.6. Regulation of the clathrin-cage disassembly ATPase Hsc70 in AP2 CCV

As it was described in the introduction (in Section 1.10), stCCV are more stable than wt stable CCV, because of the alterations in three CCV proteins. The stCCV have less of the clathrin-cage disassembly ATPase Hsc70, they have more of the AP2 activating kinase AAK1 and less of the PI-4,5-P_2 phosphatase Synaptojanin1 [85], [164]. After we had resolved the CCV protein network, which determines CCV levels of Synaptojanin1, I focused on the analysis of the molecular mechanisms, which regulate CCV levels of Hsc70. While AP1/σ1B ko canCCV contain wt levels of Hsc70, the stCCV contain 50% less Hsc70 compared to wt stable CCV [85], [164]. My predecessors in this project already demonstrated that the levels of the two Hsc70 J-domain co-chaperones auxilin1 and GAK/auxilin2 and as well as the pre-synapse specific AP2 CCV chaperone CSPα are not differentially regulated between two AP2 CCV classes [85], [102], [164]. Therefore, I started with the analysis of the CCV levels of additional proteins, which have been implicated in the regulation of Hsc70 functions in CCV. These are the neuronal cell adhesion protein CHL1 [222], the Hsc70 nucleotide-exchange-factor (NEF) and chaperone Hsp110 [223] and also the Hsc70 working-partner chaperone Hsp90 [224].

3.6.1. CHL1 does not recruit Hsc70 into AP2 CCV

Pre-synaptic neuronal cell adhesion molecule (NCAM) close homolog of L1 (CHL1), also called as NCAM-like 1 (NCAM-L1) protein, has been identified as a binding partner for the clathrin-uncoating ATPase, Hsc70. A Hsc70 binding motif was detected at the intracellular domain of CHL1 [222]. Furthermore, CHL1 deficiency leads to decrease in the levels of Hsc70 on SVs. The subsequent distruption of CHL1:Hsc70 complexes causes the accumulation of CCVs in the synapses of CHL1 deficient mice [222]. Based on these data, a model was proposed by Leshchyns'ka *et al.* 2006 and colleagues, that CHL1 determines the levels of Hsc70 in synapses and, most importantly, also in synaptic CCV, thereby regulating the uncoating of synaptic CCVs [222]. To test the correctness of their model, the alterations in the levels of CHL1 in AP1/σ1B ko synapses and in synaptic CCVs are were investigated. Previous published work of our group showed that Hsc70 levels were not changed in AP1/σ1B ko synapses [102]. Therefore, it was expected to detect no changes in the AP1/σ1B ko

synapse levels of CHL1 compared to wt levels, based on the model proposed by Leshchyns´ka *et al.* 2006 [222]. However, the CHL1 level is increased in AP1/σ1B ko synapses to 130 % of wt levels (Figure 3.7). If the proposed synaptic function of CHL1 by Leshchyns´ka *et al.* 2006 was correct, there would be wt levels of CHL1 in ko canCCV, but ko stCCV would contain less CHL1 than the wt stable CCV. The ko canCCV contain 70 % of wt CHL1 levels. However, in contrast to the expected reduction in stCCV CHL1 levels, the obtained results clearly demonstrate an enrichment of CHL1 in ko stCCV to 230 % wt stable CCV levels (115 % wt CHL1 levels per CCV). Therefore, our data speak against the suggested function of CHL1 in the regulation of Hsc70 levels in synapses and in synaptic CCV.
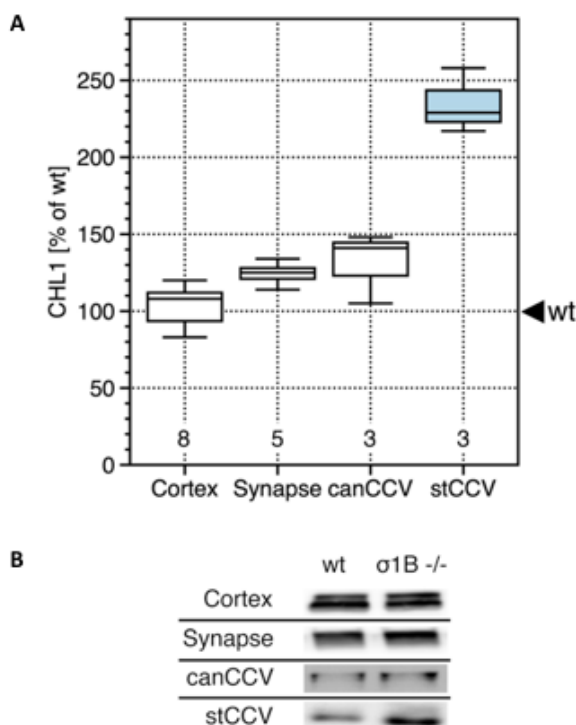
Figure 3.7. The comparison of CHL1 levels between wt-ko subcellular fractions. (A) The changes in the levels of CHL1 protein in AP1/σ1B ko cellular fractions relative to the corresponding wt samples are displayed. The quantified band intensities from wt proteins are set to 100 % and ko protein levels are expressed as compared to wt values. Numbers of biological replicates are denoted at the bottom part of the box-plot for each wt-ko subfractions **(B)** Representative semi-quantitative Western-blot images used for the quantifications are indicated for each wt-ko cellular fraction. The estimated molecular weight of CHL1 is 175 kDa. G.F. Sengül performed all the experiments to generate the complete figure.

3.6.2. The Hsc70 NEF, Hsp110 and Hsc70 co-worker Hsp90 are not involved in the stabilization of AP2 CCV

Hsc70 is recruited to the center of clathrin triskelia by its co-chaperons auxilin1 and GAK/auxilin2 for the uncoating of CCV. Clathrin basket disassembly takes place upon ATP hydrolysis. However, clathrin forms a stable complex with Hsc70*ADP [53]. This persistent clathrin:Hsc70*ADP complex can be dissociated by nucleotide exchange factors (NEFs) that release ADP from Hsc70 and allow ATP to bind and to induce the distruption of Hsc70 and clathrin associations [143]. Hsp110 is a NEF for Hsc70 and it has been shown that Hsp110 regulates the amount and ATPase activity of Hsc70 in CCV uncoating process [143], [223], [225], [226]. Therefore, next the levels of Hsp110 are compared between wt and AP1/σ1B ko cortex, synaptosome and both CCV fractions. Whilst there are 130 % of wt Hsp110 levels in AP1/σ1B ko cortices, its levels are decreased down to 40 % of wt levels in AP1/σ1B ko synapses (Figure 3.8.A). This was surprizing since the level of Hsc70 in AP1/σ1B ko synapses was maintained at the wt levels [102]. Even though any details are not known yet, appearently Hsp110 functions are altered in AP1/σ1B ko synapses. A reduction in Hsp110 levels is also sustained in AP1/σ1B ko synaptic CCVs. It is reduced down to 50 % of wt levels in AP1/σ1B ko canCCV whereas ko stCCV contain only 30 % of wt stable CCV levels (Figure 3.8.A). However, there were wt levels of Hsc70 in AP1/σ1B ko canCCV and it was reduced down to 50 % of wt stable CCV levels in AP1/σ1B ko stCCV [85], [102]. In Figure 3.8.B, it can be easily detected that the ratios of Hsc70:Hsp110 are maintained in ko stCCV as compared to ko canCCV. Therefore, the amount/activity of Hsp110 in ko canCCV is sufficient or in other words is not limiting the activity of Hsc70 for CCV uncoating. Furthermore, the reduction in the levels of Hsp110 in ko stCCV exclaims that it is not responsible for the formation of stabilized CCV in AP1/σ1B ko synapses.
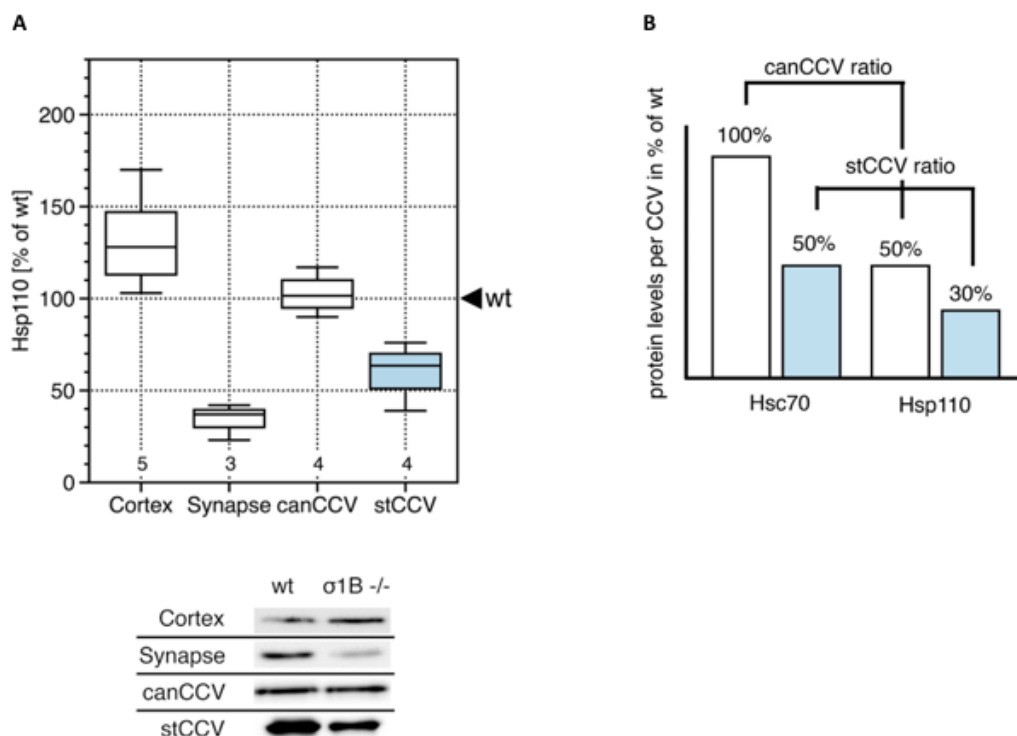
Figure 3.8. The comparison of Hsc70 NEF Hsp110 levels between wt-ko subcellular fractions and the comparison of Hsc70:Hsp110 ratios in AP2 CCV. (A) Changes in the amunts of the Hsc70 NEF, Hsp110 and representative semi-quantitative Western blot images are shown in wt and AP1/σ1B ko cellular fractions. The band signal intensities from wt proteins are defined as 100 % and ko values are calculated relative to wt. Numbers below each box-plot diagram denote the numbers of independent biological wt-ko replicates for each data set. The estimated molecular weight of Hsp110 is 110 kDa. **(B)** Bar plots summarizes the changes in the levels of Hsc70, Hsc70 bar diagrams are drawn based on the published data in Kratzke *et al.* 2015 and Candiello *et al.* 2017 [85], [102], and Hsp110 in canCCV and stCCV levels, in % per CCV. Hsc70:Hsp110 ratios in canCCV and in stCCV are shown in black arrow-lines. Data contribution: R. Mishra contributed to cortex (Hsp110), synapse (Hsp110), canCCV (Hsp110) and stabilized CCV (Hsp110) and G.F Sengül contributed to canCCV (Hsp110).

Heat shock protein 90 (Hsp90) is also one another CCV chaperon with intrinsic ATPase activity like Hsc70 and Hsp70, which takes role in the folding and remodeling of the proteins. Therefore, both Hsp90 and Hsc70 or Hsp70 are accepted as the key players of protein homeostasis in several cellular pathways. They can either work together or separately in many protein refolding processes [224]. The interaction of Hsp90 with Hsc70 [224], [227] makes it a strong candidate to discover novel regulatory mechanism(s) behind the Hsc70-mediated CCV uncoating. It could be highly possible that Hsc70 activity in the uncoating of AP2 CCV is regulated by Hsp90 protein. In order to test this assumption, the levels of Hsp90 in cortex, synapse and CCV fractions from wt and AP1/σ1B ko mice are assesed. The Hsp90 levels are increased to 150 % of wt levels in AP1/σ1B ko cortices, but its level slightly reduced

down to 80 % of wt Hsp90 levels in AP1/σ1B ko synapses (Figure 3.9). The levels of Hsp90 are not changed in AP1/σ1B ko canCCV, there are wt canCCV Hsp90 levels in AP1/σ1B ko synapses. Similiarly, Hsp90 is also present at almost the wt levels in ko stCCV which contains 80 % of wt stable CCV levels (Figure 3.9). In contrast to the expected results, the levels of Hsp90 in ko stCCV are not reduced to or even below Hsc70 levels, which were reduced down to 50 % of wt stable CCV levels [85]. Therefore, it can be assumed that Hsp90 does not collaborate with Hsc70 for the regulation of the AP2 CCV life cycle, thereby stabilization of AP2 CCV. However, it is still possible that Hsp90 does it indirectly by interacting with intrinsically disordered domains of CCV coat and/or endocytic cargo-adaptor proteins such as Epsin1, CALM and AP180 [228].
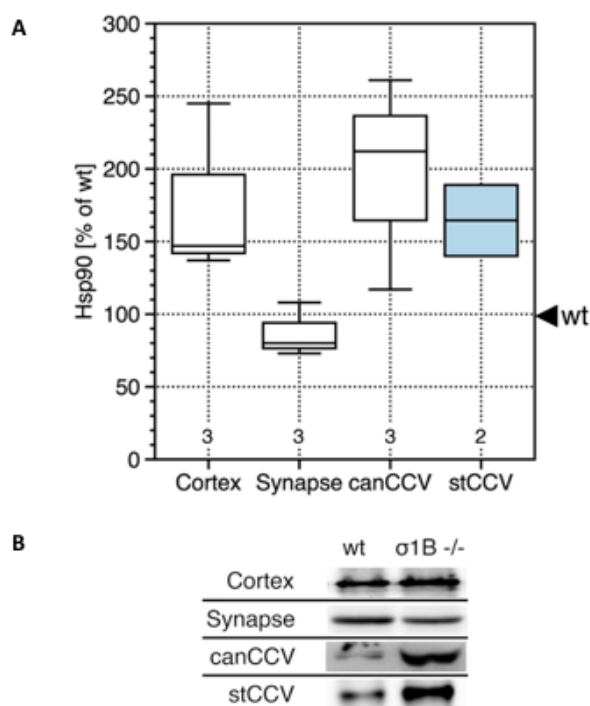
Figure 3.9. The comparisons of Hsc90 between wt-ko subcellular fractions. (A) Alterations in the amount of the Hsc70 co-chaperone Hsp90 are demonstrated in AP1/σ1B ko cellular fractions as compared to wt samples. The quantified band signal intensities from wt samples are defined as 100 % and ko values are expressed relative to wt. Numbers below each box-plot diagram designate the numbers of biological wt-ko replicates for each subfractions. **(B)** Representative semi-quantitative Western-blot images used for quantifications are illustrated for each cellular fraction; Hsp90 MW is 90 kDa. Data contribution: R. Mishra contributed to cortex, synapse and stabilized CCV and E. Candiello contributed to canCCV experiments for Hsp90 protein.

3.7. CCV class specific Hsc70 phosphorylation patterns

All known Hsc70 activity regulators were tested, as discussed in detail above, but none of them has CCV class specific protein levels, which would indicate their involvement in the enhanced stabilization of stCCV by reducing Hsc70 CCV levels. Therefore, we speculated that post-translational modifications (PTM), specifically phosphorylation (Pi), of Hsc70 and also of its two co-chaperons auxilin1 and GAK/auxilin2 might regulate Hsc70 recruitment into AP2 CCV. Therefore, I compare the Pi levels of them between the two wt and ko AP2 CCV classes. For this purpose, synaptosome and purified CCV proteins are separated on phos-tag ^{TM} SDS- PAGE (see Material and Methods section 2.2.10). The immobilized phos-tag ^{TM} functional group and Mn^{2+} bind to a phosphate group of a protein, which results in slower migration of a phosphorylated protein compared to its non-phosphorylated variant or even between hyper-Pi and hypo-Pi versions of a protein [172]. Proteins separated in this gel system can be transferred onto membranes as described in Material and Methods section 2.2.7 and proteins can be identified by immunoblotting as described in Material and Methods section 2.2.8. The migration behaviors of two co-chaperons auxilin1 and GAK/auxilin2 (auxilins) do not show significant differences between wt and AP1/σ1B ko synapses and canCCV under the tested phos-tag^{TM} SDS-PAGE conditions. However, Hsc70 migrates as two well-separated and strong bands in wt and AP1/σ1B ko synaptosomes, and in wt and AP1/σ1B ko synaptic canCCV as well as wt stable CCV and ko stCCV. The positions of hypo-Pi Hsc70 and of hyper-Pi Hsc70 bands are identical in wt and AP1/σ1B ko synapse proteins and in all AP2 CCV classes. The intensities of hyper-pi Hsc70 bands are higher than the hypo-Pi Hsc70 bands in all protein samples. The fractions of hypo-Pi Hsc70 in wt and AP1/σ1B ko synapses are 22 % and 17 % of total Hsc70, respectively (Figure 3.10.A-B). The wt canCCV have ~8 % and the AP1/σ1B ko canCCV have ~18 % of hypo-Pi Hsc70 (Figure 3.10). This difference does not lead to a measurable difference in their stability. However, wt stable CCV and ko stCCV have larger hypo-Pi Hsc70 protein fractions. The wt stable CCV contain 33 % hypo-Pi Hsc70 and AP1/σ1B ko stCCV contain 37 % hypo-Pi Hsc70 (Figure 3.10.A-B). These results from wt and AP1/σ1B ko canCCV and wt stable CCV and AP1/σ1B ko stCCV suggest that hypo-Pi Hsc70 might be responsible for the stabilization of wt stable CCV and of the ko stCCV. Additionally, the hypo-

Pi:hyper-Pi Hsc70 ratio of 18%:82% in AP1/σ1B ko canCCV enables fast CCV uncoating, while a 33%:67% ratio contributes to an increased stability of wt stable CCV (Figure 3.10.A-B). However, the ratio in AP1/σ1B ko stCCV is with 37%:63% relatively similar, questioning whether such a small difference can be responsible for the comparably increased stability of the AP1/σ1B ko stCCV. The study of Sousa *et al.* 2016 demonstrates that clathrin cage disassembly requires Hsc70 homodimers (shown in Figure 3.10.C-D) and possibly even larger Hsc70 homooligomers, which is in line with the excess of Hsc70 over clathrin in CCV [142]. Therefore, it is possible that modifications of Hsc70 inhibit its homodimerization, even with its unmodified version. Given these circumstances, the 4 % differences between hyper-Pi:hypo-Pi Hsc70 ratios of wt stable CCV and AP1/σ1B ko stCCV would double and lead to 8 % less Hsc70 for clathrin cage disassembly. The ko canCCV have 15 % less hypo-Pi Hsc70 than wt stable CCV and this leads to a difference in their stability. Therefore, the further increase of 8% hypo-Pi Hsc70 in stCCV compared to wt stable CCV could be responsible for the increased stability of stCCV. As a result, the phosphorylation level of Hsc70 can be proposed to be one mechanism regulating the Hsc70 uncoating activity in AP2 CCV.

3.8. Regulation of Hsc70 by binding of CaM/Ca^{2+} and CaM

Stevenson and Calderwood *et al.* 1990 identified a CaM/Ca^{2+} binding sequence motif within a 20 amino acid long helical domain in Hsc70. Interestingly, this sequence motif in the 257-277 amino acid residues of Hsc70, did not interact with CaM. Binding of CaM/Ca^{2+} to this Hsc70 domain blocks Hsc70 homodimerization [229]. PhosphoSitePlus summarizes the phosphoprotein mass spectrometry screens, which identified a total of 49 Pi sites in Hsc70. Among these 49 residues is also the T265 residue, which is located in the center of the CaM/Ca^{2+} binding domain of Hsc70 and it is also one of the most frequently detected Pi sites on Hsc70 [230]. Therefore, it is possible that phosphorylation of Hsc70 T265 by a yet unknown kinase regulates the formation of a Hsc70-CaM/Ca^{2+} complex and thus Hsc70 homodimerization and Hsc70 enrichment in AP2 CCV (Figure 3.10).

In order to answer the question whether CCV associated Hsc70 proteins are regulated by CaM/Ca^{2+} binding, I incubated Ca^{2+} loaded and Ca^{2+} free CaM agarose

beads (CABs) with purified wt and AP1/σ1B ko canCCV and as well as with wt stable CCV and AP1/σ1B ko stCCV. CCV Hsc70 proteins associated with Ca^{+2} treated and Ca^{+2} free CABs and as well as the proteins that remained in the pull-down supernatants were separated on phos-tag™ SDS-PAGE and upon the transfer of proteins, membranes are immunoblotted with anti-Hsc70 antibody (see Material and Method section 2.2.4, 2.2.7-8, 2.2.10).

The CaM/Ca^{2+} beads isolate from wt and from AP1/σ1B ko canCCV comparable amounts of hyper-Pi Hsc70 CCV, and only trace amounts of hypo-Pi Hsc70 (Figure 3.10.E). However, the majority of Hsc70 proteins are detected in the supernatants of the pull-down experiments (Figure 3.10.E). These data suggest, that the majority of hyper-Pi and hypo-Pi Hsc70 proteins of wt and ko canCCV are T265-Pi Hsc70 proteins and that CaM/Ca^{2+} does not inhibit the activity of canCCV associated hyper-Pi and hypo-Pi Hsc70 proteins (T265-Pi). Surprisingly, also the Ca^{2+} free CaM beads immunoisolated a second fraction of wt and AP1/σ1B ko canCCV, which also do not differ between the two genetic backgrounds. Also, CaM isolate more hyper-Pi Hsc70 from wt and AP1/σ1B ko canCCV than hypo-Pi canCCV, but less canCCV compared to CaM/Ca^{2+}. Importantly, the CaM beads isolate hypo-Pi and hyper-Pi Hsc70 from wt and AP1/σ1B ko canCCVs which migrated slightly faster than those isolated by CaM/Ca^{2+} beads (Figure 3.10.E). The difference in their migration is small and within the band widths of total hyper-Pi and hypo-Pi Hsc70 protein bands and thus these proteins may differ in just one phosphorylation side (Figure 3.10.E). This difference in Hsc70 phosphorylation uncovers a previously unknown and uncharacterized CaM binding motif in Hsc70, because the CaM/Ca^{2+} motif is not bound by CaM. However, the differences in canCCV Hsc70 phosphorylation patterns are more complex, because the Hsc70 proteins in the supernatants also migrate as fast, but are not bound by CaM (Figure 3.10.E). As a result of this experiment, four different Hsc70-Pi variants within the particular fractions of wt and AP1/σ1B ko canCCV are identified via CaM/Ca^{2+} and CaM beads binding.

These results about the differential Pi patterns of CCV Hsc70 proteins can be interpreted as canCCV in different maturation stages. The canCCV with hyper-Pi and T265 Hsc70 could be inhibited by CaM/Ca^{2+} and CaM to prevent clathrin cage disassembly before cage assembly is completed so that a CCV can be formed. So, these

canCCV could be younger canCCV. The other fraction of canCCV containing hyper-Pi and T265-Pi Hsc70 and hypo-Pi and T265-Pi Hsc70 proteins is not inhibited by CaM/Ca^{2+} and so, these canCCVs are presumably fully matured canCCV, whose coat can be readily disassembled so that their vesicles can fuse with early endosomes.

Contrary to the experiments with wt and AP1/σ1B ko canCCV, only hypo-Pi and no hyper-Pi Hsc70 proteins have been isolated by CaM/Ca^{2+} and by CaM beads, when wt stable CCV and AP1/σ1B ko stCCV were incubated with the beads (Figure 3.10.E). In addition, all these hypo-Pi Hsc70 proteins from longer-lived CCV migrated slightly faster than those of the hypo-Pi Hsc70 proteins of canCCV isolated specifically by CaM/Ca^{2+} beads. They migrated to the same positions of hypo-Pi Hsc70 of canCCV isolated by CaM beads and those which are not bound at all (Figure 3.10.E). Thus, the dimerizations of hypo-Pi Hsc70 proteins of wt stable CCV and ko stCCV are inhibited by CaM/Ca^{2+} (T265) and by CaM.

However, pull-down supernatants of both CaM/Ca^{2+} and CaM experiments with wt stable CCV and AP1/σ1B ko stCCV contain neither hyper-Pi, T265-Pi, Hsc70 nor hypo-Pi, T265-Pi Hsc70 proteins (Figure 3.10.E). This could be due to the fact that these proteins weakly interact with CaM/Ca^{2+} and CaM beads, so that hyper-Pi Hsc70 proteins are isolated, but they are lost in the wash fractions. However, hyper-Pi Hsc70 proteins are not also detected in the wash fractions. Even though the Western-blot membranes are overexposed for a longer period of time, only negligible amounts of hyper-Pi Hsc70 proteins are observed in the wash fractions. Therefore, it is most likely that hyper-Pi Hsc70 proteins of wt stable CCV and ko stCCV are dephosphorylated during the pull-down experiments and converted into hypo-Pi Hsc70 proteins, which exhibit increased binding affinity towards CaM/Ca^{2+} and CaM beads. Apparently, phosphatase activities are not sufficiently inhibited in wt stable CCV and ko stCCV, whereas this is not the case for canCCV. Thus, this demonstrates that wt stable and ko stCCV show higher Hsc70-Pi phosphatase activities than canCCV. Furthermore, the small differences in migration behaviour indicate additional Pi Hsc70 residues, which weaken Hsc70 binding to CaM/Ca^{2+} and CaM. The Hsc70 residue S275-Pi is a candidate, because it is positioned at the end of the helical Hsc70 domain to which CaM/Ca^{2+} binds (Figure 3.10.C-D). This domain does not bind CaM and thus another Hsc70 residue should interfere with CaM binding.
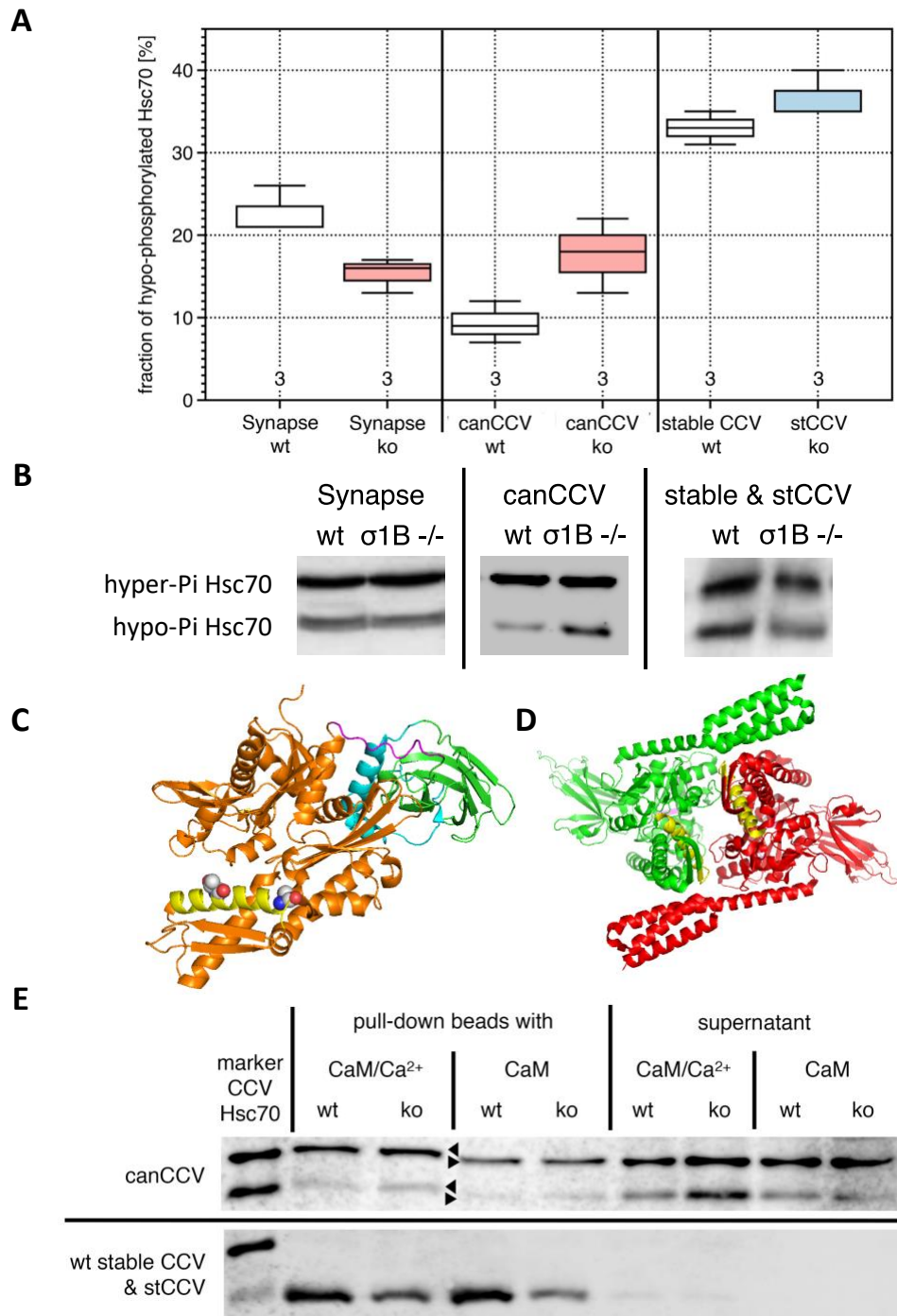
Figure 3.10. The regulation of Hsc70 uncoating activity in AP2 CCV via phosphorylation. (A) CCV class specific changes in Hsc70 Pi levels are analysed by phos-tag[TM] SDS-PAGE in wt and AP1/σ1B ko synapse and AP2 CCV. The numbers below the box-plot indicates the numbers of wt-ko independent biological replicates. **(B)** Representative semi-quantitative Western-blot images are demonstrated for each tested condition in wt-ko canCCV and wt stable and ko stCCV. **(C)** The structure of Hsc70 as obtained from Protein Data Bank (2kho.pdb) is indicated. Color codes: yellow shows CaM/Ca^{2+} binding domain involving T265 and S275 side chains, orange shows nucleotide binding domain, pink shows J-domain binding domain, cyan and green show substrate binding domain α and β, respectively. **(D)** The structure of Hsc70 dimer as obtained from Protein Data Bank (4jne.pdb) is indicated. Color codes: dimer is formed between red and green Hsc70s and the CaM/Ca^{2+} binding domain is shown with yellow in each Hsc70. **(E)** Representative semi-quantitative Western blot images of CaM/Ca^{2+} and CaM pull-down experiments with wt-ko canCCV and wt stable and ko stCCV are shown. Protein fractions are separated on phos-tag SDS-PAGE and then membarnes are developed with anti-Hsc70 antibodies. Arrow heads are drawn to point out the retention differences within the groups of hyper- and hypo-Pi Hsc70 proteins. All experiments and data analysis were performed by G.F. Sengül to obtain the figure.

Collectively, these data suggest that the phosphorylation of multiple of the 49 documented Hsc70 residues can alter the Hsc70 function in clathrin cage disassembly. This result unravels a much more complicated regulatory network as expected and makes it impossible to come up with a simple Hsc70 model. Therefore, the levels of CCV-associated kinases and as well as of phosphatases are compared between the AP2 CCV classes in order to reveal the novel mechanisms behind the regulation of CCV assembly and disassembly processes. The sequence specificities of differentially regulated kinases and/or phosphatases can point to the Hsc70 residues which regulate its activity in clathrin-cage disassembly.

3.9. Identification of CCV-specific Hsc70 phosphorylation sites using protein mass spectrometry

We also used protein mass spectrometry (MS) to identify CCV class specific phosphorylation sites in hyper-Pi and hypo-Pi Hsc70 proteins. The mouse Hsc70 sequence is 646 amino-acid long and contains 36 serine residues (50 % lower frequency than on average in the mouse proteome), 47 threonine residues (50 % higher frequency than on average in the mouse proteome) and 15 tyrosine residues (corresponding to the average frequency in the mouse proteome). As already mentioned in sections 3.7 and 3.8, a total of 49 Pi sites have been identified in Hsc70 in protein MS screens [230], which means that 50 % of its serine, threonine and tyrosine residues are substrates for kinases. The CaM/Ca^{2+} and CaM CCV Hsc70 binding assays revealed complex Pi-patterns of CCV associated Hsc70 proteins (see sections 3.8) and therefore, several of these 49 Pi sites should play a regulatory role(s) in Hsc70 activity, either alone, but more likely, in a combinatory manner. A 100% sequence coverage of Hsc70 is required to identify the Pi-patterns of CCV associated hypo-Pi Hsc70 and hyper-Pi Hsc70 proteins. This is of cause difficult to achieve and indeed previous studies analyzing regulatory Hsc70 Pi-residues were without success [231].

The hyper-Pi and hypo-Pi Hsc70 proteins of wt and ko canCCV are isolated out of phos-tag™ SDS-PAGE gels (see Materials and Methods section 2.2.10). The isolated proteins were digested with trypsin and the generated peptides were analyzed by MS, as described in section 2.2.12. Indeed, we also did not achieve a 100%

sequence coverage of the hyper-Pi and hypo-Pi Hsc70 proteins. Therefore, we are unable to identify the various Hsc70 Pi-patterns or even single residues important for the regulation of CCV associated Hsc70 proteins.

Several of the previously identified 49 Pi sites on Hsc70 could affect the homodimerization of Hsc70, thereby determining its concentration under each vertex of the clathrin cage and thus regulating Hsc70 activity in clathrin cage disassembly and the initiation of AP2 CCV uncoating. It has been shown that Hsc70 is able to homodimerize in more than one orientation. So, different Hsc70 homodimers can take part in the regulation of CCV uncoating. The structure of a dimer may affect the extent of Hsc70 volume change during its ADP/ATP cycle. In order to determine which Hsc70 residues play a key role in the regulation of CCV life cycle, *in-vitro* and *in-vivo* assays with Hsc70 mutants have to be performed. These sets of experiments can also enable to quantify the influence of specific Hsc70 residues on its homodimerization and the disassembly of the clathrin cage. The involvement of multiple Pi sites of Hsc70 also strengthens the idea that its activity in the CCV life cycle can be regulated by several kinases and/or phosphatases. Our data on CCV-associated kinases and PP2A phosphatases will be helpful to verify Hsc70 residues regulating its concentration in AP2 CCV *in-vivo*. These enzymes may also support the identification of Hsc70 regulation in clathrin-cage disassembly in other cell types and tissues.

3.10. The levels of PP2A regulatory subunits are not differentially regulated between two AP2 CCV classes

Current knowledge is still unable to fully explain the regulatory mechanisms behind the CCV assembly and disassembly processes. However, most of the studies indicated that phosphorylation and dephosphorylation cycles of coat proteins determine the CCV lifespan [232]. The AP2 complex itself is also modified via phosphorylation of its subunits. Phosphatases hold an equally important role as kinases for the dynamics between the phosphorylation and dephosphorylation ratios of AP2 subunits. Previously performed studies indicated that Protein phosphatase 2A (PP2A) dephosphorylates AP2 β2 and µ2 adaptins [232], [233]. PP2A is a holoenzyme phosphatase which comprises a scaffolding A subunit, a regulatory B subunit and a catalytic C subunit. Whilst scaffolding A and catalytic C subunits share a high degree

of sequence homologies among eukaryotes, the most variable regulatory B subunits determine the substrate specificity of the various PP2A enzymes [233], [234]. Alterations in the levels of two regulatory subunits of CCV associated phosphatase PP2A namely, PP2R2B (B55β) and PP2R2C (B55γ), are analyzed between wt and AP1/σ1B ko cellular fractions. The levels of PP2R2B and PP2R2C are with 110-120 % of wt levels, slightly increased in both AP1/σ1B ko cortex and synapse. This upregulation in the protein levels of PP2A regulatory domains appears not to be for synapse-specific plasticity, because such an increase is also observed in AP1/σ1B ko cortices as well (Figure 3.11).
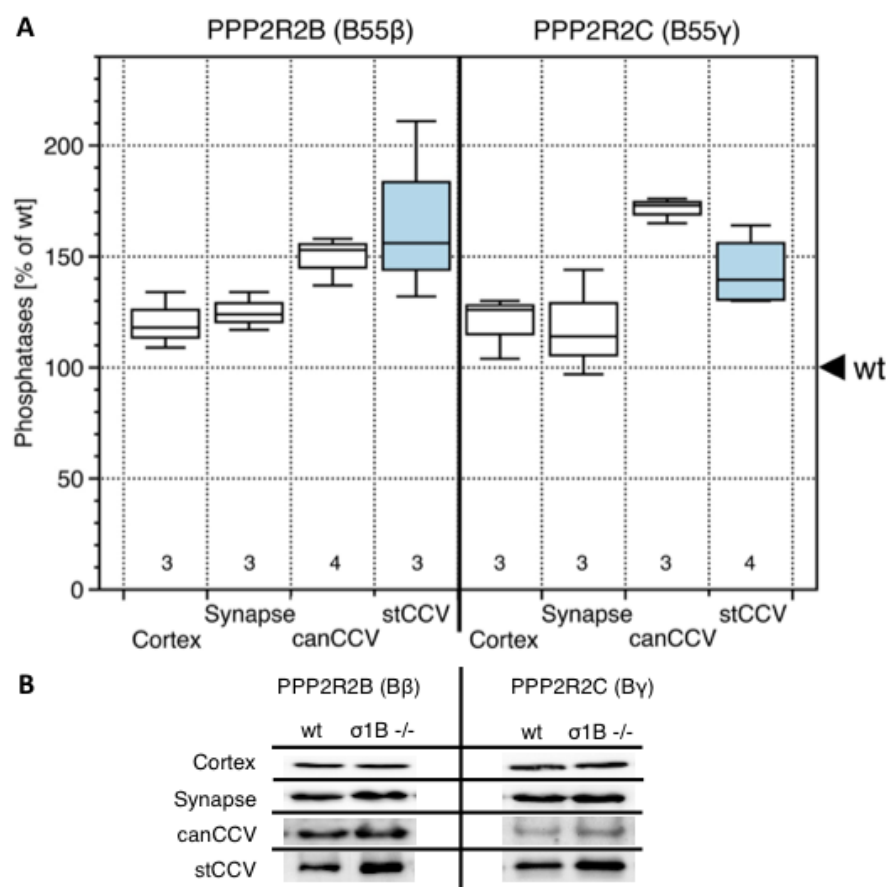
Figure 3.11. The comparison of PP2A regulatory subunits between wt-ko subfractions. (A) Changes in PP2A phosphatase regulatory subunits PPP2R2B (B55β) and PPP2R2C (B55γ) protein levels in wt and AP1/σ1B ko subfractions are indicated. The signal intensities of wt proteins are set to 100% and ko protein signals are expressed relative to wt. Numbers below each box-plot diagram indicate the numbers of independent biological wt-ko replicates for each data set. **(B)** Representative semi-quantitative Western-blot images used for quantifications are shown for each wt and AP1/σ1B ko cellular fractions. The molecular weight of PPP2R2B (B55β) is 50 kDa and of PPP2R2C (B55γ) is 50 kDA. Data contribution: R. Mishra contributed to canCCV (PPP2R2B, PPP2R2C), E.C. contributed to stable CCV (PPP2R2B) and G.F. Sengül contributed to cortex (PPP2R2B, PPP2R2C), synapse (PPP2R2B, PPP2R2C), stable CCV (PPP2R2C).

Both ko canCCV and ko stCCV contain almost the same amount of PPP2R2B (B55β) relative to their corresponding wt CCV levels (Figure 3.11). There are 75 % of wt PPP2R2B (B55β) levels in ko canCCV and in ko stCCV. Our results also indicate that ko canCCV contain almost wt levels of PP2R2C (B55γ) and ko stCCV have 70 % wt stable CCV PP2R2C (B55γ) levels (Figure 3.11). Apparently, the levels of PPP2R2B and PPP2R2C in both AP2 CCV classes are not differentially regulated. Therefore, the regulatory subunits of PP2A do not take role in the extension of the stCCV life span.

3.11. Kinases in the regulation of AP2 CCV stability and life span

To identify the protein kinases that are responsible for the regulation of AP2 CCV lifespan, the levels of six known CCV kinases are screened between wt and AP1/σ1B ko synaptic CCVs. Kratzke *et al.* 2015 and Candiello *et al.* 2017 revealed the differential recruitment of AAK1 between two CCV classes (Figure 3.12.A) [85], [102]. Both the amount and activity of AAK1 kinase were enriched in ko stCCV [85], [102]. As it was elaborately described in the introduction (Section 1.10), the hyperactivation of AAK1 ensures high-affinity AP2 membrane binding. Therefore, it has been proposed as one of the mechanisms that is responsible for the stabilization of AP2 CCV thereby regulating the AP2 CCV life cycle [85], [102]. Cyclin-G-associated kinase (GAK), also known as auxilin 2, serves as a co-chaperon for the CCV uncoating ATPase Hsc70 together with auxilin 1. Unlike auxilin1, GAK/auxilin2 contains a N-terminal kinase domain which can phosphorylate AP1 and AP2 on their μ1 and μ2 subunits, respectively [235]. Also because of this property, the changes in the levels of GAK/auxilin2 were checked in two synaptic CCV pools. Even though its levels were enriched in both ko canCCV and ko stCCV as compared to respective wt CCVs, GAK/auxilin2 levels were not differentially regulated between two CCV classes (Figure 3.12.B) [85], [102]. Thus, current data do not suggest the involvement of GAK/auxilin2 kinase in the AP2 CCV stabilization [85], [102].

3.11.1. The CCV kinases LRRK2, CVAK104, CK2 and DYRK1A

One candidate kinase proposed to be a regulator of the CME pathway is LRRK2 [165], [189], [223], [236]. As it is described in the context of the analysis of

an Endophilin A1 function in the regulation of Synaptojanin1 CCV levels (Section 3.1), neither LRRK2 levels nor its activity is differentially regulated between the two wt and AP1/σ1B ko synaptic CCV classes (Figure 3.12.A) [164]. Three more established CCV kinases, namely coated vesicle-associated kinase of 104 kDa (CVAK104) [237], Casein Kinase 2 (CK2) [238], [239] and Dual specificity tyrosine phosphorylation-regulated serine-threonine kinase 1A (DYRK1A) [240], [241] were studied in this thesis.
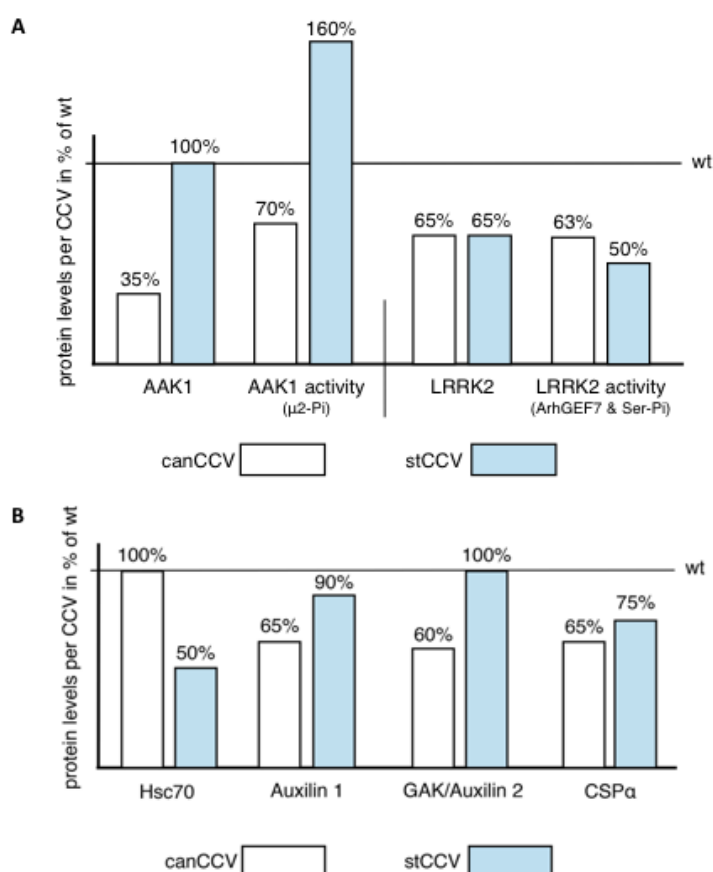
Figure 3.12. The summary of AAK1, LRRK2 and GAK/auxilin2 kinases and their activities in wt-ko AP2 CCV. (A) Summary of AAK1 and LRRK2 kinases and their activities in wt-ko AP2 CCVs are shown as bar-plots based on the published data in Candiello *et al.* 2017 and Mishra *et al.* 2021 [85], [164]. **(B)** Summary of Hsc70, its co-chaperons and pre-synaptic chaperone CSPα levels in wt-ko synaptic CCVs are displayed as bar-diagrams based on the published data in Kratzke *et al.* 2015 and Candiello *et al.* 2017 [85], [102]. Changes in the levels of proteins are given in % per CCV.

CVAK104, also known as SCYL2, is a member of SCY1-like family (Saccharomyces cerevisiae-like pseudokinase 1) protein kinases. Based on the MS analysis of CCV preparations from isolated CCV proteins, CVAK104 was identified as a CCV serine-threonine kinase. Furthermore, a direct interaction of CVAK104 with

clathrin and as well as with AP2 has been shown. Besides its autophosphorylation capability, *in-vitro* kinase assays indicated CVAK104-mediated phosphorylation of the AP2 adaptin β2 in the presence of poly-L-lysine [237]. Even though the β subunits of AP2 and AP1 complexes share 85 % amino acid sequence homology [48], CVAK104 does not phosphorylate β1 adaptin of the AP1 complex [237]. This result was surprising given the high conservation of β adaptins, which are even functionally redundant as they can compensate the absence of one another in many cellular pathways [48]. Furthermore, CVAK104 also associates with AP1 CCV [237], but AP1 CCV are not stabilized in AP1/σ1B ko synapses [66], [102]. So, CVAK104 was a candidate kinase that may regulate the AP2 CCV life cycle. CVAK104 levels are not changed in AP1/σ1B ko cortices compared to the wt, whereas it is slightly increased to 110 % of wt levels in AP1/σ1B ko synapses (Figure 3.13.A). Since the alterations in the protein levels of CVAK104 are AP1/σ1B ko synapse-specific, this also suggests that CVAK104 has a function in AP2 CCV life cycle regulation and most likely also in other pathways of the synaptic plasticity. The levels of CVAK104 are reduced down to 45 % of wt canCCV levels in ko canCCV and are decreased to 60 % of wt stable CCV in AP1/σ1B ko stCCV (Figure 3.13.A). The fact that CVAK104 is not recruited extra into the canCCV formed in ko synapses, but is actively recruited into stCCV, even so not to the levels of wt stable CCV, indicating CVAK104 may be involved in AP2 CCV life cycle regulation, but not so much in the extension of the AP2 CCV lifespan.

Casein Kinase 2 (CK2) has been identified as a Ser/Thr kinase that phosphorylates several CCV-associated proteins after their isolation *in-vitro*. Unlike many other CCV kinases such as GAK/auxilin2, CK2 is inactive when it associates with the PM enriched PI-4,5-P_2. However, it should become active during uncoating of CCV, because of the dephosphorylation of PI-4,5-P_2 [238], [239]. This suggests that its activity is required for the uncoating of CCV [238], [239]. CK2 forms a tetramer, which is composed of two α catalytic subunits and two β regulatory subunits [242] Since regulatory β domain of CK2 mediates its kinase activity [242], the levels of CK2β are investigated between wt and AP1/σ1B ko cortex, synapse and CCV fractions in the current study. CK2β levels are increased to 130 % of wt in AP1/σ1B ko cortices as well as in ko synapses (Figure 3.13.B). So, the alterations in the CK2β levels may

not be related to AP1/σ1B ko-induced synaptic plasticity, because they are not synapse specific. The recruitment of CK2β into two CCV classes are not differentially regulated. Both AP1/σ1B ko canCCV and ko stCCV contain approximately 70 % of wt CK2β levels per canCCV and per stCCV, respectively (Figure 3.13.B). Therefore, it seems that CK2β may not take on a role in the regulation of the AP2 CCV lifespan.

Dual-specificity tyrosine phosphorylation regulated-kinase 1A (DYRK1A) is a member of a proline-directed Ser/Thr protein kinase family. Its homologue in *Drosophila melanogaster* is highly conserved, also known as *minibrain* kinase, and regulates neuroblast proliferation during neurogenesis [240], [241]. It has been also shown that DYRK1A plays an important role in neurodevelopmental processes in vertebrates. Moreover, the discovery of the location of the *Dyrk1A* gene on human chromosome 21 revealed its association with Down Syndrome (DS) [243], [244]. The upregulation of *Dyrk1A* gene expression in patients with DS and also the overexpression of this gene in transgenic mice with certain DS phenotypes, including neurodevelopmental delay, cognitive decline and problems in memory and learning, further supported this finding with experimental evidences [243], [244]. Furthermore, the significant increase in the *Dyrk1A* mRNA expression in the hippocampus of Alzheimer´s Disease (AD) individuals convinces the scientists that DYRK1A is also important for adult brain functions [243], [244]. The later analysis of DYRK1A protein kinase led to the identification of its several substrates in the rat brain, ranging from microtubule-associated protein tau to transcription factors (TFs) such as forkhead TF family member FKHR [241], [245], in addition to R-synuclein and caspase 9 [241], [246], [247]. Intriguingly, DYRK1A kinase has been proposed to inhibit CME via the phosphorylation of endocytic proteins such as Dynamin1, Synaptojanin1 and Amhiphysin1 [240], [241]. Besides the putative inhibitory action of DYRK1A on the CME pathway, it has also been shown to trigger the uncoating of synaptic CCVs [240], [241]. Bearing all these publications in mind, DYRK1A is included into the investigated CCV kinase list. The levels of DYRK1A are not changed in AP1/σ1B ko cortices compared to the wt (Figure 3.13.C). However, it is increased to 140 % of wt DYRK1A levels in AP1/σ1B ko synapses (Figure 3.13.C). This ko synapse-specific upregulation of DYRK1A may alter its functions in SV exocytosis [240], [241] and in cytoskeleton organization [243], [244]. In contrary to literature about the inhibitory

effect of DYRK1A on CME, this increase does not prevent the stimulation of AP2 CME in AP1/σ1B ko synapses [85], [102]. The ko canCCV have 95% essentially wt DYRK1A levels (Figure 3.13.C). Since DYRK1A enhances CCV uncoating, ko stCCV should contain less DYRK1A than wt stable CCV. In ko stCCV, the levels of DYRK1A are reduced down to 50 % wt stable CCV levels (Figure 3.13.C). These results indicate that DYRK1A does not play an inhibitory role in the formation of CCV, but that it triggers the uncoating of CCV.
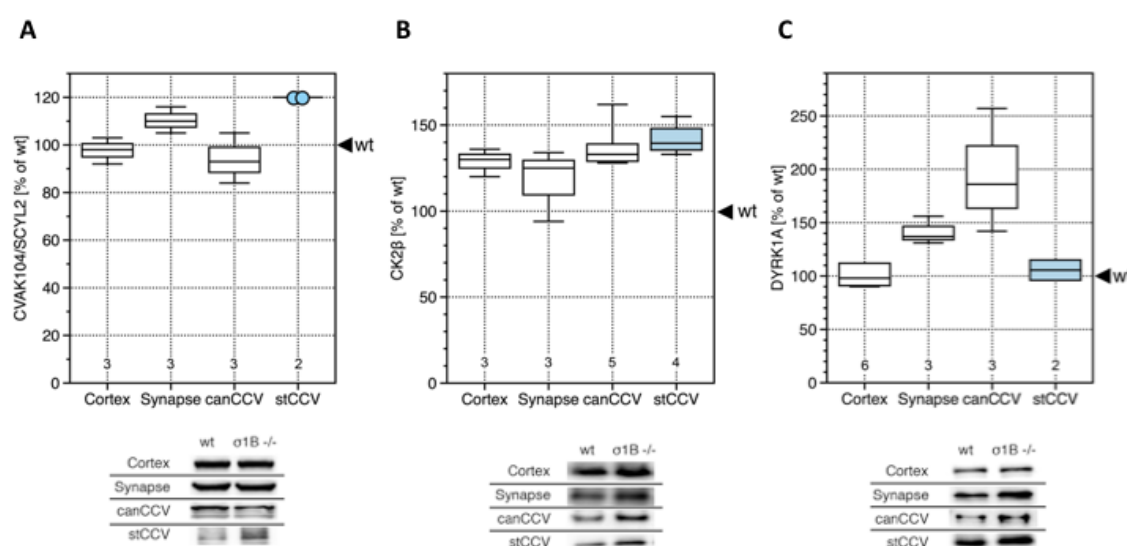
Figure 3.13. The alterations in the levels of of CVAK104, CK2β and DYRK1A CCV kinases in wt-ko subcellular fractions. Changes in the levels of **(A)** CVAK104/SCYL2, **(B)** CK2β and **(C)** DYRK1A kinases are shown in wt and AP1/σ1B ko cellular fractions. The signal intensities of protein bands in wt samples are set to 100 % and ko protein levels are calculated relative to wt. Numbers below each of the box-plots denote the numbers of the independent biological wt-ko replicates used for the quantifications. Representative semi-quantitative Western blot images used for quantifications are demonstrated below the diagrams for CVAK104/SCYL2 (75 kDa), CK2β (25 kDa) and DYRK1A (75 kDa) kinases. Data contribution: G.F. Sengül contributed to cortex (CVAK104, DYRK1A), synapse (CVAK104, CK2β, DYRK1A), canCCV (CVAK104, CK2β, DYRK1A), stabilized CCV (CVAK104, CK2β, DYRK1A) and R. Mishra contributed to cortex (CK2β), synapse (CK2β).

3.11.2 The roles of novel CCV kinases in AP2 CCV life cycle regulation

Previously performed MS analysis of synaptic CCV proteins identified kinases which did not belong to the group of well-characterized CCV-associated kinases. In our study, I have also analyzed these putative CCV kinases to reveal their involvement in the regulation of AP2 CCV life cycle. Therefore, the levels of Activated Cdc42-associated kinase 1 (ACK1), whose protein encoding gene is also known as Tyrosine-kinase non-receptor protein 2 (TNK2) [248], [249], of Doublecortin-like kinase 1 (DCLK1) [250], [251], of Calcium/Calmodulin-dependent kinase II δ (CaMK-IIδ), of

Ser/Thr protein kinase 39, which is also called as STE20/SPS1-related proline-alanine-rich protein kinase (SPAK) [252], and of its activator Calcium-binding protein 39 (CAB39), also known as Mouse protein 25 α (MO25α) [253], [254], were tested as well.

ACK1 protein levels are elevated to 140 % of wt levels in both AP1/σ1B ko cortices and synapses (Figure 3.14.A). Since ACK1 has been shown to phosphorylate a myriad of synaptic proteins [248], the increases in its levels in AP1/σ1B ko cortices and synapses imply the involvement of this kinase in neuronal plasticity. The pool of AP1/σ1B ko canCCV contain 130 % of wt ACK1 levels, corresponding to 65 % of wt ACK1 levels per canCCV (Figure 3.14.A). The ACK1 protein is found in the ko stCCV pool at 110 % of wt stable CCV levels, corresponding to 55% of wt ACK1 levels in a single stCCV (Figure 3.14.A). All these findings support the notion that ACK1 maintains its neuronal functions in AP1/σ1B ko brains, but it appears not to regulate the AP2 CCV life cycle. Interestingly, a ACK1 ko mouse model shows no apparent phenotype, while *in-vitro* and cell line studies revealed its association with distinct cellular processes [249]. Furthermore, there is no homologous kinase known and many of the binding partners and/or substrates of ACK1 have been implied to play a role in endosomal protein transport and in endocytosis processes [255]. Therefore, the elevated levels of ACK1 in AP1/σ1B ko brain can be linked to the stimulated CME and endolysosomal protein trafficking [66], [85], [102].

Next, the protein levels and the distribution of DCLK1 kinase are compared between wt and AP1/σ1B ko cellular fractions. DCLK1 levels are almost doubled to 170% of wt levels in AP1/σ1B ko cortices. In stark contrast, AP1/σ1B ko synapses contain with 40% of wt, less than half the amount of wt DCLK1 levels (Figure 3.14.B). The lower level of DCLK1 in ko synapses does not cause lower levels of it in synaptic CCV, but DCLK1 is not recruited into the enlarged pools of ko synaptic CCV (Figure 3.14.B). A ko canCCV contains 70 % and a stCCV contains 60 % of DCLK1 wt canCCV and wt stable CCV levels, respectively (Figure 3.14.B). This small difference between ko canCCV and stCCV strongly suggests that DCLK1 is not responsible for the stabilization of AP2 CCV. As it was reported in Chen *et al.* 2015 and Lipka *et al.* 2017, DCLK1 takes part in cytoskeletal organization to steer selective axonal and dendritic cargo transport [250], [251]. Based on the literature, the drastically decreased

DCLK1 levels in AP1/σ1B ko synapses may stabilize cytoskeletal networks so that transport of the fewer SV and as well as the endosomal maturation are promoted [102], [250], [251].

One other MS-detected candidate kinase was the CaMK-II isoform CaMK-IIδ. The alterations in the levels of CaMK-IIδ in AP1/σ1B ko cortices and synapses were published previously [102]. As it was shown by Kratzke, M. *et al.* 2015, CaMK-IIδ was increased to 120 % wt levels in AP1/σ1B ko cortices, whereas it was elevated to 160 % of wt levels in AP1/σ1B ko synapses [102]. The activity of CaMK-II enzymes is regulated via their binding of CaM/Ca^{2+} and their subsequent autophosphorylation [256]. After the CaMK-II enzymes are activated, they take on roles in the regulation of multiple cellular processes such as Ca^{2+} homeostasis [256], SV exocytosis [256], [257], cytoskeleton organization [256], [257] and memory and learning [256], [258], [259]. Therefore, the changes in the levels of CaM were also compared between wt and AP1/σ1B ko cellular fractions. As it was expected, the CaM levels are also elevated to 120 % of wt levels in AP1/σ1B ko cortices and to 135 % of wt levels in AP1/σ1B ko synapses. Intriguingly, this enrichment in the levels of CaMK-IIδ is not sustained in synaptic CCV. The levels of CaMK-IIδ are reduced down to 60 % of wt levels in AP1/σ1B ko canCCV. The recruitment of CaMK-IIδ into ko stCCV is further decreased and thus inhibited down to 33 % of a wt stable CCV (Figure 3.14.C). These data suggest that synaptic CCV require CaMK-IIδ for CCV uncoating and that reduced CaMK-IIδ levels are responsible for the extended stabilization of AP2 stCCV in AP1/σ1B ko synapses. As it is described in the Material and Methodology chapter, CCV isolation requires the inclusion of EGTA in the buffer solution (Section 2.1). Therefore, only the levels of Ca^{2+}-free CaM can be determined in synaptic CCV. In AP1/σ1B ko canCCV, CaM are reduced down to 64 % of wt, but CaM is recruited into ko stCCV reaching 82 % of wt stable CCV levels (Figure 3.14.D). This relative increase in stCCV CaM levels compared to ko canCCV may be linked to its enhanced binding to the hypo-Pi Hsc70 proteins of stCCV, however it may bind to other CCV proteins as well. Taken together, the synapse and CCV protein level data support a CaMK-IIδ function in AP2 CCV lifespan regulation, especially via the regulation of the activity of synaptic Hsc70 proteins.
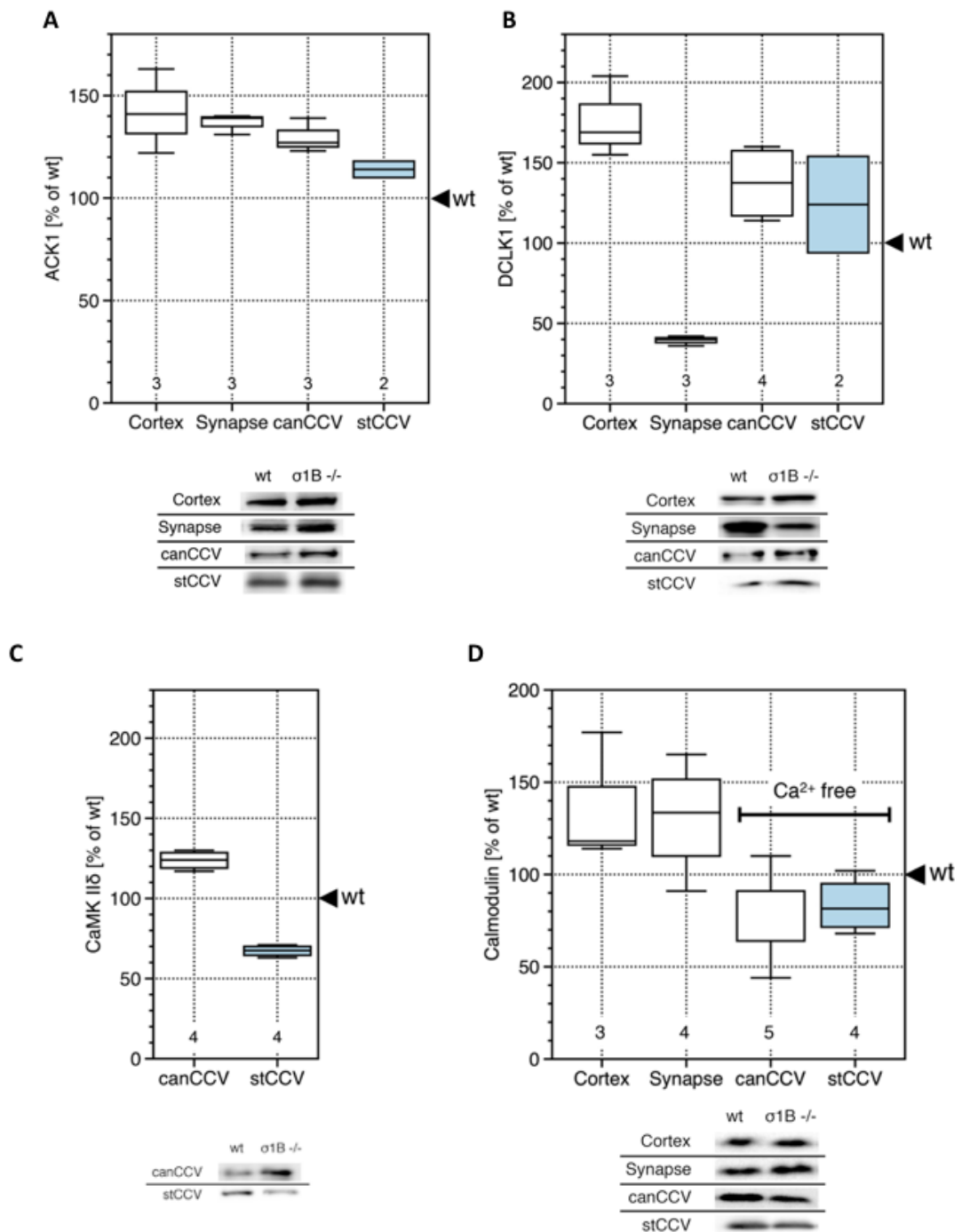
Figure 3.14. The comparison of ACK1, DCLK1, CaMKIIδ kinases and CaM levels between wt-ko cellular fractions. Changes in the levels of **(A)** ACK1, **(B)** DCLK1 **(C)** CaMKIIδ kinases and **(D)** CaM in wt and AP1/σ1B ko cellular fractions are shown. The signal intensities of protein bands in wt samples are set to 100 % and ko protein levels are calculated relative to wt. Numbers below each box-plot diagram denote the numbers of independent biological wt-ko replicates used for quantifications. Representative semi-quantitative Western-blot images used for quantifications are demonstrated below the diagrams for ACK1 (75 kDa), DCLK1 (70 kDa), CaMKIIδ (55 kDa) and CaM (20 kDa). Data contribution: G.F. Sengül contributed to cortex (ACK1), synapse (ACK1), canCCV (ACK1), stabilized CCV (ACK1). R. Mishra contributed to cortex (DCLK1, CaM), synapse (DCLK1, CaM), canCCV (DCLK1, CaM). E. Candiello contributed to canCCV (CaMKIIδ), stabilized CCV (DCLK1, CaMKIIδ, CaM).

94

The sterile20/SPS1 (Ste20)-related proline alanine rich kinase SPAK, also called as serine-threonine kinase 39 (STK39), is a member of the mitogen-activated protein kinase family [252]. The Ste20-related protein kinases comprise highly conserved protein sequences among fungi, plants and animals, thereby emphasizing their important regulatory roles [252]. Previous scientific research have described the expression pattern, the protein interactome, altered signaling pathways and physiological functions of SPAK (STK39) in different organ systems [252]. Based on the published works, SPAK (STK39) is involved in the modulation of excitatory and inhibitory neurotransmission [260], [261], Na^+-K^+-Cl^- ion cotransport [262], motor movement coordination and balance [252], [260]–[262] and is also in schizophrenia [262]. However, the substrates of SPAK (STK39) protein kinase in these distinct cellular processes are yet unidentified. Therefore, it is interesting that we have detected SPAK (STK39) in our previously performed MS analysis in isolated synaptic CCV. The semi-quantitative Western-blot analysis indicates that, SPAK (STK39) is slightly increased in AP1/σ1B ko cortices compared to wt, but that it is reduced down to 40 % of wt levels in AP1/σ1B ko synapses (Figure 3.15.A). However, the lower level of SPAK (STK39) in synapses does not hamper its recruitment into synaptic CCVs. There are 80 % and 95 % of wt SPAK (STK39) canCCV and of wt stable CCV levels in AP1/σ1B ko canCCV and in ko stCCV, respectively (Figure 3.15.A). Even though these data do not clearly suggest a role of SPAK (STK39) activity in the extension of the AP2 CCV lifespan these results still imply its involvement in the formation of AP2 CCV. Published *in-vitro* studies indicated that CAB39 stimulates the catalytic activity of SPAK (STK39) [253], [254]. Therefore, the levels of CAB39 are also compared between wt and AP1/σ1B ko cellular fractions. The increase in the levels of CAB39 in AP1/σ1B ko cortices are consistent with the SPAK (STK39) cortex data (Figure 3.15). However, there is only a 10 % reduction in the levels of CAB39 in AP1/σ1B ko synapses, which does not match the 60 % reduction of SPAK (STK39) in ko synapses (Figure 3.15). The ko canCCV contain 80 % of wt canCCV CAB39 levels. So, CAB39 is recruited into the ko canCCV to levels comparable with those of SPAK (STK39) and the wt ratio of SPAK (STK39)/CAB39 is maintained in ko canCCV. However, the ko stCCV contain only 60 % CAB39 of a wt stable CCV. So, it can be inferred that the reduced recruitment of CAB39 into ko stCCV leads to lower activation of SPAK

(STK39), even though its amount is not limited in ko stCCV. However, the recruitment of SPAK (STK39) into synaptic CCV, despite the dramatic decrease in its synapse levels, indicates its functions in CME, but more so in synaptic functions besides the CME pathway.
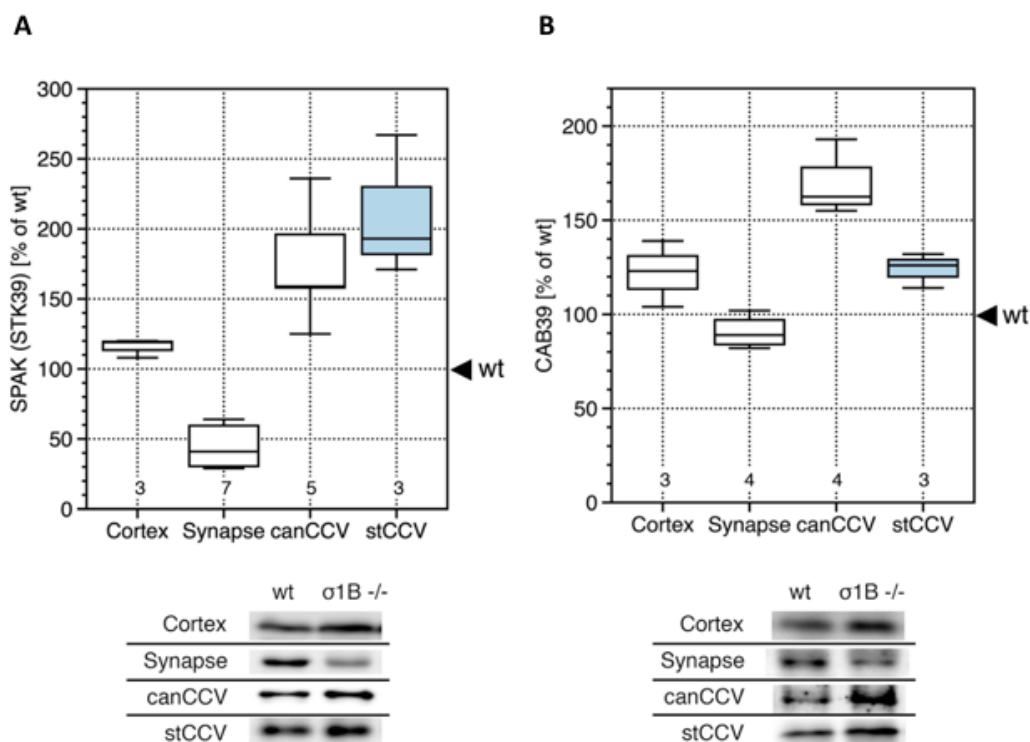
Figure 3.15. The comparison of SPAK (STK39) kinase and its activator CAB39 between wt-ko subfractions. Alterations in the levels of **(A)** SPAK (STK39) and **(B)** CAB39 in AP1/σ1B ko cellular fractions are compared to wt samples. The signal intensities of protein bands in wt samples are defined as 100 % and ko protein levels are calculated relative to wt. Numbers below each box-plot diagram denote the numbers of independent biological wt-ko replicates used for quantifications. Representative semi-quantitative Western blot images used for quantifications are shown below the box-plot diagrams for SPAK (STK39) (50 kDa) and CAB39 (40 kDa). Data contribution: G.F. Sengül contributed to cortex (CAB39), canCCV (STK39, CAB39), stabilized CCV (STK39, CAB39). R. Mishra contributed to cortex (STK39) and synapse (STK39, CAB39).

3.11.3. Kinases regulating AAK1 as AP2 CCV kinases

As described in the introduction, previously published studies of our lab demonstrate the crucial function of AAK1 kinase in AP2 CCV life cycle regulation and AP2 CCV lifespan extension [85]. Not only the amount of AAK1, but also its activity towards the AP2 µ2-adaptin is stimulated in ko stCCV [85]. AAK1 kinase activity is known to be regulated by several kinases in other pathways than AP2 CME and thus I tested whether those kinases are associated with CCV and subsequently

whether their levels are altered in CCV of AP1/σ1B ko synapses. Naturally, these kinases may also control the activity of Hsc70 in the CCV uncoating process.

These AAK1 kinases are LRRK2 [263], STK38S (serine-threonine protein kinase 38), that is also called as nuclear Dbf2-related kinase 1 (NDR1) [264], and STK38L (STK38-like or also known as NDR2) [264]. As it was already explained, neither LRRK2 activity nor its levels were differentially regulated between the two CCV classes [164]. The level of STK38S is elevated to 150 % wt levels in AP1/σ1B ko cortices, whereas it is reduced down to 70 % of wt levels in AP1/σ1B ko synapses (Figure 3.16.A). Nevertheless, STK38S is recruited into both ko synaptic CCV classes to wt canCCV and wt stable CCV levels, respectively (Figure 3.16.A). These results suggest that STK38S plays a crucial role in the regulation of AP2 CCV formation, even though the data cannot clearly depict the involvement of this kinase in the extension of the AP2 CCV lifespan. In addition to STK38S, the levels of STK38L are also compared between wt and AP1/σ1B ko cortices, synapses and the synaptic CCV. Its changes in AP1/σ1B ko cortex and synapse levels exhibit a similar profile to STK38S levels, but the changes are marginal (Figure 3.16.B). The levels of STK38L are increased to 110 % of wt in AP1/σ1B ko cortices and slightly reduced down to 90 % of wt in AP1/σ1B ko synapses (Figure 3.16.B). There are 80 % wt levels of STK38L (almost wt levels) in ko canCCV, as in the case of STK38S. However, a ko stCCV contains only 55 % STK38L of a wt stable CCV. The STK38L kinase is not actively recruited into stCCV and therefore, it can be responsible for a destabilization of AP2 CCV. This suggests that CCV STK38L modifies and inhibits CCV AAK1 activity, which may cause the reduced recruitment of AAK1 into ko canCCV. Furthermore, these data suggest that STK38S and/or STK38L may regulate the AP2 CME pathway via phosphorylating other CCV proteins including Hsc70.
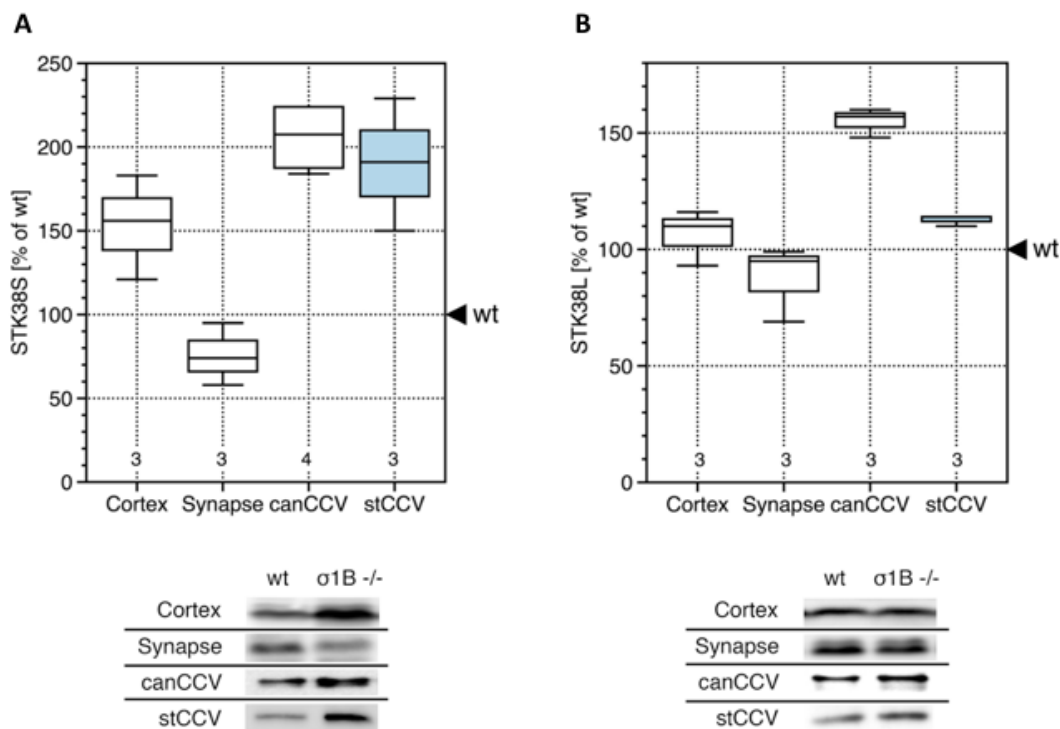
Figure 3.16. The levels of AAK1 regulating STK38S and STK38L kinases in AP2 CME pathway.
Changes in the levels of **(A)** STK38S and **(B)** STK38L kinases in AP1/σ1B ko cellular fractions as compared to wt samples are shown. The signal intensities of protein bands in wt samples are set to 100 % and ko protein levels are calculated relative to wt. Numbers below each box-plot diagram designate the numbers of independent biological wt-ko replicates used for quantifications. Representative semi-quantitative Western blot images used for quantifications are illustrated below each box-plot diagram for STK38S (50 kDa) and STK38L (50 kDa). Data contribution: G.F. Şengül contributed to canCCV (STK38S, STK38L), stabilized CCV (STK38S, STK38L). R. Mishra contributed to cortex (STK38S, STK38L) and synapse (STK38S, STK38L).

3.12. Stabilized AP2 CCV specific cargo proteins

A major question remains to be answered, is the question about specific functions of stabilized and thus longer lived AP2 CCV in protein sorting and protein transport. Previously, my predecessors in this project have shown that the scaffolding active zone proteins Git1 and Stonin2 are specific cargo proteins of stCCV [85]. Both surround the AZ in synapses and take part in the regulation of SV recycling [187], [265], by yet unknown molecular mechanisms. The analysis of a CHL1 function in Hsc70 regulation (described in Section 3.6.1) revealed that CHL1 is also a specific cargo protein of stCCV. These data suggested to test whether the specialized AP2 CCV endocytic route is preferentially followed by the other NCAM proteins as well. Therefore, the levels of the Ig-L1 NCAM family member NrCAM [266], and Ig-NCAM proteins NCAM1 (alias TenascinR) [266] and SynCAM1 [266], [267] are also

compared between wt and AP1/σ1B ko cellular fractions. Moreover, two additional chondroitin sulfate proteoglycan (CSPG)-NCAM proteins, namely Neurocan [268] and phosphotyrosine phosphatase receptor-type protein (PTPRZ1, alias PTPRβ) [268] are also included to this study as they have been identified as cargo proteins of synaptic AP2 CCVs in previously performed MS analysis (P.Schu unpublished data).

The levels of NCAM1 are not changed in isolated cortices and synapses from AP1/σ1B ko brains as compared to the corresponding wt fractions (Figure 3.17.A). However, SynCAM1, the master regulator of synapse formation [267], is slightly increased to 130 % of wt cortex and as well as wt synapse levels (Figure 3.17.B) while, NrCAM is slightly decreased to 85 % of wt cortex levels and to 95 % of wt synapse levels in AP1/σ1B ko mice (Figure 3.17.C). Even though the cortex levels of CHL1 from AP1/σ1B ko brains are not altered as compared to wt cortex levels, it is elevated to 130 % of wt levels in AP1/σ1B ko synapses (Figure 3.7). Therefore, it could be concluded that CHL1 is the only Ig-NCAM proteins analyzed whose level is specifically increased in AP1/σ1B ko synapses (Figure 3.7, Figure 3.17). Moreover, the levels of other Ig-NCAM proteins are slightly elevated (Figure 3.17) due to the stimulated AP2 CCV mediated-endocytosis in both synaptic CCV classes [85]. The levels of NCAM1 and NrCAM in ko canCCV are 120 % of wt canCCV levels, corresponding to 60 % of wt levels per CCV whereas their levels are slightly higher in ko stCCV which contains with 75 % and 70 % of wt stable CCV NCAM1 and NrCAM levels, in per CCV, respectively (Figure 3.17.A, C). Although ko canCCV has almost identical amounts of NCAM1, NrCAM, and SynCAM1, 60 % of their wt canCCV levels, ko stCCV contains less SynCAM1 levels than NCAM1 and NrCAM, 55 % of wt stable CCV SynCAM1 levels, in per CCV (Figure 3.17). Therefore, these data suggest that all of the analyzed neuronal cell adhesion proteins show a preference for their sorting via stCCV, while SynCAM1 is the only one which tends to be endocytosed via canCCV. Overall, CHL1 is the only Ig-NCAM protein specifically endocytosed via the stabilized AP2 stCCV pathway.
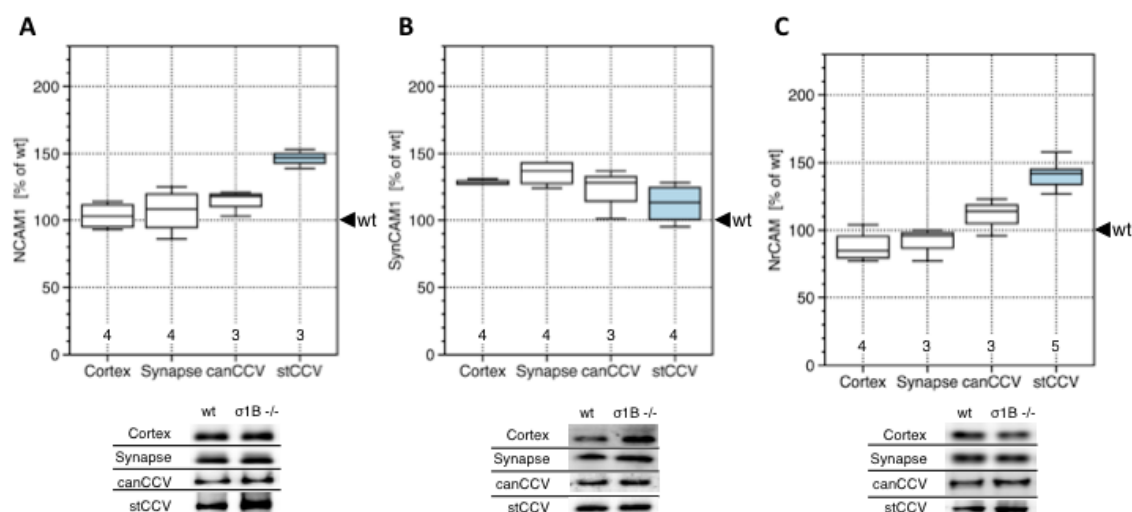
Figure 3.17. The alterations in the levels of Ig-NCAM proteins in wt-ko subfractions. The changes in the levels of **(A)** NCAM1, **(B)** SynCAM1 and **(C)** NrCAM in AP1/σ1B ko cellular fractions as compared to wt samples are shown. The signal intensities from protein bands in wt samples are defined as 100 % and ko protein levels are calculated relative to wt. Numbers below each box-diagram denote the numbers of independent biological wt-ko replicates used for quantifications. The representative semi-quantitative Western blot images used for quantifications are shown below each box-plot diagram for NCAM1 (170 kDa), SynCAM1 (37 kDa) and NrCAM (150 kDa). Data contribution: G.F. Sengül performed the cortex (NCAM1, SynCAM1, NrCAM), synapse (NCAM1, SynCAM1, NrCAM), canCCV (NCAM1, SynCAM1, NrCAM) and stabilized CCV (NCAM1, SynCAM1, NrCAM) experiments and data analysis to obtain the complete figure.

The levels of the CSPG-NCAM proteins, Neurocan and PTPRZ1 are not changed in AP1/σ1B ko cortices compared to wt cortices (Figure 3.18). However, the levels of Neurocan and PTPRZ1 are elevated to 140 % and 120 % of wt levels in AP1/σ1B ko synapses, respectively (Figure 3.18). So, there is a synapse specific increase in their levels as in the case of CHL1 (Figure 3.7, 3.18). The levels of PTPRZ1 in both ko CCVs are comparable to those of NCAM1 and NrCAM, which are 60 % of wt canCCV and 80 % of wt stable CCV, in per CCV, respectively (Figure 3.17, 3.18). So, also PTPRZ1 is preferentially sorted via stCCV like the Ig-NCAM proteins. However, endocytosis of Neurocan is increased due to the stimulated AP2 CME pathway [85], and it is enriched in stCCV as in the case of CHL1. The ko canCCV contains 60% of the wt canCCV, but ko stCCV contains 110 % of wt stable CCV Neurocan levels, in per CCV (Figure 3.18.A).
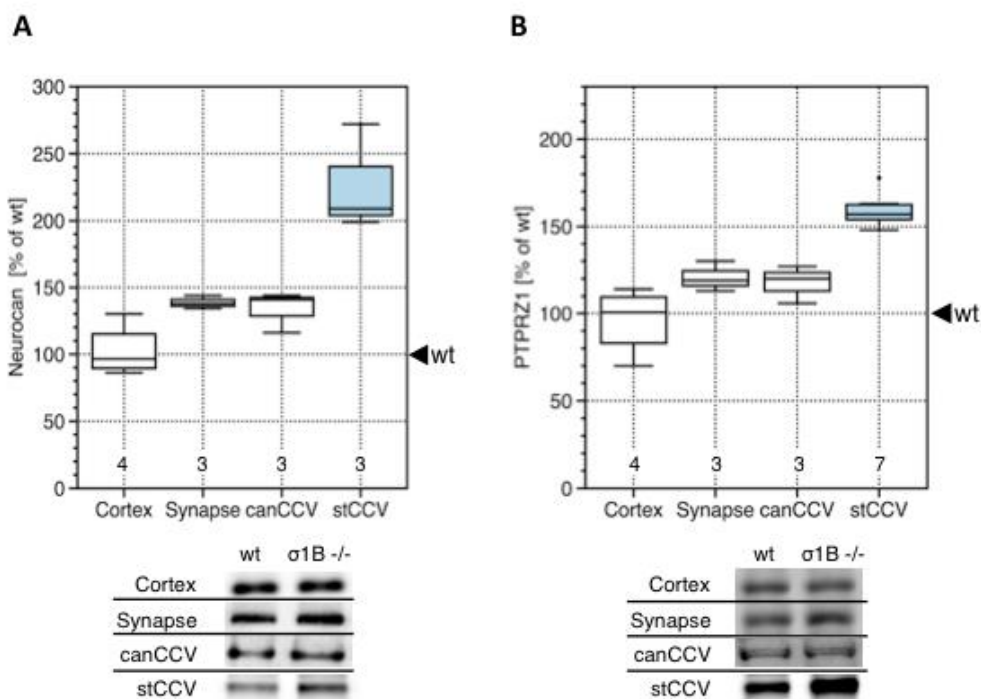
Figure 3.18. The changes in the levels of CSPG-NCAM proteins in wt-ko cellular fractions. The alteration in the levels of (A) Neurocan and (B) PTPRZ1 proteins in AP1/σ1B ko cellular fractions as compared to wt samples are shown. The signal intensities from protein bands in wt samples are set to 100 % and ko protein levels are expressed relative to wt. Numbers below each box-plot denote the numbers of independent biological wt-ko replicates used for quantifications. The representative semi-quantitative Western blot images used for quantifications are indicated below each box-plot diagram for Neurocan (140 kDa) and PTPRZ1 (250 kDa). Data contribution: G.F. Sengül performed the cortex (Neurocan, PTPRZ1), synapse (Neurocan, PTPRZ1), canCCV (Neurocan, PTPRZ1) and stabilized CCV (Neurocan, PTPRZ1) experiments and data analysis to obtain the complete figure.

The analysis of NCAM proteins revealed that all of the investigated proteins, except SynCAM1, are preferentially sorted via stCCV. However, the Ig-NCAM protein CHL1 and the CSPG-NCAM protein Neurocan are specifically endocytosed via stabilized AP2 stCCV. The endocytosis of certain NCAM proteins via stCCV strongly supports our previously proposed function of this specialized AP2 CME pathway in synaptic function-related plasticity [85].

CHAPTER 4

4. DISCUSSION

4.1. Regulation of AP2 CCV life cycle

The AP2 CCV mediated endocytosis of PM proteins starts with the stable binding of AP2 to the PM phospholipid PI-4,5-P_2 and to the cytoplasmic domain of a cargo protein, which is bound by the AP2/μ2 or AP2/σ2 adaptins [116]. The tripartite AP2-Eps15/ Eps15L1-Sgip1 complex accelerates CCV formation [208]. AP2 co-adaptors, like Eps15 and Eps15L1, collect additional cargo-proteins, which are not recognized by AP2 to expand the repertoire of AP2 CCV cargo proteins [89]. After the recruitment of clathrin, mostly but not exclusively by AP2, a shallow clathrin-coated-pit is formed [116]. This pit grows and invaginates into a round clathrin-coated-vesicle, which is connected with the PM via a narrow membrane neck. This process is driven by the continuous recruitment of coat proteins and clathrin [116]. The assembly of a large GTPase Dynamin into rings around the nascent CCV neck and the subsequent constriction of these rings pinch off the AP2 CCV from the donor membrane [116], [127], [128]. The formation of AP2 CCV involves more than 60 additional proteins, which can be part of the vesicle coat during this process [119]. However, the numbers of interaction domains in the coat proteins are limited. Moreover, they are often in a close proximity, thereby restricting different protein:protein interactions due to steric hindrance [119]. Therefore, coat protein:protein interactions must be strictly regulated in time [115], [119]. This makes CCV formation a highly complex process. Eventually, the AP2 CCV disassembly starts with the most outer coat, the clathrin cage [116]. Clathrin cage uncoating requires the Hsc70 ATPase, its two co-chaperones auxilin1 and GAK/auxilin2, and its NEF protein Hsp110 [143]. While the molecular mechanisms of clathrin cage disassembly by these proteins have been studied in detail, the knowledge about the regulation of this process is quite restricted. We also do not know how exactly the

protein:protein interactions of coat proteins are released, but numerous protein phosphorylations and dephosphorylations take place for the regulation of AP2 CCV life cycle [232]. Lastly, the activity of the Synaptojanin1 phosphatase is known to be essential for the dissociation of AP2 and additional PI-4,5-P_2 binding coat proteins from the vesicle membrane [151]. Only after the uncoating of AP2 CCV, the vesicle will be able to fuse with the membrane of the acceptor organelle, usually an early endosome, to deliver its cargo content [116]. As mentioned above, a given coat protein interacts with several different proteins and thus the consequences of the absence of one protein for CCV formation can be difficult to envision. Therefore, the data obtained from the perturbation of protein functions using knockdown, knockout, or overexpression approaches can only be interpreted in the context of AP2 CCV formation but is not applicable in terms of AP2 CCV stability and lifetime.

In our group, a mouse knockout model of the AP2 homologous AP1 complex, AP1/σ1B ko mice, had been generated [100], which has multiple alterations in synaptic protein sorting [102]. The alterations in tissue specific AP1/σ1B ko mice are induced as secondary phenotypes in AP2 CME. These synapse-specific phenotypes are the upregulation of AP2 CME and the formation of a class of AP2 CCV with enhanced stability thereby with an extended lifetime [85]. The analysis of the alterations in the coat protein composition of these AP2 CCV enabled us to study and to identify the molecular mechanisms regulating AP2 CCV uncoating and thus their life-span [85].

Neurons contain the ubiquitous AP1/σ1A complex, whose protein sorting and transport functions between the TGN and endosomes are indispensable for embryonic development and tissue-functions. Additionally, neurons and a limited number of cell types in other tissues, also contain the tissue-specific AP1/σ1B complex. The absence of this complex is compatible with life [100]. However, the deficiency of the X-chromosome encoded AP1/σ1B gene leads to severe impairments in memory and learning in mice and as well as in human [100], [269]. Additionally, AP1/σ1B ko mice exhibit problems in motor coordination and human patients show delayed motor development. They start to walk only at the age of 4-6 years [100], [269]. These patients require life-long comprehensive care. The AP1/σ1B ko mice serve as a model organism for this severe human X-linked mental retardation disorder [100], [269]. The

hippocampal synapse of the AP1/σ1B ko animals contains less SVs compared to the wt due to slowed down and inefficient SV recycling [100]. At the same time, enlarged endosomes and AP2 CCV accumulate in the AP1/σ1B ko synapses. Moreover, numerous synaptic proteins are degraded in the endolysosomes [100], [102]. These disturbances in protein sorting induce secondary phenotypes which are the upregulation of AP2 CME and the formation of a subclass of AP2 CCV with a more stable coat and thus with an extended lifetime [85]. These phenotypes enabled us to work on the molecular mechanisms behind the AP2 CCV life cycle regulation without having to mutate AP2 CME proteins [85]. Our group identified two AP2 CCV classes in synapses. Firstly, the class of canonical CCV, canCCV, corresponding to the 85 % of the total synaptic AP2 CCV pool. The second class contains AP2 CCV with a comparably more stable coat and they form the remaining 15 % of the total synaptic AP2 CCV pool [85]. Both AP2 CCV classes are doubled in size in AP1/σ1B ko synapses. Moreover, the latter class of AP2 CCV is more stable than canCCV, even more stabilized in AP1/σ1B ko synapses, named as stCCV [85]. This AP2 CCV phenotype is only established in AP1/σ1B ko synapses and thus it is a form of synaptic plasticity [85]. Due to the extended life-span of stCCV, there will be delay in the fusion of these endocytic vesicles with their acceptor membranes, mostly early endosomes. Therefore, the transported cargo and its recycling between endosomes and the PM will be slowed down also the activation of receptor signaling cascades will be comparably slower [270].

The comparison of AP2 CCV coat composition between wt and AP1/σ1B ko synapses led my predecessors in this project to the identify three molecular mechanisms regulating the enhanced stabilization thereby extended life-span of AP2 CCV [85]. Firstly, stabilized stCCV contain less of the disassembly ATPase, Hsc70 [4]. Second mechanism suggests that hyperphosphorylation of AP2/μ2 subunit by AAK1 stabilizes high-affinity AP2-membrane binding. Thirdly, the reduced recruitment of Synaptojanin1, the PI-4,5-P$_2$ phosphatase, into these AP2 stCCV also leads to their enhanced stabilization [85]. To understand the molecular mechanism that determine the amount and activity of Synaptojanin1 in AP2 CCV is not only important for the regulation of the AP2 CCV life cycle. Synaptojanin1 has additional functions in membrane and protein transport and its defects are associated with the development

of several neurological diseases such as PD, AD and Down-syndrome [164], [271]– [273]. Therefore, the mechanisms regulating its recruitment into AP2 CCV is studied first in this Thesis.

4.2. Regulation of Synaptojanin1 recruitment into stCCV

The Synaptojanin1 CCV protein interactome consists of 9 proteins implying that the regulation of its recruitment depends on several protein-protein interactions [85], [164]. Moreover, most of these proteins also bind to one another, which does not only emphasize the complexity of its protein network, but also makes it difficult to come up with a simple explanation for the regulatory mechanisms behind its recruitment into stCCV. Of all Synaptojanin1 interacting CCV proteins, Endophilin A1 was proposed to play the most important role in the regulation of Synaptojanin1 recruitment and its activity in CCV uncoating [162], [163], [186]. However, our data did not show the differential regulation of Endophilin A1 recruitment into the different AP2 CCV classes [164]. Moreover, Endophilin A1 is not differentially phosphorylated by LRRK2 in its BAR-domain between two CCV classes, a modification which would impair Synaptojanin1 binding [164]. The comparison of LRRK2 levels and of its activity between wt and ko AP2 CCV did not support the regulation of Synaptojanin1 recruitment by Endophilin A1 [164]. The previously suggested Endophilin A1 function in the regulation of Synaptojanin1 activity in uncoating CCV was shown in neuronal cell cultures of triple Endophilin A1-3 isoform ko mice, because a single Endophilin A1 ko exhibit no apparent phenotypes [162], [163], [186]. The cumulative protein sorting defects in the triple Endophilin A1-3 isoform ko can be responsible for the changes in the CME pathway and eventually in the CCV uncoating process. Our data indicated that other CCV proteins than Endophilin A1 regulate the CCV life cycle [164]. The enhanced ITSN1-Endophilin A1 interaction in both ko AP2 CCV classes as compared to the respective wt CCV is most likely associated with the stimulation of the AP2 CME pathways [85], [164]. Pacsin1 is another Synaptojanin1 interacting protein. Its level did not change in ko canCCV as compared to wt canCCV levels, while it was decreased down to 30 % of wt levels in ko stCCV. However, more of these Pacsin1 proteins were activated in the ko stCCV via a higher phosphorylation level [164]. Therefore, the compensation of reduced Pacsin1 levels by its increased

activity excluded its potential involvement in the regulation of Synaptojanin1 levels in ko stCCV [164]. The affinity of the Pacsin1 antibody was insufficient for the analysis of a CCV class specific Pacsin1:Synaptojanin1 interaction, in contrast to the ITSN1 antibody (Figure 3.4). The activation of Pacsin1 via phosphorylation was also a reason to determine the master regulatory kinase(s) and/or phosphatase(s) in the AP2 CME pathway that will be discussed throughly in Section 4.4. It could be also possible that the Pacsin1 level in ko stCCV might be limited by the increased transportation of CCV coat or cargo proteins, like the AZ scaffolding Git1 protein [85]. These Pacsin1 data demonstrate one more time the complexity of CCV life cycle regulation.

The reduction of the ITSN1 protein in ko stCCV closely resembles the reduction in Synaptojanin1 levels [164]. This suggested that ITSN1 might be the major regulator of the Synaptojanin1 amount in AP2 CCV. This conclusion was verified by the co-immunoprecipitation experiments of Synaptojanin1 and of Endophilin A1 with the anti-ITSN1 antibody [164]. In the solubilized coat protein mixtures of two different AP2 CCV classes, ITSN1 bound preferentially to Synaptojanin1 in a CCV class specific manner, but not to Endophilin A1 [164], [186]. It has been proposed that ITSN1 coordinates the binding of Synaptohanin1 with Endophilin A1, which is based on the fact that ITSN1 is able to interact with both proteins independent of each other [186]. However, the co-immunoprecipitation experiments are not in line with such a scaffolding function of ITSN1 [186]. Collectively, we can conclude that ITSN1 determines the amount of Synaptojanin1 incorporated into an AP2 CCV so that it plays a role in the regulation of the AP2 CCV life cycle [164]. The excessive amount of AP2/Sgip1 complex over ITSN1 can be responsible for the further reduction in the recruitment of Synaptojanin1 below the ITSN1 level in ko stCCV. Sgip1 interacts with ITSN1 via its SH3A domain [201], like Synaptojanin1 [198], and AP2 binds to ITSN1 via its SH3A-SH3B linker domain [199]. The excess amount of the Sgip1/AP2 complex over ITSN1 competes with Synaptojanin1 for ITSN1 binding, which further lower the levels of Synaptojanin1 in ko stCCV [164], [186]. Next, it was intended to investigate why the level of ITSN1 is reduced in ko stCCV. The analysis of several potential ITSN1 recruiters, selected based on the well-established ITSN1 CCV protein interactome, showed that only Eps15 levels are differentially regulated between the two AP2 CCV classes in line with the alteration in the ITSN1 CCV amounts. Eps15

and its homolog Eps15L1 bind ITSN1 via its coiled-coil domain. Those interactions restrain the homodimerization of ITSN1, thereby preventing its inactivation [164], [198], [274]. It is quite interesting that not Eps15L1, but Eps15 determines the ITSN1 AP2 CCV level [164]. Since Eps15L1 ko mice are lethal and display strong neurological defects, whereas Eps15 ko mice have no severe neurological phenotypes, suggesting the compensation of Eps15 deficiency by its homolog Eps15L1 in the converging cellular pathways [164], [275]. Numerous phosphorylation and ubiquitination sites in the less conserved regions of Eps15 and Eps15L1 imply the regulation of their functions via modifications, which could also alter their incorporation into an AP2 CCV coat [220], [276]. These modifications may not only play a role in the regulation of the AP2 CCV life cycle, but also in the selection of specific AP2 CCV cargo proteins [220], [221], [276]. Eps15 functions as a cargo co-adaptor CCV protein, so that its level is also dependent on the sorted CCV cargo protein(s) [275]. It could be also possible that cargo and/or other coat proteins may impede the recruitment of Eps15 into a CCV or those proteins can efficiently distrupt the interaction between Eps15 and ITSN1 [164]. In the light of our results, we developed a model in which Eps15 regulates the levels of ITSN1 stably bind to a CCV, which then controls the levels of Synaptojanin1 stably incorporated into AP2 CCV [164], as summarized in Figure 4.1. The proposed model in our study collectively accounts for the regulation of AP2 CCV lifespan by its co-adaptor proteins and thus by its cargo proteins [164].
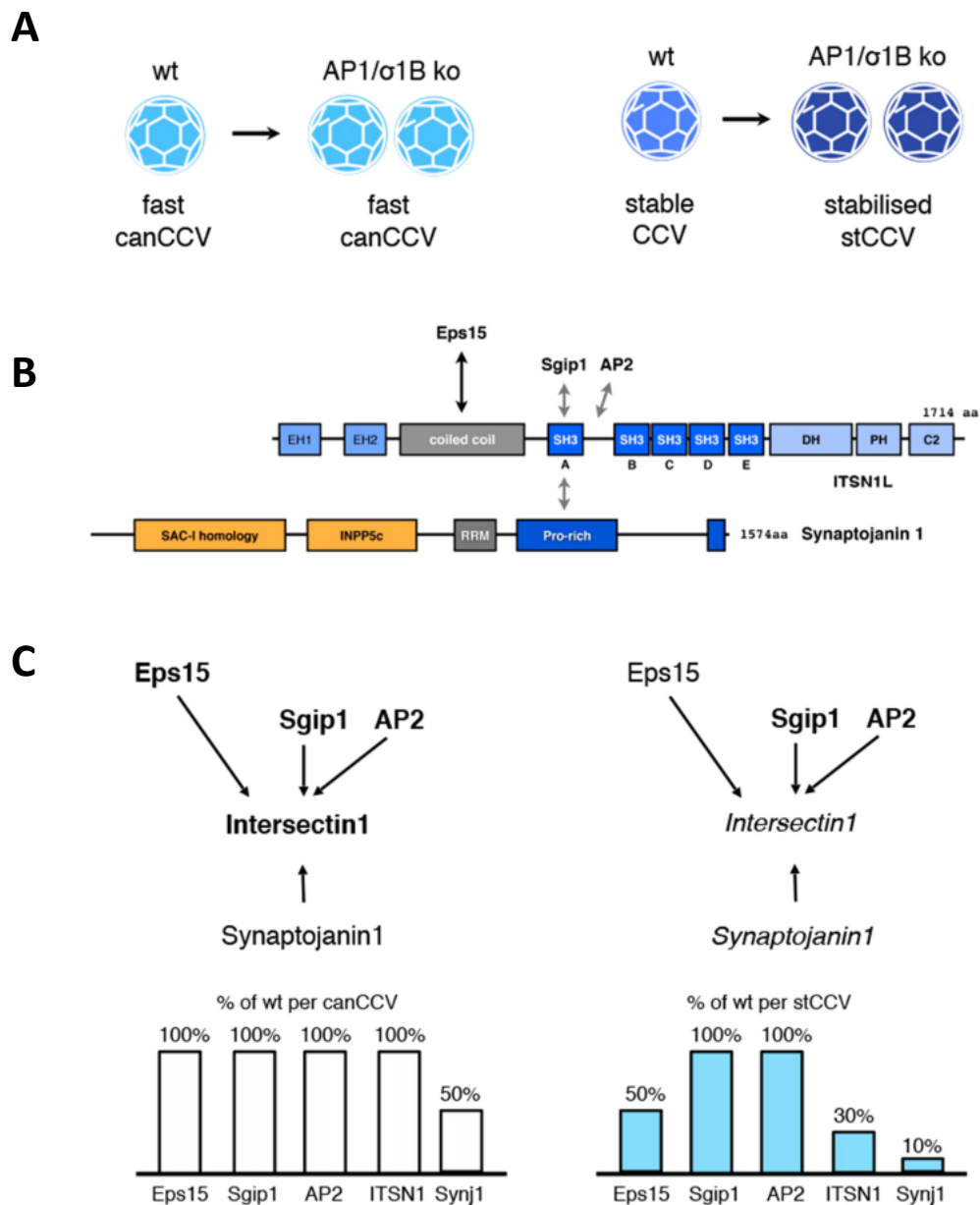
Figure 4.1. Model for the regulation of Synaptojanin1 levels stably incorporated into AP2 CCV.
(A) The alterations in the coat composition and extended life-span of AP2 CCV in wt and AP1/σ1B ko synapses are demonstrated. (B) The protein domain organization and interaction sites of ITSN1 and Synaptojanin1 are depicted. (C) The analysis of Synaptojanin1 recruitment into canCCV (left) and stCCV (right) by its CCV protein interactome is summarized. Eps15 regulates the ITSN1 levels stably bind to a CCV which then, determines the levels of Synaptojanin1 stably incorporated into AP2 CCV. The competition among Sgip1/AP2 complex and Synaptojanin1 for the ITSN1 binding further reduces the recruitment of Synaptojanin1 into stCCV. Proteins written in bold letters represent 100 % wt levels, in regular letters are reduced down to 50 % wt levels and in italic letters are reduced well-below 50 % of wt levels in the drawn interaction schemes. The bar-diagrams show the changes in the protein levels in two AP1/σ1B ko AP2 CCV classes relative to wt, given in % per CCV. The figure is adapted from Mishra, R., Sengül, G.F. et al. 2021. The figure is reprinted with the permission from Nature Springer, Scientific Reports open access created common CC BY provided a licence for the unrestricted use of any part of the manuscript without special permission. The schematic summary diagram figure (model) is drawn based on the obtained experimental results by R. Mishra, G.F. Sengül and E. Candiello in the referred paper [164]. Individual contributions are described in detail for each figure (see Results section 3.1-3.5).

4.3. Regulation of Hsc70 for clathrin-cage disassembly

Another molecular mechanism which has been found to be responsible for the stabilization of AP2 CCV coat was a reduction of the uncoating ATPase, Hsc70, in ko stCCV [85]. Hsc70 levels were reduced down to 50 % of wt levels, although its CCV co-chaperons auxilin1 and auxilin2/GAK were present almost at the wt levels in ko stCCV [85]. Plenty of Hsc70 proteins, which is present in molar excess over clathrin in CCV, are required to initiate clathrin-cage disassembly. Hsc70s are positioned under each clathrin triskelia vertex [142], [143]. The Hsc70:ADP complex is stably associated with clathrin triskelia [146]. The well-known regulator of the Hsc70 ADP-ATP cycle is the nucleotide exchange factor (NEF) Hsp110, which replaces ADP for ATP, inducing the release of Hsc70 from clathrin [142], [143], [146]. As described in result section 3.7, the Hsp70:Hsp110 ratio in short-lived canCCV is maintained in the longer-lived stCCV (Figure 3.8). Therefore, Hsp110 most probably does not take part in the extension of the stCCV life-span. Hsp90 is another CCV chaperon protein and it works together with Hsc70 in numerous cellular pathways [224], [231] [20-21]. The analysis of Hsp90 reveals that its level is not changed in ko stCCV as compared to wt stable CCV (Figure 3.9). Therefore, Hsp90 also appears not to be involved in the regulation Hsc70 activity in the stabilized AP2 CCV. Next, we hypothesized that the AP2 CCV class specific phosphorylation patterns of Hsc70 itself and of the two auxilins might control Hsc70 recruitment. Two major Hsc70-Pi variants in wt-ko AP2 CCV and in wt-ko synapse were separated by phos-tag[TM] SDS PAGE (Figure 3.10.B demonstrates the upper, hyper-Pi Hsc70 and the lower, hypo-Pi Hsc70 proteins), but no such differences were detected for the two auxilins. In wt stable AP2 CCV and in ko stCCV, an increase in hypo-Pi Hsc70 relative to hyper-Pi Hsc70 proteins compared to wt and ko canCCV were detected. This implies that hypo-Pi Hsc70 proteins are not concentrated by their Hsc70 homodimerization in stable, longer-lived AP2 CCV.

The homodimerization of Hsc70 is shown to be inhibited by the formation of a Hsc70:CaM/Ca^{2+} complex [229]. The phosphorylation of Hsc70 on its T265 residue, which is located in the central CaM/Ca^{2+} binding domain, hinders the formation of a Hsc70:CaM/Ca^{2+} complex [229]. The Hsc70 T265 amino acid has been found to be among the most frequently modified residue of Hsc70 [230]. The pull-down experiments demonstrated that hypo-Pi Hsc70 proteins in wt stable and ko stCCV can

bind to CaM/Ca^{2+}, while the hypo-Pi Hsc70 proteins in wt and ko canCCV cannot. This indicates the important point that hypo-Pi Hsc70 proteins of wt and ko canCCV are phosphorylated on the T265 residue, whereas hypo-Pi Hsc70 proteins of wt stable AP2 CCV and ko stCCV are not phosphorylated on T265 residue. This conclusion is also supported by the fact that hypo-Pi Hsc70 proteins of long-lived CCV migrates slightly further in the phos-tag^{TM} SDS-PAGE than the hypo-Pi Hsc70 proteins of wt and ko canCCV. The Hsc70 proteins of canCCV which bind CaM migrate faster than those bound by CaM/Ca^{2+}. Therefore, the phosphorylation patterns of these Hsc70 proteins of canCCV are complex and reveal the existence of a previously unnoticed and uncharacterized CaM binding motif(s) in Hsc70. These data strongly suggest that the reduced levels of Hsc70 in ko stCCV are caused by the inhibition of Hsc70 homodimerization by binding of CaM/Ca^{2+} and most likely also by CaM. The detected differences in the hypo-Pi/hyper-Pi Hsc70 ratios between wt stable AP2 CCV and ko stCCV are so small that their involvement in the enhanced stability and extended life-span of AP2 stCCV might be insignificant. However, a modified Hsc70 is not able to form a Hsc70 homodimer with an unmodified Hsc70 version (Figure 4.2) [21]. Therefore, the reduction in the Hsc70 CCV level will be two times more than the modified Hsc70 proteins. It also must be kept in mind that clathrin-cage disassembly requires the coordinated Hsc70 activity under each clathrin vertex of the cage. Therefore, even such small differences between the hypo-Pi Hsc70 proteins of wt stable CCV and ko stCCV can lead to an extension in the CCV life-span.
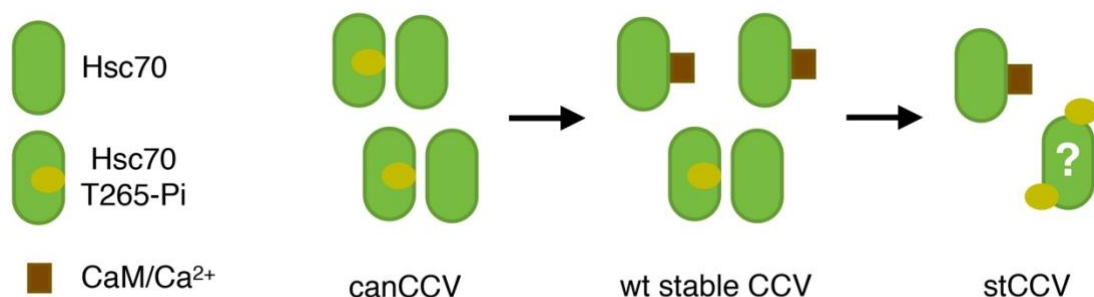

Figure 4.2. Model for the regulation of Hsc70 homodimerization in wt-ko synaptic AP2 CCV. The cartoon displays CaM/Ca^{2+} and T265-Pi dependent regulation of Hsc70 homodimerization and thus its concentration in synaptic AP2 CCV.

Empty clathrin-cages, containing no vesicle inside, are formed spontaneously in the cytoplasm. This self-assembly property of clathrin triskelia has been shown to limit the availability of clathrin for the CME cycles, if these clathrin-cages will not be disassembled by Hsc70 and its co-chaperones auxilin1 and auxilin2/GAK [277], [278]. Even though AP1/σ1B ko synapses contain wt levels of Hsc70 [85], relatively more hyper-Pi Hsc70 than hypo-Pi Hsc70 are present in ko synapses compared to wt synapses. This may be because the activation of CME requires also a stimulation of the constitutive clathrin-cage disassembly activity of Hsc70 in the cytoplasm.

4.4. CCV kinases in the regulation of CCV coat-stability and CCV lifetime extension

Our data repeatedly pointed out the necessity to look for alterations in the AP2 CCV class specific association of kinases and phosphatases, which might be linked to the increase in AP2 CCV stability and thus their life span extension. Furthermore, the changes in the levels of such enzymes enable prediction of their sequence specificities for potential substrates. This might also assist in the identification of the Hsc70 residues whose phosphorylation controls the recruitment and activity of Hsc70 in uncoating CCV. Based on the literature and our previously performed CCV MS analysis, a total of 12 protein kinases were determined to be studied. The data from three of these kinases, the AP2 kinases AAK1, auxilin2/GAK and LRRK2 have been already published by our group [85], [102], [164]. The other nine kinases and two PP2A phosphatase regulatory domains were investigated in this thesis. Our findings suggest that the associations of eight of these 12 kinases with AP2 CCV are tightly regulated. These are AAK1, CVAK104, DYRK1A, DCLK1, CaMKIIδ, SPAK (STK39)/CAB39, STK38S and STK38L. The levels of DCLK1 and STK38S are two-fold increased in the pools of both ko AP2 CCV classes and thus a single CCV has wt levels of these two kinases (Figures 3.14.B and 3.16.A). Even though they apparently play key roles in the regulation of the two AP2 CME pathways, they are not shown to be involved in the extension of the AP2 CCV life span. The levels of DYRK1A, CaMKIIδ, SPAK (STK39)/CAB39, and STK38L are specifically decreased in ko stCCV compared to wt stable AP2 CCV, while they are present at wt canCCV levels in ko canCCV. These results imply that these kinases stimulate the destabilization of

AP2 CCV thereby shortening the AP2 CCV half-life. Exclusively the levels of AAK1 are increased in ko stCCV, whereas its recruitment into ko synapse canCCV is inhibited [85], [102]. CVAK104 levels exhibits a similar pattern as AAK1 levels. However, the changes in the CVAK104 levels are minimal compared to AAK1. Overall, our kinase data set suggests that AAK1 is the major kinase, whose activity directly serves AP2 CCV coat stabilization and AP2 CCV life-span extension [85], [102].

What could be the CCV protein substrates of DYRK1A, CaMKIIδ, SPAK(STK39)/CAB39 and STK38L? AAK1 is characterized as a substrate for STK38L kinase in another AAK1 dependent pathway [264]. Our data suggest that CCV STK38L inhibits the activity of AAK1 in AP2 CCV. The CaMKIIδ and DYRK1A levels are elevated in ko synapses and not in ko cortices compared to the wt fractions [102]. As just mentioned above, ko synapses contain a larger fraction of hyper-Pi Hsc70 proteins than wt synapses. This suggest that CaMKIIδ and DYRK1A are of the strongest candidates for the formation of hyper-Pi Hsc70 and the stimulation of Hsc70 activity for the disassembly of the clathrin-cage. The sequence specificity of CaMKIIδ and of SPAK(STK39)/CAB39 indicate that both are able to phosphorylate Hsc70 on its T265 residue to prevent inhibition of Hsc70 homodimerization by CaM/Ca^{2+}. GPS 5.0 kinase-specific phosphorylation site prediction database reported 18 more kinases which are able to phosphorylate Hsc70 on its T265 residue out of the total of 479 kinases in the database [279]. Therefore, more than one kinase may modify the Hsc70 activity to ensure the robustness of the regulation. Furthermore, DYRK1A has been demonstrated to phosphorylate several CCV coat proteins *in-vitro,* but the functions of these modifications for the dynamics of the AP2 CCV life-cycle remain unknown [240], [241]. Even though the levels of PP2A regulatory subunits PPP2R2B (B55β) and PP2R2C (B55γ) were not differentially regulated between two AP2 CCV classes, their levels in ko stCCV should be synergistic with the reduced activities of these four kinases.

4.5. The preferential sorting of specific neuronal cell adhesion proteins by AP2 stCCV

The wt stable CCV and ko stCCV correspond to 15 % of the total synaptic AP2 CCV pools in wt and AP1/σ1B ko brains, which due to the small pool sizes, one may consider being irrelevant for synaptic function and plasticity. Therefore, an important point that needs to be addressed is what could be the physiological function(s) of these longer-lived AP2 CCV? In order to answer this question, stCCV specific cargo protein(s) should be identified first. Secondly, the physiological consequences of the altered trafficking of these cargo protein(s) should be further investigated, which would of cause be limited by the current knowledge of their functions. My predecessors have identified the AZ scaffolding protein, Git1 and AP2 CCV co-adaptor protein, Stonin2 as being cargo proteins of AP2 CCV [85]. Both of these proteins form a ring around the AZ [187], [265]. Therefore, it is very likely that the stimulated endocytosis and transport of Git1 and Stonin2 via stCCV play a role in AZ plasticity [85], [164], [265]. However, Git1 is a scaffolding protein functioning in numerous signal transduction pathways [187], [265]. Moreover, the specific sorting of Git1 by AP2 CCV may alter its functions in remodeling of focal adhesions, dendritic spine morphogenesis and synapse formation [187], [265], [280], [281]. Indeed, two new AP2 stCCV-specific cargo proteins, namely CHL1 and Neurocan, which belong to the neuronal cell adhesion molecule (NCAM) superfamily, were identified in the current study.

Leshchyns´ka *et al.* 2006 proposed that CHL1 regulates the amounts of Hsc70 in synapses and as well as in synaptic CCVs [222]. The comparison of CHL1 and Hsc70 levels in wt and ko synapses and its content in wt-ko synaptic AP2 CCV are not in line with the model proposed by Leshchyns´ka *et al.* 2006 [222]. The CHL1 AP1/σ1B ko synapse level is increased relative to the wt, but Hsc70 is present at the wt level in ko synapses. Moreover, CHL1 is enriched in stCCV of AP1/σ1B ko synapses, while their Hsc70 content is reduced down to 50% of wt levels. Therefore, it can be concluded that CHL1 is not involved in the regulation of the AP2 CCV life cycle. However, we wondered whether stCCV are specialized for the sorting of NCAMs due to the enrichment of CHL1 in stCCV.

Besides CHL1, vertebrates also express three other members of the Ig-family NCAM proteins namely, NCAM1, NrCAM and SynCAM1. These are not enriched in the ko stCCV (Figures 3.17). Moreover, CSPG NCAM protein PTPRZ1 is not increased in stCCV, but the CSPG Neurocan is also enriched in ko stCCV, just like CHL1 (Figure 3.7-3.18). Although the endocytosis of other NCAMs is not stimulated, they all exhibit a preference for their sorting via stCCV. The only exception is SynCAM, which is preferentially sorted by canCCV. SynCAM is able to direct synapse formation in non-neuronal cells and is thus a master regulator of synaptogenesis [267]. It enhances synapse stability and strength, while other Ig-NCAM proteins restrict synapse formation and stability [282]. These novel data corroborate our previously proposed function of long-lived AP2 CCV in synaptic plasticity [85].

CHL1 and the Ig-NCAM family members NrCAM, NCAM-L1 and Neurofacsin form numerous complexes with integrins, receptors and ion channels. The formation of such complexes induces the recruitment of ankyrins to anchor these proteins to the actin cytoskeleton [283]–[287]. CHL deficient mice cannot immobilize many PM proteins, and thus they are endocytosed constitutively by AP2 CCV and recycled repeatedly between the PM and endosomes [284]. Therefore, the accumulation of AP2 CCV in CHL1 ko synapses is most likely a secondary phenotype of CHL1 deficiency [222].

It is interesting that the endocytosis of CHL1 and Neurocan via ko stCCV is stimulated. Neurocan inhibits homodimerization of CHL1 and thus, its inactivation [288]. This relation can explain the correlative increase in their stCCV levels. Neurocan also regulates NrCAM and NCAM1 in the same manner. Therefore, the interdependent regulations of NCAMs can remodel the dendritic spine and modify the synaptic activity and functioning [288], [289]. The specific enrichment of just CHL1 and Neurocan in stCCV strengthens our model that stCCV-mediated sorting fulfills particular functions in synaptic plasticity [85].

What might be the specific functions of Neurocan and CHL1 proteins transported by stCCV? CHL1 is the only member of the L1 family of Ig-class NCAMs which exclusively forms cis homo- and heterodimers. The key function of CHL1 is to organize the distribution of proteins at the presynaptic PM [266], [290], [291]. The

loss of CHL1 function is associated with 3p-deletion syndrome, which is caused by a chromosomal truncation, a disease characterized by intellectual disability, developmental delay in motor skills, autism and schizophrenia [292], [293]. Importantly, parents who carry the mutated CHL1 gene may not develop the disease symptoms, but their children can have intellectual disabilities due to mutations in CHL1 gene locus [294]. CHL heterozygous mice also exhibit variable phenotypes [293]. The variability in the disease phenotype penetrance could be due to the differences in the levels of CHL1 expression among mice and/or the compensation of CHL1 function through the other cell adhesion proteins [293], [294]. The functional redundancies among the NCAMs stipulated even the generation of quadruple knockouts mice, which showed only mild alterations in synaptic transmission [295]–[297]. Therefore, it is quite difficult to develop a model for the functional consequences of specialized CHL1 sorting via the AP2 stCCV pathway. The transportation of CHL1 and Neurocan via longer-lived stCCV would enable their transport to the sites distal from their site of endocytosis. This would allow their incorporation into different pre-synaptic PM domains. In addition, the endocytosis of these proteins within the pro-longed stCCV could lead to relatively slow recycling of these cargos between PM and EE. So, there would be inevitable delay in the activation or inhibition of signaling pathways which require these proteins [102]. It could be also possible that stCCV protect these proteins from being degraded. The endolysosomal degredation of SV proteins were upregulated in AP1/σ1B ko synapses [102]. EEs mature into MVB endosomal compartments where some cargo proteins are destined for their degradation. The transportantion of these cargo proteins within the stabilized AP2 CCV may prevent their fusion with EE so that those proteins would not be conveyed to endolysososmes for their degradation. The higher levels of CHL1 and Neurocan in AP1/σ1B ko synapses as compared to their wt levels strongly suggest that the transportation of these cargo proteins within the stCCV prevents their degradation [102]. Collectively, all these modifications can rearrange the cell-to-cell and cell-to-ECM interactions of AP1/σ1B ko synapses, which can be suggested as a mechanism of synaptic plasticity suppressing the memory and learning deficiencies caused by the absence of AP1/σ1B complex [100], [298]–[300].

The improvements in microscopic technologies and computational power allowed scientists to visualize the dynamics of CME, that are CCP growth, and CCV formation and CCV life time [301]. However, determining the life time of CCV would require to follow a given CCV along its way from the PM into the cell and through the cytoplasm. This is technically challenging as it would require automatic tracking of a single CCV by the microscope [302]. Therefore, we do not have *in-vivo* life span measurements of CCV [164]. Moreover, to follow specific AP2 CCV classes enriched in certain cargos and those AP2 CCV with an extended life span requires their specific labelling to discriminate them from the canCCV. The fact that these represent the minority of CCV, 15% in the case of longer lived AP2 CCV, makes a microscopic approach even more challenging, if not impossible. Even though we determined the differences between the coat composition of wt and ko canCCV and between wt stable and ko stCCV in our study, the data do not point to biomarker protein(s) suitable to differentiate the AP2 CCV classes. Those proteins only differ in their levels; moreover, none of them is unique for a given CCV class. For example, the significant reduction in the levels of Synaptojanin1 makes it a candidate to differentiate between the two AP2 CCV classes in ko synapses [85], [164]. However, the immunoreactivity of the antibody on the brain slices must be validated first. If the previously obtained biochemical results are confirmed, then it can be used to differentially label and analyze these two AP2 CCV. Alternatively, a fluorescently tagged Synaptojanin1 could be expressed. However, it is questionable whether the differences in its incorporation levels in stCCV would allow to identify stCCV and canCCV unequivocally. Therefore, future studies should identify additional differences in CCV coat protein compositions that enable the microscopic analysis of CCV class-specific life times and transport functions.

Which mechanisms decide whether an AP2 canCCV or an AP2 stable CCV or stCCV is being formed? The lipid and protein composition of PM micro domains can determine the type of AP2 CCV being formed by coordinating the association of the regulatory proteins, e.g., the kinases, with AP2 CCV [270], [303]. AP2 CME does not take place randomly. For instance, AP2 CME is stimulated at specific PM domains in the axonal growth cone, whereas it can be suppressed in other regions of PM at the tips of growing axons [304]. Finally, AP2 CCV coat and/or cargo proteins might also

regulate the recruitment of kinases and/or phosphatases into a CCV. Even though this study investigates the regulation of AP2 CME pathways exclusively in synapses, the comparable pathways can also exist in other tissues and cell types because these enzymes and proteins are not solely expressed in neurons. However, detecting such specialized AP2 CME pathways could be more difficult in other tissues due to their lower activation as compared to synapses.

CHAPTER 5

5. CONCLUSIONS AND PERSPECTIVES

Three molecular mechanisms that regulate AP2 CCV coat stabilization and life-span extension were identified and two of them have been studied in this PhD thesis. Firstly, we analyzed the molecular mechanism that determines the AP2 CCV levels of Synaptojanin1. It has been indicated by previous publications that Synaptojanin1 is recruited to the neck of budding CCV via Endophilin A1 right before the membrane scission [162], [163]. However, the changes in the levels of Endophilin A1 in AP1/σ1B ko AP2 CCV relative to their wt counterparts indicated that Endophilin A1 is not involved in the regulation of Synaptojanin1 AP2 CCV levels [164]. However, phosphorylation of Endophilin A1 BAR domain by LRRK2 is expected to switch the mode of Endophilin A1 recruitment from the membrane binding to protein binding. Its interaction with different CCV proteins would reduce its ability to recruit Synaptojanin1 [165]. Nevertheless, the LRRK2 CCV levels as well as its kinase activity are not regulated in a CCV class specific manner and thus we conclude that Endophilin A1 does not regulate Synaptojanin1 CCV levels [164]. Next, distributions of additional CCV proteins belonging to the Synaptojanin1 CCV interactome were compared between wt and AP1/σ1B ko synaptic AP2 CCV. Based on our results, ITSN1 is indicated as being the major regulator of Synaptojanin1 AP2 CCV levels. Moreover, it is also indicated that excessive Sgip1/AP2 complexes over ITSN1 can efficiently impede Synaptojanin1 binding to ITSN1, which causes a further reduction in Synaptojanin1 stCCV levels. Furthermore, Eps15 determines the levels of ITSN1 stably incorporated into AP2 CCV. Interestingly, its homolog Eps15L1, which apparently can substitute Eps15 functions in several pathways, does not play a role in the extension of the AP2 CCV half-life. Additionally, the fact that a reduction in the level of Pacsin1 in stCCV is compensated via its higher activation demonstrates the tight regulation of stCCV formation. We published these data and proposed a

model for the regulation of Synaptojanin1 AP2 CCV levels by coat and cargo proteins in Mishra *et al.* 2021 with myself as a second co-author [164].

I continued with the analysis of another molecular mechanism contributing to the increased stability and thus extended lifetime of stCCV, the regulation of Hsc70 activity in clathrin-cage disassembly. Numerous Hsc70 proteins are required for clathrin-cage disassembly, because Hsc70 proteins have to be simultaneously active under each of the vertices of the clathrin-cage [142]. Therefore, the 50% lower Hsc70 levels in ko stCCV will result in enhanced CCV coat stabilization and CCV life time extension [85], [102]. None of the CCV proteins known to regulate Hsc70 activity, like its co-chaperons, auxilin1 and GAK/auxilin2 [85], [102] and its NEF Hsp110 and its co-worker Hsp90, appears to be responsible for the reduction in Hsc70 association with stCCV. Therefore, I focused on Hsc70 itself and searched for CCV class specific Hsc70 phosphorylation patterns(s), which might regulate its levels and uncoating activity in AP2 CCV. This analysis revealed the association of hyper-Pi and hypo-Pi Hsc70 proteins in wt and ko synaptic AP2 CCV. Both, wt stable CCV and ko stCCV contain more hypo-phosphorylated Hsc70 proteins than wt and ko short lived canCCV. The hypo-Pi Hsc70 proteins present in stCCV cannot homodimerize and cannot concentrate Hsc70 proteins, because their dimerization is inhibited by the formation of Hsc70-CaM/Ca^{2+} and most likely also by Hsc70-CaM complexes. These Hsc70 CaM/Ca^{2+} and CaM binding specifities are controlled by the unique phosphorylation pattern of these Hsc70 proteins. Regulation of Hsc70 and of Pacsin1 activities via phosphorylation and the stimulation of AAK1 kinase activity stipulated the involvement of kinases and phosphatases in AP2 CCV life cycle regulation. Of all 12 kinases analyzed, only the amounts of DYRK1A, CaMK-IIδ, STK38L and STK39/CAB39 are specifically reduced in ko stCCV suggesting these kinases take role in the destabilization of AP2 CCV thereby shortening their life span. Even though the PP2A phosphatase regulatory subunit PPP2R2B (B55β) and PP2R2B (B55γ) levels are not differentially regulated between two AP2 CCV pools, their ko stCCV levels possibly support low phosphorylation levels of the substrates of these four kinases. The analysis of all investigated kinases revealed that only the AAK1 level and its kinase activity were specifically elevated in ko stCCV. Therefore, AAK1 appears to be the master kinase in the regulation of the AP2 CCV life cycle [85], [102].

An important question is remained to be answered is about the functions of the AP2 stCCV pathway in synaptic plasticity. Previously, the AZ scaffolding protein Git1 and its CCV co-adaptor protein Stonin2 had been identified as specific cargo proteins of AP2 CCV [85]. I identified the Ig-NCAM family member CHL1 and the CSPG NCAM family member Neurocan as novel specific cargo proteins of ko AP2 stCCV, while the transport other NCAMs via this specialized pathway is not stimulated. Overall, through these new findings the functional association of AP2 stCCV with synaptic plasticity is fortified. In conclusion, we have successfully clarified the involvement of two molecular mechanisms for the regulation of AP2 CCV life cycle and suggested the functional relation of this specialized AP2 CME pathway in the synaptic plasticity.

Even though we obtained data which explain the reduced recruitment of the Synaptojanin1 phosphatase and of the Hsc70 uncoating ATPase into stCCV, there are still open questions to be answered. In the model for Synaptojanin1 regulation, the reasons for the specificity of Eps15 in the recruitment of ITSN1 have to be studied. In our model about the Hsc70 regulation, (Section 3.8) *in-vitro* and *in-vivo* assays have to be established to determine the phosphorylated residues in Hsc70, which are responsible for the regulation of the AP2 CCV life-cycle.

The second molecular mechanism is the hyperactivation of stable AP2 membrane binding by AAK1 phosphorylation. My predecessors in this project identified an inhibition of AAK1 recruitment in ko canCCV and a stimulation of AAK1 recruitment into the stCCV, accompanied with an increase in its catalytic activity towards the AP2 μ2-adaptin [85], [102]. They also found CCV class specific Pi patterns of AAK1 (unpublished data, P. Schu). These specific changes are expected to regulate AAK1 recruitment and activity. Therefore, wt and AAK1 mutants have to be expressed in *E.coli* to perform *in-vitro* kinase assays. Afterwards, the expression of AAK1 mutants in cells should clarify their functions in AP2 CCV stabilization and in life-cycle regulation. Furthermore, it has to be tested whether one or more of the CCV class specific regulated kinases identified in this study take part in the regulation of AAK1.

Finally, the analysis of AP2 CME pathway functions should be supported by a more detailed characterization of the cargo proteins enriched in stCCV. Since the CCV

coat-proteins are numerous and present in high copy numbers, a proteome analysis by a quantitative MS of uncoated, stripped AP2 CCV should be screened. The obtained results might enable the identification of additional stCCV enriched cargo proteins.

All these suggested experiments will definitely extend our knowledge about the novel functions and regulatory mechanisms of AP2 CME pathways. Overall, they will not only contribute to the better comprehension of protein sorting functions and mechanisms in neurons and neuronal cell types, but also in cell types of other tissues. Ultimately, these data will lay the basis for the treatment of diseases caused by altered protein sorting in endocytic routes.

References

[1]   B. Alberts, A. Johnson, J. Lewis, M. Raff, K. Roberts, and P. Walter, *Molecular Biology of the Cell*, 4 th editi. Newyork: Garland Science, 2002.

[2]   D. P. Clark, N. J. Pazdernik, and M. R. McGehee, "Chapter 13 - Protein Synthesis," D. P. Clark, N. J. Pazdernik, and M. R. B. T.-M. B. (Third E. McGehee, Eds. Academic Cell, 2019, pp. 397–444.

[3]   F. A. Agarraberes and J. F. Dice, "Protein translocation across membranes," *Biochim. Biophys. Acta - Biomembr.*, vol. 1513, no. 1, pp. 1–24, 2001, doi: https://doi.org/10.1016/S0304-4157(01)00005-3.

[4]   T. Szul and E. Sztul, "COPII and COPI Traffic at the ER-Golgi Interface," *Physiology*, vol. 26, no. 5, pp. 348–364, Oct. 2011, doi: 10.1152/physiol.00017.2011.

[5]   S. Huang and Y. Wang, "Golgi structure formation, function, and post-translational modifications in mammalian cells," *F1000Research*, vol. 6, p. 2050, Nov. 2017, doi: 10.12688/f1000research.11900.1.

[6]   W. Garten, "Characterization of Proprotein Convertases and Their Involvement in Virus Propagation," *Act. Viruses by Host Proteases*, pp. 205–248, Feb. 2018, doi: 10.1007/978-3-319-75474-1_9.

[7]   M. J. DALLING and P. L. BHALLA, "CHAPTER 5 - Mobilization of Nitrogen and Phosphorus from Endosperm," D. R. B. T.-G. and R. M. Murray, Ed. Academic Press, 1984, pp. 163–199.

[8]   J. S. Bonifacino and B. S. Glick, "The Mechanisms of Vesicle Budding and Fusion," *Cell*, vol. 116, no. 2, pp. 153–166, Jan. 2004, doi: 10.1016/S0092-8674(03)01079-1.

[9]   V. W. Hsu, S. Y. Lee, and J.-S. Yang, "The evolving understanding of COPI vesicle formation," *Nat. Rev. Mol. Cell Biol.*, vol. 10, no. 5, pp. 360–364, 2009, doi: 10.1038/nrm2663.

[10]   L. M. Traub, S. I. Bannykh, J. E. Rodel, M. Aridor, W. E. Balch, and S. Kornfeld, "AP-2-containing clathrin coats assemble on mature lysosomes.," *J. Cell Biol.*, vol. 135, no. 6, pp. 1801–1814, Dec. 1996, doi: 10.1083/jcb.135.6.1801.

[11]   P. Schu, "Vesicular protein transport," *Pharmacogenomics J.*, vol. 1, no. 4, pp. 262–271, 2001, doi: 10.1038/sj.tpj.6500055.

[12]   E. C. Arakel and B. Schwappach, "Formation of COPI-coated vesicles at a glance," *J. Cell Sci.*, vol. 131, no. 5, p. jcs209890, Mar. 2018, doi: 10.1242/jcs.209890.

[13]   T. Kirchhausen, "Adaptors for Clathrin-Mediated Traffic," *Annu. Rev. Cell*

Dev. Biol., vol. 15, no. 1, pp. 705–732, Nov. 1999, doi: 10.1146/annurev.cellbio.15.1.705.

[14]   X. Ren, G. G. Farías, B. J. Canagarajah, J. S. Bonifacino, and J. H. Hurley, "Structural Basis for Recruitment and Activation of the AP-1 Clathrin Adaptor Complex by Arf1," *Cell*, vol. 152, no. 4, pp. 755–767, 2013, doi: https://doi.org/10.1016/j.cell.2012.12.042.

[15]   X. Yu, M. Breitman, and J. Goldberg, "A Structure-Based Mechanism for Arf1-Dependent Recruitment of Coatomer to Membranes," *Cell*, vol. 148, no. 3, pp. 530–542, 2012, doi: https://doi.org/10.1016/j.cell.2012.01.015.

[16]   H. T. McMahon and I. G. Mills, "COP and clathrin-coated vesicle budding: different pathways, common approaches," *Curr. Opin. Cell Biol.*, vol. 16, no. 4, pp. 379–391, 2004, doi: https://doi.org/10.1016/j.ceb.2004.06.009.

[17]   K. Matsuoka *et al.*, "COPII-Coated Vesicle Formation Reconstituted with Purified Coat Proteins and Chemically Defined Liposomes," *Cell*, vol. 93, no. 2, pp. 263–275, 1998, doi: https://doi.org/10.1016/S0092-8674(00)81577-9.

[18]   J. T. Weissman, H. Plutner, and W. E. Balch, "The Mammalian Guanine Nucleotide Exchange Factor mSec12 is Essential for Activation of the Sar1 GTPase Directing Endoplasmic Reticulum Export," *Traffic*, vol. 2, no. 7, pp. 465–475, Jul. 2001, doi: https://doi.org/10.1034/j.1600-0854.2001.20704.x.

[19]   M. C. S. Lee, L. Orci, S. Hamamoto, E. Futai, M. Ravazzola, and R. Schekman, "Sar1p N-Terminal Helix Initiates Membrane Curvature and Completes the Fission of a COPII Vesicle," *Cell*, vol. 122, no. 4, pp. 605–617, 2005, doi: https://doi.org/10.1016/j.cell.2005.07.025.

[20]   A. Bielli, C. J. Haney, G. Gabreski, S. C. Watkins, S. I. Bannykh, and M. Aridor, "Regulation of Sar1 NH2 terminus by GTP binding and hydrolysis promotes membrane deformation to control COPII vesicle fission," *J. Cell Biol.*, vol. 171, no. 6, pp. 919–924, Dec. 2005, doi: 10.1083/jcb.200509095.

[21]   B. L. Tang, Y. Wang, Y. S. Ong, and W. Hong, "COPII and exit from the endoplasmic reticulum," *Biochim. Biophys. Acta - Mol. Cell Res.*, vol. 1744, no. 3, pp. 293–303, 2005, doi: https://doi.org/10.1016/j.bbamcr.2005.02.007.

[22]   X. Cao, N. Ballew, and C. Barlowe, "Initial docking of ER-derived vesicles requires Uso1p and Ypt1p but is independent of SNARE proteins," *EMBO J.*, vol. 17, no. 8, pp. 2156–2165, Apr. 1998, doi: 10.1093/emboj/17.8.2156.

[23]   X. Cao and C. Barlowe, "Asymmetric Requirements for a Rab Gtpase and Snare Proteins in Fusion of Copii Vesicles with Acceptor Membranes," *J. Cell Biol.*, vol. 149, no. 1, pp. 55–66, Apr. 2000, doi: 10.1083/jcb.149.1.55.

[24]   R. Behnia, F. A. Barr, J. J. Flanagan, C. Barlowe, and S. Munro, "The yeast orthologue of GRASP65 forms a complex with a coiled-coil protein that contributes to ER to Golgi traffic," *J. Cell Biol.*, vol. 176, no. 3, pp. 255–261, Jan. 2007, doi: 10.1083/jcb.200607151.

[25]   A. Eugster, G. Frigerio, M. Dale, and R. Duden, "COP I domains required for coatomer integrity, and novel interactions with ARF and ARF-GAP," *EMBO J.*, vol. 19, no. 15, pp. 3905–3917, Aug. 2000, doi: 10.1093/emboj/19.15.3905.

[26]   C. Lee and J. Goldberg, "Structure of Coatomer Cage Proteins and the Relationship among COPI, COPII, and Clathrin Vesicle Coats," *Cell*, vol. 142, no. 1, pp. 123–132, 2010, doi: https://doi.org/10.1016/j.cell.2010.05.030.

[27]   G. R. Hoffman, P. B. Rahl, R. N. Collins, and R. A. Cerione, "Conserved Structural Motifs in Intracellular Trafficking Pathways: Structure of the γCOP Appendage Domain," *Mol. Cell*, vol. 12, no. 3, pp. 615–625, 2003, doi: https://doi.org/10.1016/j.molcel.2003.08.002.

[28]   R. A. Kahn *et al.*, "Arf family GTPases: Roles in membrane traffic and microtubule dynamics," *Biochem. Soc. Trans.*, vol. 33, no. 6, pp. 1269–1272, 2005, doi: 10.1042/BST20051269.

[29]   C. L. Jackson and J. E. Casanova, "Turning on ARF: the Sec7 family of guanine-nucleotide-exchange factors," *Trends Cell Biol.*, vol. 10, no. 2, pp. 60–67, 2000, doi: https://doi.org/10.1016/S0962-8924(99)01699-2.

[30]   S. V Pipaliya, A. Schlacht, C. M. Klinger, R. A. Kahn, and J. Dacks, "Ancient complement and lineage-specific evolution of the Sec7 ARF GEF proteins in eukaryotes," *Mol. Biol. Cell*, vol. 30, no. 15, pp. 1846–1863, Jul. 2019, doi: 10.1091/mbc.E19-01-0073.

[31]   J. B. Sáenz *et al.*, "Golgicide A reveals essential roles for GBF1 in Golgi assembly and function," *Nat. Chem. Biol.*, vol. 5, no. 3, pp. 157–165, Mar. 2009, doi: 10.1038/nchembio.144.

[32]   R. A. Kahn *et al.*, "Consensus nomenclature for the human ArfGAP domain-containing proteins," *J. Cell Biol.*, vol. 182, no. 6, pp. 1039–1044, Sep. 2008, doi: 10.1083/jcb.200806041.

[33]   S. Y. Lee, J.-S. Yang, W. Hong, R. T. Premont, and V. W. Hsu, "ARFGAP1 plays a central role in coupling COPI cargo sorting with vesicle formation," *J. Cell Biol.*, vol. 168, no. 2, pp. 281–290, Jan. 2005, doi: 10.1083/jcb.200404008.

[34]   J. Goldberg, "Decoding of Sorting Signals by Coatomer through a GTPase Switch in the COPI Coat Complex," *Cell*, vol. 100, no. 6, pp. 671–679, Mar. 2000, doi: 10.1016/S0092-8674(00)80703-5.

[35]   R. Luo, V. L. Ha, R. Hayashi, and P. A. Randazzo, "Arf GAP2 is positively regulated by coatomer and cargo," *Cell. Signal.*, vol. 21, no. 7, pp. 1169–1179, 2009, doi: https://doi.org/10.1016/j.cellsig.2009.03.006.

[36]   C. T. A. Meiringer *et al.*, "The Dsl1 Protein Tethering Complex Is a Resident Endoplasmic Reticulum Complex, Which Interacts with Five Soluble NSF (N-Ethylmaleimide-sensitive Factor) Attachment Protein Receptors (SNAREs): IMPLICATIONS FOR FUSION AND FUSION REGULATION*," *J. Biol.*

Chem., vol. 286, no. 28, pp. 25039–25046, 2011, doi: https://doi.org/10.1074/jbc.M110.215327.

[37]   Y. Ren *et al.*, "A Structure-Based Mechanism for Vesicle Capture by the Multisubunit Tethering Complex Dsl1," *Cell*, vol. 139, no. 6, pp. 1119–1129, Dec. 2009, doi: 10.1016/j.cell.2009.11.002.

[38]   B. M. Pearse, "Clathrin: a unique protein associated with intracellular transfer of membrane by coated vesicles," *Proc. Natl. Acad. Sci. U. S. A.*, vol. 73, no. 4, pp. 1255–1259, Apr. 1976, doi: 10.1073/pnas.73.4.1255.

[39]   S. L. Schmid, "CLATHRIN-COATED VESICLE FORMATION AND PROTEIN SORTING: An Integrated Process," *Annu. Rev. Biochem.*, vol. 66, no. 1, pp. 511–548, Jun. 1997, doi: 10.1146/annurev.biochem.66.1.511.

[40]   A. Fotin *et al.*, "Molecular model for a complete clathrin lattice from electron cryomicroscopy," *Nature*, vol. 432, no. 7017, pp. 573–579, 2004, doi: 10.1038/nature03079.

[41]   R. M. Twyman, "Clathrin and Clathrin-Adaptors," L. R. B. T.-E. of N. Squire, Ed. Oxford: Academic Press, 2009, pp. 1013–1017.

[42]   M. Boehm and J. S. Bonifacino, "Adaptins," *Mol. Biol. Cell*, vol. 12, no. 10, pp. 2907–2920, Oct. 2001, doi: 10.1091/mbc.12.10.2907.

[43]   M. S. Robinson and J. S. Bonifacino, "Adaptor-related proteins," *Curr. Opin. Cell Biol.*, vol. 13, pp. 444–453, 2001.

[44]   I. Strazic Geljic *et al.*, "Viral Interactions with Adaptor-Protein Complexes: A Ubiquitous Trait among Viral Species," *Int. J. Mol. Sci.*, vol. 22, no. 10, p. 5274, May 2021, doi: 10.3390/ijms22105274.

[45]   J. Hirst *et al.*, "The Fifth Adaptor Protein Complex," *PLOS Biol.*, vol. 9, no. 10, p. e1001170, Oct. 2011, [Online]. Available: https://doi.org/10.1371/journal.pbio.1001170.

[46]   J. Hirst, C. Irving, and G. H. H. Borner, "Adaptor Protein Complexes AP-4 and AP-5: New Players in Endosomal Trafficking and Progressive Spastic Paraplegia," *Traffic*, vol. 14, no. 2, pp. 153–164, 2013, doi: 10.1111/tra.12028.

[47]   J. Hirst, D. N. Itzhak, R. Antrobus, G. H. H. Borner, and M. S. Robinson, "Role of the AP-5 adaptor protein complex in late endosome-to-Golgi retrieval," *PLOS Biol.*, vol. 16, no. 1, p. e2004411, Feb. 2018, doi: 10.1371/journal.pbio.2004411.

[48]   T. Kirchhausen *et al.*, "Structural and functional division into two domains of the large (100- to 115-kDa) chains of the clathrin-associated protein complex AP-2," *Proc. Natl. Acad. Sci. U. S. A.*, vol. 86, no. 8, pp. 2612–2616, Apr. 1989, doi: 10.1073/pnas.86.8.2612.

[49]   T. J. Brett, L. M. Traub, and D. H. Fremont, "Accessory Protein Recruitment Motifs in Clathrin-Mediated Endocytosis," *Structure*, vol. 10, no. 6, pp. 797–

809, 2002, doi: https://doi.org/10.1016/S0969-2126(02)00784-0.

[50] L. M. Traub, "Sorting it out: AP-2 and alternate clathrin adaptors in endocytic cargo selection," *J. Cell Biol.*, vol. 163, no. 2, pp. 203–208, Oct. 2003, doi: 10.1083/jcb.200309175.

[51] M. A. Edeling, C. Smith, and D. Owen, "Life of a clathrin coat: insights from clathrin and AP structures," *Nat. Rev. Mol. Cell Biol.*, vol. 7, no. 1, pp. 32–44, 2006, doi: 10.1038/nrm1786.

[52] D. J. Owen, Y. Vallis, B. M. F. Pearse, H. T. McMahon, and P. R. Evans, "The structure and function of the β2-adaptin appendage domain," *EMBO J.*, vol. 19, no. 16, pp. 4216–4227, Aug. 2000, doi: https://doi.org/10.1093/emboj/19.16.4216.

[53] L. M. Traub, "Common principles in clathrin-mediated sorting at the Golgi and the plasma membrane," *Biochim. Biophys. Acta - Mol. Cell Res.*, vol. 1744, no. 3, pp. 415–437, 2005, doi: https://doi.org/10.1016/j.bbamcr.2005.04.005.

[54] M. A. Edeling *et al.*, "Molecular Switches Involving the AP-2 β2 Appendage Regulate Endocytic Cargo Selection and Clathrin Coat Assembly," *Dev. Cell*, vol. 10, no. 3, pp. 329–342, 2006, doi: https://doi.org/10.1016/j.devcel.2006.01.016.

[55] M. S. Robinson, "The role of clathrin, adaptors and dynamin in endocytosis," *Curr. Opin. Cell Biol.*, vol. 6, no. 4, pp. 538–544, 1994, doi: https://doi.org/10.1016/0955-0674(94)90074-4.

[56] E. M. Schmid and H. T. McMahon, "Integrating molecular and network biology to decode endocytosis," *Nature*, vol. 448, no. 7156, pp. 883–888, 2007, doi: 10.1038/nature06031.

[57] L. M. Traub and B. Wendland, "How to don a coat," *Nature*, vol. 465, no. 7298, pp. 556–557, 2010, doi: 10.1038/465556a.

[58] L. M. Traub and J. S. Bonifacino, "Cargo recognition in clathrin-mediated endocytosis," *Cold Spring Harb. Perspect. Biol.*, vol. 5, no. 11, pp. a016790–a016790, Nov. 2013, doi: 10.1101/cshperspect.a016790.

[59] C. Thurieau *et al.*, "Molecular Cloning and Complete Amino Acid Sequence of AP50, an Assembly Protein Associated with Clathrin-Coated Vesicles," *Dna*, vol. 7, no. 10, pp. 663–669, 1988, doi: 10.1089/dna.1988.7.663.

[60] Y. NAKAYAMA, M. GOEBL, B. O'BRINE GRECO, S. LEMMON, E. PINGCHANG CHOW, and T. KIRCHHAUSEN, "The medium chains of the mammalian clathrin-associated proteins have a homolog in yeast," *Eur. J. Biochem.*, vol. 202, no. 2, pp. 569–574, Dec. 1991, doi: https://doi.org/10.1111/j.1432-1033.1991.tb16409.x.

[61] L. M. Traub, "Clathrin couture: fashioning distinctive membrane coats at the

cell surface," *PLoS Biol.*, vol. 7, no. 9, pp. e1000192–e1000192, Sep. 2009, doi: 10.1371/journal.pbio.1000192.

[62] L. M. Traub, "Tickets to ride: selecting cargo for clathrin-regulated internalization," *Nat. Rev. Mol. Cell Biol.*, vol. 10, no. 9, pp. 583–596, 2009, doi: 10.1038/nrm2751.

[63] J. Baltes *et al.*, "σ1B adaptin regulates adipogenesis by mediating the sorting of sortilin in adipose tissue," *J. Cell Sci.*, vol. 127, no. 16, pp. 3477–3487, Aug. 2014, doi: 10.1242/jcs.146886.

[64] K. Dib, I. G. Tikhonova, A. Ivetic, and P. Schu, "The cytoplasmic tail of L-selectin interacts with the adaptor-protein complex AP-1 subunit μ1A via a novel basic binding motif," *J. Biol. Chem.*, vol. 292, no. 16, pp. 6703–6714, Apr. 2017, doi: 10.1074/jbc.M116.768598.

[65] S. Y. Park and X. Guo, "Adaptor protein complexes and intracellular transport," *Biosci. Rep.*, vol. 34, no. 4, p. e00123, Jul. 2014, doi: 10.1042/BSR20140069.

[66] D. Zizioli *et al.*, "γ2 and γ1AP-1 complexes: Different essential functions and regulatory mechanisms in clathrin-dependent protein sorting," *Eur. J. Cell Biol.*, vol. 96, no. 4, pp. 356–368, 2017, doi: https://doi.org/10.1016/j.ejcb.2017.03.008.

[67] D. Zizioli, C. Meyer, G. Guhde, P. Saftig, K. von Figura, and P. Schu, "Early Embryonic Death of Mice Deficient in γ-Adaptin*," *J. Biol. Chem.*, vol. 274, no. 9, pp. 5385–5390, 1999, doi: https://doi.org/10.1074/jbc.274.9.5385.

[68] P. G. Adamopoulos, C. K. Kontos, M. A. Diamantopoulos, and A. Scorilas, "Molecular cloning of novel transcripts of the adaptor-related protein complex 2 alpha 1 subunit (AP2A1) gene, using Next-Generation Sequencing," *Gene*, vol. 678, pp. 55–64, 2018, doi: https://doi.org/10.1016/j.gene.2018.08.008.

[69] C. Meyer *et al.*, "mu1A-adaptin-deficient mice: lethality, loss of AP-1 binding and rerouting of mannose 6-phosphate receptors," *EMBO J.*, vol. 19, no. 10, pp. 2193–2203, May 2000, doi: 10.1093/emboj/19.10.2193.

[70] J. Burgess *et al.*, "AP-1 and clathrin are essential for secretory granule biogenesis in Drosophila," *Mol. Biol. Cell*, vol. 22, no. 12, pp. 2094–2105, Apr. 2011, doi: 10.1091/mbc.e11-01-0054.

[71] A. A. Peden, V. Oorschot, B. A. Hesser, C. D. Austin, R. H. Scheller, and J. Klumperman, "Localization of the AP-3 adaptor complex defines a novel endosomal exit site for lysosomal membrane proteins," *J. Cell Biol.*, vol. 164, no. 7, pp. 1065–1076, Mar. 2004, doi: 10.1083/jcb.200311064.

[72] E. C. Dell'Angelica, V. Shotelersuk, R. C. Aguilar, W. A. Gahl, and J. S. Bonifacino, "Altered Trafficking of Lysosomal Proteins in Hermansky-Pudlak Syndrome Due to Mutations in the β3A Subunit of the AP-3 Adaptor," *Mol. Cell*, vol. 3, no. 1, pp. 11–21, 1999, doi: https://doi.org/10.1016/S1097-

2765(00)80170-7.

[73]   G. C. P., P. S. D., L. Anna, C. A. L., and F. A. P., "Regulation of large dense-core vesicle volume and neurotransmitter content mediated by adaptor protein 3," *Proc. Natl. Acad. Sci.*, vol. 103, no. 26, pp. 10035–10040, Jun. 2006, doi: 10.1073/pnas.0509844103.

[74]   A. C. Theos *et al.*, "Functions of adaptor protein (AP)-3 and AP-1 in tyrosinase sorting from endosomes to melanosomes," *Mol. Biol. Cell*, vol. 16, no. 11, pp. 5356–5372, Nov. 2005, doi: 10.1091/mbc.e05-07-0626.

[75]   B. H. Ross, Y. Lin, E. A. Corales, P. V Burgos, and G. A. Mardones, "Structural and Functional Characterization of Cargo-Binding Sites on the μ4-Subunit of Adaptor Protein Complex 4," *PLoS One*, vol. 9, no. 2, p. e88147, Feb. 2014, [Online]. Available: https://doi.org/10.1371/journal.pone.0088147.

[76]   T. Simmen, S. Höning, A. Icking, R. Tikkanen, and W. Hunziker, "AP-4 binds basolateral signals and participates in basolateral sorting in epithelial MDCK cells," *Nat. Cell Biol.*, vol. 4, no. 2, pp. 154–159, 2002, doi: 10.1038/ncb745.

[77]   S. Matsuda *et al.*, "Accumulation of AMPA Receptors in Autophagosomes in Neuronal Axons Lacking Adaptor Protein AP-4," *Neuron*, vol. 57, no. 5, pp. 730–745, 2008, doi: 10.1016/j.neuron.2008.02.012.

[78]   R. Mattera, S. Y. Park, R. De Pace, C. M. Guardia, and J. S. Bonifacino, "AP-4 mediates export of ATG9A from the trans-Golgi network to promote autophagosome formation," *Proc. Natl. Acad. Sci.*, vol. 114, no. 50, pp. E10697–E10706, Dec. 2017, doi: 10.1073/PNAS.1717327114.

[79]   D. Ivankovic *et al.*, "Axonal autophagosome maturation defect through failure of ATG9A sorting underpins pathology in AP-4 deficiency syndrome," *Autophagy*, vol. 16, no. 3, pp. 391–407, Mar. 2020, doi: 10.1080/15548627.2019.1615302.

[80]   M. Khundadze *et al.*, "A mouse model for SPG48 reveals a block of autophagic flux upon disruption of adaptor protein complex five," *Neurobiol. Dis.*, vol. 127, pp. 419–431, 2019, doi: https://doi.org/10.1016/j.nbd.2019.03.026.

[81]   R. Lisa *et al.*, "Clathrin light chain diversity regulates membrane deformation in vitro and synaptic vesicle formation in vivo," *Proc. Natl. Acad. Sci.*, vol. 117, no. 38, pp. 23527–23538, Sep. 2020, doi: 10.1073/pnas.2003662117.

[82]   K. T. *et al.*, "Clathrin Light Chains LCA and LCB Are Similar, Polymorphic, and Share Repeated Heptad Motifs," *Science (80-.).*, vol. 236, no. 4799, pp. 320–324, Apr. 1987, doi: 10.1126/science.3563513.

[83]   J. D. Wilbur, C.-Y. Chen, V. Manalo, P. K. Hwang, R. J. Fletterick, and F. M. Brodsky, "Actin binding by Hip1 (huntingtin-interacting protein 1) and Hip1R (Hip1-related protein) is regulated by clathrin light chain," *J. Biol. Chem.*, vol. 283, no. 47, pp. 32870–32879, Nov. 2008, doi: 10.1074/jbc.M802863200.

[84] F. M. Brodsky, "Diversity of Clathrin Function: New Tricks for an Old Protein," *Annu. Rev. Cell Dev. Biol.*, vol. 28, no. 1, pp. 309–336, Oct. 2012, doi: 10.1146/annurev-cellbio-101011-155716.

[85] E. Candiello, R. Mishra, B. Schmidt, O. Jahn, and P. Schu, "Differential regulation of synaptic AP-2/clathrin vesicle uncoating in synaptic plasticity," *Sci. Rep.*, vol. 7, no. 1, pp. 1–11, 2017, doi: 10.1038/s41598-017-16055-4.

[86] P. K. Nandi, K. Prasad, R. E. Lippoldt, A. Alfsen, and H. Edelhoch, "Reversibility of coated vesicle dissociation," *Biochemistry*, vol. 21, no. 25, pp. 6434–6440, Dec. 1982, doi: 10.1021/bi00268a018.

[87] A. Di Cerbo, P. K. Nandi, and H. Edelhoch, "Interaction of basic compounds with coated vesicles," *Biochemistry*, vol. 23, no. 25, pp. 6036–6040, Dec. 1984, doi: 10.1021/bi00320a021.

[88] P. K. Nandi and H. Edelhoch, "The effects of lyotropic (Hofmeister) salts on the stability of clathrin coat structure in coated vesicles and baskets.," *J. Biol. Chem.*, vol. 259, no. 18, pp. 11290–11296, 1984, doi: https://doi.org/10.1016/S0021-9258(18)90861-6.

[89] R. Pascolutti *et al.*, "Molecularly Distinct Clathrin-Coated Pits Differentially Impact EGFR Fate and Signaling," *Cell Rep.*, vol. 27, no. 10, pp. 3049-3061.e6, 2019, doi: https://doi.org/10.1016/j.celrep.2019.05.017.

[90] E. M. Bennett, C.-Y. Chen, Å. E. Y. Engqvist-Goldstein, D. G. Drubin, and F. M. Brodsky, "Clathrin Hub Expression Dissociates the Actin-Binding Protein Hip1R from Coated Pits and Disrupts Their Alignment with the Actin Cytoskeleton," *Traffic*, vol. 2, no. 11, pp. 851–858, Nov. 2001, doi: https://doi.org/10.1046/j.1398-9219.2001.x.

[91] V. Poupon *et al.*, "Clathrin light chains function in mannose phosphate receptor trafficking via regulation of actin assembly," *Proc. Natl. Acad. Sci.*, vol. 105, no. 1, pp. 168 LP – 173, Jan. 2008, doi: 10.1073/pnas.0707269105.

[92] F. Ferreira *et al.*, "Endocytosis of G Protein-Coupled Receptors Is Regulated by Clathrin Light Chain Phosphorylation," *Curr. Biol.*, vol. 22, no. 15, pp. 1361–1370, 2012, doi: https://doi.org/10.1016/j.cub.2012.05.034.

[93] S. Ahle and E. Ungewickell, "Purification and properties of a new clathrin assembly protein," *EMBO J.*, vol. 5, no. 12, pp. 3143–3149, Dec. 1986, [Online]. Available: https://pubmed.ncbi.nlm.nih.gov/3816757.

[94] F. Blondeau *et al.*, "Tandem MS analysis of brain clathrin-coated vesicles reveals their critical involvement in synaptic vesicle recycling," *Proc. Natl. Acad. Sci.*, vol. 101, no. 11, pp. 3833–3838, Mar. 2004, doi: 10.1073/PNAS.0308186101.

[95] P. S. McPherson, "Proteomic analysis of clathrin-coated vesicles," *Proteomics*, vol. 10, no. 22, pp. 4025–4039, Nov. 2010, doi: https://doi.org/10.1002/pmic.201000253.

[96]   D. A. Lewin *et al.*, "Cloning, expression, and localization of a novel γ-adaptin-like molecule," *FEBS Lett.*, vol. 435, no. 2–3, pp. 263–268, Sep. 1998, doi: https://doi.org/10.1016/S0014-5793(98)01083-7.

[97]   D. Zizioli *et al.*, "Characterization of the AP-1 μ1A and μ1B adaptins in zebrafish (Danio rerio)," *Dev. Dyn.*, vol. 239, no. 9, pp. 2404–2412, Sep. 2010, doi: https://doi.org/10.1002/dvdy.22372.

[98]   E.-L. Eskelinen, C. Meyer, H. Ohno, K. von Figura, and P. Schu, "The polarized epithelia-specific μ1B-adaptin complements μ1A-deficiency in fibroblasts," *EMBO Rep.*, vol. 3, no. 5, pp. 471–477, May 2002, doi: https://doi.org/10.1093/embo-reports/kvf092.

[99]   H. Fölsch, "Role of the epithelial cell-specific clathrin adaptor complex AP-1B in cell polarity," *Cell. Logist.*, vol. 5, no. 2, pp. e1074331–e1074331, Jul. 2015, doi: 10.1080/21592799.2015.1074331.

[100]   N. Glyvuk *et al.*, "AP-1/sigma1B-adaptin mediates endosomal synaptic vesicle recycling, learning and memory," *EMBO J.*, vol. 29, no. 8, pp. 1318–1330, Apr. 2010, doi: 10.1038/emboj.2010.15.

[101]   E. Candiello, M. Kratzke, D. Wenzel, D. Cassel, and P. Schu, "AP-1/σ1A and AP-1/σ1B adaptor-proteins differentially regulate neuronal early endosome maturation via the Rab5/Vps34-pathway," *Sci. Rep.*, vol. 6, no. 1, p. 29950, 2016, doi: 10.1038/srep29950.

[102]   M. Kratzke, E. Candiello, B. Schmidt, O. Jahn, and P. Schu, "AP-1/σ1B-Dependent SV Protein Recycling Is Regulated in Early Endosomes and Is Coupled to AP-2 Endocytosis," *Mol. Neurobiol.*, vol. 52, no. 1, pp. 142–161, 2015, doi: 10.1007/s12035-014-8852-0.

[103]   S. P. V., T. Kaoru, F. M. J., S. J. H., W. M. D., and E. S. D., "Phosphatidylinositol 3-Kinase Encoded by Yeast VPS34 Gene Essential for Protein Sorting," *Science (80-.).*, vol. 260, no. 5104, pp. 88–91, Apr. 1993, doi: 10.1126/science.8385367.

[104]   C. E. Futter, L. M. Collinson, J. M. Backer, and C. R. Hopkins, "Human VPS34 is required for internal vesicle formation within multivesicular endosomes," *J. Cell Biol.*, vol. 155, no. 7, pp. 1251–1264, Dec. 2001, doi: 10.1083/jcb.200108152.

[105]   M. Takashi *et al.*, "Clathrin Adaptor AP-2 Is Essential for Early Embryonal Development," *Mol. Cell. Biol.*, vol. 25, no. 21, pp. 9318–9323, Nov. 2005, doi: 10.1128/MCB.25.21.9318-9323.2005.

[106]   R. Thomas Sosa, M. M. Weber, Y. Wen, and T. J. O'Halloran, "A Single β Adaptin Contributes to AP1 and AP2 Complexes and Clathrin Function in Dictyostelium," *Traffic*, vol. 13, no. 2, pp. 305–316, 2012, doi: 10.1111/j.1600-0854.2011.01310.x.

[107]   W. Li, R. Puertollano, J. S. Bonifacino, P. A. Overbeek, and E. T. Everett,

"Disruption of the murine Ap2β1 gene causes nonsyndromic cleft palate," *Cleft Palate. Craniofac. J.*, vol. 47, no. 6, pp. 566–573, Nov. 2010, doi: 10.1597/09-145.

[108] S. O. Rizzoli, "Synaptic vesicle recycling: steps and principles," *EMBO J.*, vol. 33, no. 8, pp. 788–822, Apr. 2014, doi: 10.1002/embj.201386357.

[109] T. C. Südhof, "THE SYNAPTIC VESICLE CYCLE," *Annu. Rev. Neurosci.*, vol. 27, no. 1, pp. 509–547, Jun. 2004, doi: 10.1146/annurev.neuro.26.041002.131412.

[110] O. Mundigl and P. De Camilli, "Formation of synaptic vesicles," *Curr. Opin. Cell Biol.*, vol. 6, no. 4, pp. 561–567, 1994, doi: https://doi.org/10.1016/0955-0674(94)90077-9.

[111] Y. Saheki and P. De Camilli, "Synaptic vesicle endocytosis," *Cold Spring Harb. Perspect. Biol.*, vol. 4, no. 9, pp. a005645–a005645, Sep. 2012, doi: 10.1101/cshperspect.a005645.

[112] D. Ricotta, S. D. Conner, S. L. Schmid, K. von Figura, and S. Höning, "Phosphorylation of the AP2 μ subunit by AAK1 mediates high affinity binding to membrane protein sorting signals," *J. Cell Biol.*, vol. 156, no. 5, pp. 791–795, Mar. 2002, doi: 10.1083/jcb.200111068.

[113] S. D. Conner and S. L. Schmid, "Identification of an adaptor-associated kinase, AAK1, as a regulator of clathrin-mediated endocytosis," *J. Cell Biol.*, vol. 156, no. 5, pp. 921–929, Mar. 2002, doi: 10.1083/jcb.200108123.

[114] S. D. Conner, T. Schröter, and S. L. Schmid, "AAK1-Mediated μ2 Phosphorylation is Stimulated by Assembled Clathrin," *Traffic*, vol. 4, no. 12, pp. 885–890, Dec. 2003, doi: https://doi.org/10.1046/j.1398-9219.2003.0142.x.

[115] K. Takei and V. Haucke, "Clathrin-mediated endocytosis: membrane factors pull the trigger," *Trends Cell Biol.*, vol. 11, no. 9, pp. 385–391, 2001, doi: https://doi.org/10.1016/S0962-8924(01)02082-7.

[116] M. Mettlen, P.-H. Chen, S. Srinivasan, G. Danuser, and S. L. Schmid, "Regulation of Clathrin-Mediated Endocytosis," *Annu. Rev. Biochem.*, vol. 87, no. 1, pp. 871–896, Jun. 2018, doi: 10.1146/annurev-biochem-062917-012644.

[117] B. Antonny *et al.*, "Membrane fission by dynamin: what we know and what we need to know," *EMBO J.*, vol. 35, no. 21, pp. 2270–2284, Nov. 2016, doi: https://doi.org/10.15252/embj.201694613.

[118] T. C. Südhof and J. E. Rothman, "Membrane fusion: grappling with SNARE and SM proteins," *Science*, vol. 323, no. 5913, pp. 474–477, Jan. 2009, doi: 10.1126/science.1161748.

[119] L. M. Traub, "Regarding the amazing choreography of clathrin coats," *PLoS*

Biol., vol. 9, no. 3, pp. e1001037–e1001037, Mar. 2011, doi: 10.1371/journal.pbio.1001037.

[120] H. W. Mike *et al.*, "FCHo Proteins Are Nucleators of Clathrin-Mediated Endocytosis," *Science (80-.).*, vol. 328, no. 5983, pp. 1281–1284, Jun. 2010, doi: 10.1126/science.1188462.

[121] A. Reider *et al.*, "Syp1 is a conserved endocytic adaptor that contains domains involved in cargo selection and membrane tubulation," *EMBO J.*, vol. 28, no. 20, pp. 3103–3116, Oct. 2009, doi: 10.1038/emboj.2009.248.

[122] H. E. M. Stimpson, C. P. Toret, A. T. Cheng, B. S. Pauly, and D. G. Drubin, "Early-Arriving Syp1p and Ede1p Function in Endocytic Site Placement and Formation in Budding Yeast," *Mol. Biol. Cell*, vol. 20, no. 22, pp. 4640–4651, Sep. 2009, doi: 10.1091/mbc.e09-05-0429.

[123] D. M. Henderson and S. D. Conner, "A Novel AAK1 Splice Variant Functions at Multiple Steps of the Endocytic Pathway," *Mol. Biol. Cell*, vol. 18, no. 7, pp. 2698–2706, May 2007, doi: 10.1091/mbc.e06-09-0831.

[124] H. Volker and C. Pietro De, "AP-2 Recruitment to Synaptotagmin Stimulated by Tyrosine-Based Endocytic Motifs," *Science (80-.).*, vol. 285, no. 5431, pp. 1268–1271, Aug. 1999, doi: 10.1126/science.285.5431.1268.

[125] L. Hinrichsen, A. Meyerholz, S. Groos, and E. J. Ungewickell, "Bending a membrane: How clathrin affects budding," *Proc. Natl. Acad. Sci.*, vol. 103, no. 23, pp. 8715 LP – 8720, Jun. 2006, doi: 10.1073/pnas.0600312103.

[126] H. Maib, F. Ferreira, S. Vassilopoulos, and E. Smythe, "Cargo regulates clathrin-coated pit invagination via clathrin light chain phosphorylation," *J. Cell Biol.*, vol. 217, no. 12, pp. 4253–4266, Sep. 2018, doi: 10.1083/jcb.201805005.

[127] T. Kosaka and K. Ikeda, "Reversible blockage of membrane retrieval and endocytosis in the garland cell of the temperature-sensitive mutant of Drosophila melanogaster, shibirets1.," *J. Cell Biol.*, vol. 97, no. 2, pp. 499–507, 1983, doi: 10.1083/jcb.97.2.499.

[128] T. Kosaka and K. Ikeda, "Possible temperature-dependent blockage of synaptic vesicle recycling induced by a single gene mutation in drosophila," *J. Neurobiol.*, vol. 14, no. 3, pp. 207–225, 1983, doi: 10.1002/neu.480140305.

[129] P. Wigge *et al.*, "Amphiphysin heterodimers: potential role in clathrin-mediated endocytosis," *Mol. Biol. Cell*, vol. 8, no. 10, pp. 2003–2015, Oct. 1997, doi: 10.1091/mbc.8.10.2003.

[130] S. M. Ferguson *et al.*, "Coordinated actions of actin and BAR proteins upstream of dynamin at endocytic clathrin-coated pits," *Dev. Cell*, vol. 17, no. 6, pp. 811–822, Dec. 2009, doi: 10.1016/j.devcel.2009.11.005.

[131] A. Sundborger, C. Soderblom, O. Vorontsova, E. Evergren, J. E. Hinshaw,

and O. Shupliakov, "An endophilin-dynamin complex promotes budding of clathrin-coated vesicles during synaptic vesicle recycling," *J. Cell Sci.*, vol. 124, no. Pt 1, pp. 133–143, Jan. 2011, doi: 10.1242/jcs.072686.

[132] S. M. Sweitzer and J. E. Hinshaw, "Dynamin Undergoes a GTP-Dependent Conformational Change Causing Vesiculation," *Cell*, vol. 93, no. 6, pp. 1021–1029, Jun. 1998, doi: 10.1016/S0092-8674(00)81207-6.

[133] M. H. B. Stowell, B. Marks, P. Wigge, and H. T. McMahon, "Nucleotide-dependent conformational changes in dynamin: evidence for a mechanochemical molecular spring," *Nat. Cell Biol.*, vol. 1, no. 1, pp. 27–32, 1999, doi: 10.1038/8997.

[134] A. Roux, K. Uyhazi, A. Frost, and P. De Camilli, "GTP-dependent twisting of dynamin implicates constriction and tension in membrane fission," *Nature*, vol. 441, no. 7092, pp. 528–531, 2006, doi: 10.1038/nature04718.

[135] P. V Bashkirov, S. A. Akimov, A. I. Evseev, S. L. Schmid, J. Zimmerberg, and V. A. Frolov, "GTPase cycle of dynamin is coupled to membrane squeeze and release, leading to spontaneous fission," *Cell*, vol. 135, no. 7, pp. 1276–1286, Dec. 2008, doi: 10.1016/j.cell.2008.11.028.

[136] M. Kaksonen and A. Roux, "Mechanisms of clathrin-mediated endocytosis," *Nat. Rev. Mol. Cell Biol.*, vol. 19, no. 5, pp. 313–326, 2018, doi: 10.1038/nrm.2017.132.

[137] W. A. Braell, D. M. Schlossman, S. L. Schmid, and J. E. Rothman, "Dissociation of clathrin coats coupled to the hydrolysis of ATP: role of an uncoating ATPase," *J. Cell Biol.*, vol. 99, no. 2, pp. 734–741, Aug. 1984, doi: 10.1083/jcb.99.2.734.

[138] D. M. Schlossman, S. L. Schmid, W. A. Braell, and J. E. Rothman, "An enzyme that removes clathrin coats: purification of an uncoating ATPase," *J. Cell Biol.*, vol. 99, no. 2, pp. 723–733, Aug. 1984, doi: 10.1083/jcb.99.2.723.

[139] U. Scheele, J. Alves, R. Frank, M. Düwel, C. Kalthoff, and E. Ungewickell, "Molecular and Functional Characterization of Clathrin- and AP-2-binding Determinants within a Disordered Domain of Auxilin *," *J. Biol. Chem.*, vol. 278, no. 28, pp. 25357–25368, Jul. 2003, doi: 10.1074/jbc.M303738200.

[140] Y. Xing, T. Böcking, M. Wolf, N. Grigorieff, T. Kirchhausen, and S. C. Harrison, "Structure of clathrin coat with bound Hsc70 and auxilin: mechanism of Hsc70-facilitated disassembly," *EMBO J.*, vol. 29, no. 3, pp. 655–665, Feb. 2010, doi: 10.1038/emboj.2009.383.

[141] S. L. Newmyer, A. Christensen, and S. Sever, "Auxilin-Dynamin Interactions Link the Uncoating ATPase Chaperone Machinery with Vesicle Formation," *Dev. Cell*, vol. 4, no. 6, pp. 929–940, 2003, doi: https://doi.org/10.1016/S1534-5807(03)00157-6.

[142] R. Sousa *et al.*, "Clathrin-coat disassembly illuminates the mechanisms of

Hsp70 force generation," *Nat. Struct. Mol. Biol.*, vol. 23, no. 9, pp. 821–829, 2016, doi: 10.1038/nsmb.3272.

[143] R. Sousa and E. M. Lafer, "The role of molecular chaperones in clathrin mediated vesicular trafficking," *Frontiers in Molecular Biosciences*, vol. 2. p. 26, 2015, [Online]. Available: https://www.frontiersin.org/article/10.3389/fmolb.2015.00026.

[144] P. De Los Rios, A. Ben-Zvi, O. Slutsky, A. Azem, and P. Goloubinoff, "Hsp70 chaperones accelerate protein translocation and the unfolding of stable protein aggregates by entropic pulling," *Proc. Natl. Acad. Sci.*, vol. 103, no. 16, pp. 6166 LP – 6171, Apr. 2006, doi: 10.1073/pnas.0510496103.

[145] P. Goloubinoff and P. D. L. Rios, "The mechanism of Hsp70 chaperones: (entropic) pulling the models together," *Trends Biochem. Sci.*, vol. 32, no. 8, pp. 372–380, 2007, doi: https://doi.org/10.1016/j.tibs.2007.06.008.

[146] J. P. Schuermann *et al.*, "Structure of the Hsp110:Hsc70 Nucleotide Exchange Machine," *Mol. Cell*, vol. 31, no. 2, pp. 232–243, 2008, doi: https://doi.org/10.1016/j.molcel.2008.05.006.

[147] S. L. Newmyer and S. L. Schmid, "Dominant-Interfering Hsc70 Mutants Disrupt Multiple Stages of the Clathrin-Coated Vesicle Cycle in Vivo," *J. Cell Biol.*, vol. 152, no. 3, pp. 607–620, Feb. 2001, doi: 10.1083/jcb.152.3.607.

[148] L. Packschies, H. Theyssen, A. Buchberger, B. Bukau, R. S. Goody, and J. Reinstein, "GrpE Accelerates Nucleotide Exchange of the Molecular Chaperone DnaK with an Associative Displacement Mechanism," *Biochemistry*, vol. 36, no. 12, pp. 3417–3422, Mar. 1997, doi: 10.1021/bi962835l.

[149] J. R. Morgan *et al.*, "A Role for an Hsp70 Nucleotide Exchange Factor in the Regulation of Synaptic Vesicle Endocytosis," *J. Neurosci.*, vol. 33, no. 18, pp. 8009 LP – 8021, May 2013, doi: 10.1523/JNEUROSCI.4505-12.2013.

[150] K. Ishihara, N. Yamagishi, and T. Hatayama, "Protein kinase CK2 phosphorylates Hsp105 alpha at Ser509 and modulates its function," *Biochem. J.*, vol. 371, no. Pt 3, pp. 917–925, May 2003, doi: 10.1042/BJ20021331.

[151] R. M. Perera, R. Zoncu, L. Lucast, P. De Camilli, and D. Toomre, "Two synaptojanin 1 isoforms are recruited to clathrin-coated pits at different stages," *Proc. Natl. Acad. Sci.*, vol. 103, no. 51, pp. 19332 LP – 19337, Dec. 2006, doi: 10.1073/pnas.0609795104.

[152] P. S. McPherson *et al.*, "A presynaptic inositol-5-phosphatase," *Nature*, vol. 379, no. 6563, pp. 353–357, 1996, doi: 10.1038/379353a0.

[153] O. Cremona *et al.*, "Essential Role of Phosphoinositide Metabolism in Synaptic Vesicle Recycling," *Cell*, vol. 99, no. 2, pp. 179–188, 1999, doi: https://doi.org/10.1016/S0092-8674(00)81649-9.

[154] R. Zoncu *et al.*, "Loss of endocytic clathrin-coated pits upon acute depletion of phosphatidylinositol 4,5-bisphosphate," *Proc. Natl. Acad. Sci.*, vol. 104, no. 10, pp. 3793 LP – 3798, Mar. 2007, doi: 10.1073/pnas.0611733104.

[155] G. Di Paolo *et al.*, "Impaired PtdIns(4,5)P2 synthesis in nerve terminals produces defects in synaptic vesicle trafficking," *Nature*, vol. 431, no. 7007, pp. 415–422, 2004, doi: 10.1038/nature02896.

[156] K. S. Erdmann *et al.*, "A Role of the Lowe Syndrome Protein OCRL in Early Steps of the Endocytic Pathway," *Dev. Cell*, vol. 13, no. 3, pp. 377–390, 2007, doi: https://doi.org/10.1016/j.devcel.2007.08.004.

[157] R. Choudhury *et al.*, "Lowe Syndrome Protein OCRL1 Interacts with Clathrin and Regulates Protein Trafficking between Endosomes and the Trans-Golgi Network," *Mol. Biol. Cell*, vol. 16, no. 8, pp. 3467–3479, May 2005, doi: 10.1091/mbc.e05-02-0120.

[158] A. Ungewickell, M. E. Ward, E. Ungewickell, and P. W. Majerus, "The inositol polyphosphate 5-phosphatase Ocrl associates with endosomes that are partially coated with clathrin," *Proc. Natl. Acad. Sci. U. S. A.*, vol. 101, no. 37, pp. 13501–13506, Sep. 2004, doi: 10.1073/pnas.0405664101.

[159] L. P. Jackson *et al.*, "A Large-Scale Conformational Change Couples Membrane Recruitment to Cargo Binding in the AP2 Clathrin Adaptor Complex," *Cell*, vol. 141, no. 7, pp. 1220–1229, 2010, doi: https://doi.org/10.1016/j.cell.2010.05.006.

[160] I. Augustin, C. Rosenmund, T. C. Südhof, and N. Brose, "Munc13-1 is essential for fusion competence of glutamatergic synaptic vesicles," *Nature*, vol. 400, no. 6743, pp. 457–461, 1999, doi: 10.1038/22768.

[161] H. Kawabe *et al.*, "ELKS1 localizes the synaptic vesicle priming protein bMunc13-2 to a specific subset of active zones," *J. Cell Biol.*, vol. 216, no. 4, pp. 1143–1161, Apr. 2017, doi: 10.1083/jcb.201606086.

[162] I. Milosevic *et al.*, "Recruitment of endophilin to clathrin-coated pit necks is required for efficient vesicle uncoating after fission," *Neuron*, vol. 72, no. 4, pp. 587–601, Nov. 2011, doi: 10.1016/j.neuron.2011.08.029.

[163] I. Milosevic, "Revisiting the Role of Clathrin-Mediated Endoytosis in Synaptic Vesicle Recycling," *Front. Cell. Neurosci.*, vol. 12, p. 27, Feb. 2018, doi: 10.3389/fncel.2018.00027.

[164] R. Mishra, G. F. Sengül, E. Candiello, and P. Schu, "Synaptic AP2 CCV life cycle regulation by the Eps15, ITSN1, Sgip1/AP2, synaptojanin1 interactome," *Sci. Rep.*, vol. 11, no. 1, pp. 1–16, 2021, doi: 10.1038/s41598-021-87591-3.

[165] S. Matta *et al.*, "LRRK2 Controls an EndoA Phosphorylation Cycle in Synaptic Endocytosis," *Neuron*, vol. 75, no. 6, pp. 1008–1021, 2012, doi: https://doi.org/10.1016/j.neuron.2012.08.022.

[166] J. C. Trinidad, "Synaptosomes and Synaptic Vesicles," R. A. Bradshaw and P. D. B. T.-E. of C. B. Stahl, Eds. Waltham: Academic Press, 2016, pp. 293–301.

[167] T. Böcking *et al.*, "Key interactions for clathrin coat stability," *Structure*, vol. 22, no. 6, pp. 819–829, Jun. 2014, doi: 10.1016/j.str.2014.04.002.

[168] "A Guide to Polyacrylamide Gel Electrophoresis and Detection Part I : Theory and Product Selection Part II : Methods Part III : Troubleshooting Part IV : Appendices."

[169] L. Biosciences, "Technical Note: Protein Electrotransfer Methods and the Odyssey Infrared Imaging Imaging System," no. September 2008, 2009, [Online]. Available: https://www.licor.com/bio/guide/westerns/transfer_options.

[170] C. M. O´Connor, "Exercise 1 - Preparing the membrane replica." Boston College, 2021, [Online]. Available: https://bio.libretexts.org/@go/page/17591.

[171] G. León, "Membrane Stripping," *Encycl. Membr.*, pp. 1–2, 2014, doi: 10.1007/978-3-642-40872-4_1633-1.

[172] *Phostag SDS-OAGE Guidebook*. FUJIFILM Wako Pure Chemical Corporation.

[173] X. Wang, X. Li, and Y. Li, "A modified Coomassie Brilliant Blue staining method at nanogram sensitivity compatible with proteomic analysis," *Biotechnol. Lett.*, vol. 29, no. 10, pp. 1599–1603, 2007, doi: 10.1007/s10529-007-9425-3.

[174] M. Pink, N. Verma, A. W. Rettenmeier, and S. Schmitz-Spanke, "CBB staining protocol with higher sensitivity and mass spectrometric compatibility," *Electrophoresis*, vol. 31, no. 4, pp. 593–598, Jan. 2010, doi: https://doi.org/10.1002/elps.200900481.

[175] L. Brown and J. H. Beynon, "Mass Spectrometry," *Encyclopedia Britannica*, 2020. https://www.britannica.com/science/mass-spectrometry (accessed Feb. 08, 2022).

[176] S. Rosati *et al.*, "Qualitative and Semiquantitative Analysis of Composite Mixtures of Antibodies by Native Mass Spectrometry," *Anal. Chem.*, vol. 84, no. 16, pp. 7227–7232, Aug. 2012, doi: 10.1021/ac301611d.

[177] P. L. Urban, "Quantitative mass spectrometry: an overview," *Philos. Trans. A. Math. Phys. Eng. Sci.*, vol. 374, no. 2079, p. 20150382, Oct. 2016, doi: 10.1098/rsta.2015.0382.

[178] S. R. Piersma, M. O. Warmoes, M. de Wit, I. de Reus, J. C. Knol, and C. R. Jiménez, "Whole gel processing procedure for GeLC-MS/MS based proteomics," *Proteome Sci.*, vol. 11, no. 1, p. 17, 2013, doi: 10.1186/1477-5956-11-17.

[179] J. V Olsen, S.-E. Ong, and M. Mann, "Trypsin Cleaves Exclusively C-

terminal to Arginine and Lysine Residues*," *Mol. Cell. Proteomics*, vol. 3, no. 6, pp. 608–614, 2004, doi: https://doi.org/10.1074/mcp.T400003-MCP200.

[180] C. V Smythe, "THE REACTION OF IODOACETATE AND OF IODOACETAMIDE WITH VARIOUS SULFHYDRYL GROUPS, WITH UREASE, AND WITH YEAST PREPARATIONS," *J. Biol. Chem.*, vol. 114, no. 3, pp. 601–612, 1936, doi: https://doi.org/10.1016/S0021-9258(18)74789-3.

[181] A. Aitken and M. Learmonth, "Carboxymethylation of Cysteine Using Iodoacetamide/ Iodoacetic Acid," in *The Protein Protocols Handbook*, J. M. Walker, Ed. Totowa, NJ: Humana Press, 2002, pp. 455–456.

[182] V. Mirabet *et al.*, "Long-term storage in liquid nitrogen does not affect cell viability in cardiac valve allografts," *Cryobiology*, vol. 57, no. 2, pp. 113–121, 2008, doi: https://doi.org/10.1016/j.cryobiol.2008.07.008.

[183] L. de Abreu Costa *et al.*, "Dimethyl Sulfoxide (DMSO) Decreases Cell Proliferation and TNF-α, IFN-γ, and IL-2 Cytokines Production in Cultures of Peripheral Blood Lymphocytes," *Molecules*, vol. 22, no. 11, p. 1789, Nov. 2017, doi: 10.3390/molecules22111789.

[184] I. Kratochvílová *et al.*, "Theoretical and experimental study of the antifreeze protein AFP752, trehalose and dimethyl sulfoxide cryoprotection mechanism: correlation with cryopreserved cell viability," *RSC Adv.*, vol. 7, no. 1, pp. 352–360, 2017, doi: 10.1039/C6RA25095E.

[185] Y. Dong, Y. Gou, Y. Li, Y. Liu, and J. Bai, "Synaptojanin cooperates in vivo with endophilin through an unexpected mechanism," *Elife*, vol. 4, p. e05660, Apr. 2015, doi: 10.7554/eLife.05660.

[186] A. Pechstein *et al.*, "Vesicle uncoating regulated by SH3-SH3 domain-mediated complex formation between endophilin and intersectin at synapses," *EMBO Rep.*, vol. 16, no. 2, pp. 232–239, Feb. 2015, doi: 10.15252/embr.201439260.

[187] W. Zhou, X. Li, and R. T. Premont, "Expanding functions of GIT Arf GTPase-activating proteins, PIX Rho guanine nucleotide exchange factors and GIT-PIX complexes," *J. Cell Sci.*, vol. 129, no. 10, pp. 1963–1974, May 2016, doi: 10.1242/jcs.179465.

[188] X. Li *et al.*, "Phosphorylation-dependent 14-3-3 binding to LRRK2 is impaired by common mutations of familial Parkinson's disease," *PLoS One*, vol. 6, no. 3, pp. e17153–e17153, Mar. 2011, doi: 10.1371/journal.pone.0017153.

[189] D. R. Alessi and S. Esther, "LRRK2 kinase in Parkinson's disease," *Science (80-.).*, vol. 360, no. 6384, pp. 36–37, Apr. 2018, doi: 10.1126/science.aar5683.

[190] S. Liu, X. Xiong, X. Zhao, X. Yang, and H. Wang, "F-BAR family proteins,

emerging regulators for cell membrane dynamic changes—from structure to human diseases," *J. Hematol. Oncol.*, vol. 8, no. 1, p. 47, 2015, doi: 10.1186/s13045-015-0144-2.

[191] A. Quan and P. J. Robinson, "Syndapin – a membrane remodelling and endocytic F-BAR protein," *FEBS J.*, vol. 280, no. 21, pp. 5198–5212, Nov. 2013, doi: https://doi.org/10.1111/febs.12343.

[192] J. Modregger, B. Ritter, B. Witter, M. Paulsson, and M. Plomann, "All three PACSIN isoforms bind to endocytic proteins and inhibit endocytosis," *J. Cell Sci.*, vol. 113, no. 24, pp. 4511–4521, Dec. 2000, doi: 10.1242/jcs.113.24.4511.

[193] T. I. Strochlic *et al.*, "Identification of neuronal substrates implicates Pak5 in synaptic vesicle trafficking," *Proc. Natl. Acad. Sci. U. S. A.*, vol. 109, no. 11, pp. 4116–4121, Mar. 2012, doi: 10.1073/pnas.1116560109.

[194] A. Halbach, M. Mörgelin, M. Baumgarten, M. Milbrandt, M. Paulsson, and M. Plomann, "PACSIN 1 forms tetramers via its N-terminal F-BAR domain," *FEBS J.*, vol. 274, no. 3, pp. 773–782, Feb. 2007, doi: https://doi.org/10.1111/j.1742-4658.2006.05622.x.

[195] W. X. Schulze and M. Mann, "A Novel Proteomic Screen for Peptide-Protein Interactions *," *J. Biol. Chem.*, vol. 279, no. 11, pp. 10756–10764, Mar. 2004, doi: 10.1074/jbc.M309909200.

[196] E. L. Huttlin *et al.*, "A tissue-specific atlas of mouse protein phosphorylation and expression," *Cell*, vol. 143, no. 7, pp. 1174–1189, Dec. 2010, doi: 10.1016/j.cell.2010.12.001.

[197] L. Almeida-Souza *et al.*, "A Flat BAR Protein Promotes Actin Polymerization at the Base of Clathrin-Coated Pits," *Cell*, vol. 174, no. 2, pp. 325-337.e14, Jul. 2018, doi: 10.1016/j.cell.2018.05.020.

[198] A. Pechstein, O. Shupliakov, and V. Haucke, "Intersectin 1: A versatile actor in the synaptic vesicle cycle," *Biochem. Soc. Trans.*, vol. 38, no. 1, pp. 181–186, 2010, doi: 10.1042/BST0380181.

[199] A. Pechstein *et al.*, "Regulation of synaptic vesicle recycling by complex formation between intersectin 1 and the clathrin adaptor complex AP2," *Proc. Natl. Acad. Sci. U. S. A.*, vol. 107, no. 9, pp. 4206–4211, 2010, doi: 10.1073/pnas.0911073107.

[200] Å. M. E. Winther *et al.*, "The dynamin-binding domains of Dap160/intersectin affect bulk membrane retrieval in synapses," *J. Cell Sci.*, vol. 126, no. 4, pp. 1021–1031, Feb. 2013, doi: 10.1242/jcs.118968.

[201] O. Dergai *et al.*, "Intersectin 1 forms complexes with SGIP1 and Reps1 in clathrin-coated pits," *Biochem. Biophys. Res. Commun.*, vol. 402, no. 2, pp. 408–413, 2010, doi: 10.1016/j.bbrc.2010.10.045.

[202] C. Pucharcos, C. Casas, M. Nadal, X. Estivill, and S. de la Luna, "The human intersectin genes and their spliced variants are differentially expressed," *Biochim. Biophys. Acta - Gene Struct. Expr.*, vol. 1521, no. 1, pp. 1–11, 2001, doi: https://doi.org/10.1016/S0167-4781(01)00276-7.

[203] L. Tsyba *et al.*, "Alternative splicing of mammalian Intersectin 1: domain associations and tissue specificities," *Genomics*, vol. 84, no. 1, pp. 106–113, 2004, doi: https://doi.org/10.1016/j.ygeno.2004.02.005.

[204] F. Gerth *et al.*, "Exon Inclusion Modulates Conformational Plasticity and Autoinhibition of the Intersectin 1 SH3A Domain," *Structure*, vol. 27, no. 6, pp. 977-987.e5, 2019, doi: https://doi.org/10.1016/j.str.2019.03.020.

[205] Y. Zhang, Y. Feng, Y. Xin, and X. Liu, "SGIP1 dimerizes via intermolecular disulfide bond in μHD domain during cellular endocytosis," *Biochem. Biophys. Res. Commun.*, vol. 505, no. 1, pp. 99–105, 2018, doi: 10.1016/j.bbrc.2018.09.075.

[206] A. Shimada, A. Yamaguchi, and D. Kohda, "Structural basis for the recognition of two consecutive mutually interacting DPF motifs by the SGIP1 μ homology domain," *Sci. Rep.*, vol. 6, no. 1, p. 19565, 2016, doi: 10.1038/srep19565.

[207] G. Hollopeter *et al.*, "The membrane-associated proteins FCHo and SGIP are allosteric activators of the AP2 clathrin adaptor complex," *Elife*, vol. 3, p. e03648, 2014, doi: 10.7554/eLife.03648.

[208] A. Uezu *et al.*, "SGIP1α is an endocytic protein that directly interacts with phospholipids and Eps15," *J. Biol. Chem.*, vol. 282, no. 36, pp. 26481–26489, 2007, doi: 10.1074/jbc.M703815200.

[209] M. T. Drake, M. A. Downs, and L. M. Traub, "Epsin Binds to Clathrin by Associating Directly with the Clathrin-terminal Domain: EVIDENCE FOR COOPERATIVE BINDING THROUGH TWO DISCRETE SITES*," *J. Biol. Chem.*, vol. 275, no. 9, pp. 6479–6489, 2000, doi: https://doi.org/10.1074/jbc.275.9.6479.

[210] M. G. J. Ford *et al.*, "Curvature of clathrin-coated pits driven by epsin," *Nature*, vol. 419, no. 6905, pp. 361–366, 2002, doi: 10.1038/nature01020.

[211] J. W. Kyung, J. R. Bae, D.-H. Kim, W. K. Song, and S. H. Kim, "Epsin1 modulates synaptic vesicle retrieval capacity at CNS synapses," *Sci. Rep.*, vol. 6, no. 1, p. 31997, 2016, doi: 10.1038/srep31997.

[212] M. J. Hawryluk, P. A. Keyel, S. K. Mishra, S. C. Watkins, J. E. Heuser, and L. M. Traub, "Epsin 1 is a polyubiquitin-selective clathrin-associated sorting protein," *Traffic*, vol. 7, no. 3, pp. 262–281, 2006, doi: 10.1111/j.1600-0854.2006.00383.x.

[213] M. Kazazic *et al.*, "Epsin 1 is involved in recruitment of ubiquitinated EGF receptors into clathrin-coated pits," *Traffic*, vol. 10, no. 2, pp. 235–245, 2009,

doi: 10.1111/j.1600-0854.2008.00858.x.

[214] R. A. Hom *et al.*, "pH-dependent Binding of the Epsin ENTH Domain and the AP180 ANTH Domain to PI(4,5)P2-containing Bilayers," *J. Mol. Biol.*, vol. 373, no. 2, pp. 412–423, 2007, doi: https://doi.org/10.1016/j.jmb.2007.08.016.

[215] M. Messa *et al.*, "Epsin deficiency impairs endocytosis by stalling the actin-dependent invagination of endocytic clathrin-coated pits," *Elife*, vol. 3, p. e03311, 2014, doi: 10.7554/eLife.03311.

[216] H. Chen *et al.*, "Embryonic arrest at midgestation and disruption of Notch signaling produced by the absence of both epsin 1 and epsin 2 in mice," *Proc. Natl. Acad. Sci.*, vol. 106, no. 33, pp. 13838–13843, Aug. 2009, doi: 10.1073/PNAS.0907008106.

[217] C. Milesi *et al.*, "Redundant and nonredundant organismal functions of EPS15 and EPS15L1," *Life Sci. Alliance*, vol. 2, no. 1, p. e201800273, Feb. 2019, doi: 10.26508/lsa.201800273.

[218] A. Majumdar, S. Ramagiri, and R. Rikhy, "Drosophila homologue of Eps15 is essential for synaptic vesicle recycling," *Exp. Cell Res.*, vol. 312, no. 12, pp. 2288–2298, 2006, doi: https://doi.org/10.1016/j.yexcr.2006.03.030.

[219] T.-W. Koh *et al.*, "Eps15 and Dap160 control synaptic vesicle membrane retrieval and synapse development," *J. Cell Biol.*, vol. 178, no. 2, pp. 309–322, Jul. 2007, doi: 10.1083/jcb.200701030.

[220] M. Gschweitl *et al.*, "A SPOPL/Cullin-3 ubiquitin ligase complex regulates endocytic trafficking by targeting EPS15 at endosomes," *Elife*, vol. 5, p. e13841, 2016, doi: 10.7554/eLife.13841.

[221] L. M. Traub, "A nanobody-based molecular toolkit provides new mechanistic insight into clathrin-coat initiation," *Elife*, vol. 8, p. e41768, 2019, doi: 10.7554/eLife.41768.

[222] I. Leshchyns'ka, V. Sytnyk, M. Richter, A. Andreyeva, D. Puchkov, and M. Schachner, "The Adhesion Molecule CHL1 Regulates Uncoating of Clathrin-Coated Synaptic Vesicles," *Neuron*, vol. 52, no. 6, pp. 1011–1025, 2006, doi: 10.1016/j.neuron.2006.10.020.

[223] Z. Dragovic, S. A. Broadley, Y. Shomura, A. Bracher, and F. U. Hartl, "Molecular chaperones of the Hsp110 family act as nucleotide exchange factors of Hsp70s," *EMBO J.*, vol. 25, no. 11, pp. 2519–2528, Jun. 2006, doi: 10.1038/sj.emboj.7601138.

[224] O. Genest, S. Wickner, and S. M. Doyle, "Hsp90 and Hsp70 chaperones: Collaborators in protein remodeling," *J. Biol. Chem.*, vol. 294, no. 6, pp. 2109–2120, Feb. 2019, doi: 10.1074/jbc.REV118.002806.

[225] H. Raviol, H. Sadlish, F. Rodriguez, M. P. Mayer, and B. Bukau, "Chaperone network in the yeast cytosol: Hsp110 is revealed as an Hsp70 nucleotide

exchange factor," *EMBO J.*, vol. 25, no. 11, pp. 2510–2518, Jun. 2006, doi: 10.1038/sj.emboj.7601139.

[226] J. P. Schuermann *et al.*, "Structure of the Hsp110:Hsc70 nucleotide exchange machine," *Mol. Cell*, vol. 31, no. 2, pp. 232–243, Jul. 2008, doi: 10.1016/j.molcel.2008.05.006.

[227] S. Kishinevsky *et al.*, "HSP90-incorporating chaperome networks as biosensor for disease-related pathways in patient-specific midbrain dopamine neurons," *Nat. Commun.*, vol. 9, no. 1, p. 4345, Oct. 2018, doi: 10.1038/s41467-018-06486-6.

[228] D. J. Busch, J. R. Houser, C. C. Hayden, M. B. Sherman, E. M. Lafer, and J. C. Stachowiak, "Intrinsically disordered proteins drive membrane curvature," *Nat. Commun.*, vol. 6, no. 1, p. 7875, 2015, doi: 10.1038/ncomms8875.

[229] M. A. Stevenson and S. K. Calderwood, "Members of the 70-kilodalton heat shock protein family contain a highly conserved calmodulin-binding domain," *Mol. Cell. Biol.*, vol. 10, no. 3, pp. 1234–1238, 1990, doi: 10.1128/mcb.10.3.1234-1238.1990.

[230] P. V Hornbeck, B. Zhang, B. Murray, J. M. Kornhauser, V. Latham, and E. Skrzypek, "PhosphoSitePlus, 2014: mutations, PTMs and recalibrations," *Nucleic Acids Res.*, vol. 43, no. D1, pp. D512–D520, Jan. 2015, doi: 10.1093/nar/gku1267.

[231] N. Morgner *et al.*, "Hsp70 Forms Antiparallel Dimers Stabilized by Post-translational Modifications to Position Clients for Transfer to Hsp90," *Cell Rep.*, vol. 11, no. 5, pp. 759–769, 2015, doi: https://doi.org/10.1016/j.celrep.2015.03.063.

[232] J. P. H. Lauritsen, C. Menné, J. Kastrup, J. Dietrich, N. Ødum, and C. Geisler, "β2-Adaptin is constitutively de-phosphorylated by serine/threonine protein phosphatase PP2A and phosphorylated by a staurosporine-sensitive kinase," *Biochim. Biophys. Acta - Mol. Cell Res.*, vol. 1497, no. 3, pp. 297–307, 2000, doi: https://doi.org/10.1016/S0167-4889(00)00065-3.

[233] D. Ricotta, J. Hansen, C. Preiss, D. Teichert, and S. Höning, "Characterization of a Protein Phosphatase 2A Holoenzyme That Dephosphorylates the Clathrin Adaptors AP-1 and AP-2*," *J. Biol. Chem.*, vol. 283, no. 9, pp. 5510–5517, 2008, doi: https://doi.org/10.1074/jbc.M707166200.

[234] U. S. Cho and W. Xu, "Crystal structure of a protein phosphatase 2A heterotrimeric holoenzyme," *Nature*, vol. 445, no. 7123, pp. 53–57, 2007, doi: 10.1038/nature05351.

[235] A. Umeda, A. Meyerholz, and E. Ungewickell, "Identification of the universal cofactor (auxilin 2) in clathrin coat dissociation," *Eur. J. Cell Biol.*, vol. 79, no. 5, pp. 336–342, 2000, doi: https://doi.org/10.1078/S0171-9335(04)70037-0.

[236] G. Piccoli *et al.*, "LRRK2 controls synaptic vesicle storage and mobilization within the recycling pool," *J. Neurosci.*, vol. 31, no. 6, pp. 2225–2237, Feb. 2011, doi: 10.1523/JNEUROSCI.3730-10.2011.

[237] S. D. Conner and S. L. Schmid, "CVAK104 Is a Novel Poly-l-lysine-stimulated Kinase That Targets the β2-Subunit of AP2*," *J. Biol. Chem.*, vol. 280, no. 22, pp. 21539–21544, 2005, doi: https://doi.org/10.1074/jbc.M502462200.

[238] V. I. Korolchuk and G. Banting, "CK2 and GAK/auxilin2 Are Major Protein Kinases in Clathrin-Coated Vesicles," *Traffic*, vol. 3, no. 6, pp. 428–439, Jun. 2002, doi: https://doi.org/10.1034/j.1600-0854.2002.30606.x.

[239] V. I. Korolchuk, G. Cozier, and G. Banting, "Regulation of CK2 Activity by Phosphatidylinositol Phosphates *," *J. Biol. Chem.*, vol. 280, no. 49, pp. 40796–40801, Dec. 2005, doi: 10.1074/jbc.M508988200.

[240] N. Murakami, D. Bolton, and Y.-W. Hwang, "Dyrk1A Binds to Multiple Endocytic Proteins Required for Formation of Clathrin-Coated Vesicles," *Biochemistry*, vol. 48, no. 39, pp. 9297–9305, Oct. 2009, doi: 10.1021/bi9010557.

[241] N. Murakami, D. C. Bolton, E. Kida, W. Xie, and Y.-W. Hwang, "Phosphorylation by Dyrk1A of clathrin coated vesicle-associated proteins: identification of the substrate proteins and the effects of phosphorylation," *PLoS One*, vol. 7, no. 4, pp. e34845–e34845, 2012, doi: 10.1371/journal.pone.0034845.

[242] D. W. Litchfield, "Protein kinase CK2: structure, regulation and role in cellular decisions of life and death," *Biochem. J.*, vol. 369, no. Pt 1, pp. 1–15, Jan. 2003, doi: 10.1042/BJ20021469.

[243] J. Park and K. C. Chung, "New Perspectives of Dyrk1A Role in Neurogenesis and Neuropathologic Features of Down Syndrome," *Exp. Neurobiol.*, vol. 22, no. 4, pp. 244–248, Dec. 2013, doi: 10.5607/en.2013.22.4.244.

[244] J. Wegiel, C.-X. Gong, and Y.-W. Hwang, "The role of DYRK1A in neurodegenerative diseases," *FEBS J.*, vol. 278, no. 2, pp. 236–245, Jan. 2011, doi: 10.1111/j.1742-4658.2010.07955.x.

[245] Y. L. Woods *et al.*, "The kinase DYRK1A phosphorylates the transcription factor FKHR at Ser329 in vitro, a novel in vivo phosphorylation site," *Biochem. J.*, vol. 355, no. Pt 3, pp. 597–607, May 2001, doi: 10.1042/bj3550597.

[246] A. Seifert, L. A. Allan, and P. R. Clarke, "DYRK1A phosphorylates caspase 9 at an inhibitory site and is potently inhibited in human cells by harmine," *FEBS J.*, vol. 275, no. 24, pp. 6268–6280, Dec. 2008, doi: https://doi.org/10.1111/j.1742-4658.2008.06751.x.

[247] A. Laguna *et al.*, "The Protein Kinase DYRK1A Regulates Caspase-9-

Mediated Apoptosis during Retina Development," *Dev. Cell*, vol. 15, no. 6, pp. 841–853, 2008, doi: https://doi.org/10.1016/j.devcel.2008.10.014.

[248] M. Del Mar Masdeu, B. G. Armendáriz, A. La Torre, E. Soriano, F. Burgaya, and J. M. Ureña, "Identification of novel Ack1-interacting proteins and Ack1 phosphorylated sites in mouse brain by mass spectrometry," *Oncotarget*, vol. 8, no. 60, pp. 101146–101157, Sep. 2017, doi: 10.18632/oncotarget.20929.

[249] R. Brandao, M. Q. Kwa, Y. Yarden, and C. Brakebusch, "ACK1 is dispensable for development, skin tumor formation, and breast cancer cell proliferation," *FEBS Open Bio*, vol. 11, no. 6, pp. 1579–1592, Jun. 2021, doi: https://doi.org/10.1002/2211-5463.13149.

[250] L. Chen, M. Chuang, T. Koorman, M. Boxem, Y. Jin, and A. D. Chisholm, "Axon injury triggers EFA-6 mediated destabilization of axonal microtubules via TACC and doublecortin like kinase," *Elife*, vol. 4, p. e08695, 2015, doi: 10.7554/eLife.08695.

[251] J. Lipka, L. C. Kapitein, J. Jaworski, and C. C. Hoogenraad, "Microtubule-binding protein doublecortin-like kinase 1 (DCLK1) guides kinesin-3-mediated cargo transport to dendrites," *EMBO J.*, vol. 35, no. 3, pp. 302–318, Feb. 2016, doi: 10.15252/embj.201592929.

[252] K. B. Gagnon and E. Delpire, "Molecular physiology of SPAK and OSR1: two Ste20-related protein kinases regulating ion transport," *Physiol. Rev.*, vol. 92, no. 4, pp. 1577–1617, Oct. 2012, doi: 10.1152/physrev.00009.2012.

[253] J. Ponce-Coria *et al.*, "A Novel Ste20-related Proline/Alanine-rich Kinase (SPAK)-independent Pathway Involving Calcium-binding Protein 39 (Cab39) and Serine Threonine Kinase with No Lysine Member 4 (WNK4) in the Activation of Na-K-Cl Cotransporters*," *J. Biol. Chem.*, vol. 289, no. 25, pp. 17680–17688, 2014, doi: https://doi.org/10.1074/jbc.M113.540518.

[254] B. M. Filippi *et al.*, "MO25 is a master regulator of SPAK/OSR1 and MST3/MST4/YSK1 protein kinases," *EMBO J.*, vol. 30, no. 9, pp. 1730–1741, May 2011, doi: https://doi.org/10.1038/emboj.2011.78.

[255] R. Tahir *et al.*, "Proximity-Dependent Biotinylation to Elucidate the Interactome of TNK2 Nonreceptor Tyrosine Kinase," *J. Proteome Res.*, vol. 20, no. 9, pp. 4566–4577, Sep. 2021, doi: 10.1021/acs.jproteome.1c00551.

[256] K.-U. Bayer, J. Löhler, H. Schulman, and K. Harbers, "Developmental expression of the CaM kinase II isoforms: ubiquitous γ- and δ-CaM kinase II are the early isoforms and most abundant in the developing nervous system," *Mol. Brain Res.*, vol. 70, no. 1, pp. 147–154, 1999, doi: https://doi.org/10.1016/S0169-328X(99)00131-X.

[257] L. Hoffman, M. M. Farley, and M. N. Waxham, "Calcium-Calmodulin-Dependent Protein Kinase II Isoforms Differentially Impact the Dynamics and Structure of the Actin Cytoskeleton," *Biochemistry*, vol. 52, no. 7, pp. 1198–1207, Feb. 2013, doi: 10.1021/bi3016586.

[258] G. Zalcman, N. Federman, and A. Romano, "CaMKII Isoforms in Learning and Memory: Localization and Function," *Frontiers in Molecular Neuroscience*, vol. 11. p. 445, 2018, [Online]. Available: https://www.frontiersin.org/article/10.3389/fnmol.2018.00445.

[259] G. Zalcman *et al.*, "Sustained CaMKII Delta Gene Expression Is Specifically Required for Long-Lasting Memories in Mice," *Mol. Neurobiol.*, vol. 56, no. 2, pp. 1437–1450, 2019, doi: 10.1007/s12035-018-1144-3.

[260] A. Abousaab, J. Warsi, B. Elvira, I. Alesutan, Z. Hoseinzadeh, and F. Lang, "Down-Regulation of Excitatory Amino Acid Transporters EAAT1 and EAAT2 by the Kinases SPAK and OSR1," *J. Membr. Biol.*, vol. 248, no. 6, pp. 1107–1119, 2015, doi: 10.1007/s00232-015-9826-5.

[261] Y. Geng, N. Byun, and E. Delpire, "Behavioral analysis of Ste20 kinase SPAK knockout mice," *Behav. Brain Res.*, vol. 208, no. 2, pp. 377–382, Apr. 2010, doi: 10.1016/j.bbr.2009.12.005.

[262] S.-S. Yang, C.-L. Huang, H.-E. Chen, C.-S. Tung, H.-P. Shih, and Y.-P. Liu, "Effects of SPAK knockout on sensorimotor gating, novelty exploration, and brain area-dependent expressions of NKCC1 and KCC2 in a mouse model of schizophrenia," *Prog. Neuro-Psychopharmacology Biol. Psychiatry*, vol. 61, pp. 30–36, 2015, doi: https://doi.org/10.1016/j.pnpbp.2015.03.007.

[263] L. Qinfang, B.-G. Judith, H. D. A., Y. Jianzhong, and X. Yulan, "Dysregulation of the AP2M1 phosphorylation cycle by LRRK2 impairs endocytosis and leads to dopaminergic neurodegeneration," *Sci. Signal.*, vol. 14, no. 693, p. eabg3555, Jul. 2021, doi: 10.1126/scisignal.abg3555.

[264] S. K. Ultanir *et al.*, "Chemical genetic identification of NDR1/2 kinase substrates AAK1 and Rabin8 Uncovers their roles in dendrite arborization and spine development," *Neuron*, vol. 73, no. 6, pp. 1127–1142, Mar. 2012, doi: 10.1016/j.neuron.2012.01.019.

[265] J. Podufall *et al.*, "A Presynaptic Role for the Cytomatrix Protein GIT in Synaptic Vesicle Recycling," *Cell Rep.*, vol. 7, no. 5, pp. 1417–1425, 2014, doi: https://doi.org/10.1016/j.celrep.2014.04.051.

[266] B. W. Duncan, K. E. Murphy, and P. F. Maness, "Molecular Mechanisms of L1 and NCAM Adhesion Molecules in Synaptic Pruning, Plasticity, and Stabilization," *Frontiers in Cell and Developmental Biology*, vol. 9. p. 10, 2021, [Online]. Available: https://www.frontiersin.org/article/10.3389/fcell.2021.625340.

[267] J. A. Frei and E. T. Stoeckli, "SynCAMs extend their functions beyond the synapse," *Eur. J. Neurosci.*, vol. 39, no. 11, pp. 1752–1760, 2014, doi: 10.1111/ejn.12544.

[268] X. Yang, "Chondroitin sulfate proteoglycans: Key modulators of neuronal plasticity, long-term memory, neurodegenerative, and psychiatric disorders," *Rev. Neurosci.*, vol. 31, no. 5, pp. 555–568, 2020, doi: 10.1515/revneuro-

2019-0117.

[269] P. S. Tarpey *et al.*, "Mutations in the gene encoding the Sigma 2 subunit of the adaptor protein 1 complex, AP1S2, cause X-linked mental retardation," *Am. J. Hum. Genet.*, vol. 79, no. 6, pp. 1119–1124, Dec. 2006, doi: 10.1086/510137.

[270] H. Wang, C. Zhang, and H. Xiao, "Mechanism of membrane fusion: protein-protein interaction and beyond," *Int. J. Physiol. Pathophysiol. Pharmacol.*, vol. 11, no. 6, pp. 250–257, Dec. 2019, [Online]. Available: https://pubmed.ncbi.nlm.nih.gov/31993099.

[271] C. E. Krebs *et al.*, "The Sac1 domain of SYNJ1 identified mutated in a family with early-onset progressive Parkinsonism with generalized seizures," *Hum. Mutat.*, vol. 34, no. 9, pp. 1200–1207, Sep. 2013, doi: 10.1002/humu.22372.

[272] S. B. Martin *et al.*, "Synaptophysin and synaptojanin-1 in Down syndrome are differentially affected by Alzheimer's disease," *J. Alzheimers. Dis.*, vol. 42, no. 3, pp. 767–775, 2014, doi: 10.3233/JAD-140795.

[273] Y. Arai, T. Ijuin, T. Takenawa, L. E. Becker, and S. Takashima, "Excessive expression of synaptojanin in brains with Down syndrome," *Brain Dev.*, vol. 24, no. 2, pp. 67–72, 2002, doi: 10.1016/S0387-7604(01)00405-3.

[274] O. Gubar *et al.*, "Intersectin: The Crossroad between Vesicle Exocytosis and Endocytosis," *Front. Endocrinol. (Lausanne).*, vol. 4, p. 109, Aug. 2013, doi: 10.3389/fendo.2013.00109.

[275] C. Milesi *et al.*, "Redundant and nonredundant organismal functions of EPS15 and EPS15L1," *Life Sci. Alliance*, vol. 2, no. 1, pp. 1–11, 2019, doi: 10.26508/lsa.201800273.

[276] M. Kohansal-Nodehi, J. J. E. Chua, H. Urlaub, R. Jahn, and D. Czernik, "Analysis of protein phosphorylation in nerve terminal reveals extensive changes in active zone proteins upon exocytosis," *Elife*, vol. 5, p. e14530, 2016, doi: 10.7554/eLife.14530.

[277] W. K. den Otter, M. R. Renes, and W. J. Briels, "Asymmetry as the key to clathrin cage assembly," *Biophys. J.*, vol. 99, no. 4, pp. 1231–1238, Aug. 2010, doi: 10.1016/j.bpj.2010.06.011.

[278] J. Hirst, D. A. Sahlender, S. Li, N. B. Lubben, G. H. H. Borner, and M. S. Robinson, "Auxilin depletion causes self-assembly of clathrin into membraneless cages in vivo," *Traffic*, vol. 9, no. 8, pp. 1354–1371, Aug. 2008, doi: 10.1111/j.1600-0854.2008.00764.x.

[279] C. Wang *et al.*, "GPS 5.0: An Update on the Prediction of Kinase-specific Phosphorylation Sites in Proteins," *Genomics. Proteomics Bioinformatics*, vol. 18, no. 1, pp. 72–80, Feb. 2020, doi: 10.1016/j.gpb.2020.01.001.

[280] H. Zhang, D. J. Webb, H. Asmussen, and A. F. Horwitz, "Synapse formation is regulated by the signaling adaptor GIT1," *J. Cell Biol.*, vol. 161, no. 1, pp.

131–142, 2003, doi: 10.1083/jcb.200211002.

[281] H. Zhang, D. J. Webb, H. Asmussen, S. Niu, and A. F. Horwitz, "A GIT1/PIX/Rac/PAK signaling module regulates spine morphogenesis and synapse formation through MLC," *J. Neurosci.*, vol. 25, no. 13, pp. 3379–3388, Mar. 2005, doi: 10.1523/JNEUROSCI.3553-04.2005.

[282] S. Cameron and A. K. McAllister, "Immunoglobulin-Like Receptors and Their Impact on Wiring of Brain Synapses," *Annu. Rev. Genet.*, vol. 52, no. 1, pp. 567–590, Nov. 2018, doi: 10.1146/annurev-genet-120417-031513.

[283] M. Buhusi, B. R. Midkiff, A. M. Gates, M. Richter, M. Schachner, and P. F. Maness, "Close Homolog of L1 Is an Enhancer of Integrin-mediated Cell Migration*," *J. Biol. Chem.*, vol. 278, no. 27, pp. 25024–25031, 2003, doi: https://doi.org/10.1074/jbc.M303084200.

[284] U. Cavallaro and E. Dejana, "Adhesion molecule signalling: not always a sticky business," *Nat. Rev. Mol. Cell Biol.*, vol. 12, no. 3, pp. 189–197, 2011, doi: 10.1038/nrm3068.

[285] D. Guseva *et al.*, "Cell Adhesion Molecule Close Homolog of L1 (CHL1) Guides the Regrowth of Regenerating Motor Axons and Regulates Synaptic Coverage of Motor Neurons," *Frontiers in Molecular Neuroscience*, vol. 11. 2018, [Online]. Available: https://www.frontiersin.org/article/10.3389/fnmol.2018.00174.

[286] L. R. Herron, M. Hill, F. Davey, and F. J. Gunn-Moore, "The intracellular interactions of the L1 family of cell adhesion molecules," *Biochem. J.*, vol. 419, no. 3, pp. 519–531, Apr. 2009, doi: 10.1042/BJ20082284.

[287] A. Kotarska, L. Fernandes, R. Kleene, and M. Schachner, "Cell adhesion molecule close homolog of L1 binds to the dopamine receptor D2 and inhibits the internalization of its short isoform," *FASEB J.*, vol. 34, no. 4, pp. 4832–4851, Apr. 2020, doi: https://doi.org/10.1096/fj.201900577RRRR.

[288] V. Mohan *et al.*, "Neurocan Inhibits Semaphorin 3F Induced Dendritic Spine Remodeling Through NrCAM in Cortical Neurons," *Frontiers in Cellular Neuroscience*, vol. 12. 2018, [Online]. Available: https://www.frontiersin.org/article/10.3389/fncel.2018.00346.

[289] X. H. Zhou *et al.*, "Neurocan is dispensable for brain development," *Mol. Cell. Biol.*, vol. 21, no. 17, pp. 5970–5978, Sep. 2001, doi: 10.1128/MCB.21.17.5970-5978.2001.

[290] D. R. Friedlander, P. Milev, L. Karthikeyan, R. K. Margolis, R. U. Margolis, and M. Grumet, "The neuronal chondroitin sulfate proteoglycan neurocan binds to the neural cell adhesion molecules Ng-CAM/L1/NILE and N-CAM, and inhibits neuronal adhesion and neurite outgrowth," *J. Cell Biol.*, vol. 125, no. 3, pp. 669–680, May 1994, doi: 10.1083/jcb.125.3.669.

[291] C. H. Wei and S. E. Ryu, "Homophilic interaction of the L1 family of cell

adhesion molecules," *Exp. Mol. Med.*, vol. 44, no. 7, pp. 413–423, Jul. 2012, doi: 10.3858/emm.2012.44.7.050.

[292] D. Angeloni, N. M. Lindor, S. Pack, F. Latif, M.-H. Wei, and M. I. Lerman, "CALL gene is haploinsufficient in a 3p− syndrome patient," *Am. J. Med. Genet.*, vol. 86, no. 5, pp. 482–485, Oct. 1999, doi: https://doi.org/10.1002/(SICI)1096-8628(19991029)86:5<482::AID-AJMG15>3.0.CO;2-L.

[293] S. G. M. Frints *et al.*, "CALL interrupted in a patient with non-specific mental retardation: gene dosage-dependent alteration of murine brain development and behavior," *Hum. Mol. Genet.*, vol. 12, no. 13, pp. 1463–1474, Jul. 2003, doi: 10.1093/hmg/ddg165.

[294] C. Cuoco *et al.*, "Microarray based analysis of an inherited terminal 3p26.3 deletion, containing only the CHL1 gene, from a normal father to his two affected children," *Orphanet J. Rare Dis.*, vol. 6, p. 12, Apr. 2011, doi: 10.1186/1750-1172-6-12.

[295] J. Emperador-Melero, G. de Nola, and P. S. Kaeser, "Intact synapse structure and function after combined knockout of PTPδ, PTPσ, and LAR," *Elife*, vol. 10, p. e66638, 2021, doi: 10.7554/eLife.66638.

[296] M. Geissler *et al.*, "Primary hippocampal neurons, which lack four crucial extracellular matrix molecules, display abnormalities of synaptic structure and function and severe deficits in perineuronal net formation," *J. Neurosci.*, vol. 33, no. 18, pp. 7742–7755, May 2013, doi: 10.1523/JNEUROSCI.3275-12.2013.

[297] C. Gottschling, D. Wegrzyn, B. Denecke, and A. Faissner, "Elimination of the four extracellular matrix molecules tenascin-C, tenascin-R, brevican and neurocan alters the ratio of excitatory and inhibitory synapses," *Sci. Rep.*, vol. 9, no. 1, p. 13939, Sep. 2019, doi: 10.1038/s41598-019-50404-9.

[298] D. Carulli and J. Verhaagen, "An Extracellular Perspective on CNS Maturation: Perineuronal Nets and the Control of Plasticity," *Int. J. Mol. Sci.*, vol. 22, no. 5, p. 2434, Feb. 2021, doi: 10.3390/ijms22052434.

[299] J. W. Fawcett, T. Oohashi, and T. Pizzorusso, "The roles of perineuronal nets and the perinodal extracellular matrix in neuronal function," *Nat. Rev. Neurosci.*, vol. 20, no. 8, pp. 451–465, 2019, doi: 10.1038/s41583-019-0196-3.

[300] J. C. Wingert and B. A. Sorg, "Impact of Perineuronal Nets on Electrophysiology of Parvalbumin Interneurons, Principal Neurons, and Brain Oscillations: A Review," *Frontiers in Synaptic Neuroscience*, vol. 13. 2021, [Online]. Available: https://www.frontiersin.org/article/10.3389/fnsyn.2021.673210.

[301] M. Mettlen and G. Danuser, "Imaging and modeling the dynamics of clathrin-mediated endocytosis," *Cold Spring Harb. Perspect. Biol.*, vol. 6, no. 12, pp.

a017038–a017038, Aug. 2014, doi: 10.1101/cshperspect.a017038.

[302] T. Kirchhausen, "Imaging endocytic clathrin structures in living cells," *Trends Cell Biol.*, vol. 19, no. 11, pp. 596–605, Nov. 2009, doi: 10.1016/j.tcb.2009.09.002.

[303] A. J. Laude and I. A. Prior, "Plasma membrane microdomains: organization, function and trafficking," *Mol. Membr. Biol.*, vol. 21, no. 3, pp. 193–205, 2004, doi: 10.1080/09687680410001700517.

[304] T. Tojima, R. Itofusa, and H. Kamiguchi, "Asymmetric Clathrin-Mediated Endocytosis Drives Repulsive Growth Cone Guidance," *Neuron*, vol. 66, no. 3, pp. 370–377, 2010, doi: https://doi.org/10.1016/j.neuron.2010.04.007.

Acknowledgements

During my PhD study, I really had a great time for being in the lab to complete my experiments with great people around me. I could not imagine that I would achieve to complete my Thesis project without their support and guidance. Therefore, I would like to thank to express my gratitude towards all the wonderful people and scientists around me during my PhD journey. First and foremost, I would like to thank my supervisor, Prof. Dr. Peter Schu for accepting me as a PhD student in his lab and providing me a great mentorship during my PhD studies. I am grateful for his constant support, motivative talks and experienced outlook for the difficult situations that I have been gone through. He always shares his extended and endless scientific knowledge with me whenever I have questions. His great knowledge and expertise in the area of Neurobiochemistry always helped me to identify the problems in the experiments and eliminate the trouble shooting quickly. I also specifically put emphasis on his helps and efforts for his finishing touches in my presentations, posters and as well as in my written PhD thesis. I also would like to appreciate his patience and persistence for the corrections on my Thesis and also on my misunderstandings or on my wrong assumptions during our scientific discussion meetings. Therefore, I was not able to complete my PhD studies without his guidance and support.

Secondly, I would like to thank my TAC members, Prof. Dr. Silvio Rizzoli and Prof. Dr. Martin Oppermann for the warm and encouraging environment that they have provided during my TAC meetings. In particular, I would like to thank Prof. Dr. Silvio Rizzoli for his great advices to improve my PhD project with his endless knowledge and expertise in the area of synaptic vesicle recycling. I am also grateful for accepting our group to have joint lab seminars. It was really a great opportunity to visualize the molecular architecture of synapses and synaptic vesicles through the presented progress reports of his wonderful team. Additionally, I also want to thank Prof. Dr. Rizzoli for his questions and suggestions during the TAC meetings and lab seminars which definitely put my project forward so that we had a chance to revise our conclusions and interpretations based on his kind feedback. I would like to appreciate Prof. Dr. Martin Oppermann for his helpful and motivative attitudes. His expertise in the different scientific areas aids me in improvin my PhD project.

I also would like to thank my extended thesis comitee examination board members, Prof. Dr. Michael Thumm, Prof. Dr. Susanne Lutz and Prof. Dr. Alexander Stein. I am greatful for accepting to attend my thesis defense presentation and also investing time to read and revise my PhD thesis. I appreciate all of their supports, understandings and helps for their interest in my project.

I would like to thank the GGNB office and Molecular Biology of Cells programme coordinators for their professional and personal support and helps during my PhD studies about my questions. Their expertise and quick responses to my emails all the time gratify my hesitations and questions. I also would like to specifically thank to GGNB for offering great courses, workshops and retreats. They helped me to improve my scientific knowledge and my scientific network. I also want to thank GGNB board for suppoting my last three months of PhD thesis period financially by awarding me with GGNB bridging fund. I am also greateful to DFG, German Research Foundation, for the financial support of my PhD project. Through DFG funding, we had a chance to conduct effective and outstanding scientific research.

I would like to thank my precedessors, Dr. Ratnakar Mishra and Dr. Ermes Candiello for their contribution to my PhD project. They put great effort for the optimization and establishment of the protocols. Moreover, I also would like to thank them for their initial data contribution to my project that were important basis to proceed in this study. I specifically would like to thank Dr. Mishra for his mentorship and supervision to teach me the methods and biochemical assays required to perform the experiments for my thesis and for our scientific papers. I am also greatful to him to describing and sharing every single details of the project that I have taken over from him. I also would like to thank Olaf Benhard for his technical support and collaboration for the preparation of samples for MS analysis. I am also greatful to Dr. Oliver Valerious from the Department of Molecular Microbiology and Genetics for his collobartions to perform the phosphoproteome analysis of isolated synaptic CCVproteins. It was a great opportunity for me to collobrate with all these great scientists to enrich and to complete my PhD project.

I would like to thank Prof. Dr. Peter Rehling for providing a laboratory for us at the Department of Cellular Biochemistry. I also would like to thank all the great people in the department from Prof. Rehling, Prof. Thumm, Prof. Richter-Dennerlein

and from Prof. Meinecke lab groups for provoding a warm and great working environment during my PhD studies. I would like to thank department secretory, Eva Ausmeier for her support and helps in administrative duties and tasks that she conducted for me during my PhD study.

I also would like to thank my dearest colliques and friends namely, Anusha Valpadashi, Roya Yousefi, Metin Özdemir, Matthew Taylor, Dr. Lisa Marquardt, Dr. Sabine Poerschke, Dr. Bettina Homberg, Dr. Ridhima Gomkale, Dr. Daryna Tarasenko, Angela Boshnakovska, Naintara Jain, Venkat, Arun, Dr. Elena Lavdovskaia and Dr. Cong Wang for their personal and scientific support especially whenever I feel demotivated and exhausted. We altogether share our burdens, negative feelings and as well as happiness in our department. I also specifically thank to Post. Doc researchers, Dr. Abhishek Aich, Dr. Arpita Chowdhury, Dr. Silvio Callegari, Dr. David Paceu-Grau and Dr. Luis Daniel Cruz for sharing their scientific expertise and wisdom with me whenever I need to confront with difficulties during my experiments. Additionally, I also would like to thank all of you for your advice and support during the writing of this thesis.

I also would like to thank my great colliques, Tanja Gall, Mirjam Wissel, and Petra Schlotterhose for the supplement and recruitment of equipments and chemicals to conduct my experiments. I also want to thank Carmen and Anita for their technical supports. I especially thank to Tanja Gall for her support and friendship. Even though we worked in a short time at the same laboratory, her positive attitude towards life and her warm heart made my working environment great. I also would like to especially thank to her for her constant support to motivate me while I was writing my thesis. I also would like to thank Dairovys Anner Jimenez Fundora for her support and helps during my PhD studies. Although we could not spend so long time in the laboratory, she constantly motivated and guided me about my job applications. Therefore, I will be always grateful for her tactics and guidance about my job applications.

Last but not least, I would like to thank my family for supporting to continue my Academic career in abroad. It was too hard for me to stay away from them for a long time. Although it contributed to my professional and personal growth, I all the time feel their asence and I always miss them a lot. Whenever I feel demotivated and exhausted, their support from thousands of miles away keep me focus on my work and

achieve my goals to complete my PhD studies. I am also greatful to them for providing a great environment during my short visits to Turkey. Since their helps and supports were priceless, this thesis also belongs to them.

I also would like to thank my old best friends, MSc Özge Pelin Burhan, Dr. Nuray Gündüz and MSc Özge Uysal. They all the listen my problems and find a way to make me happier again. They also made me feel like their precious princes and do their best to realize my wishes and requests. I am really glad to them for their constant support and helps during my thesis writing period. I know that I am so lucky to have such great friends in my life.

Once more time, I would like to thank all the people around me during my PhD thesis. I apriciate all of their supports, understandings and helps in this journey.

Curriculum Vitae

Göksemin SENGÜL
Date of Birth: 03.02.1991
Place of Birth: Ankara, Turkey
Current Work Address: Humboldtallee 23, 37073 Göttingen, Germany
E-Mail: goekseminfatma.senguel@med.uni-goettingen.de
gokseminsengul@gmail.com
Phone: 0152-510-91782

EDUCATION

08/2018–06/2022   **PhD in Biochemistry**

Georg-August University Göttingen, Germany

University Medical Centre Göttingen

Department of Cellular Biochemistry

PhD Thesis: Modifications in AP2 and Clathrin-Mediated Endocytosis

as a Mechanism of Synaptic Plasticity

Supervisor: Prof. Dr. Peter Schu

09/2015 – 06/2018   **Master of Science in Interdisciplinary Neurosciene**

Department of Neuroscience, Bilkent University, Turkey

Master's Thesis: Analysis of Movement Disorder-Related Genes

Following the Knockdowns of *ANO10, WDR81* and *VLDLR* in Zebrafish

(*Danio Rerio*)

Supervisor: Prof. Dr. Michelle Adams

09/2011 – 06/2015   **Bachelor of Science in Molecular Biology and Genetics**

Bilkent University, Department of Molecular Biology and Genetics,
Turkey

ACADEMIC & RESEARCH EXPERIENCE

08/2018 – current   **Graduate student (PhD Student)**

Georg-August University Göttingen, Germany

University Medicine Center Göttingen

Department of Cellular Biochemistry

Supervisor: Prof. Dr. Peter Schu

09/2015 – 06/2018   **Graduate student (MSc student, researcher)**

Bilkent University, Department of Neuroscience, Turkey

Supervisor: Prof. Dr. Michelle Adams

09/2014-06/2015.   **Senior student (BSc student, researcher)**

Bilkent University, Department of Molecular Biology and Genetics,

Turkey, Supervisor: Assoc. Prof. Ebru Erbay, Project: The

investigation of the novel roles of protein kinase R in lipotoxicity

06/2014-09/2014.   **Visiting internship student**
Cambridge UniversityDepartment of Genetics, UK,
Supervisor: Prof. Dr. Cahir O'Kane
Project: Characterization of a novel Drosophila motor neuron
disease model

06/2012-06/2014   **Research assistant internship (BSc student, researcher)**
Bilkent University, Department of Molecular Biology and Genetics,
Turkey
Supervisor: Prof. Dr. Özlen Konu
Project: qPCR validation of breast cancer diagnostic markers

TEACHING EXPERIENCE
02/2016 – current   **Teaching assistant**

10/2020-03/2022   **Practical course Enzymology II**
Georg-August University Göttingen
Department of Cellular Biochemistry
Supervisor: Prof. Dr. Peter Schu

10/2021-12/2021   **Fast Forward productivity and time management course**
Georg-August University Göttingen, Germany, Dr. Nadine Sinclair

02/2017-06/2018   **Research Methods in Neuroscience (NSC 512)**
Bilkent University, Department of Neuroscience, Turkey
Supervisor: Prof. Michelle Adams

09/2016-01/2017   **Genetics (MBG 210)**
Bilkent University, Department of Molecular Biology and Genetics
Turkey
Supervisor: Prof. Dr. Özlen Konu

02/2016-05/2016   **Molecular Genetics (MBG 223)**
Bilkent University, Department of Molecular Biology and Genetics,
Turkey, Supervisor: Asst. Prof. Murat Cevher

HONORS&AWARDS
04/2022-06/2022   GGNB Bridging Fund stipend
05/2015-12/2017   Tubitak scientific and technological research (1001) project stipend
01/2015   High-honour student, Bilkent University, Department of Molecular
Biology and Genetics
06/2014-09/2014   Erasmus scholarship for summer internship
05/2012-05/2015   Honour student, Bilkent University**,** Department of Molecular Biology
and Genetics

SCIENTIFIC PUBLICATIONS (Peer-reviewed journal articles)

D. Celebi-Birand, N.I. Ardic, E.T. Karoglu-Eravsar, **G.F. Sengul,** H. Kafaligonul, and M.M. Adams. Dietary and Pharmacological Interventions that Inhibit Mammalian Target of Rapamycin (mTOR) Activity Alter the Brain Expression Levels of Neurogenic and Glial Markers in An Age- and Treatment-Dependent Manner. *Rejuvenation Research*. 2020 Dec;23(6):485-497. doi: 10.1089/rej.2019.2297. Epub 2020 May 19. PMID: 32279604.

Mishra, R., **Sengül, G.F.,** Candiello, E. and Schu, P. Synaptic AP2 CCV life cycle regulation by the Eps15, ITSN1, Sgip1/AP2, synaptojanin1 interactome. *Sci Rep* **11,** 8007 (2021). https://doi.org/10.1038/s41598-021-87591-3.

Sengul, G.F., Celebi-Birand, D., Keskus, A.G., Tuz-Sasik, M.U., Karoglu-Eravsar, E.T., Doldur-Ballı, F., Arslan-Ergül, A., Konu, O., Ozcelik, T., Topaloglu, H. and Adams, M.M.
Functional knocdowns of *ano10, wdr81,* and *vldlr* reveal a potential network of genes involved in the Cerebellar Ataxia pathogenesis. *In submission*.

Sengul, G.F., Mishra, R., Candiello, E., Bernhard, O., Valerious, O., and Schu, P. Hsc70 phosphorylation pattern and calmodulin regulate formation of stabilized AP2 CCV for cell adhesion protein transport. *In submission.*

CONFERENCES and PRESENTATIONS
03/2021 14 th German Neuroscience Society Meeting, Georg-August University Göttingen
09/2020 17 th Horizons in Molecular Biology, Georg-August University Göttingen, Germany
10/2019 GGNB Cell retreat, Georg-August University Göttingen, Germany
11/2014 EMBO Winter retreat, Bilkent University, Turkey

Poster presentations
09/2020 17 th Horizons in Molecular Bilogy, Georg-August University Göttingen, Germany
10/2019 GGNB Cell retreat, Georg-August University Göttingen, Germany
05/2018 16 th ITU USK Neuroscience Symposium, Istanbul Technical University, Turkey
04/2017 4 th International Symposium on Brain and Cognitive Science, Hacettepe University, Turkey
05/2016 NanoDays, National Nanobiotechnology Research Center, Bilkent University, Turkey